

Copyright is owned by the Author of the thesis. Permission is given for a copy to be downloaded by an individual for the purpose of research and private study only. The thesis may not be reproduced elsewhere without the permission of the Author.

**Characterisation of food fibres and their effect on  
starch digestion in an *in-vitro* system at  
physiological shear rates**

A thesis presented in partial fulfilment of the requirements for the  
degree of Doctor of Philosophy in Anatomy and Physiology at  
Massey University, New Zealand.

**SIA-YEN, YAP**

**2017**



**MASSEY UNIVERSITY**  
**TE KUNENGA KI PŪREHUROA**  
**UNIVERSITY OF NEW ZEALAND**



## ABSTRACT

The fast pace of life promotes the excessive consumption of processed starchy food containing high levels of sugar, salt and oil; which can increase the prevalence of type II diabetes, colon and cardiovascular diseases. The addition of dietary fibres in the diet increases the viscosity of digesta, delays mixing in the gut, and promotes laxation. However, few studies attempt to quantify the possible physical and chemical effects of either soluble (food gums) and insoluble (largely cellulose) fibre in the diet. These effects may encompass the retention of water inside the fibre particles, between particles in the fibre mass and direct effects of the chemical nature of the fibre on the digestion process. In this study, the fractions of water held in the various partitions of insoluble particulate dietary fibres are quantified. The relationship between the volume fraction of soluble and insoluble dietary fibres in simulated digesta at physiological concentrations and the rheological properties of the suspension at physiological shear rates is determined. Furthermore, the impact of fibre and shear rates on the digestion of starch *in-vitro* at physiological shear rates was measured. This work provides the first quantitative assessment of the effects of the physical attributes of dietary fibre on the digestion of starch *in-vitro*, at physiological shear rates.

In this work, four insoluble fibre types were used to construct aqueous suspensions containing solid volume fractions similar to those of pig digesta from the small intestine, these suspensions also were shown to have similar rheological properties to those of pig digesta at physiological shear rates. In addition, a soluble fibre (Guar gum) was used to construct solutions with viscosities comparable to those of the

particulate suspensions. Gelatinised and partially gelatinised starch was added to these suspensions and its rate of digestion at 37°C under simulated small intestinal conditions was measured at shear rates covering the reported physiological range.

Important results from this work include:

- The proportion of water retained by a given volume of hydrated mass of large fibre particles (AllBran®) was double that of smaller particles (wheat fibre). For all of the solid particles used, the proportion of water sequestered by the intra-particulate voids was less than 4% of the volume of the particles, similar proportions were determined for indigestible particles recovered from the colon of pigs and from human faeces.
- Food fibre systems containing less than 20% by volume (solid volume fraction,  $\phi = 0.20$ ) of insoluble dietary fibres showed Newtonian rheological properties and the viscosity of these suspensions could be predicted from  $\phi$  by the Maron-Pierce model. Starch/fibre suspensions prepared with  $\phi$  below 20% ( $\phi = 0.68-0.98$ ) had a similar viscosity to that of starch/guar suspension comprising 10% (w/v) starch and 0.4% (w/v) guar.

During *in-vitro* digestion, the viscosity of the starch/fibre suspensions decreased logarithmically over the first 20 minutes during which about 30% of the starch was hydrolysed, this was followed by a prolonged period of slow digestion as the slowly digested starch (SDS) and resistant starch (RS) were hydrolysed. The rate of starch digestion was independent of the type of insoluble fibre and was not affected by suspension viscosities used

providing shear rates could be maintained within physiological levels. For guar, rates of digestion were slowed probably due to non-competitive inhibition of the amylase by the guar.

- When shear rates were below the physiological range ( $0.1 \text{ s}^{-1}$ ) or gelatinisation was incomplete, the rate of digestion became linear over the first 20 minutes of digestion suggesting that the rate of digestion was limited by transport processes at low shear in viscous suspensions.
- This study provides useful information regarding the limiting concentration of particles and hence viscosity of digesta in the gut if rates of digestion are to be maximised. Additionally, it is suggested that guar, even at low concentration may reduce glycemia by reducing rates of amylolysis.

## **ACKNOWLEDGMENTS**

The beginning of a PhD study, resembles a single way journey which with the ultimate goal of graduation. This journey has been enjoyable yet accompanied with hardships which would not have been possible without the help of many people. Firstly, I am grateful to the Lord God Almighty for giving me the opportunity to complete my research and making all things possible.

I would like to express my most honoured gratitude to my enthusiastic chief supervisor, Professor Dr. Roger Lentle to accept me in as his student. My PhD has been an amazing experience and I thank Professor Roger not only for giving me so many wonderful opportunities, but also for his tremendous academic support by continually inspired me with his insightful comments on the scope of my study and patiently guide me to think like a scientist. My deepest thanks go to my co-supervisor, Mr. Allan Hardacre for his invaluable guidance and comments on my research methodology and scientific writing, also his kind hospitality exposing me to the kiwi culture. Special mention goes to my second co-supervisor, Dr. John Monro, for his advice and insightful scientific suggestions to the project. I have learned a lot from them, especially their enthusiasm and innovation in research.

Special thanks go to the Riddet Institute and Plant and Food Research for funding this project.

To the Director of Postgraduate Studies of School of Food and Nutrition (SFN), Professor Julian Heyes and to the Head of department, Professor Steve Flint, thank you for your caring support and encouragement throughout my study.

I am thankful to all the staff of SFN especially the laboratory managers, Michelle Tamehana, Corrin Hulls, Steve Glasgow, Garry Radford, Warwick Johnson, Fliss Jackson and Ann-Marie Jackson for their invaluable technical assistance in using various equipment. I also appreciate the generous assistance from Miria Busby, Yvonne Parkes, Christine Ramsey and Matthew Levin for their support in administration and computer networking setting throughout the years. I would like to give my sincere thanks to Anja Moebis, for her help to access the lab and use the gas pycnometer; Doug Hopcroft, for his help in preparing the images from scanning electron microscope. My thanks also address to Dr. Patrick Janssen who wrote the custom software using Image J that enabled me to estimate particle volumes.

I would like to thank my friends, especially Dr. Zeinab Dehghan-Shoar, Drs. Reza Abdollahi and Faegheh Zaefarian for their kind hospitality. My sincere thanks also go to Farihan, Soffalina, Anges, Karren, Elham, Sayaka, and Tanya for the de-stressed and fun outings to “hunt” for cuppa, delicious pizzas and cakes. Special thanks go to Pla, Pang, Chalida, Pilirani, Sandra, and Thu for their invaluable support, encouragement, and friendship.

Last but not least, to my beloved family members, my father, Mr. Yap Wei Keong, my mother, Mdm. Lee Siew Moey, my sister, Sin Ling and my brother, Chee Yoong. Thank you for their unconditional love and moral support.



## TABLE OF CONTENTS

ABSTRACT .....	i
ACKNOWLEDGMENTS .....	iv
TABLE OF CONTENTS .....	vi
LIST OF FIGURES .....	xi
LIST OF TABLES .....	xvi
LIST OF EQUATIONS .....	xviii
LIST OF ABBREVIATIONS .....	xix
LIST OF PUBLICATIONS AND CONFERENCES .....	xxii

<b>Chapter 1</b>	<b>General introduction .....</b>	<b>1</b>
------------------	-----------------------------------	----------

<b>Chapter 2</b>	<b>Review of literature .....</b>	<b>10</b>
2.1.	Dietary carbohydrate .....	10
2.1.1.	Definition and classification of dietary fibre .....	10
2.1.2.	Sources of dietary fibre .....	15
2.1.3.	Chemical compositions of dietary fibre .....	17
2.1.3.1.	Insoluble dietary fibre .....	18
2.1.3.2.	Soluble dietary fibre .....	19
2.1.4.	Fermentability of dietary fibre .....	21
2.1.5.	Hydration properties of insoluble fibres .....	22
2.1.5.1.	Factors affecting water holding capacity (WHC) .....	23
2.1.5.1.1	Chemical composition and WHC .....	23
2.1.5.1.2	Particle sizes, processing methods and health benefits .....	24
2.2.	Starch granules .....	26
2.2.1.	The size and shape of starch granules .....	26
2.2.2.	Amylose and amylopectin .....	26
2.2.3.	Other minor components .....	32
2.2.4.	The structure of starch granules .....	32
2.2.5.	Gelatinisation .....	34
2.3.	Viscosity of starch and dietary fibres suspensions .....	36
2.3.1.	Viscosity of digesta .....	39
2.3.2.	Factors affecting viscosity .....	40
2.3.2.1.	Solid volume fractions ( $\phi$ ) and shear rate .....	40
2.3.2.2.	Ratio of solid volume fraction to the maximum packing fraction, ( $\phi/\phi_{\max}$ ) .....	42
2.3.2.3.	Aspect ratio of particles sizes .....	44
2.3.3.	Viscosity of starch suspensions .....	46
2.3.3.1.	Defining gelatinisation by viscosity .....	46
2.3.3.2.	Hydration and viscous properties of starch .....	48
2.4.	Starch digestion .....	50
2.4.1.	<i>In-vitro</i> and <i>in-vivo</i> starch digestion .....	51
2.4.1.1.	Measurement of rate of digestion <i>in-vitro</i> .....	52
2.4.2.	Factors affecting the rate of starch digestion <i>in-vitro</i> .....	54

2.4.2.1.	Kinetic of alpha amylase and amyloglucosidase .....	55
2.4.2.2.	Physico-chemical properties of raw starch granules .....	56
2.4.2.3.	Degree of gelatinisation (DG) .....	58
2.4.2.4.	Presence of insoluble and soluble dietary fibres .....	60
2.4.2.5.	Effect of shear rate .....	62
2.5.	Concluding remarks .....	63
<b>Chapter 3</b>	<b>General materials and methods .....</b>	<b>64</b>
3.1.	Introduction .....	64
3.2.	Selection of materials .....	64
3.2.1.	Digestive residues of pig and human .....	64
3.2.2.	Food fibres .....	68
3.2.3.	Starch .....	69
3.2.4.	Glass beads .....	70
3.3.	Chemical properties of dietary fibre and starch .....	70
3.3.1.	Proportion of cellulose, hemicellulose and lignin in food dietary fibre .....	70
3.3.2.	Protein content .....	73
3.3.3.	Fat content (Soxtec <sup>TM</sup> method) .....	74
3.3.4.	Moisture content .....	74
3.3.5.	Water activity ( $A_w$ ) .....	75
3.4.	Physical properties of fibre suspensions .....	75
3.4.1.	Density of solid residues from digesta and faeces .....	76
3.4.2.	Density of liquid used to prepare fibre suspensions .....	77
3.4.2.1.	Selection of the Newtonian liquid phase .....	77
3.4.3.	Microscopy .....	79
3.4.3.1.	Light microscope .....	79
3.4.3.2.	Scanning electron microscope .....	81
3.5.	Starch digestion .....	82
3.5.1.	Removal of digestible components from fibre particles .....	82
3.5.2.	<i>In-vitro</i> digestion system - using rheometer .....	83
3.5.3.	Determination of total starch content .....	85
3.6.	Data analysis .....	86
<b>Chapter 4</b>	<b>Quantification of water partitioned in undigested and digested dietary fibres.....</b>	<b>90</b>
4.1.	Abstract .....	91
4.2.	Introduction .....	91
4.3.	Materials and methods .....	95
4.3.1.	Proximate chemical compositions of fibre particulates .....	95
4.3.2.	Physical characteristics of fibre particulates .....	95
4.3.3.	Particulates recovered from human faeces and pig digesta .....	95
4.3.4.	Selection of drying temperature for digesta particles .....	95
4.3.5.	<i>In-vitro</i> digestion of commercial fibre particles .....	96
4.3.6.	SEM .....	96
4.3.7.	Light microscope .....	97
4.3.8.	Determination of the volume of fibre particles .....	97

4.3.9.	Determination of the water content of saturated particles .....	98
4.3.9.1.	Water of saturation ( $W_s$ ) .....	98
4.3.9.2.	Water holding capacity (WHC) .....	99
4.3.9.3.	Intra-particulate and extra-particulate water .....	100
4.3.10.	Statistical analysis .....	100
4.4.	Results .....	101
4.4.1.	Chemical composition of fibre particles .....	101
4.4.2.	Particle morphology .....	103
4.4.2.1.	Scanning electron micrographs .....	103
4.4.2.2.	Light micrographs .....	105
4.4.3.	Distributions of particles .....	111
4.4.3.1.	Cumulative distribution of particles .....	111
4.4.3.2.	Distribution of particles volume .....	113
4.4.4.	Particle density .....	115
4.4.5.	Hydration of particles .....	116
4.4.6.	Intra- and extra-particulate water .....	119
4.5.	Discussion .....	120
4.6.	Conclusions .....	124

<b>Chapter 5</b>	<b>The effect of the solid phase of digesta on the viscosity of digesta .....</b>	<b>126</b>
5.1.	Abstract .....	126
5.2.	Introduction .....	127
5.3.	Materials and Methods .....	130
5.3.1.	Solid particles .....	130
5.3.2.	Dry matter contents (DMC) .....	130
5.3.3.	Density of solid particles from pig digesta .....	131
5.3.4.	Solid volume fraction ( $\phi$ ) .....	131
5.3.5.	Apparent viscosity of pig digesta .....	131
5.3.6.	Fitting the Maron-Pierce equation for fibre and glass bead suspensions .....	132
5.3.7.	Image analysis .....	135
5.3.8.	Data analysis .....	135
5.4.	Results .....	137
5.4.1.	Validation of parameters used to characterise the viscosity of digesta .....	137
5.4.2.	Model particle system .....	139
5.4.3.	Properties of particles from pig digesta .....	144
5.5.	Discussion .....	148
5.6.	Conclusions .....	151

<b>Chapter 6</b>	<b>The effect of fibre and gelatinised starch type on the rate of amylolysis and apparent viscosity reduction during in-vitro digestion at a physiological shear rate .....</b>	<b>152</b>
6.1.	Abstract .....	153

6.2.	Introduction .....	154
6.3.	Materials and methods .....	157
6.3.1.	Fibre types .....	157
6.3.2.	Preparation of AllBran® fibre .....	157
6.3.3.	The concentration of fibres used .....	158
6.3.4.	Starch .....	158
6.3.5.	Pasting temperature .....	158
6.3.6.	Preparation of starch/fibre suspensions .....	160
6.3.7.	<i>In-vitro</i> digestion using rheometer .....	161
6.3.8.	Total starch and sugar determination .....	162
6.3.9.	SEM of starch granules .....	162
6.3.10.	Data analysis .....	163
6.4.	Results .....	165
6.4.1.	Fibre types .....	165
6.4.2.	Physico-chemical properties of starches .....	166
6.4.3.	RDS, SDS, and RS as a proportion of total starch .....	166
6.4.4.	Relationship between viscosity and starch .....	168
6.5.	Discussion .....	186
6.6.	Conclusions .....	192

## **Chapter 7      The effects of degree of gelatinisation and process conditions on the digestibility of starch suspensions during in-vitro digestion at physiological shear rates .....**

7.1.	Abstract .....	194
7.2.	Introduction .....	195
7.3.	Materials and methods .....	198
7.3.1.	Starch .....	198
7.3.2.	Determination of %DG .....	198
7.3.3.	Hydration properties .....	201
7.3.4.	Preparation of starch samples for digestion .....	203
7.3.5.	Light microscope .....	203
7.3.6.	Experiment designs for <i>in-vitro</i> digestion .....	204
7.3.7.	<i>In-vitro</i> digestion .....	204
7.3.8.	Rheology .....	205
7.3.9.	Total starch and sugar determination .....	206
7.3.10.	Data analysis .....	206
7.4.	Results .....	206
7.4.1.	Pasting properties of starches .....	206
7.4.2.	RDS as a proportion of total starch .....	207
7.4.3.	Water absorption, solubility and apparent viscosity .....	209
7.4.4.	Digestion of starch .....	211
7.4.5.	Effect of %DG .....	215
7.4.6.	Effects on starch viscosity .....	216
7.4.7.	Relationship between digestion starch and % viscosity .....	218
7.5.	Discussion .....	220
7.6.	Conclusion .....	224

<b>Chapter 8</b>	<b>General discussion and conclusions .....</b>	<b>226</b>
8.1.	Introduction .....	226
8.2.	Outcomes from the study .....	226
8.3.	Applications .....	228
8.4.	Limitations .....	229
8.5.	Recommended future research .....	229
Bibliography	.....	230
Appendix 1	.....	256
Appendix 2	.....	257
Appendix 3	.....	258
Appendix 4	.....	259
Appendix 5	.....	260
Appendix 6	.....	269
Appendix 7	.....	278

## LIST OF FIGURES

Figure 2.1:	Analytical methodology for quantitatively assessing the components of dietary fibre (Asp et al., 1983).....	14
Figure 2.2:	Structural model of a cellulose microfibril. The microfibril has homopolymeric regions of highly crystallinity intermixed with less organised heteropolymeric amorphous regions (adapted from Taiz & Zeiger, 2002).....	18
Figure 2.3:	Three dimensional view of the arrangement of plant cell wall polymers that made up of insoluble and soluble fibres (adapted from Thakur, Singh, Handa, & Rao, 1997).....	20
Figure 2.4:	Basic structure of the main starch polymers: the quasi-linear amylose (above) and highly branched amylopectin (below) (adapted from Delcour et al., 2010).....	27
Figure 2.5:	From starch granules to building blocks; a schematic showing organization of the unit chains in amylopectin illustrated according to the cluster model and the building block backbone model. (a) the granule consisting of alternating ring with a hilum region, normally considered as amorphous and centred to their middle. (b) The principal arrangement of the semi-crystalline rings according to the cluster structure of amylopectin. (c) The principal arrangement of the semi-crystalline rings according to the building block backbone structure of amylopectin. The structure of the amorphous rings is not established, but consists of amylose as well as amylopectin. The semi-crystalline rings consist of alternating crystalline (C) and amorphous (A) lamellae, which are enlarged in the lower figures. The details of double helices (cylinders) and building blocks (encircled) are depicted in the centre lower figure (circles depict glucose residues). Inter-block segments (IBS) and inter-cluster segments (ICS) are indicated and are found in both models, but the principal unit in (b) is the cluster and in (c) is the much smaller and more tightly branched building block. Note that a major difference between the models is that in (b) the amylopectin molecules penetrate the stacks of lamellae, whereas in (c) the AP molecules do not penetrate the stacks. The blocklets or super helices of AP are not shown, but are supposed to be structures in between the granular rings and the molecular levels (adapted from Vamadevan & Bertoft, 2015).....	30
Figure 2.6:	Schematic diagram of starch granule structure (a) a single granule with alternating amorphous and pseudo-crystalline layers; (b) expanded view alternating crystalline and amorphous lamellae in the pseudo-crystalline layers (adapted from Jenkins et al., 1994); (c) blocklet structure in association with amorphous radial channels. Blocklet size is smaller in the semi-crystalline layer than in the crystalline layer; (d) Scanning electron micrographs of starch granules after $\alpha$ -amylolysis showing the occurrence of spherical blocklet-like structures (adapted from Gallant et al.,	

	1992).....	33
Figure 2.7:	Scanning electron micrographs of residual starch granules after pancreatic alpha-amylase hydrolysis: (a) wheat; (b) potato. “Blocklets” are shown by arrows (adapted from Gallant et al., 1992).....	34
Figure 2.8:	An illustration of the gelatinisation process and the changes in ordered structures of a starch granule during heating in excess water (adapted from Biliaderis, 1991).....	35
Figure 2.9:	The dispersed soluble fibre forming entangled network in a solution (adapted from Ellis, Rayment, & Wang, 1996).....	38
Figure 2.10:	Schematic model of a suspension of spherical particles in response to applied shear (arrows). Particle-particle interaction increases as the gap (h) between particles decreases and the mean particle diameter (d) increases (adapted from Petford, 2009).....	41
Figure 2.11:	The effect of shear rate on apparent viscosity of a particulate suspension.....	42
Figure 2.12:	The relationship between relative viscosity and the $\phi/\phi_{\max}$ (adapted from Stickel & Powell, 2005) using hard polystyrene spheres and polymethyl methacrylate beads suspended in polymer solutions such as polyethylene glycol-ran-propylene glycol monobutylether.....	43
Figure 2.13:	A typical RVA viscogram for starch gelatinisation, viscosity profile (dotted line) and temperature profile (bold line).....	47
Figure 2.14:	Hydrolytic mechanism of enzymes on amylose and amylopectin. Alpha-amylase is an endo-acting enzyme hydrolysing $\alpha$ -(1-4) bonds at random giving rise to malto-oligosaccharides (linear or branched, typically DP 2-6); it does not hydrolyse $\alpha$ -(1-6) bonds. Amyloglucosidase is an exo-acting hydrolase which releases single glucose molecules from the non-reducing end of $\alpha$ -(1-4) oligo- or polysaccharides. This enzyme is unique because it can hydrolyse $\alpha$ -(1-6) branching points, converting starch completely to glucose (adapted from Tester & Sommerville, 2000).....	55
Figure 2.15:	Action of salivary and pancreatic alpha-amylase on amylopectin. Each circle represents a glucose residue linked with either alpha-1,4 (horizontally) or alpha-1,6 (vertically) bond. The final products from amylolysis are maltose, maltotriose and the branched alpha-dextrins (adapted from Gray, 1992).....	56
Figure 2.16:	Diffusion of amylase and its hydrolysis patterns in raw corn and potato starches: (A) corn starch showing pores and channels; (B) corn starch hydrolysed by amylase with enlarged pores; (C) potato starch granules have fewer pores, (D) channels and cavity of potato starch by amylase. Adapted from (left: Dhital, Shrestha, & Gidley, 2010); (right: Sujka & Jamroz, 2007).....	58
Figure 3.1:	SEM images of the starch particles (i-ii), to the same scale.....	69
Figure 3.2:	The small strain oscillation time sweep test on 70% (w/v) fructose in which 50% (w/v) of glass beads was suspended.....	79
Figure 3.3:	The light microphotography of (a) cellulosic wheat fibre (Prolux) and (b) Wood fibre stained with toluidine blue O (left) and safranin (right).....	80
Figure 4.1:	Chemical compositions of the “as supplied” fibre particles.....	101

Figure 4.2:	Chemical compositions of the fibre particles after <i>in-vitro</i> digestion.....	102
Figure 4.3:	SEM images of the various commercial fibre particles used. Left column: commercial fibre particles ‘as supplied’; Right column: commercial fibre particles after <i>in-vitro</i> digestion.....	104
Figure 4.4:	Light microscope images of (a) WF600 and (b) Prolux wheat fibres after staining with Toluidine blue O; particles from (c) wood, (d) AllBran®, (e) human faeces and (f) pig digesta were stained with safranin. For fibre particles from (a) to (d): (Left) commercial fibre particles ‘as supplied’; (Right) commercial fibre particles after <i>in-vitro</i> digestion. All photos were taken in the same scale as WF600.....	108
Figure 4.5:	Light microscope images after analysis of volume using Image J software (a) WF600 and (b) Prolux wheat fibres after staining with Toluidine blue O; particles from (c) wood, (d) AllBran®, (e) human faeces and (f) pig digesta were stained with safranin. For fibre particles from (a) to (d): (Left) commercial fibre particles ‘as supplied’; (Right) commercial fibre particles after <i>in-vitro</i> digestion. All photos were taken in the same scale.....	111
Figure 4.6:	Volume of particles plotted against cumulative volume weighted from Image J analysis; (a) all commercial fibre types before and after <i>in-vitro</i> digestion (IV) and solid particles recovered from human faeces and pig digesta; (b) Cellulosic WF600 and Prolux wheat fibres before and after <i>in-vitro</i> digestion.....	112
Figure 4.7:	Percent of particles (left) and the proportion of particle volume (right) for each of the 5 size categories. (a) Commercial fibre particles before <i>in-vitro</i> digestion, (b) commercial fibre particles following <i>in-vitro</i> digestion, (c) Particles collected from colonic pig digesta and human faeces.....	114
Figure 5.1:	SEM micrograph of glass beads.....	139
Figure 5.2:	Light micrographs (x200) of food particles recovered from <i>in-vitro</i> digestion with various R values.....	140
Figure 5.3:	The relationship between $\eta_r$ of the food fibre suspensions to $\phi/\phi_{\max}$ ; ■ = WF600 after <i>in-vitro</i> digestion, ▲ = Prolux after <i>in-vitro</i> digestion; + = wood fibre after <i>in-vitro</i> digestion, ◆ = AllBran® after <i>in-vitro</i> digestion, x = glass beads, and — = Maron-Pierce equation fit. Apparent viscosity of the suspending 70% fructose solution, $\eta_s = 0.032$ Pa.s.....	142
Figure 5.4:	The relationship between $\phi_{\max}$ and aspect ratio (R) for the glass bead and fibre suspensions from this study and for other suspensions (Kitano et al., 1981; Pabst, Gregorova, et al., 2006). Coefficients from the linear regression: This study (Equation 5.4); $\phi_{\max} = 0.528 - 0.042 R$ , Kitano; $\phi_{\max} = 0.54 - 0.0125 R$ , Pabst; $\phi_{\max} = 0.51 - 0.0223 R$ .....	143
Figure 5.5:	Optical microscopic images (x200) of digesta particles recovered from (a) the proximal; (b) the distal segments of porcine small intestine.....	147
Figure 6.1:	Chemical compositions of the five fibre types.....	165
Figure 6.2:	SEM images of the starch particles (i-ii), to the same scale.....	166
Figure 6.3:	Proportions of RDS, SDS, and RS as a percentage of total starch,	



	with and without the inclusion of the fibre types. P, potato starch; C, corn starch; WF600, WF600 wheat fibre; P, Prolux wheat fibre; W, wood fibre; Ab, <i>In-vitro</i> digested AllBran®; G, guar gum; RDS, rapidly digestible starch; SDS, slowly digestible starch; RS, resistant starch. Mean values labelled with different superscripts (a–e) are significantly different (GLM and Tukey’s pair wise test, $p \leq 0.05$ ).....	167
Figure 6.4:	The proportion of starch remaining during <i>in-vitro</i> digestion of the ■=Control starch (left, potato; right, corn), and various starch/fibre suspensions, □=WF600, ▲=Prolux fibre, △=Wood fibre, ●=AllBran® fibre, ○=Guar. Each point is the mean of two replicates. The line is the best fit for all points using an exponential decay function (Equation 3.10).....	171
Figure 6.5:	The proportion of apparent viscosity measured during <i>in-vitro</i> digestion of the ■=Control starch (left, potato; right, corn), and various starch/fibre suspensions, □=WF600, ▲=Prolux fibre, △=Wood fibre, ●=AllBran® fibre, ○=Guar. Each point is the mean of two replicates. The line is the best fit for all points using an exponential decay function (Equation 3.10).....	173
Figure 6.6:	The proportion of starch remaining (Ln-transformed data) during the first 20 min (Figure 6.4) of <i>in-vitro</i> digestion of the ■=Control starch (left, potato; right, corn), and various starch/fibre suspensions, □=WF600, ▲=Prolux fibre, △=Wood fibre, ●=AllBran® fibre, ○=Guar. Each point is the mean of two replicates. The line is the linear regression (Equation 3.11) fitted to all points.....	178
Figure 6.7:	The proportion of initial viscosity measured (Ln-transformed data) during the first 20 min (Figure 6.5) of <i>in-vitro</i> digestion of ■=Control starch (left, potato; right, corn), and various starch/fibre suspensions, □=WF600, ▲=Prolux fibre, △=Wood fibre, ●=AllBran® fibre, ○=Guar. Each point is the mean of two replicates. The line is the linear regression (Equation 3.11) fitted to all points.....	180
Figure 6.8:	The relationship between the proportion of starch remaining in suspension and apparent suspension viscosity during 20 min of <i>in-vitro</i> digestion for ■=Control starch (left, potato; right, corn), and various starch/fibre suspensions, □=WF600, ▲=Prolux fibre, △=Wood fibre, ●=AllBran® fibre, ○=Guar. Each point is the mean of two replicates.....	185
Figure 7.1:	Rheology of starches during gelatinisation: RVA pasting profile for aqueous suspensions of 10% (w/w) potato (P) and corn (C) starch, △ = DG0%, ●=DG50%, DG100% marked on graph.....	199
Figure 7.2:	Differences in RDS as a percentage of total starch, with %DG and cooking duration at different shear rates (10s, shear rate at $10 \text{ s}^{-1}$ ; 1s, shear rate at $1 \text{ s}^{-1}$ ; 0.1s, shear rate at $0.1 \text{ s}^{-1}$ ). Proportion of RDS was plotted as means; values with superscripts (a-h) are significantly different (Two way ANOVA and Tukey’s pair-wise test, $p < 0.05$ ). Other notation similar to Table 7.2.....	208
Figure 7.3:	Light micrographs (x40) of starch granules gelatinised at different DG and cooking duration. Upper row: Potato starch, lower row:	

	corn starch. The $A_w$ for all starch/water suspension was 0.99 and $A_w$ for all starch/70% fructose suspensions was 0.74.....	210
Figure 7.4:	Ln proportion of starch remaining during the first 20 min of simulated small intestinal digestion (Start value = 100%). DG, degree of gelatinisation; Ck, cook time (min); Starch cooked in fructose and measured at shear rates of $0.1 \text{ s}^{-1}$ , $1 \text{ s}^{-1}$ and $10 \text{ s}^{-1}$ (open symbols as per legend); starch cooked in water and measured at a shear rate of $0.1 \text{ s}^{-1}$ (filled symbols as per legend); starch cooked in water measured at a shear rate of $1 \text{ s}^{-1}$ and $10 \text{ s}^{-1}$ (Shear rate $> 0.1 \text{ s}^{-1}$ ) is the remaining data. Linear regressions of the Ln-transformed data plotted against time are fitted to all data within each of the 3 data sets and are the annotated lines on the graphs.....	212
Figure 7.5:	Ln proportion of apparent viscosity remaining during the first 20 min of simulated small intestinal digestion (Start value = 100%). Notations were similar to those in Figure 7.4.....	213
Figure 7.6:	The relationship between the proportion of undigested starch and the proportion of apparent viscosity remaining for all treatments during the 20 min of digestion; $\boxplus=10 \text{ s}^{-1}$ FrucCk30, $\blacksquare=10 \text{ s}^{-1}$ DG50%Ck30, $\blacksquare=10 \text{ s}^{-1}$ DG100%Ck10, $\square=10 \text{ s}^{-1}$ DG100%Ck30, $\blacktriangle=1 \text{ s}^{-1}$ FrucCk30, $\blacktriangle=1 \text{ s}^{-1}$ DG50%Ck30, $\blacktriangle=1 \text{ s}^{-1}$ DG100%Ck10, $\triangle=1 \text{ s}^{-1}$ DG100%Ck30, $\oplus=0.1 \text{ s}^{-1}$ FrucCk30, $\bullet=0.1 \text{ s}^{-1}$ DG50%Ck30, $\bullet=0.1 \text{ s}^{-1}$ DG100%Ck10, $\circ=0.1 \text{ s}^{-1}$ DG100%Ck30, - - - - Shear rate at $0.1 \text{ s}^{-1}$ , ——— Shear rate at 10 and $1 \text{ s}^{-1}$ ( $R^2=0.97$ ), - - - - Predicted from the Einstein model and Fructose treatment data. All treatments set to 100% starch and viscosity at the start of digestion. Digestion proceeds from left to right.....	219

## LIST OF TABLES

Table 2.1:	The dietary fibre content in some common food sources (g/100g edible portion) analysed using AOAC method (adapted from (Dreher, 1999; Hollmann, Themeier, Neese, & Lindhauer, 2013; Li, Andrews, & Pehrsson, 2002; Menkovska et al., 2017).....	16
Table 2.2:	Proximate composition (%) of dietary fibre isolated from plant cell wall analysed using methods adapted from (Englyst, 1989; Holloway & Greig, 1984).....	17
Table 2.3:	Hydration properties of various fibre types with different particle sizes.....	25
Table 2.4:	Shapes and sizes of starch granules from different botanical origin...	26
Table 3.1:	Dietary records of the volunteer on three consecutive days on 100 g Kellogg's AllBran® fibre supplement.....	66
Table 3.2:	Calculated nutritional values of carbohydrate, protein and fats for the daily food intake of the volunteer for three consecutive days using NutriPRO Inc. software.....	67
Table 3.3:	The densities and apparent viscosities of fructose solutions at 37°C..	78
Table 4.1:	The hydration characteristics of centrifuged pellets of various fibres before and after <i>in-vitro</i> digestion.....	118
Table 4.2:	Relative proportions of dry matter, $W_E$ and $W_I$ in the water saturated centrifuged particle pellets prepared for the measurement of $W_S$ .....	119
Table 5.1:	Values for DMC, $\phi$ and $\phi/\phi_{\max}$ for particulates recovered from the small intestine (SI) of pigs.....	138
Table 5.2:	The relative viscosities ( $\eta_r$ ) and, the estimated $\phi_{\max}$ of the fibre suspensions using <i>in-vitro</i> digested particles at a range of $\phi$ . Results relative to the viscosity of glass bead suspensions.....	141
Table 5.3:	Comparisons of constants relating $\phi_{\max}$ with R for various studies....	144
Table 6.1:	The PT and peak hot PV for the four concentrations of the two starches.....	159
Table 6.2:	Experimental treatments of starch/fibre suspensions used.....	162
Table 6.3:	Viscosity (Pa.s) of the potato (P) and corn (C) starch suspensions with the various fibre types before intestinal digestion (0 min) and during <i>in-vitro</i> intestinal digestion at 20 and 120 min.....	169
Table 6.4:	Differences in coefficients $a$ and $b$ from Eq. 3.10 ( $y = ae^{-(bx)}$ ) for the relative rate of decay in the proportion of potato and corn starch for six treatments over 120 min of stimulated small intestinal digestion.....	174
Table 6.5:	Differences in coefficients $a$ and $b$ from Eq. 3.10 ( $y = ae^{-(bx)}$ ) for the reduction in initial viscosity of potato and corn starch for six treatments over 120 min of stimulated small intestinal digestion.....	175
Table 6.6:	Differences in constants $m$ and $n$ ( $\ln Y = \ln m + n \cdot \ln t$ ), the relative rate of decay in the proportion of potato and corn starch for six treatments over 20 min of stimulated small intestinal digestion...	181
Table 6.7:	Differences in constants $m$ and $n$ ( $\ln Y = \ln m + n \cdot \ln t$ ), the relative rate of decay in viscosity as a proportion of initial viscosity for potato and corn starch suspensions for six treatments over 20 min of stimulated small intestinal digestion.....	182

Table 6.8:	Differences in the relative rate of digestion of potato and corn starch ( $\text{min}^{-1}$ ) for six treatments over 20 min of stimulated small intestinal digestion.....	183
Table 6.9:	$T_{1/2}$ values (min) for starch digestion and viscosity for the two starch controls (P, C) and 10 treatments during 120 min of <i>in-vitro</i> digestion of suspensions of various fibres with potato (left) and corn (right) starch.....	184
Table 7.1:	Pasting properties of 10% (w/w) potato and corn starch suspensions determined by the RVA.....	199
Table 7.2:	Experimental treatments: P, Potato; C, Corn; Fruc, starch suspension cooked in 70% (w/v) fructose solution; DG50% or DG100%, 50% or 100% gelatinisation temperature treatments; Ck10 or Ck30, cooked for 10 min or 30 min.....	204
Table 7.3:	Calculated shear stress required ( <i>Italics</i> ) to generate the shear rates for materials of the apparent viscosities listed. The value for shear stress = 1 ( <i>italics</i> , bold) is close to the maximum reported for the small intestine and shear stress values to the right of this in each row represent suspensions with viscosities that are unlikely to be mixed effectively in the small intestine.....	205
Table 7.4:	Effect of cooking duration (Ck10 min or Ck30 min) and %DG on Q (swelling factor), $\phi_w$ (volume proportion of water in the granules), and S (weight proportion of granule solubles) and the apparent viscosity at the three (3) shear rates for all treatments at the end of the gastric digestion phase. Other notation similar to Table 7.2.....	209
Table 7.5:	Variation in the relative rate of digestion of potato (P) and corn (C) starch ( $\text{min}^{-1}$ ) for the four gelatinisation treatments and three shear rates over 20 min of simulated small intestinal digestion. Other notation similar to Table 7.2.....	214
Table 7.6:	Variation in $T_{1/2}$ values with starch digestion and apparent viscosity for all treatments over 20 minutes. Data points are derived by solving from the linear regression fitted to the data in Figures 7.3 and 7.4.....	217

## LIST OF EQUATIONS

$\eta_r = \eta_s (1 + [k] \phi)$	(Equation 2.1).....	42
$\eta_r = (1 - (\phi/\phi_{\max}))^{-[k] \phi_{\max}}$	(Equation 2.2).....	43
$\eta_r = (1 - (\phi/\phi_{\max}))^{-2}$	(Equation 2.3).....	44
$Y = c - m X$	(Equation 2.4).....	46
$\phi_{\max} = 0.54 - 0.0125 R$	(Equation 2.5).....	46
$\phi_{\max} = 0.51 - 0.0223 R$	(Equation 2.6).....	46
$\phi_w = cQ$	(Equation 2.7).....	49
$\phi_w = [(1 - (S/100)) * cQ]$	(Equation 2.8).....	49
$NDF = 100 \times [(W_4 - W_5) - (B_4 - B_5)] / [W_1 * W_3]$	(Equation 3.1).....	71
$ADF = [(W_3 - W_2) - (B_3 - B_2)] W_1 \times 100$	(Equation 3.2).....	72
$ADL = [(W_4 - W_5) - (B_4 - B_5)] W_1 \times 100$	(Equation 3.3).....	73
$\% \text{Fat in starch} = [(W_2 - W_3)/W_1] * 100$	(Equation 3.4).....	74
$\% \text{Moisture} = [(W_2 - W_1)/W_1] * 100$	(Equation 3.5).....	75
Density of solid = (weight of solid / volume of solid)	(Equation 3.6).....	76
Density of liquid = (weight of liquid / volume of liquid)	(Equation 3.7).....	77
$t = 18\eta h / [g(\rho_s - \rho_w)d^2]$	(Equation 3.8).....	78
Reducing sugar = $[((OD * k) / (W * \text{starch})) \times 0.9]$	(Equation 3.9).....	86
$y = ae^{-(bx)}$	(Equation 3.10).....	87
$\ln y = \ln m + n. \ln t$	(Equation 3.11).....	88
$Y = A + [(B) / (1 + \exp(-(s-C)/D))]$	(Equation 3.12).....	88
Proportion of intra-particulate water = $[(\text{Fully hydrated volume} - \text{dehydrated volume}) / \text{dehydrated volume} \times 100]$	(Equation 4.1).....	100
Total intra-particulate water = Weight of dry fibre used to determine $W_s \times \text{Volume \% of shrinkage}$	(Equation 4.2).....	100
Total extra-particulate water = $W_s - \text{Total } W_1$	(Equation 4.3).....	100
$\phi = [(m_s / d_s) / V_1]$	(Equation 5.1).....	131
Average relative error = $(A / B) \times 100$	(Equation 5.2).....	134
$\eta_r = (0.58 \pm 4.35) + (-0.70 \pm 0.22 \text{ DMC}) + (-59.19 \pm 21.39 \phi) + (53.31 \pm 4.55 \phi / \phi_{\max})$	(Equation 5.3).....	138
$t = \frac{b_1 - b_2}{SEb_1 - b_2}$	(Equation 6.1).....	164
$SEb_1 - b_2 = \sqrt{SEb_1^2 - SEb_2^2}$	(Equation 6.2).....	164
$t = \frac{b - b_0}{SE_b}$	(Equation 6.3).....	164
$Q \text{ (g/g)} = (\text{weight of gelatinised granules} / \text{dry weight of starch})$	(Equation 7.1).....	201
$S (\%) = [(Ss / st) \times 100]$	(Equation 7.2).....	202

## LIST OF ABBREVIATIONS

ADF	Acidic detergent fibre
ADL	Acidic detergent lignin
$\alpha$	alpha
ANOVA	Analysis of variance
$\eta_s$	Apparent viscosity
R	Aspect ratio
AOAC	Association of Official Analytical Chemists
$\beta$	beta
BD	Breakdown
$\text{CaCl}_2$	Calcium chloride
$c$	Concentration of starch in a suspension
$c^*$	critical concentration
$^{\circ}\text{C}$	Degree celsius
DG	Degree of gelatinisation
$\rho$	density
DMC	Dry matter content
DNS	dinitrosalicylic acid
$\text{Na}_2\text{EDTA}\cdot 2\text{H}_2\text{O}$	Disodium ethylenediaminetetraacetate dihydrate
dwb	dry weight basis
GLM	Generalised linear model
g	gram
$g$	Gravity force
h	hour
HCl	Hydrochloric acid
kg	kilogram
LiCl	Lithium chloride
L	litre
$\mu\text{l}$	Microlitre
$\mu\text{m}$	Micrometer
mg	Milligram

mL	Millilitre
mm	Millimeter
mmol/L	Millimolar/litre
min	minutes
M	Molar
MW	Molecular weight
nKat	nanokatal
NDF	Neutral detergent fibre
$\eta_a$	Newtonian suspending liquid
NSP	Non starch polysaccharides
Pa	Pascal
Pa.s	Pascal per second
PT	Pasting temperature
PV	Pasting viscosity
%	Percentage
s <sup>-1</sup>	Per seconds
KCl	Potassium chloride
W <sub>E</sub>	Proportion of extra particulate water
W <sub>I</sub>	Proportion of intra-particulate water
RDS	Rapid digested starch
RVA	Rapid Visco Analyser
$\eta_r$	Relative viscosity
RS	Resistant starch
rpm	Revolutions per minute
SEM	Scanning electron microscope
SDS	Slow digested starch
NaHCO <sub>3</sub>	Sodium bicarbonate
NaCl	Sodium chloride
Na <sub>2</sub> HPO <sub>4</sub> • 2H <sub>2</sub> O	Sodium phosphate dibasic dihydrate
Na <sub>2</sub> B <sub>4</sub> O <sub>7</sub> • 10H <sub>2</sub> O	Sodium tetraborate decahydrate
$\phi$	Solid volume fraction
$\phi/\phi_{\max}$	Solid volume fraction to their maximum packing fraction
H <sub>2</sub> SO <sub>4</sub>	Sulfuric acid

Q	Swelling capacity
$\phi_w$	Volume fraction of gelatinised starch
v/v	volume/volume
$A_w$	Water activity
WHC	Water holding capacity
$W_s$	Water in the saturated fibre
S	Water solubility index
w/w	weight/weight
w/v	weight/volume
wwb	Wet weight basis



## LIST OF PUBLICATIONS AND CONFERENCES

Studies completed during candidature, some of which are reported in this thesis, have been published or presented in the following communications:

### Peer-reviewed papers:

Allan K. Hardacre, Roger G. Lentle, Sia-Yen Yap, John A. Monroe. (2018). Predicting the viscosity of digesta from the physical characteristics of particle suspensions using existing rheological models. Manuscript submitted to the Journal of the Royal Society Interface for publication.

Allan, K. Hardacre, Roger, G. Lentle, Sia-Yen, Yap, John, A. Monroe. (2016). Does viscosity or structure govern the rate at which starch granules are digested? *Carbohydrate Polymers*. 136: 667-675.

Allan, K. Hardacre, Sia-Yen, Yap, Roger, G. Lentle, John, A. Monroe. (2015). The effect of fibre and gelatinised starch type on amylolysis and apparent viscosity during *in-vitro* digestion at a physiological shear rate. *Carbohydrate Polymers*. 123:80-88

Allan, K. Hardacre, Sia-Yen, Yap, Roger, G. Lentle, Patrick, W. M. Janssen, John, A. Monroe. (2014). The partitioning of water in aggregates of undigested and digested dietary particles. *Food Chemistry*. 142: 446-454

### Conferences, seminars:

Hardacre, A., Lentle, R., Yap, S. Y., Monroe, J. (2014). Functional fibres: Will they reduce carbohydrate digestion? Conducted oral presentation in NZIFST Annual Conference 2014 (1<sup>st</sup>-3<sup>th</sup> July, 2014), Christchurch, New Zealand.

Yap, S. Y., Hardacre, A., Lentle, R., Monro, J. (2013). Factors affecting the digestibility of starch in an *in-vitro* rheological system. Conducted poster presentation in NZIFST Annual Conference 2013 (2-4<sup>th</sup> July, 2013), Hawke's Bay, New Zealand.

Yap, S. Y., Hardacre, A., Lentle, R., Monro, J. (2012). The partitioning of intraparticulate water in insoluble dietary fiber. Conducted poster presentation in 2012. The Riddet Institute Student Colloquium. (19-21<sup>th</sup> November, 2012), Palmerston North, New Zealand.

Yap, S. Y., Hardacre, A., Lentle, R., Monro, J. (2011). Characterization of the rheological properties of dietary fibers using fructose solutions. Conducted poster presentation in 7<sup>th</sup> Asia Pacific Conference on Clinical Nutrition (5-8<sup>th</sup> June, 2011), Bangkok, Thailand.

Yap, S. Y., Hardacre, A., Lentle, R., Monro, J. (2011). A quantitative exploration of the influence of the solid phase of digesta on its rheological properties and digestibility. Conducted oral presentation in 2011 Riddet Institute Annual conference (4-6<sup>th</sup> July, 2011), Palmerston North, New Zealand.

Yap, S. Y., Hardacre, A., Lentle, R., Monro, J. (2010). The digestion of starchy foods. Conducted oral presentation in the 2010 Riddet Institute Annual conference (10-11<sup>th</sup> June, 2010), Palmerston North, New Zealand.



## **Chapter 1      General introduction**

The addition of dietary fibres into the human diet is one of the steps to help prevent chronic digestive diseases (Lunn & Buttriss, 2007). Dietary fibres are getting increased attention after the announcement of the 2005 Dietary Guidelines for Americans which recommended an increase in the intake of fibre-enriched foods, such as fruits, vegetables, and whole grains (Stephen et al., 2017) as an alternative to processed starchy foods which tend to be low in fibre and protein but contain high levels of saturated fat, salt, and particularly gelatinised starch (Biliaderis, 1991; Monteiro, Levy, Claro, de Castro, & Cannon, 2010).

Diets high in insoluble fibre are associated with a high volume of colonic digesta (Painter & Burkitt, 1971) and reduced the risk of bowel disorders, such as constipation (Cummings, 1984; Taylor, 1990), diverticulitis (Marchand et al., 1997), and in extreme cases, colonic carcinoma (Larsson, Giovannucci, Bergkvist, & Wolk, 2005). Clinical studies reported that inclusions of dietary fibres in diet have dual beneficial health effects, i.e. they reduce the risk of colon cancer and may lower postprandial blood glucose and insulin levels although the mechanism by which this occurs is not clear. Increasing the consumption of insoluble fibres from cereal, grains, wheat bran, vegetable and fruits in diet by two fold, reduced the risk of colorectal cancer by up to 40% in population of European, American, Japan, and Asia multi-ethnic cohort studies (Anderson, Smith, & Gustafson, 1994; Aune et al., 2011; Bingham et al., 2003; Crowe, Appleby, Allen, & Key, 2011; Freudenheim et al., 1990; Giacco et al., 2000; Gonzalez, Riboli, & (EPIC), 2010). In comparison, diets containing high levels of soluble fibres, from gums, barley, oat and psyllium

lead to lower levels of blood glucose and insulin and reduce the risk of type II diabetes (Kendall, Esfahani, & Jenkins, 2010; Maki et al., 2010; Papathanasopoulos & Camilleri, 2010; Schulze et al., 2007).

Dietary fibre is a general term of heterogeneous compounds which usually derived from the cell walls of plants and indigestible in the small intestine (Asp, Johansson, Hallmer, & Siljestrom, 1983; Cummings & Stephen, 2007; Williams, Grant, Gidley, & Mikkelsen, 2017; Yangilar, 2013). Dietary fibre is classified as soluble or insoluble based on its solubility in the aqueous medium of starch digestion in fibre analysis. Typical examples of insoluble fibre are the cellulosic and lignified tissues making up the bulk of structural tissues in plants. This material may have a low fermentability in the colon (Trowell et al., 1976). Soluble fibres are typically the soluble cell wall materials such as pectin,  $\beta$ -glucans, and gums such as guar, xanthan or agar and they may be fully or partially fermented in the colon by the colonic bacteria (Dikeman & Fahey, 2006; Williams et al., 2017).

The benefits associated with insoluble fibre are due to its ability to associate with significant volume of water and hence increase the faecal bulk and promote laxation. Furthermore, insoluble fibres also sequester toxins (Painter & Burkitt, 1971) such as deconjugated bile from colonic digesta (Konstantinov, 2017; Vahouny, Tombes, Cassidy, Kritchevsky, & Gallo, 1980) into voids between the fibre particles. About 60% of insoluble dietary fibres and almost all soluble fibre are degraded by diverse population of colonic bacteria into soluble sugars (Nyman, Asp, Cummings, & Wiggins, 1986) and short chain fatty acids (Cummings, Pomare, Branch, Naylor, & Macfarlane, 1987; Koh, Vadder, Kovatcheva-Datchary, & Bäckhed, 2016).

The ability of dietary fibre to sequester water is expressed as water holding capacity (WHC), which measures the total amount of water retained by the hydrated fibre after centrifugation at 6000 *g* for 15 min (Robertson & Eastwood, 1981b). Reported values of WHC in food fibre (1.4 to 11.0 g water/g pellet) varied with their physico-chemical properties (Heller et al., 1980; Robertson & Eastwood, 1981b) including particle size (Auffret, Ralet, Guillon, Barry, & Thibault, 1994; Li, Mense, Brewer, Lau, & Shi, 2017) the effect of processing methods on fibre matrices (Cadden, 1987) and centrifugation force used to quantify WHC (Chen, Piva, & Labuza, 1984; Parrott & Thrall, 1978).

During digestion, the chemical composition of the gut contents is changed by the removal of proteins, starches and other digestible materials in the small intestine. It is expected that small intestinal digestion rapidly removes a large amount of material from the food, leaving a porous skeleton of fibre. Little work has been carried out that measures changes in WHC and the distribution of water within (intra-particular) and between (extra-particulate) the fibre mass in the colon. Intra-particulate water ( $W_I$ ) is closely associated with the fibre particles and is less active in physiological functions, such as increasing stool volume (Robertson & Eastwood, 1981c) in comparison with the loosely associated extra-particulate water ( $W_E$ ) which is more mobile (Lentle & Janssen, 2008) and is a high proportion (~75%) of stool volume and is available for transport processes in the colon.

Studies reported that inclusion of different fibres in diets (Fuentes-Zaragoza, Riquelme-Navarrete, Sánchez-Zapata, & Pérez-Álvarez, 2010; Parada & Aguilera, 2011; Tudorica, Kuri, & Brennan, 2002) slows the rate of starch digestion. Soluble

fibre, such as guar gum, a typical soluble polysaccharide extracted from the Indian cluster bean (*Cyamopsis tetragonoloba*) is classified as “generally recognised as safe” (GRAS), and being effective in controlling hyperglycaemia by United States Food and Drug Administration (FDA) (Finley et al., 2013). It solubilises in water forming a viscous liquid at a concentration about 0.05% (w/w) and the addition of about 0.4% (w/w) guar gum to foods reduces post-prandial glycaemia in normal and diabetic humans (Ells, Seal, Kettlitz, Bal, & Mathers, 2005; Jenkins, Leeds, Gassull, Cochet, & Alberti, 1977; Jenkins, Marchie, Augustin, Ros, & Kendall, 2004). This has been attributed to increases of the viscosity of digesta (Blackburn & Johnson, 1981) that hinders the rate of glucose absorption or by interfering with amylolysis (Hasinoff, Dreher, & Davey, 1987; Slaughter, Ellis, & Butterworth, 2001).

Unlike soluble fibres, insoluble fibres are thought to be inert and less important in increasing the apparent viscosity ( $\eta$ ) of the whole digesta. As such they receive less attention as methods of reducing the incidence of post-prandial glycaemia (Jenkins et al., 2004; Johansen & Knudsen, 1994). A recent study reported that the digesta is a non-Newtonian, shear thinning suspension (Lentle, Stafford, Kennedy, & Haslett, 2002). After removal of the solid particles from the digesta by centrifugation, the liquid phase of digesta is a Newtonian liquid with a viscosity that is usually similar to water (Bedford & Classen, 1992; Takahashi & Sakata, 2002). Digesta is therefore a two phase system that behaves like a particulate system in which the mobility of the continuous phase is restricted by the concentration of solid particles contained therein.

The viscosity of a suspension increases in direct proportion to the proportion of suspended solid particles. The concentration of solid particles in digesta is typically characterised by dry matter content (DMC) rather than solid volume fraction ( $\phi$ ). However, DMC is simply the ratio of the dry mass of the suspended particles to the total weight of digesta, and the total volume occupied by these particles varies with their densities. Therefore, DMC does not encompass the significance of the interaction of solid particles that occupy the total volume of the suspension and hence the increase of viscosity (Lentle, Stafford, et al., 2007).

The ratio of the viscosity ( $\eta$ ) of a whole suspension containing spherical solid particles of  $\phi$  to the viscosity of the suspending Newtonian liquid ( $\eta_0$ ) is reported as relative viscosity ( $\eta_r$ ). The relationship between  $\eta_r$  and  $\phi$  of spherical solid particles is linear when less than 15% of the total volume of a Newtonian liquid is occupied by spherical hard particles (Einstein, 1906). However,  $\eta_r$  does not always increase linearly with  $\phi$  (Dikeman, Murphy, & Fahey, 2007; Krieger & Dougherty, 1959; Lentle, Hemar, Hall, & Stafford, 2005; Takahashi & Sakata, 2004). Studies on particulate suspensions reported that when spherical solids are suspended in a Newtonian liquid at a concentration of more than  $\phi \geq 0.20$  (20%), the  $\eta_r$  of the suspension becomes increasingly dependent on interactions among the solid particles that restrict the flow of the liquid phase (Stickel & Powell, 2005). Therefore,  $\eta_r$  for a suspension of rigid spherical particles is dependent on the ratio of the volume fraction of solid particles relative to their maximum packing volume fraction,  $\phi/\phi_{\max}$  (Krieger & Dougherty, 1959; Maron & Pierce, 1956) and  $\eta_r$  increases exponentially with  $\phi/\phi_{\max}$ . Such a relationship has also been adapted to model suspensions containing non-spherical solid particles such as fibres by



incorporating a term for aspect ratio (R) into the equation (Brenner, 1974; Pabst, Gregorova, & Berthold, 2006).

The insoluble fibre content contributes to the viscosity of digesta and could contribute to reducing the rate of starch digestion. It seems reasonable that the rate of digestion of solids contained within digesta such as starch could be reduced as the mass transfer of digestate (solutes) is slowed by high concentrations of insoluble fibres, particularly at values of  $\phi > 0.2$ . Possible mechanisms by which fibres delay digestion have been reported, they include trapping glucose molecules into voids within the fibres (Ou, Kwok, Li, & Fu, 2001) and increasing the viscosity of the suspension, slowing the movement of enzymes to and product from the substrate (Braaten et al., 1991; Braaten et al., 1994; Jenkins et al., 1987). Guar gum, at a concentration higher than 0.5% (w/v) also reduced the rate of starch digestion (Blackburn et al., 1984; Wood, Braaten, Scott, Riedel, & Poste, 1990). It has been reported that the molecular structure of Guar is similar to starch polymers and will bind to amylase so inhibiting hydrolysis of starch (Slaughter et al., 2001) and therefore its primary mode of action may be in inhibiting amylolysis and not in increasing viscosity.

Food processing methods such as cooking (Gunaratne, Ranaweera, & Corke, 2007; Noda et al., 2008) gelatinise starch granules, the degree of gelatinisation depending on cooking duration and temperature (Tester, Karkalas, & Qi, 2004). Upon heating to temperatures above 60°C in excess water, starch granules begin to gelatinise and lose their ordered pseudo-crystalline structure; swelling by 10 to 50 times in volume as water binds to the starch molecules. The degree of starch gelatinisation is greatest

when the starch suspension is heated to around 95°C in excess water or when processed dry at temperatures around 120°C (extrusion processing) (Bagley & Christianson, 1982; Bauer & Knorr, 2005; Eliasson, 1986). As the degree of gelatinisation increases the susceptibility to amylolysis also increases (Dona, Pages, Gilbert, & Kuchel, 2010; Holm, Lundquist, Bjorck, Eliasson, & Asp, 1988; Parada & Aguilera, 2009).

The degrees of gelatinisation of starch granules can be characterised by using Differential Scanning Calorimetry (DSC) to identify changes in the ordered starch structure (Baks, Bruins, Master, Janssen, & Boom, 2008; Holm et al., 1988; Parada & Aguilera, 2009); using microscopy to measure the increase of volume of starch granules and the loss of birefringence when observed in polarised light (Liu & Zhao, 1990; López, Rolee, & Meste, 2004); and by using a rheometer or rapid visco-analyser (RVA) to measure the increase of viscosity of starch suspension in water as it is heated (Doublier, 1987; Limpisut & Jindal, 2002; Mishra & Rai, 2006). The degree of starch gelatinisation in aqueous suspensions is proportional to Q (swelling capacity), S (water solubility index) and  $\phi_w$  (volume fraction of water in the hydrated granules) (Bagley & Christianson, 1982; Donovan, 1979).

Apart from the degree to which the food is cooked, physiological limitations in the gut such as the low shear stress that can be generated by the muscle of the gut wall could also reduce the rate of digestion (Hasinoff et al., 1987). Shear stress developed by the gut has rarely been estimated but values up to 1.2 Pa has been reported (Jeffrey, Udaykumar, & Schulze, 2003). The reported viscosity of digesta from animals ranged from 0.2 Pa.s to 28 Pa.s when measured at physiological shear

rates of  $1 \text{ s}^{-1}$  to  $10 \text{ s}^{-1}$  (de Loubens, Lentle, Love, Hulls, & Janssen, 2013; Lentle & Janssen, 2008). Therefore, highly viscous digesta may lead to poor mixing (Lentle et al., 2002) and restrict the accessibility of enzymes to starch. The relationship between shear rate the apparent viscosity of digesta and the rate of starch digestion has not been fully explored. However, assessing this is complicated given that viscosity in human gut varies from person to person, as does the type of food consumed and the segment of gut from which the digesta may be sampled (Dikeman, Murphy, & Fahey, 2007; Lentle, Stafford, et al., 2007). Therefore, *in-vitro* systems are often used to circumvent these difficulties as the results from *in-vitro* studies are reported to be well correlated to *in-vivo* studies ( $R^2 = 0.95$ ) (Germaine et al., 2008; Hur, Lim, Decker, & McClements, 2011; Woolnough, Monro, Brennan, & Bird, 2008; van Kempen, Regmi, Matte, & Zijlstra, 2010; Zhang, Dhital, & Gidley, 2013).

Therefore, the objectives of this research are as follows:

1. To describe the partitioning of water in the undigested and digested insoluble dietary fibre used for this work.
2. To investigate the effects of solid volume fraction of these fibre particles on the viscous properties of digesta and to model viscosity using the Maron-Pierce equation.
3. To investigate and evaluate the effects of a soluble (guar gum) fibre and insoluble fibres on the rate of starch digestion and rate of viscosity reduction using an *in-vitro* system.
4. To investigate and evaluate the effects of food processing parameters (degree of gelatinisation, duration of cooking) and shear rates over the physiological

region on the rate of starch hydrolysis and rate of viscosity reduction during digestion using an *in-vitro* system.

## **Chapter 2      Review of literature**

### **2.1.            Dietary carbohydrate**

Starch and dietary fibre are the two major components of dietary carbohydrates in the human diet. Starches are main storage components in plants and are found in roots, tubers, cereals, legumes, grains and most other plant seeds (Hoover, 2001). Starches can be enzymatically hydrolysed to various soluble forms, usually the sugars (glucose and maltose); although other polysaccharides may also be produced. Dietary fibre is a broad class of dietary carbohydrates composed of the heterogeneous constituents of (usually) the cell walls and other structural components of all plants (Trowell, 1978). Dietary fibre is composed of the insoluble polysaccharides such as cellulose and lignin along with various soluble materials including the hemicelluloses, gums, inulin, pectin, and oligosaccharides usually associated with the cell wall structure although others may be storage compounds (Champ, Langkilde, Brouns, Kettlitz, & Collet, 2003). This class of materials is defined as being undigested in the mammalian small intestine but they may, to various degrees, be fermented in the colon.

#### **2.1.1.            *Definition and classification of dietary fibre***

The definition of dietary fibre has been discussed and revised over the years (Philips, 2013). Some authors define dietary fibres as non-digestible food residues in the small intestine that escape digestion and absorption in the proximal small intestine (Dahm et al., 2010), and others classified the dietary fibres as structural materials in the plant (Trowell et al., 1976) based on the chemical analysis (Zielinski, DeVries, Craig, & Bridges, 2013), which typically includes cellulose,

hemicellulose, lignin, and some associated substances such as waxes, suberin and cutin. Later, the beneficial effect of dietary fibre has been associated with health and is explained by its behaviour in the gastrointestinal tract such as faecal bulking, promoting laxation, and reducing colon cancer (Cummings et al., 1978; Dahm et al., 2010; Dhital, Gidley, & Warren, 2015; Eastwood & Kay, 1979; Murphy et al., 2012). Following these reports, several analytical procedures were developed to classify and quantify different fractions of dietary fibre (Asp et al., 1983; Capuano, 2016; Mongeau & Brassard, 1982; Southgate, Bailey, Collinson, & Walker, 1976).

The international CODEX Alimentarius Commissions of 2009 defines dietary fibre as *“carbohydrate polymers with ten or more monomeric units, which are not hydrolysed by the endogenous enzymes in the small intestine of humans. Dietary fibre consists of one or more of the following categories:*

- (1) edible carbohydrate polymers naturally occurring in the food as consumed;*
- (2) carbohydrate polymers that have been obtained from food raw material by physiological, enzymic, or chemical means and which have been shown to have a physiological effect or benefit to health as demonstrated to competent authorities by generally accepted scientific evidence;*
- (3) synthetic carbohydrate polymers which have been shown to have a physiological effect or benefit to health as demonstrated to competent authorities by generally accepted scientific evidence” (Codex, 2009).*

CODEX also proposed to standardise a method for analysis of dietary fibre, i.e. AOAC method 2009.01|AACC approved method 32-45.01 which is a gravimetric method coupled with HPLC analysis (Zielinski et al., 2013). This method was

further improved and named the AOAC method 2011.25|AACC approved method 32-50.01 to discriminate between soluble and insoluble dietary fibres and is recommended for analysis of fruits which contain high levels of fructans (Tobaruela et al., 2018). To date, these methods are the most inclusive methods of analysis for DF even though not absolutely comprehensive (Zielinski et al., 2013).

Despite there being many classifications of dietary fibres used, each of them is focused on the properties of dietary fibre in the diet that relate to the health benefits, either the naturally occurring in food or those added in as food ingredients (Capuano, 2016; Dhital et al., 2015). In this thesis, classification of dietary fibres is focused on their solubility in water (Dikeman & Fahey, 2006; Foschia, Peressini, Sensidoni, & Brennan, 2013), and fermentability in the colon (Li & Uppal, 2010). The solubility and fermentability of dietary fibres affects their hydration properties and their viscosity in suspension. These are important parameters affecting the rate of digestion and absorption in the gut (Grundy et al., 2016; Guillon & Champ, 2000).

Water insoluble dietary fibres including cellulose, hemicellulose, and lignin are partially fermented by microorganisms in the colon albeit at a slower rate than soluble fibres (Fredstrom, Lampe, Jung, & Slavin, 1994); while water soluble fibre including pectin, gums, and mucilages may contribute to the viscosity of the continuous phase in the small intestine they are fermented in the colon and with time will contribute less and less to the viscosity of the continuous phase of digesta in the colon (Harris & Ferguson, 1993).

The analytical methods used to fractionate dietary fibres into water soluble and insoluble fractions are broadly based on non-enzymatic gravimetric and enzymatic gravimetric methods. Non-enzymatic-gravimetric methods were adopted from the analysis of the constituents of animal forages using the combination of strong acid, alkalis, and solvents (Southgate, 1969). Increasing evidence shows that the presence of a significant proportion of the non-digestible non-starch polysaccharide (NSP's) in foods are fermentable by colonic microbes to produce short chain fatty acids (Topping & Clifton, 2001) and these fatty acids can reduce the colon cancer (Burkitt, Walker, & Painter, 1972). The non-enzymatic-gravimetric method does not recover a significant proportion of total dietary fibre, including the soluble fibres. Therefore, an enzymatic method was developed to accurately quantify the total dietary fibre (soluble and insoluble fibre) in foods (Asp et al., 1983; Englyst, Kingman, & Cummings, 1992; Furda, 1977).

Briefly, the enzymatic method simulates *in-vivo* digestion by adding enzymes in sequence; pepsins in an acid environment for the gastric phase and following buffering to pH 6.5, amylase and trypsin to simulate digestion in the small intestine (Robertson & van Soest, 1981; Southgate, 1976; Trowell, 1978). This sequence emulsified fats and hydrolysed most starch, and proteins after which the soluble and insoluble dietary fibre remained (Figure 2.1) (Asp et al., 1983). This method is convenient, accurate, and reproducible, hence it has been adopted by AOAC (method 985.29, 1995) (AOAC, 1995).



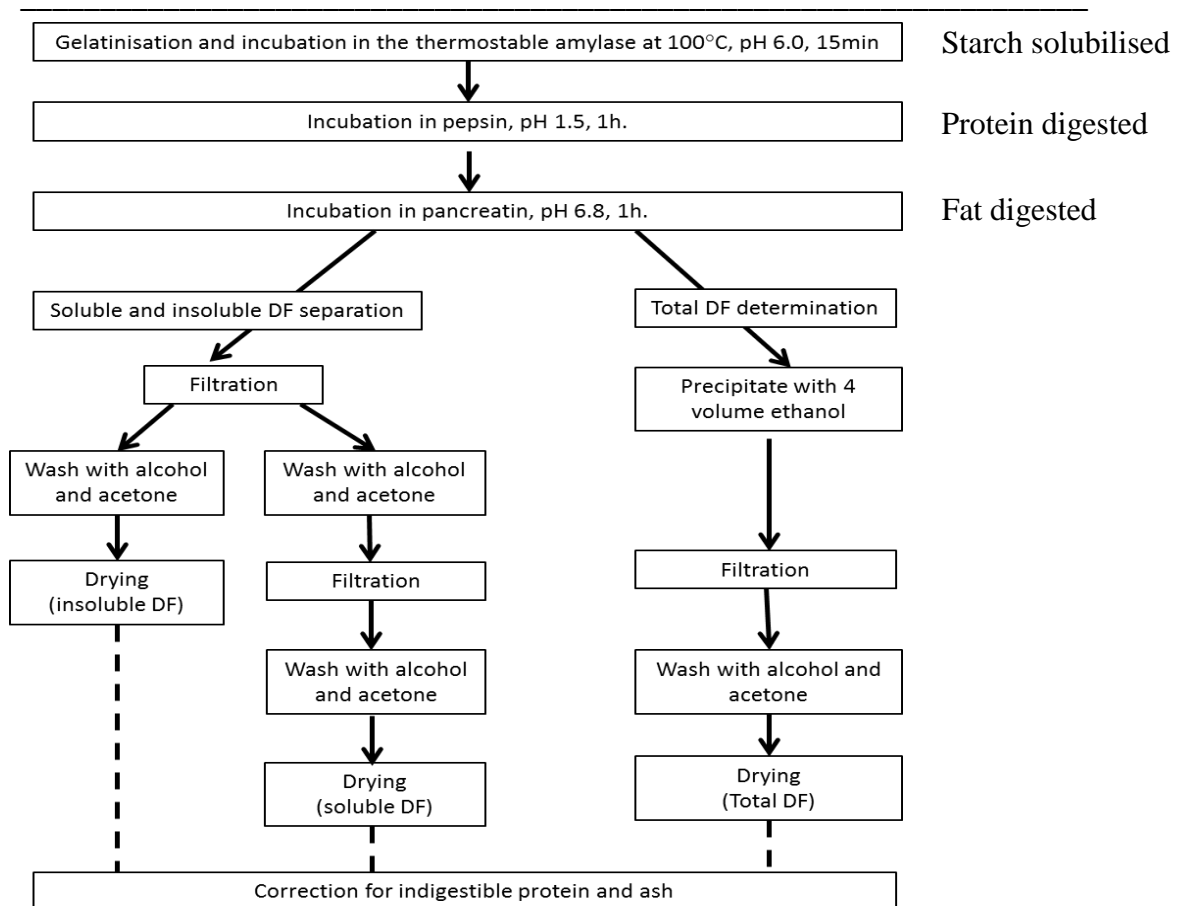


**Figure 2.1: Analytical methodology for quantitatively assessing the components of dietary fibre (Asp et al., 1983).**

The presence of large amounts of insoluble dietary fibre in the colon is typically associated with faecal bulking and laxation (Burkitt et al., 1972; Lovegrove et al., 2015), (American Dietetic Association, 2008; Murphy et al., 2012). The consumption of soluble dietary fibre may result in reductions in levels of post-prandial blood glucose, insulin, and LDL cholesterol which may occur in both healthy adults and adults with diabetes (Jenkins et al., 2004; Weickert & Pfeiffer, 2008). However, there are exceptions to this simple distinction between the physiological effects of dietary fibre, as some insoluble fibres, such as crystalline cellulose powder do not absorb water and do not promote laxation (Cummings et al., 1978; Nyman & Asp, 1982; Takahashi, 2010). Oat fibre contains soluble and

insoluble fractions which absorb large quantities of water and is effective in reducing post-prandial glycemia and in promoting laxation (Khan et al., 2017; Sturtzel & Elmadfa, 2008).

### **2.1.2.        *Sources of dietary fibre***

The proportion of soluble and insoluble components of dietary fibre in the diet varies according to the types of food consumed (Harris & Ferguson, 1993). Insoluble dietary fibre comprises mostly the cellulosic cell wall components (Davidson & McDonald, 1998), and is abundant in whole vegetables and fruits (Harris & Ferguson, 1993), nuts and in grains (Table 2.1) (Dhingra, Michael, Rajput, & Patil, 2012; Theander, Westerlund, Aman, & Graham, 1989).

All fibre from food sources includes soluble and insoluble portions (Table 2.1). The amount of fibre and its soluble and insoluble proportions depends on processing methods and the part of the plant from which dietary fibre is extracted (Selvendran, 1984). The proportion of fibre is relatively poor in fresh foods such as tomatoes, apple, and banana (Table 2.1), but the proportion is high on a dry weight basis, and fresh fruits and vegetables are an important source of fibre in the diet (Tobaruela et al., 2018).

**Table 2.1: The dietary fibre content in some common food sources (g/100g edible portion) analysed using AOAC method (adapted from (Dreher, 1999; Hollmann, Themeier, Neese, & Lindhauer, 2013; Li, Andrews, & Pehrsson, 2002; Menkovska et al., 2017)).**

Types of food	Fibre content (g/100g on an “as consumed basis”)		
	Total fibre	Insoluble	Soluble
<i>Fruits</i>			
Apple (with skin, raw and ripe)	2.21	1.54	0.67
Bananas (raw, ripe)	1.79	1.21	0.58
Mango (raw, ripe)	1.76	1.08	0.69
Oranges (raw, ripe)	2.35	0.99	1.37
Pineapple (raw, ripe)	1.46	1.42	0.04
Beans (microwaved)	4.31	2.93	1.38
Broccoli (microwaved)	4.66	2.81	1.85
Carrot (microwaved)	3.87	2.29	1.58
Chick peas (canned)	6.19	5.79	0.41
Peas (microwaved)	3.54	2.61	0.94
Peas (canned)	4.50	3.60	0.90
Peas (boiled)	6.70	5.00	1.70
Potato (fried)	4.11	3.44	0.67
Potato (boiled)	1.30	1.00	0.30
Red kidney beans (canned)	7.13	5.77	1.36
<i>Vegetables, raw</i>			
Broccoli (raw)	3.50	3.06	0.44
Cabbage (raw)	2.24	1.79	0.46
Carrots (raw)	2.88	2.39	0.49
Cauliflower (raw)	2.62	2.15	0.47
Corn (raw)	10.8	0.9	6.6
Lettuce (iceberg, raw)	0.98	0.88	0.10
Tomatoes (raw)	1.20	0.80	0.40
Spinach (raw)	3.20	2.43	0.77
<i>Cereals</i>			
Barley bran	70.0	67.0	3.0
Barley-hulled	58.7	50.6	8.1
Oats-hulled	22.2	11.7	10.5
Millet	16.13	15.94	0.19
Plain corn flakes	2.0	1.7	0.3
Oat short bread	5.2	3.3	1.9
White sourdough bread	1.9	1.3	0.6
Whole wheat sourdough bread	8.1	7.0	1.1
Wheat bran (breakfast cereals)	35.3	32.8	2.5
Wheat flakes	11.4	9.6	1.8
Wheat wholemeal toast	7.2	5.8	1.4

Insoluble fibre is consumed as a component of fresh or cooked vegetables, nuts, and fruit or it may be extracted from various sources and added to bakery, confectionary, or breakfast cereal products (Foschia et al., 2013; Parada & Aguilera, 2011). Soluble fibre is found and extracted from fruit, vegetables, seaweed, legumes and beans, seeds (psyllium husk), locust beans (guar gum), tree sap (gum arabic), bacteria (xanthan gum), bulbs (konjac gluco-mannan), and fruit and vegetable peels (pectin) (Dhingra et al., 2012; Marlett, McBurney, & Slavin, 2002).

### 2.1.3. *Chemical compositions of dietary fibre*

Fibre as part of the plant cell wall components is generally made from a few main polysaccharides, including the pentoses (arabinose and xylose), the hexoses (glucose, galactose and mannose), the 6-deoxyhexoses (rhamnose and fucose), and the uronic acids (glucuronic and galacturonic acids) (Table 2.2) (Theander et al., 1989). These components play different roles in the human diet based on their fermentability and hydration properties (Section 2.1.4 and 2.1.5.).

**Table 2.2: Proximate composition (%) of dietary fibre isolated from plant cell wall analysed using methods adapted from (Englyst, 1989; Holloway & Greig, 1984).**

Compounds / Sources	Xylose	Mannose	Arabinose	Glucose	Galactose	Rhamnose	Uronic acid
Wheat bran	60.1	0.3	31.9	4.0	12.2	0.0	0.7
Pear	19.8	3.8	17.2	27.7	13.4	1.6	8.3
Cabbage	18.0	7.5	14.3	23.0	31.4	1.8	17.0
Beans	22.0	4.1	2.0	15.7	12.3	1.0	14.4
Lettuce	23.3	8.2	19.7	0.0	0.0	1.6	24.9
Peach	18.3	4.2	9.4	19.6	11.9	1.8	9.5
Pumpkin	14.2	15.5	0.0	7.2	32.7	0.0	12.5
Tomato	27.0	12.1	3.7	31.9	6.9	0.0	9.3
Cellulose	0.0	0.0	0.0	100.0	0.0	0.0	0.0

### 2.1.3.1. Insoluble dietary fibre

Insoluble fibre is largely composed of cellulose, hemicellulose (Saha, 2003), and lignin (Vanholme, Demedts, Morreel, Ralph, & Boerjan, 2010) and forms the main structural material of the plant and its various organs. Cellulose is homopolymeric, consisting of beta-glucan molecules linked by beta-glycosidic bonds (Figure 2.2), arranged tightly to give the highly ordered skeleton of cellulose microfibrils (Taiz & Zeiger, 2002; Takahashi, 2010). It is not water soluble and its hydration is largely limited to a small proportion of water held in spaces between the fibrils (Knudsen, 2001).

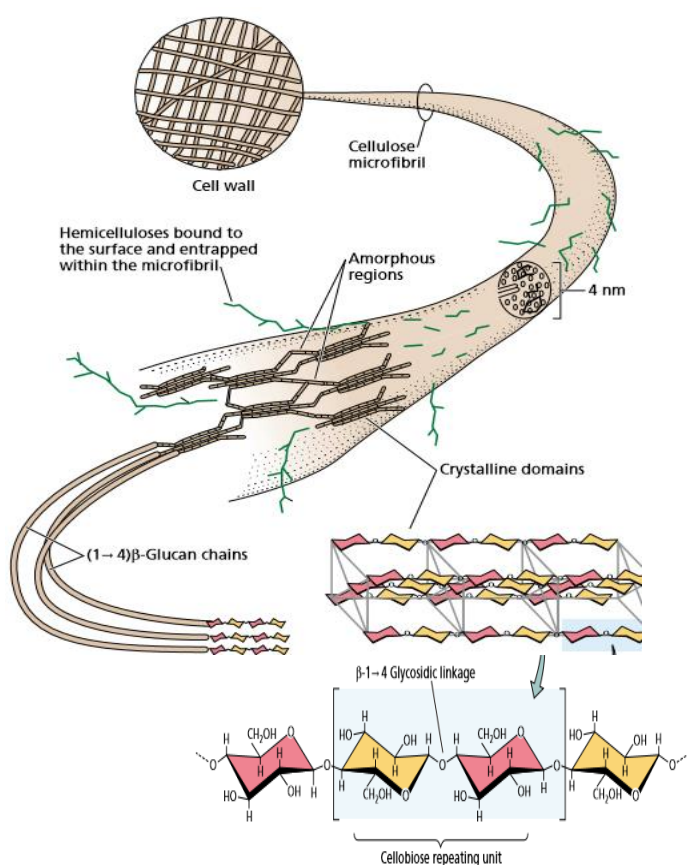


**Figure 2:2:** Structural model of a cellulose microfibril. The microfibril has homopolymeric regions of high crystallinity intermixed with less organised heteropolymeric amorphous regions (adapted from Taiz & Zeiger, 2002).

Hemicellulose is heteropolymeric, consisting of arabinoxylans such as xylan, galactan, or mannan which are linked by beta-glycosidic bonds with side chains of galactose or arabinose (Theander et al., 1989), resulting in a less ordered structure which hydrates and hydrolyses to a much greater extent than homopolymeric cellulose (Knudsen, 2001).

Lignin is a branched phenolic polymer made of three major phenylpropanoid units, namely p-hydroxyphenyl, guaiacyl, and syringyl (Boerjan, Ralph, & Baucher, 2003; Pouteau, Dole, Cathala, Averous, & Boquillon, 2003). Lignin is deposited between cellulosic and non-cellulosic polysaccharides in the cell wall, and anchors to the rigid cellulose microfibrils and other matrix polysaccharides, so providing mechanical support for cell walls (Knudsen, 2001). The ordered beta-glucan molecules linked by beta-glycosidic bonds of insoluble fibres are less accessible to alpha-amylase and thus may lower the rate of amylolysis (Grundy et al., 2016).

#### **2.1.3.2. Soluble dietary fibre**

Soluble fibre polymers, such as guar gum, pectin, or agar normally consist of various polymerised combinations of furanose and pyranose sugars such as galacturonic acid, rhamnose, mannose, xylose, and galactose molecules (Becker, Hill, & Mitchell, 2001; Elleuch et al., 2011; Oechslein, Lutz, & Amado, 2003). For example, the backbone of guar is composed of galactose and mannose residues in a ratio of 1:1.5 (Mikkonen et al., 2007). These mannose molecules are linked by beta-D-(1,4)-mannans and galactose sub-units linked to mannose C-6 sites by alpha (1→6)-alpha-D-galactopyranosyl groups (McCleary, Clark, Dea, & Rees, 1985). Inulin, extracted from chicory roots, is a fructose polymer joined by beta-(1,2) bonds

to glucose; while psyllium, derived from ispaghula husks, is a polymer of arabinoxylans with beta-(1,4) and alpha-(1,3) linkages (Chawla & Patil, 2010). Xyloglucans in the structure act as lubricating agents and prevent the aggregation of excess cellulose in the cell wall (Figure 2.3) (Carpita & Gibeaut, 1993; Cosgrove, 2005), so maintaining its flexibility.

Various (1–3,1–4)-beta-D-glucan linkages found in the cell wall of oat and other soluble fibres are indigestible by amyloglucosidase secreted in the small intestine and thus substituting these fibres in starchy food have been related to lowering the fasting blood cholesterol concentrations and postprandial glycaemia (Wang & Ellis, 2014). High molecular weight oat  $\beta$ -glucan that solubilises in the small intestine increases the intra-luminal viscosity compared to its low molecular weight counterpart and may delay the rate of amylolysis (Grundy et al., 2016; Regand, Chowdhury, Tosh, Wolever, & Wood, 2011).

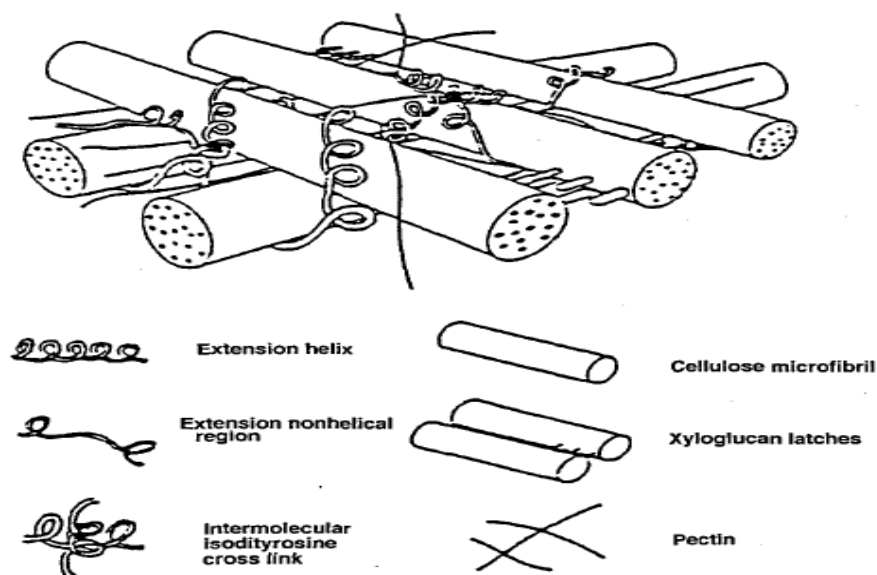


**Figure 2.3:** Three dimensional view of the arrangement of plant cell wall polymers that made up of insoluble and soluble fibres (adapted from Thakur, Singh, Handa, & Rao, 1997).

#### **2.1.4.        *Fermentability of dietary fibre***

Fibres are either partially or totally fermented in the colon (Foschia et al., 2013) by colonic bacteria. The fermentability of fibre in the colon is high when the cell wall fibre matrix consists of polysaccharides of short chain length that are not highly ordered (Grundy et al., 2016; Takahashi, 2010). For instance, highly ordered microfibrils such as crystalline cellulose (Solka Floc® ) are about 10% hydrolysed in the colon (Slavin, Brauer, & Marlett, 1981) compared to hemicellulose and pectin that have less ordered structure and, which are more than 50% hydrolysed by colonic bacteria (Hillman, Peters, Fisher, & Pomare, 1986; Slavin et al., 1981). Similar findings were recorded from a clinical study using high fibre diets containing fruit and vegetables, approximately 88% of hemicelluloses were degraded compared with only 42% of cellulose and 18% lignin (Kelsay, Goering, Behall, & Elizabeth, 1981).

Soluble fibre, such as guar, is almost completely fermented in the colon. As a result when added to rat diet at 100g/kg (Nyman & Asp, 1982) faecal bulking was poor compared with wheat bran added at the same concentration (w/w) (Jacobs & Lupton, 1986). Comparing the fermentability of insoluble fibre (hemicellulose) to soluble fibres (pectin, fruit and vegetables) showed that the latter was more fermentable and consequently the water holding capacity reduced by 26% (Chudzikowski, 1971; Cummings, 2001; Stephen & Cummings, 1979).

#### **2.1.5.        *Hydration properties of insoluble fibres***

The benefits of insoluble fibre are associated with their hydration properties which are generally measured in terms of their water holding capacity (WHC) (Robertson



& Eastwood, 1981b; Zhao et al., 2018). The WHC of insoluble fibre is the mass proportion of water retained by the fully hydrated fibre (Robertson & Eastwood, 1981b) following centrifugation at a given gravity force ( $g$ ) levels (Chen et al., 1984; Parrott & Thrall, 1978). The  $g$  force used to assess the hydration level varies from 2,000  $g$  for 10 min (Mongeau & Brassard, 1982) to 6000  $g$  for 15 min (Eastwood, Robertson, Brydon, & MacDonald, 1983) and up to 14,000  $g$  for 1 h (Cadden, 1987) has been used for human faecal material.

In most human clinical studies, 6000  $g$  to 8000  $g$  for 15 to 30 min are used for WHC measurements (Eastwood et al., 1983). The higher  $g$  force forces more water from voids between particles and reduces variation in WHC measurements due to better packing of the particles (Eastwood et al., 1983). The high  $g$  force used to measure WHC is far greater than the pressure exerted by the gut wall.

#### **2.1.5.1. Factors affecting WHC**

The WHC of insoluble fibre decreases with particle size (Cadden, 1987; Li et al., 2017; Robertson et al., 2000) as does the porosity of the cell wall of these particles following digestion or mechanical grinding (Auffret et al., 1994; Cadden, 1987; Cummings, 2001; Holloway & Greig, 1984; Juntunen et al., 2003; Slavin et al., 1981; Stephen & Cummings, 1979). The high porosity of fibre particles is usually associated with a higher proportion of hemicellulose or larger sized particles and, as a consequence, either of these two factors lead to a lower particle density (Mwaikambo & Ansell, 2001; Sacilik, Ozturk, & Keskin, 2003; Sangnark & Noomhorm, 2004; Walker, 2006). As particle density decreases it is expected that

the larger particles would have greater void volumes within and between them and hence greater water holding capacity (Sacilik et al., 2003).

#### **2.1.5.1.1. Chemical composition and WHC**

Generally, insoluble dietary fibres are supplied in a dry form. They absorb between 4 to 8 times their dry mass of water (Hillman, Peters, Fisher, & Pomare, 1983) and swell by between 4% and 12% of their original volume (Auffret et al., 1994) when fully hydrated. The WHC of insoluble dietary fibres that contain lignin and cellulose is low compared to plant cell wall fractions that contain hemicellulose. The hydrophobic nature of lignin (Eastwood, 1973), and highly ordered crystalline structure in cellulose (Takahashi, 2010) result in lower WHC compared to hemicellulose which is comprised of heterogeneous polymers with a less organised molecular arrangement (Chen et al., 1984; Holloway & Greig, 1984; Saha, 2003).

Generally lignin and celluloses have lower WHC than hemicellulose, yet studies examining WHC in different fibre types with similar chemical compositions reported that WHC is more closely associated with structure than chemical composition (Robertson & Eastwood, 1981b). This may be due the fact that WHC measured by centrifugation does not distinguish between the proportions of water entrapped within the fibres (intra-particulate water,  $W_I$ ) and water either bound to the surface of fibres or trapped in voids between the fibres (extra-particulate water,  $W_E$ ) (Eastwood & Morris, 1992). There is a lack of research that quantifies the volume of water held in the intra- and extra-particulate regions (Cadden, 1987).

The manner in which water molecules are held in dietary fibre determines its ability to alter stool weight (Cummings et al., 1978; Eastwood, Anderson, Mitchell, Robertson, & Pocock, 1976) and sequester soluble toxins such as deconjugated bile acids (Li et al., 2017; Story & Kritchevsky, 1976; Zacherl, Eisner, & Engel, 2011). The  $W_E$  is more mobile and can be used as a mass transport medium for solutes in the digesta.  $W_I$  is less mobile because it is constricted in closed or near closed spaces within the matrix of the fibres (Robertson & Eastwood, 1981c). Microcrystalline cellulose has been shown to retain water in the intra-particulate voids against high osmotic pressure deficit as high as 380 mosm/kg (Cadden, 1987).

#### **2.1.5.1.2. Particle sizes, processing methods and health benefits**

In the food industry, insoluble fibre extracted from plants is available in various particle size grades. The hydration properties of insoluble fibre decrease with their particle size. Generally, but not always larger fibre particles have higher WHC than smaller particles when their chemical properties are similar (Boulos, Greenfield, & Wills, 2000; Li et al., 2017; Raghavendra, Rastogi, Raghavarao, & Tharanathan, 2004; Sanchez-Alonso, Haji-Maleki, & Borderias, 2006).

Insoluble fibre is ground to reduce particle size and this process may collapse cell-walls concomitantly reducing ( $p < 0.05$ ) WHC (Table 2.3). For instance, the WHC of wheat bran fibres with a median size of 1000  $\mu\text{m}$  was 7.00 g/g and this decreased by 60% when the particle size was reduced to 200  $\mu\text{m}$  (Table 2.3).

**Table 2.3: Hydration properties of various fibre types with different particle sizes.**

Types of fibre	Particle size (µm)	WHC (g water/g pellet)	Reference
Citrus	139	10.7	(Robertson et al., 2000)
	235	8.60	(Auffret et al., 1994)
	540	10.4	(Auffret et al., 1994)
Apple	133	5.4	(Robertson et al., 2000)
Cabbage	485	20.7	(Wrick et al., 1983)
Wheat bran	200	2.82	(Li et al., 2017)
	320	3.00	(Auffret et al., 1994)
	500	3.06	(Li et al., 2017)
	900	6.80	(Auffret et al., 1994)
	1000	7.00	(Renard, Crepeau, & Thibault, 1994)
Bran	173	2.70	(Wrick et al., 1983)
	500	3.90	(Brodribb & Groves, 1978)
	744	3.50	(Wrick et al., 1983)
	>1500	7.30	(Brodribb & Groves, 1978)
Cellulose	143	1.40	(Wrick et al., 1983)

Human studies reported that a diet containing an additional 20 grams coarse bran significantly increased ( $p < 0.01$ ) stool weight and the total faecal water content compared with a diet containing 20 grams of fine bran, despite the fact that the chemical composition of fibres was similar (Brodribb & Groves, 1978; Heller et al., 1980; Wrick et al., 1983). These results further affirmed that particles of coarse dietary fibre hold more water than fine particles.

The WHC of dietary fibre is reduced when fibres are heat treated as the drying process collapses their cell wall matrices (Hill, Norton, & Newman, 2008; Raghavendra et al., 2004; Robertson & Eastwood, 1981b). For example, one gram of 'as supplied' potato fibre contained 23.6 g water when hydrated but this reduced to only 10.3 g when the fibres was air dried at 60°C before hydration (Robertson & Eastwood, 1981b); a similar effect was noted for cauliflower fibre (Femenia, Selvendran, Ring, & Robertson, 1999).

## 2.2. Starch granules

Most starch granules are synthesised in chloroplasts and stored in organelles known as amyloplasts (Pérez & Bertoft, 2010). Starch granules are densely packed in a semi-crystalline structure with density of about  $1.5 \text{ g/cm}^3$ . The granules occur in various shapes and sizes depend on their botanical origin (Table 2.4) and the differences in these morphologies can be identified using microscopy (Park, Xu, & Seetharaman, 2011; Schirmer, Höchstötter, Jekle, Arendt, & Becker, 2013).

### 2.2.1. The size and shape of starch granules

The size and shape of starch granules vary considerably with botanical origin (Table 2.4). Generally, potato granules are larger whereas the wheat granules are smaller.

**Table 2.4: Shapes and sizes of starch granules from different botanical origin.**

Origin of starch granules	Shape	Size ( $\mu\text{m}$ )	References
Potato	oval	15-75	(Tester et al., 2004)
Corn	spherical to polyhedral	5-20	(Tester, 1997)
Rice	polygonal	2-10	(Lindeboom, Chang, & Tylera, 2004)
Large wheat	lenticular	10-35	(Veendam, 1985)
Small wheat	lenticular	2-4	(Pérez & Bertoft, 2010)
Cassava	round	7-24	(Peroni, Rocha, & Franco, 2006)
Yam/ Taro	elliptical	7-47	(Peroni et al., 2006)

### 2.2.2. Amylose and amylopectin

Starch granules are composed of two major chemical components, namely amylose and amylopectin (Schirmer et al., 2013; Tester et al., 2004). Amylose is a primarily

linear polymer, typically containing 500-600 glucose residues (Gallant, Bouchet, Buléon, & Pérez, 1992) linked by alpha-1,4 glycosidic bonds and making up of 15 – 35% of the granule weight, although larger amylose chains may have up to more than ten alpha-1,6 glycosidic branches (Pérez & Bertoft, 2010; Vamadevan & Bertoft, 2015). Amylopectin is a highly branched molecule composed of shorter linear polymers of glucose residues linked by alpha-1,4 glycosidic bonds with alpha-1,6 linked branches at an average of every 20-25 glucose residues (Parker & Ring, 2001) (Figure 2.4).

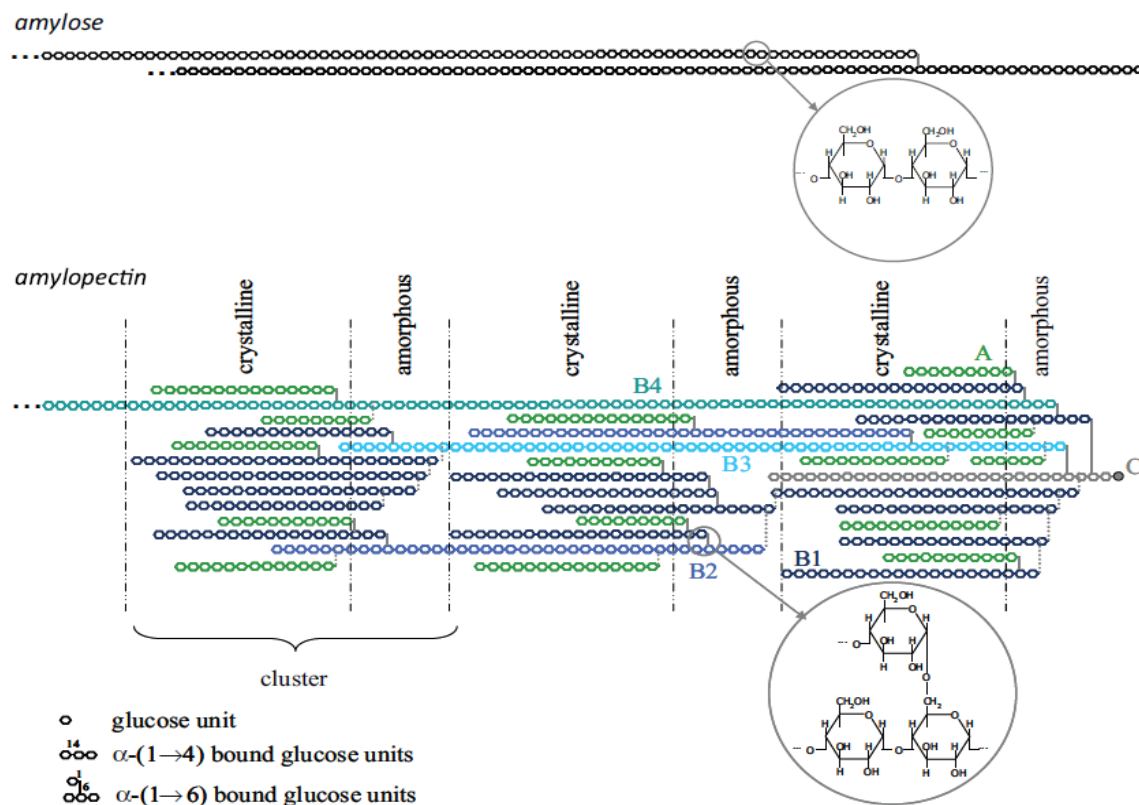


**Figure 2.4:** Basic structure of the main starch polymers: the quasi-linear amylose (above) and highly branched amylopectin (below) (adapted from Delcour et al., 2010).

Amylose in solution crystallises readily and the left-handed double helical chains pack in a parallel fashion forming either A- or B-type allomorphs (Imberty, Buléon,

Tran, & Pérez, 1991). The A-type allomorph crystals have a unit cell in a monoclinic closely packed structure which can accommodate 8 water molecules between each double helix; whereas the B-type allomorph crystals form a unit including a hexagonal space which can include up to 36 water molecules (Popov et al., 2009). The V-type allomorphs are single helices formed after retrogradation of the gelatinised starch granules and may contain lipid or protein in the lumen of the helices (Vamadevan & Bertoft, 2015).

The molecular arrangement of amylopectin is more complex than amylose, the degree of polymerisation (DP) ranges from 4800 and 15900. The average chain lengths (CL) of amylopectin are proportioned among short chain length of 6-36 and long chain length of more than polymers. The A chains consist of amylopectin with chain lengths of 19-28 (Figure 2.4) are the outermost chains and do not carry other chains, whereas B chains are chains that branch from the C chains and give rise to the A chains (Hizukuri, 1986). The A chains are linked to B chains with alpha-1,6-glycosidic bonds. The B chains can be subdivided into B1 (CL 13-24), B2 (CL 25-36), B3 (CL>37) chains, and the longest B4 (CL 110-119) chain (Hanashiro, Abe, & Hizukuri, 1996; Hizukuri, 1986). The single C chain that give rise to the B chains carry the only reducing moiety on the starch molecule (Eliasson & Gudmundsson, 1996) (Figure 2.4).

To understand the complex organisation and architecture of amylopectin, two models have been proposed, namely, the “cluster” model (Robin, Mercier, Charbonnière, & Guilbot, 1974) and the “building block backbone” model (Bertoft, 2013). The cluster model suggests that short chains (either A- or B-types) are

mostly organised into clusters in the pseudo-crystalline region which is about 5-7 nm thick; whereas the longer B and C chains are interconnected and form the amorphous lamellae region with thickness of 2-4 nm (Figure 2.5) (Jacobs & Delcour, 1998; Tester et al., 2004; Vamadevan & Bertoft, 2015). A study using  $\alpha$ -amylase from *Bacillus amyloliquefaciens* to isolate clusters of amylopectin from 20 different starches reported that the ratio of short to long chains varied from 1:5 to 1:20 (Bertoft, 2007).

The building block backbone model suggested that the clusters are made up of chains with a DP of 10 or more internal chain length of 1-3 residues (Bertoft, Koch, & Aman, 2012). The blocks inside the clusters are separated by segments with an average inter-block chain length of 5-8 residues and the inter-cluster segment has an average DP of 14 residues. These models suggest that the long amylopectin chains are spread out either side of the backbone, while the short chains are included within the block structures where they are interconnected, or serve as the branches to the backbone (Figure 2.5).



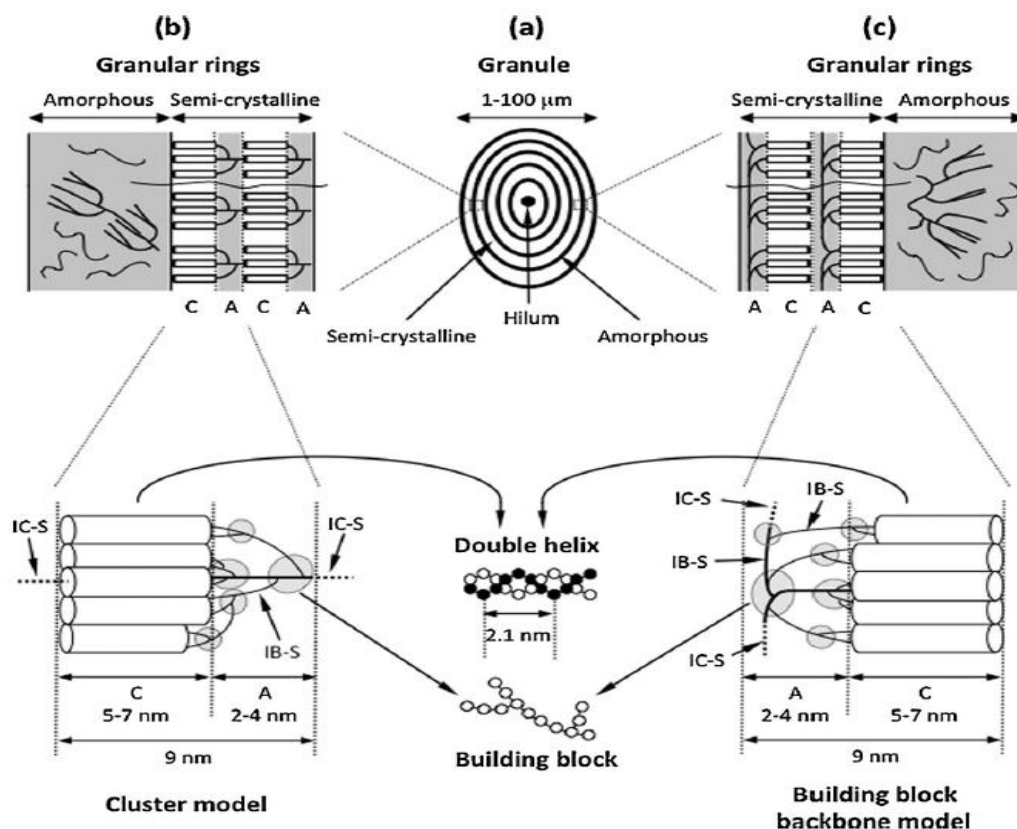


**Figure 2.5:** From starch granules to building blocks; a schematic showing organization of the unit chains in amylopectin illustrated according to the cluster model and the building block backbone model. (a) the granule consisting of alternating ring with a hilum region, normally considered as amorphous and centred to their middle. (b) The principal arrangement of the semi-crystalline rings according to the cluster structure of amylopectin. (c) The principal arrangement of the semi-crystalline rings according to the building block backbone structure of amylopectin. The structure of the amorphous rings is not established, but consists of amylose as well as amylopectin. The semi-crystalline rings consist of alternating crystalline (C) and amorphous (A) lamellae, which are enlarged in the lower figures. The details of double helices (cylinders) and building blocks (encircled) are depicted in the centre lower figure (circles depict glucose residues). Inter-block segments (IBS) and inter-cluster segments (ICS) are indicated and are found in both models, but the principal unit in (b) is the cluster and in (c) is the much smaller and more tightly branched building block. Note that a major difference between the models is that in (b) the amylopectin molecules penetrate the stacks of lamellae, whereas in (c) the AP molecules do not penetrate the stacks. The blocklets or super helices of AP are not shown, but are supposed to be structures in between the granular rings and the molecular levels (adapted from Vamadevan & Bertoft, 2015).

The ratio of amylose to amylopectin varies with the botanical species, but typically is around 3:7 for normal unmodified starch (Morrison, Tester, Snape, Law, & Gidley, 1993; Pérez & Bertoft, 2010). The most common method used to assess the amylose content relies on the affinity of amylose to bind to the iodine solution and the intensity of dark blue colour formed from the amylose-iodine complex (Knutson & Grove, 1994). Results derived from this method are often affected by the presence of lipid-protein complexes which do not bind to iodine solution, and the branched amylopectin molecules which bind to iodine solution (Chrastil, 1987; Knutson & Grove, 1994). The enzymatic debranching method, which used enzymes to hydrolyse the branching molecules in these polymers and produce various sub-fractions with different molecular weights that are then analysed using liquid chromatography, was found to be more accurate (Gérard, Planchot, Colonna, & Bertoft, 2000).

Waxy starch, a natural mutation contains less than 1% of amylose (Kim & Huber, 2010) whilst another natural mutation, high amylose starch, may contain more than 70% amylose (Tester et al., 2004). Amylose and amylopectin have different functional properties. High amylose starch promotes retrogradation, and forms tough gels and hard doughs (Gujral, Haros, & Rosell, 2004) due to the linear molecular arrangement (Jacobson, Obanni, & BeMiller, 1997), whereas amylopectin disperses in water, forms soft gels and weak films (Klucinec & Thompson, 2002; Ortega-Ojeda, Larsson, & Eliasson, 2004).

### **2.2.3.        *Other minor components***

Other minor components that occur in starch granules, such as lipid and protein, are also important in determining the functional properties of starch and their digestibility. Cereal starches (corn, wheat, rice, sorghum) normally contain ~0.6% to >1% of lipids in the form of lysophospholipid and free fatty acids, and the lipid content increases with the amylose content and these complexes less accessible by amylase (Morrison, 1988; Morrison et al., 1993; Tester & Morrison, 1990). Lipids associated with small amounts of protein (~0.5%) form lipid-protein complexes on the surface of corn granules (Buléon, Colonna, Planchot, & Ball, 1998), but are negligible in potato granules. Phosphorus at trace amounts (0.06% to 0.1%) may be present in potato (Hoover, 2001), but there is very little (<0.05%) present in corn (Mishra & Rai, 2006).

### **2.2.4.        *The structure of starch granules***

Starch granules are semi-crystalline, amylose and amylopectin polymers are organised in concentric structures with alternating pseudo-crystalline (ordered part) and amorphous lamellae into the rings that known as “growth ring”, based on the microscopic observation (Baker, Miles, & Helbert, 2001). Generally, the most acceptable concept used to explain the “growth ring” is the pseudo-crystalline lamellae are predominantly composed of shorter chain amylopectin polymers, organised into double helices and is known as the crystalline lamellae; whereas the amorphous ring is predominated by amylose molecules (Figure 2.6) (Hizukuri, 1986; Pan & Jane, 2000).

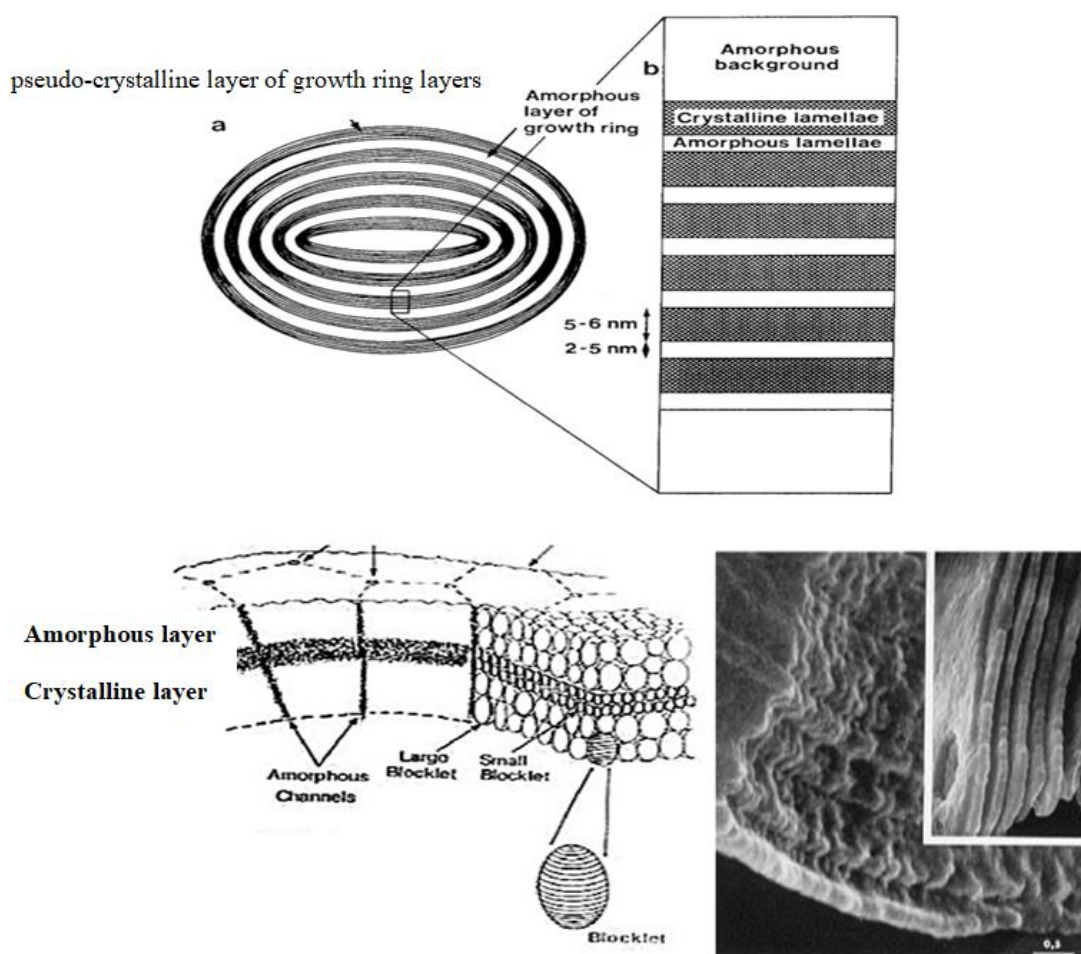


**Figure 2.6:** Schematic diagram of starch granule structure (a) a single granule with alternating amorphous and pseudo-crystalline layers; (b) expanded view alternating crystalline and amorphous lamellae in the pseudo-crystalline layers (adapted from Jenkins et al., 1994); (c) blocklet structure in association with amorphous radial channels. Blocklet size is smaller in the semi-crystalline layer than in the crystalline layer; (d) Scanning electron micrographs of starch granules after  $\alpha$ -amylolysis showing the occurrence of spherical blocklet-like structures (adapted from Gallant et al., 1992).

The cereal starch granules (e.g. corn) have shorter chains in the pseudo-crystalline regions (<20 glucose subunits) and are arranged into a relatively compact hexagonal close packing array and are categorised as A-type allomorph crystals (same as the crystal structures described for amylose). In contrast, tuber starches, root starches, high AM cereal starches, and retrograded starches have longer chains that give a more open helical structure arrangement in the pseudo-crystalline regions having

type B allomorph crystals (Hoover, 2001; Jane, 2006). Based on differences in packing of the AP double helices, several crystal types are distinguished (Buléon et al., 1998).

Studies using scanning electron microscopy and atomic force microscopy have shown that a structural level between growth rings and lamellae consists of “blocklets” with diameters roughly from 20–100 nm (Gallant et al., 1992).

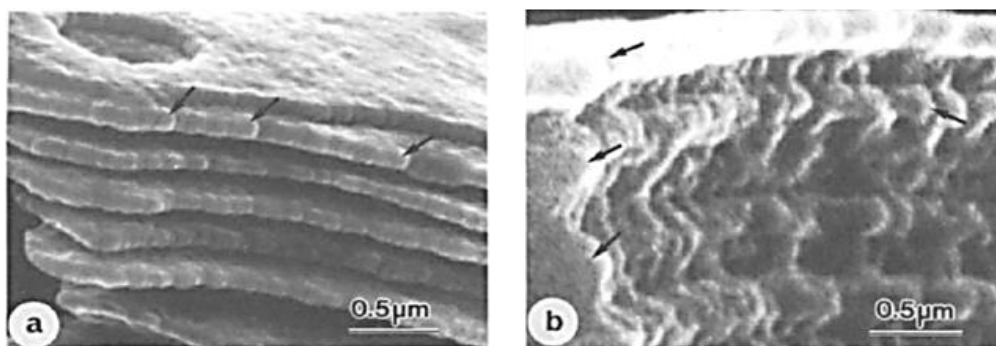


**Figure 2.7:** Scanning electron micrographs of residual starch granules after pancreatic alpha-amylase hydrolysis: (a) wheat; (b) potato. “Blocklets” are shown by arrows (adapted from Gallant et al., 1992).

Blocklets exist in both the amorphous and the semi-crystalline rings, but blocklets in the semi-crystalline rings have more perfect structure suggesting that in this region they contain the stacks of lamellae (Figures 2.6 and 2.7). The relationship of blocklets to the rest of the granular structures is still unknown.

### **2.2.5. Gelatinisation**

Starch granules are generally insoluble in cold water, but when starch granules are heated to temperatures greater than 60°C in excess water, they absorb water and

swell. The swelling is due to granules absorbing about 70% of its weight in water from the surrounding aqueous environment into the granules via hilum (López et al., 2004); the molecular bonds in the pseudo-crystalline structures are disrupted and melted (Lund & Lorenz, 1984), the granules lose birefringence (Ratnayake & Jackson, 2007), and starch polymers are solubilised and leached out (Figure 2.8). Consequently, the viscosity of starch–water suspension increases (Annison & Topping, 1994). This irreversible transition is known as gelatinisation.

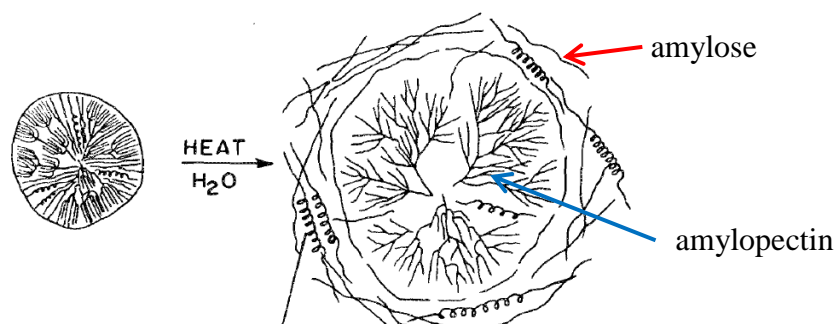


**Figure 2.8:** An illustration of the gelatinisation process and the changes in ordered structures of a starch granule during heating in excess water (adapted from Biliaderis, 1991).

The degree of swelling is measured by two different methods, namely swelling power, which is the ratio of the wet weight of the sedimented gel to its dry weight (Leach, McCowen, & Schoch, 1959); and the swelling factor, which is the ratio of the volume of swollen granules to the initial volume (Tester & Morrison, 1990). The swelling of starch granules is affected by their structural integrity which depends on the amylose to amylopectin ratio, the arrangement of amylose and amylopectin in the granules, and the percentage of lipid and protein (Morrison et al., 1993; Srichuwong, Sunarti, Mishima, Isono, & Hisamatsu, 2005). The high amylose starch is normally associated with lower swelling power, probably due to

the interaction of the amylose with the lipid-protein complexes or with the inter-block chain from amylopectin (Srichuwong et al., 2005).

The irreversible phase transition during gelatinisation in excess water can be detected and quantified using various methods. A Kofler hot stage microscope with polarised light is used to detect the loss of birefringence in starch granules (Liu & Zhao, 1990; López et al., 2004); Nuclear Magnetic Resonance spectroscopy is used to detect the loss of ordered pseudo-crystalline structure in the starch granules (Waigh, Gidley, Komanshek, & Donald, 2000). Differential Scanning Calorimetry is used to detect the heat input, enthalpy ( $\Delta H$ ) during the disruption of the hydrogen bonds in the ordered crystalline structure (Fredriksson, Silverio, Andersson, Eliasson, & Aman, 1998; Karlsson & Eliasson, 2003; Liu & Sopade, 2011; Ratnayake & Jackson, 2007).

A rapid visco-analyser (RVA) or a rheometer are used to measure changes in the viscosity of a starch suspension due to the increase in the volume of swollen granules (Gunaratne et al., 2007; Kaur, Singh, McCarthy, & Singh, 2007; Mishra & Rai, 2006; Okechukwu & Rao, 1995). The maximum viscosity is attained in a system where nearly all the amylose is leached out (Luallen, 1985) from the completely swollen intact granules (also known as “ghost granules”) suspended in a watery amylose solution (Srichuwong et al., 2005).

### **2.3. Viscosity of starch and dietary fibres suspensions**

Viscosity is defined as a quantity expressing the magnitude of internal friction in a fluid, as measured by the force per unit area resisting a uniform flow rate.

Increasing numbers of studies report that viscosity is an important property for foods manufacturing (Lille, Nurmela, Nordlund, Metsä-Kortelainen, & Sozer, 2017) and for assessment of rate of digestion (Khan et al., 2017; Lentle & Janssen, 2010; Takahashi & Sakata, 2004).

The viscosity of a Newtonian material is constant regardless of the shear stress applied. However, the apparent viscosity of a non-Newtonian material varies with applied shear, where the viscosity of a pseudoplastic material (most biological materials) decreases with shear rate and the viscosity of a dilatant material increases with shear.

For suspensions containing spherical particles above a concentration of 20% (v/v), the apparent viscosity ( $\eta_s$ ) is often normalised by the viscosity of the Newtonian suspending liquid ( $\eta_0$ ), and is reported as the relative viscosity ( $\eta_r$ ). The viscosity of this system is proportional to the solid volume fraction ( $\Phi$ ) of the particles in suspension (Genovese, Lozano, & Rao, 2007). Ungelatinised starch granules behave as hard spheres and may exhibit Newtonian properties when suspended in a Newtonian liquid. After gelatinisation, the viscosity is shear thinning (Okechukwu & Rao, 1995).

The rheological properties of soluble fibre solutions vary with the concentration; for example, a 0.5% (w/v) guar gum solution is a Newtonian solution, whereas above this concentration it is non-Newtonian shear thinning solution (Rayment, Ross-Murphy, & Ellis, 1995). Usually less than 1% (w/v) guar gum is added in most food applications.





**Figure 2.9: The dispersed soluble fibre forming entangled network in a solution (adapted from Ellis, Rayment, & Wang, 1996).**

The viscosity of guar gum solution increases in proportion to its concentration (Robinson, Ross-Murphy, & Morris, 1982) until it reaches the critical concentration ( $c^*$ ), where small increases in concentration raise the viscosity dramatically. In the  $c^*$  state, guar molecules form an entangled network (Figure 2.9) and the movement of water molecules within the solution is restricted (Ellis et al., 1996). A high proportion of the water molecules are also loosely bound to the sugar residues of the parent gum.

The viscosity of a guar solution also increases with its molecular weight (MW) (Funami et al., 2005). Compared to high MW guar, low MW guar gum has fewer galactose side chains and has less ability to establish networks with neighbouring mannan chains (Funami et al., 2005). Similarly, highly depolymerised guar gum also has lower viscosity in comparison with highly polymerised guar (Mikkonen et al., 2007), likewise starch digested to its component sugars has a much lower viscosity compared to the parent starch when gelatinised.

Few studies have compared the effect on viscosity of adding insoluble or soluble fibre to suspensions and determining the relationship between  $\phi$  and viscosity, although the effect particle concentration (Rayment, Ross-Murphy, & Ellis, 1998)

and shape (aspect ratio) on the viscosity of suspensions in Newtonian liquids has been extensively studied (Krieger & Dougherty, 1959; Maron & Pierce, 1956; Petford, 2009).

### **2.3.1. Viscosity of digesta**

Recently, studies exploring the viscosity of mammal digesta following high fibre diets reported that indigestible solid residues that accumulate in the solid phase of digesta increase the viscosity of digesta (Dikeman, Barry, Murphy, & Fahey, 2007; Shelat et al., 2015; Takahashi & Sakata, 2004).

The apparent viscosity of digesta from the digestive tract of various animals is pseudoplastic (non-Newtonian), and demonstrates yield stress properties (Lentle & Janssen, 2008). The values of viscosities vary from about 0.02 Pa.s when measured at shear rate of 1000 s<sup>-1</sup> to 600 Pa.s at shear rates of 0.001 s<sup>-1</sup> (Lentle, Stafford, et al., 2007; Piel, Montagne, Seve, & Lalles, 2005; Takahashi et al., 2008). After the removal of solid residues by centrifugation (> 10,000 g) (Takahashi & Sakata, 2004), the viscosity of the liquid digesta (supernatant) was shown to be Newtonian and low, at about 0.001 Pa.s measured at 1 s<sup>-1</sup> (Dikeman, Barry, et al., 2007; Dikeman & Fahey, 2006; Razdan & Pettersson, 1996). Although viscosity of the liquid phase of digesta is generally low and Newtonian, when significant amounts of soluble dietary fibre, e.g. guar or carboxymethylcellulose are added into the diet, the liquid phase increases in viscosity and becomes shear-thinning (pseudoplastic) (McDonald, Pethick, Mullan, & Hampson, 2001; Piel et al., 2005). When digesta contains about 18% of indigestible solid particles, the viscosity increases rapidly (Takahashi et al., 2008; Takahashi, Goto, & Sakata, 2004; Takano et al., 2013).

The solid particle concentration in the digesta is generally measured as the Dry Matter Concentration (DMC) by weight. This is the proportion of dry mass in the digesta to total digesta mass on a weight for weight basis (w/w) (Lupton & Ferrell, 1986). High DMC raises the viscosity of digesta but this relationship is not directly proportion to the mass of solids (Lentle, Stafford, et al., 2007). For example, the DMC of porcine digesta just over doubled from 12.5% to 28.5% between the caecum and the rectum, while the apparent viscosity increased 4500% (McRorie et al., 2000).

The apparent viscosity of digesta varies with the size and shape of the indigestible particles suspending in the digesta. The DMC of pig digesta fed on a diet containing 5% (g/kg) crystalline cellulose was 16% higher than that of pigs fed on a diet containing 30% (g/kg) rye-wheat diets, but the apparent viscosity of ileum digesta of the former was about 1/3 that of the rye-wheat diet (Bartelt et al., 2002). It is likely that particle interaction in digesta resembles that used in model systems (Lentle & Janssen, 2008), where the apparent viscosity is governed by the ratio of  $\phi$  of the suspended particles to its maximum packing fraction ( $\phi_{\max}$ ), ( $\phi/\phi_{\max}$ ) (Krieger & Dougherty, 1959). However, the effect of insoluble food fibres with heterogenous size and shape on viscosity is not well studied.

### **2.3.2. Factors affecting viscosity**

#### **2.3.2.1. Solid volume fractions ( $\phi$ ) and shear rate**

In a dilute suspension of spherical particulates (where  $\phi \leq 0.05$ ), the gap (h) between particles is larger than their diameter (d) (Figure 2.10) and little interaction occurs between particles. As  $\phi$  is increased above about 0.05, the viscosity of the

suspension increases due to hydrodynamic forces generated by the motion of each particle in the suspension that distort the streamline flow of Newtonian fluid of the continuous phase (Barnes, 1989).

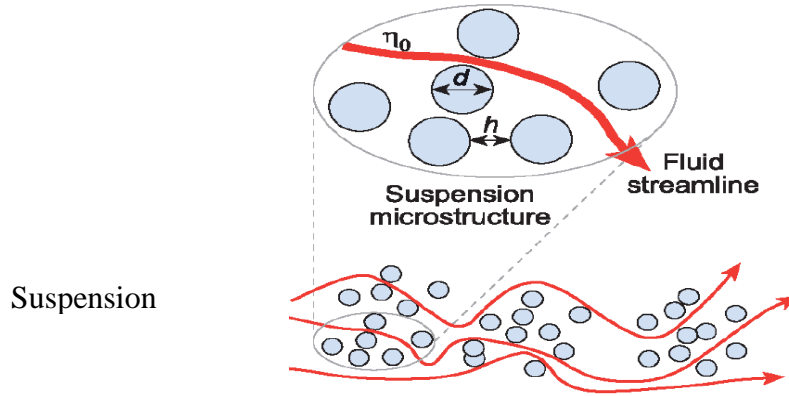


**Figure 2.10: Schematic model of a suspension of spherical particles in response to applied shear (arrows). Particle-particle interaction increases as the gap ( $h$ ) between particles decreases and the mean particle diameter ( $d$ ) increases (adapted from Petford, 2009).**

In the semi-dilute regime ( $0.05 \leq \phi \leq 0.25$ ), gaps between particles become smaller than their diameter (Figure 2.10), particle-particle interactions become important (Van Der Werff, De Kruif, & Hoff, 1989). In this region, interactions between the particles become more important than Brownian motion and the streamline flow between the particles, resulting in pseudoplastic shear thinning behaviour at intermediate shear rates (the power-law region) (Figure 2.11) (Boek, Coveney, Lekkerkerker, & van der Schoot, 1997; Marti, Hofler, Fischer, & Windhab, 2005). At very high shear rates, particles are aligned with flow streamlines rather than arranged randomly, resulting in lowered interaction between particles and the viscosity of the suspension decreases to a lower Newtonian plateau (Figure 2.11).

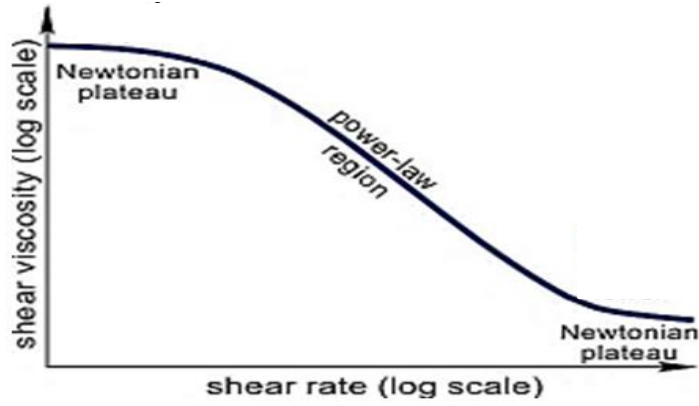


**Figure 2.11: The effect of shear rate on apparent viscosity of a particulate suspension.**

For concentrated suspensions ( $\phi \geq 0.25$ ), the gap between particles becomes smaller than their radius (Figure 2.10), this promotes inter-particle interactions and the apparent yield stress in the low shear region ( $\sim 10^{-3} \text{ s}^{-1}$ ) (Marti et al., 2005). At very high shear rates ( $10^3 \text{ s}^{-1}$ ), above those shown in Figure 2.11, a concentrated suspension will exhibit a shear thickening (dilatant) property which also known as “jamming” as streamlining cannot be established.

#### **2.3.2.2. Ratio of solid volume fraction to the maximum packing fraction, $(\phi/\phi_{max})$**

The viscosity of a dilute suspension is linearly proportional to the proportion of solid particles present ( $\phi$ ), (Equation 2.1, Einstein, 1906):

$$\eta_r = \eta_s (1 + [k] \phi) \quad (\text{Equation 2.1})$$

The assumptions made in Equation 2.1 are that the solid particles suspended in the liquid phase contribute to the viscosity of suspensions (Marti et al., 2005) and that the viscosity of the suspending fluid is Newtonian (Pabst, Gregorova, et al., 2006). In this equation,  $[k]$  is the intrinsic viscosity of particles in suspension (Brenner, 1974), and gives the contribution of solid particles in the suspension to the apparent

viscosity of the suspension (Jeffrey & Acrivos, 1976). For hard spherical particles,  $[\eta]$  equals to 2.5. This equation only predicts viscosities to values of  $\phi/\phi_{\max}$  of less than 0.6 (Figure 2.12).

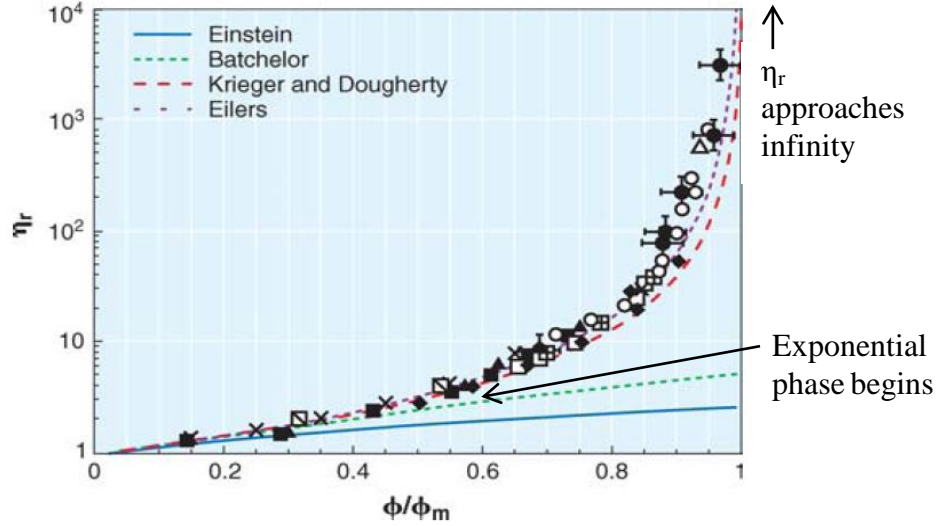


**Figure 2.12:** The relationship between relative viscosity and the  $\phi/\phi_{\max}$  (adapted from Stickel & Powell, 2005) using hard polystyrene spheres and polymethyl methacrylate beads suspended in polymer solutions such as polyethylene glycol-ran-propylene glycol monobutylether.

A suspension containing hard sphere particles of uniform size (15  $\mu\text{m}$ ) at  $\phi > 0.2$ , considered a concentrated suspension in which particles are close to being in contact, and the  $\phi$  approaches  $\phi_{\max}$  ( $\phi/\phi_{\max} \sim 0.6$ ). In such suspensions, the viscosity is too great to be measured by a rheometer (Stickel & Powell, 2005).

The most recognised semi-empirical model to predict viscosity over a wide range of  $\phi/\phi_{\max}$  was proposed by Krieger and co-workers (Krieger & Dougherty, 1959).

$$\eta_r = (1 - (\phi/\phi_{\max}))^{-[\eta] \phi_{\max}} \quad (\text{Equation 2.2})$$

Equation 2.2 was developed by suspending small, rigid, spherical particles (15 nm) in a Newtonian fluid. By adding solid particles, the viscosity of the suspension

increases. The relationship between  $\eta_r$  and  $(\phi/\phi_{\max})$  is non-linear (Krieger & Dougherty, 1959) and typical relationships are presented in Figure 2.12 where  $\eta_r$  approaches infinity as  $\phi$  approaches  $\phi_{\max}$ . At this point the rheological properties of the suspension are dominated by the interaction between the solid particles (Brown & Jaeger, 2009).

Equation 2.2 has been widely used to predict viscosity of concentrated suspensions containing solid particles of varying size and shape (Fischer, Pollard, Erni, Marti, & Padar, 2009), including suspensions of fibres and starch granules (Pabst, Berthold, & Gregorov, 2006). However, the estimation of the value  $[k]$  in the Equation 2.2 is difficult for suspensions containing non-spherical particles. In such situations, a generalised version of the Equation 2.2 is used, where  $[k]\phi_{\max} = 2$  (Maron & Pierce, 1956).

$$\eta_r = (1 - (\phi/\phi_{\max}))^{-2} \quad (\text{Equation 2.3})$$

To date, Equation 2.3 remains one of the most important equations used to predict the viscosity of concentrated suspensions containing particles of various sizes and shapes and it is used extensively in this thesis.

### **2.3.2.3. Aspect ratio of particles sizes**

For a given  $\phi_{\max}$ , the  $\eta_r$  of a suspension increases with the aspect ratio (R) of the suspended particles (Kitano, Kataoka, & Shirota, 1981; Pabst, Gregorova, et al., 2006), where R is the ratio of the longest to shortest axis of the particle (Brenner, 1974), spherical particles have an R of 1.

The  $\phi_{\max}$  of suspensions containing uniform spherical particles ( $R = 1$ ) varies from 34% to 74%, depending on the size distribution of the particles in suspension (Petford, 2009). However, the  $\phi_{\max}$  of suspensions that contain particles with  $R > 1$  increases as the  $R$  of solid particles increases (Pabst, Gregorova, et al., 2006; Wierenge & Philipse, 1996). The elongated particles rotate “end over end” with applied shear and  $\phi_{\max}$  decreases when the  $R$  of suspended particles (radius of gyration) increases (Brenner, 1974; Mueller, Llewellyn, & Mader, 2010). At very high shear rates, the alignment of elongate particles with the induced flow will reduce  $\eta_r$  (Boek et al., 1997; Mueller et al., 2010). Therefore, the  $\eta_r$  of elongated particles in suspensions such as digesta is dependent on the shear rate in the gut (Fermin & Riley, 2010; Genovese et al., 2007).

Digesta is a polydisperse suspension in which the shape of the particles is diet-dependent (Lentle & Janssen, 2008). Studies that quantified solid particles isolated from the small intestine using image analysis reported that the mean diameter of these particles are about 0.24 mm with a width of 0.06 mm, thus  $R$  values of these particles were estimated to range from 2 to 8 (Jalali, Nørgaard, Weisbjerg, & Nadeau, 2012; Krämer, Nørgaard, Lund, & Weisbjerg, 2013).

If it is assumed that the effect of the degree of polydispersity of the particles can be described by a mean value of  $R$ , then the only unknown in equation 2.3,  $\phi_{\max}$ , can be calculated by fitting  $R$  and  $\phi_{\max}$  into a general linear equation in the form of  $y = c + mx$  (Equation 2.4). Using reasonably homogenous fibre suspensions with  $R$  values between 6 and 27 (Kitano et al., 1981), the following relationship between  $R$  and  $\phi_{\max}$  has been proposed (Equation 2.4):



$$Y = c - m X \quad (\text{Equation 2.4})$$

$$\Phi_{\max} = 0.54 - 0.0125 R \quad (\text{Equation 2.5})$$

However, when particles with R values ranging from 1 to 16 were suspended in a 60% sucrose solution (Pabst, Gregorova, et al., 2006), Equation 2.4 became

$$\Phi_{\max} = 0.51 - 0.0223 R \quad (\text{Equation 2.6})$$

Equations 2.5 and 2.6 indicate that estimation of  $\Phi_{\max}$  of a suspension is dependent on the slope ( $m$ ) and the y-intercept ( $c$ ) which vary with the average values of R of solid particles in suspension. However, the determination of R of solid particles in the suspension is time consuming; hence tools such as image analysis must be used for effectively estimating R for suspensions of heterogeneous fibres such as are found in digesta. To date, little study has been carried out to relate values of R from heterogeneous distributions of plant fibres and  $\Phi_{\max}$ , and so estimate  $\eta_r$  for suspensions.

### **2.3.3. Viscosity of starch suspensions**

#### **2.3.3.1. Defining gelatinisation by viscosity**

RVA is widely used in the food industry to determine the pasting properties of starch as it simulates the actual production process (Deffenbaugh & Walker, 1989) and the results are reproducible (Becker et al., 2001). As the suspension (typically 10% (w/w) starch in water) is heated from ambient temperature (25°C) to 95°C, the starch begins to gelatinise and swell, the viscosity begins to increase between 55°C and 65°C, this point is identified as the pasting temperature (PT). Maximum

viscosity is reached at the peak hot paste viscosity (PV) where the granules are still intact and swollen to their maximum size (Figure 2.13) (Limpisut & Jindal, 2002; Mishra & Rai, 2006). Continued swelling softens the granules and the viscosity of the suspension decreases to the set-back viscosity at about 95°C (Figure 2.13).

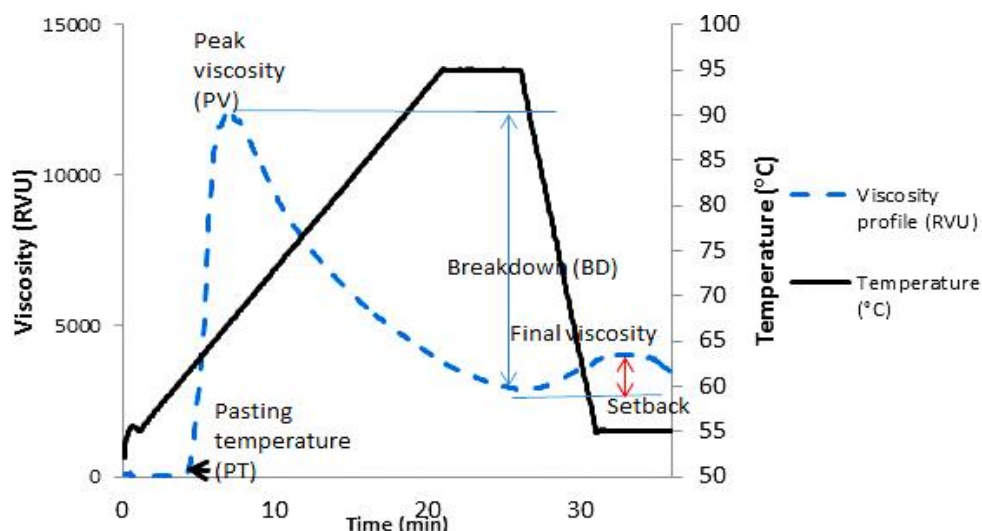


**Figure 2.13: A typical RVA viscometer profile for starch gelatinisation, viscosity profile (dotted line) and temperature profile (bold line).**

Assuming that starch granules are at their minimum volume at PT, and swollen starch granules at their maximum volume at PV and the increment in viscosity of the starch suspension against the rise in temperature is governed by volume; the degree of gelatinisation of starch granules can be set in an arbitrary unit (%) based on the swelling and viscosity properties of starch granules at PT and PV using a RVA to a given temperature.

---

**2.3.3.2. Hydration and viscous properties of starch**

The hydration of starch is characterised by the property (Q), the total amount of water absorbed by starch granules (Leach et al., 1959) and the solubility (S) (Bagley & Christianson, 1982) of amylose leached from granules (Li & Yeh, 2001) during gelatinisation. The Q and S increase with the degree to which starch is gelatinised (Blazek & Copeland, 2008; McCormick, Panozzo, & Hong, 1991) and with the source of the starch, potato starch granules having a higher Q than corn starch granules (Srichuwong et al., 2005; Zaidul, Nik Norulaini, Mohd. Omar, Yamauchi, & Noda, 2007).

Gelatinised high amylopectin (waxy) starches that have low lipid and protein contents also have greater Q values when compared to either normal or high amylose corn starch (Craig, Maningat, Seib, & Hoseney, 1989; Higley, Love, Price, Nelson, & Huber, 2003; Juhász & Salgó, 2008) or corn starch granules that have had their lipid content removed (Howling, 1980). These results suggest that amylose is associated with lipid and protein molecules to form hydrophobic complexes that lower Q and S and resist swelling (Tester, 1997).

The  $\eta_r$  of ungelatinised starch increases with  $\phi$  and can be estimated using Einstein's equation (Equation 2.1) when  $\phi/\phi_{\max}$  is below about 0.35 (Figure 2.12). However, the viscosity of gelatinised starch suspensions cannot be predicted from the Einstein equation (Okechukwu & Rao, 1995) as these granules are highly hydrated and may no longer function as rigid spheres. In this case,  $\phi$  in the Equation 2.1 needs to be modified by considering the volume of the swollen granules, a factor accounting for the flexibility of the granules and perhaps the mass of leached amylose.

The volume fraction of swollen granules ( $\phi_w$ ) is affected by the gelatinisation temperature (Wang & Seib, 1996), the concentration of starch in the suspension ( $c$ ) (Steeneken, 1989) and the amount of leached amylose ( $S$ ) (Gunaratne et al., 2007). The  $\phi_w$  for a starch suspension with concentration ( $c$ ) ranging from 7-25% (w/w), at a temperature below its PT in an aqueous suspension free of solubilised amylose can be estimated using the equation proposed by Bagley & Christianson (Bagley & Christianson, 1982),

$$\phi_w = cQ \quad (\text{Equation 2.7})$$

When amylose is leached into the aqueous phase it is accounted for by the factor  $S$  in an extended version of Equation 2.7 (Doublier, Llamas, & Le Meur, 1987),

$$\text{Where: } \phi_w = [(1 - (S/100)) * cQ] \quad (\text{Equation 2.8})$$

The  $\phi_w$  for equations 2.7 and 2.8 is expressed as (g/g) however, defining  $\phi_w$  of swollen granules as a weight ratio (g/g) may lead to errors if weight is not closely correlated with particle volume. However, as the gelatinised or partially gelatinised granules are highly hydrated in suspension, it can be assumed that  $\phi_w$  as a weight ratio (g/g) is similar to its volume ratio (v/v) (Genovese et al., 2007).

The  $\phi_w$  in Equation 2.8 is affected by the volume fraction of swollen starch granules (Steeneken, 1989). Potato starch granules have a higher  $Q$  (78.9 cm<sup>3</sup>/g) which leads to  $\phi_w$  of 0.35 (g/g) compared to corn starch which has lower  $Q$  (12.1 cm<sup>3</sup>/g) when fully gelatinised leading to  $\phi_w$  of 0.46 (g/g) (Evans & Lips, 1992). At concentrations of starch in water where granules can gelatinise fully the granules are swollen to their maximum volume and free water may be present in the suspension and  $\eta_r$  is

then dependent on the volume concentration of starch; where less water is present the swelling of granules is restricted (Evans & Lips, 1992) and no free water is present in the suspension (Bagley & Christianson, 1982), the  $\eta_r$  of the suspension is very high and may be near solid.

## **2.4. Starch digestion**

The rate of starch digestion has been related to the susceptibility of the starch granules to the hydrolytic enzymes during amylolysis. Early studies investigated the rate of starch digestion using an *in-vitro* model and have classified the starch digestibility into three largely arbitrary categories using acronyms of digestible starch (RDS), slow digestible starch (SDS), and resistant starch (RS) (Björck, Granfeldt, Liljeberg, Tovar, & Asp, 1994; Englyst, Englyst, Hudson, Cole, & Cummings, 1999). RDS is the portion of starch that is digested within 20 min of the start of simulated small intestine digestion; SDS is the portion of starch that is digested between 20 to 120 min; and RS is the portion of indigestible starch after hydrolysis for 120 min with enzymes. Since then, this classification system has been widely used in *in-vitro* starch digestibility studies.

Later studies reported that starchy foods that contain high proportion of RDS (Englyst, et al, 1999) usually release glucose at a faster rate (Björck et al., 1994) and elevate postprandial blood glucose levels rapidly (Ells et al., 2005; Parada & Aguilera, 2011); these incidences are associated with increased risk of type II diabetes (Björck et al., 1994; Brand-Miller, Hayne, Perocz, & Colagiuri, 2003). This is followed by reports that high proportions of RS in food system lower or maintain the postprandial blood glucose levels, which could reduce the risk of

obesity and type II diabetes in addition to producing higher contents of short chain fatty acids which may have protective effect against colon cancer (Ríos-Covián et al., 2016). Therefore, more research was focused on modifying the porportion of RDS or RS in the food matrices (Parada & Aguilera, 2009) by adding dietary fibre or by lowering the degree of gelatinisation of starch (Parada & Aguilera, 2009). The effect of these modifications have been studied in both *in-vitro* and *in-vivo*.

#### **2.4.1. *In-vitro* and *in-vivo* starch digestion**

The human digestion system is a complex multi-stage process. Studies involved *in-vivo* starch digestions are constrained by cost, ethical considerations, and individual variations which will affect plasma glucose and insulin responses (Englyst, Kingman, Hudson, & Cummings, 1996; Heaton, Marcus, Emmett, & Bolton, 1988). A simply, flexible and reproducible *in-vitro* model that closely mimics the *in-vivo* physiological digestive conditions is widely used in research (Germaine et al., 2008; Hur et al., 2011; Woolnough et al., 2008; Zhang et al., 2013), although *in-vitro* studies rarely consider physiological parameters such as gastric emptying, the small intestine passage rate, and the blood glucose absorption rate (Dhital, Warren, Butterworth, Ellis, & Gidley, 2017; Repin et al., 2016). Also the activity and sources of digestive enzymes used in the *in-vitro* system vary, which probably oversimplify the *in-vitro* digestion process. Given these limitations, the evidence suggests that *in-vitro* studies can predict *in-vivo* responses provided that the procedures for *in-vitro* starch digestion use similar enzymes with analogue molecular structure to the *in-vivo* enzyme and other physiological conditions such as temperature, pH, and duration of digestion are strictly controlled (Skrabanja, Elmståhl, Kreft, & Björck, 2001; Woolnough et al., 2008).

The rates of appearance of sugars in hepatic portal blood of human subjects fed on various cereal starches was less than expected from the *in-vitro* rates of digestion of the same starches (van Kempen et al., 2010). This is not surprising, as systemic glucose in the blood stream will be buffered by gastric emptying, gut content, liver function, and other metabolic processes such as the absent of mucin and digestive hormones that regulate secretion of bile salts. After correcting for some of these processes (van Kempen et al., 2010), the correlation between *in-vitro* and *in-vivo* studies was improved ( $R^2 = 0.95$ ). Therefore, results obtained from rate of starch digestion *in-vitro* model is still a useful tool to provide simplicity and approximate guide to *in-vivo* rate of starch digestion (Hasjim, Lavau, Gidley, & Gilbert, 2010; Hur et al., 2011; Zhang et al., 2013).

#### **2.4.1.1. Measurement of rate of digestion *in-vitro***

A log of slope (LOS) plot is a plot of the logarithmic concentration of starch being digested against time. It has been advocated by researchers to measure the rate of starch digestion *in-vitro* (Butterworth, Warren, Grassby, Patel, & Ellis, 2012; P. Chen et al., 2016; Dhital, Bhattarai, Gorham, & Gidley, 2014; Dhital et al., 2015; Goni, Garcia-Alonso, & Saura-Calixto, 1997). The LOS slope is used to determine the rate of starch digestion, by which the slope is greatly affected by the sub-sampling intervals (Butterworth et al., 2012). Most studies sub-sampled the digestate at every 10 to 30 min intervals (Butterworth et al., 2012; P. Chen et al., 2016; Dhital et al., 2015). LOS is widely used to estimate the products concentration at the end of amylolysis of raw starch or fully gelatinised starch granules (Dhital et al., 2015; Dona et al., 2010; Warren, Zhang, Waltzer, Gidley, & Dhital, 2015; Zhang et al., 2013). The LOS measures the rate of amylolysis of

starch or starch-containing foods with a relatively high concentration of enzymes in an *in-vitro* system by assuming that the digestibility of all starch materials in such system have the same intrinsic reactivity with respect to amylase and should follow the first-order kinetic reaction, or more correctly a pseudo-first order reaction (Butterworth, et al., 2012; P. Chen et al., 2016; Dhital et al., 2014; Dhital et al., 2015).

The first order kinetic disagrees to group the starch into classes of RDS and SDS. It argues that the rate of amylolysis gradually ceased due to the depletion in substrate concentration. A recent study showed that a partially gelatinised starch, a retrogradated starch, and a starch system containing other food components such as dietary fibre do not follow the first order kinetics; instead digestion happened in two different rates and could be described using two different constants from the LOS plots (Patel, Day, Butterworth, & Ellis, 2014). The differences in the rate of digestion are due to variations in the chemical structure of starch granules (Patel et al., 2014).

If there is only the substrate exhaustion could solely explain the rate of starch digestion, thus the rate of reaction for all substrates against the same enzyme would be the same. However, the rate of reaction was varied with starch types (Patel et al., 2014). In the system, starch granules are not only the concentration of substrate changes with time, but also the susceptibility of the starch chemical structure to the enzyme changes with time, where the digestibility of starch granules gradually moved from highly digestible starch to resistant starch (Patel et al., 2014) or by other



mechanisms such as the effects of suspension viscosity and the effects of non-competitive inhibition of amylase by starch polymers (Slaughter et al., 2001).

#### **2.4.2. Factors affecting the rate of starch digestion *in-vitro***

In the basic kinetic enzyme reaction, the rate of enzyme reaction is influenced by temperature, pH, concentrations of substrates (starch granules), and /or enzymes (amylases), and by the rate of mixing / rheological properties of the surrounding viscous materials, such as soluble fibres to increase the viscosity of digesta. High temperature increases the rate of enzyme reactions as the enzyme molecules move faster and have a higher chance of colliding with the enzyme active site, whereas optimum pH maintains the three dimensional structure of the amylase's active site for starch polymers binding (Cornish-Bowden, 2014). However, these parameters are carefully maintained at physiological level in the *in-vitro* system, thus they may have minimal effects on the rate of digestion.

The rate of starch digestion *in-vitro* might be influenced by different concentrations of starch granules and enzymes that are used in the *in-vitro* system. Comparisons of the absolute values from these data might be misleading; comparisons on the relative values might reveal more accurate information. To a greater extent, the rate of starch digestion is associated with the physico-chemical properties of raw starch granules, such as the size and shape, the ratio of amylose and amylopectin (Biliaderis, 1991; Cummings et al., 1997; Parada & Aguilera, 2011), processing of the food such as DG and cooking duration (Holm et al., 1988; Parada & Aguilera, 2009), and the presence of dietary fibres in the starchy food (Parada & Aguilera, 2011).

### 2.4.2.1. Kinetic of $\alpha$ amylase and amyloglucosidase

The  $\alpha$ -amylase (E.C.3.2.1.1) is an endo-amylase which catalyses the initial hydrolysis of starch into shorter oligosaccharides varying in molecular weight with  $\alpha$ -configuration and  $\alpha$ -limit dextrins by specifically cleaving at  $\alpha$ -D-(1,4) glycosidic bonds (Figure 2.14), but not the terminal glucose residues and  $\alpha$ -D-(1,6) glycosidic bond (de Sales, de Souza, Simeoni, Magalhaes, & Silveira, 2012). Alpha-amyloglucosidase (E.C. 3.2.1.3) is an exo-acting enzyme which hydrolyses the terminal to next to the terminal linkages at the  $\alpha$ -D-(1,4) and  $\alpha$ -D-(1,6) glycosidic bonds from the non-reducing end of the oligosaccharides at a slower rate (Weill, Burch, & Van Dyk, 1954).

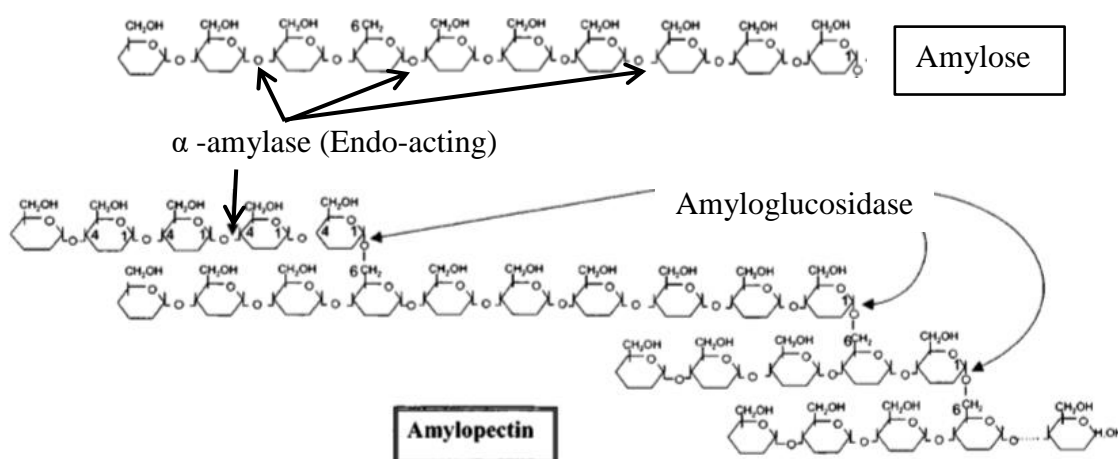


**Figure 2.14: Hydrolytic mechanism of enzymes on amylose and amylopectin.** Alpha-amylase is an endo-acting enzyme hydrolysing  $\alpha$ -(1-4) bonds at random giving rise to malto-oligosaccharides (linear or branched, typically DP 2-6); it does not hydrolyse  $\alpha$ -(1-6) bonds. Amyloglucosidase is an exo-acting hydrolase which releases single glucose molecules from the non-reducing end of  $\alpha$ -(1-4) oligo- or polysaccharides. This enzyme is unique because it can hydrolyse  $\alpha$ -(1-6) branching points, converting starch completely to glucose (adapted from Tester & Somerville, 2000).

Pancreatic alpha-amylase (E.C. 3.2.1.1) randomly locates on 5 adjacent alpha-1,4 linked glucose molecules of the starch polymer (Gray, 1992). The alpha-1,4 linkage between the 2nd and 3th molecules is cleaved to release a maltose molecule (Slaughter et al., 2001) (Figure 2.15). The maltose is further hydrolysed by amyloglycosidase (E.C. 3.2.1.3) to glucose (Dreher, Dreher, Berry, & Fleming, 1984; van der Maarel, van der Veen, Uitdehaag, Leemhuis, & Dijkhuizen, 2002) at the brush border of the small intestine from where it is finally absorbed into the blood stream.

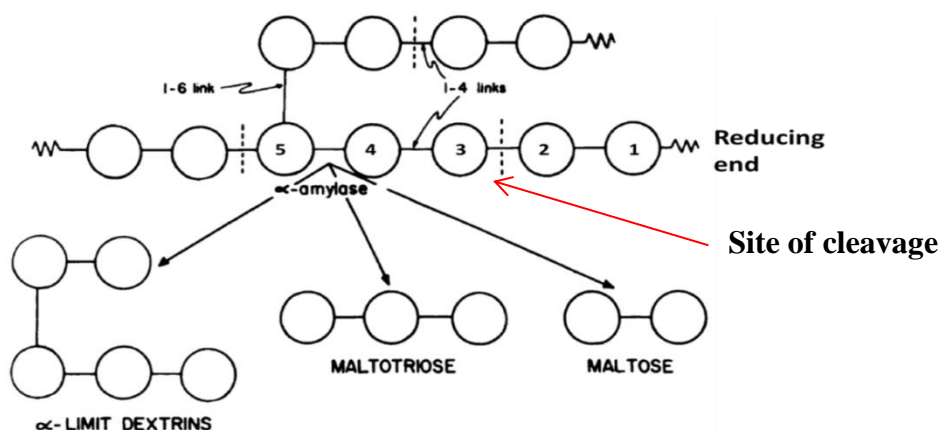


**Figure 2.15:** Action of salivary and pancreatic alpha-amylase on amylopectin. Each circle represents a glucose residue linked with either alpha-1,4 (horizontally) or alpha-1,6 (vertically) bond. The final products from amyolysis are maltose, maltotriose and the branched alpha-dextrins (adapted from Gray, 1992).

#### 2.4.2.2. *Physico-chemical properties of raw starch granules*

The digestion of ungelatinised starch is related to the size of the granules and the surface properties of the granules including porosity (Kong, Kim, Kim, & Kim, 2003). Generally, smaller corn starch granules have a higher surface to volume ratio and are digested at a faster rate than the larger potato granules (Hellman & Melvin, 1950; Kong et al., 2003). Another study reported that the hydrolysis of smaller

ungelatinised pea starch granules was 14 times faster than for potato granules during incubation with porcine pancreatic alpha-amylase (17.5 nKat/mg) for 29 h at 37°C (Planchot, Colonna, Gallant, & Bouchet, 1995).

Ungelatinised corn starch granules have irregular pores ranging from 2-3 nm in diameter (Sujka & Jamroz, 2010) which were formed by *in-situ* hydrolysis by amylases secreted by tissues in the corn kernels (Jane et al., 2003). These pores act as channels to facilitate the diffusion of amylase into the granule (Gallant et al., 1992) and hence initiate amylolysis (Buléon et al., 1998; Sujka & Jamroz, 2007). These reports lead to further studies on the formation of pores/channels in maize starch and found that the channels are associated with the integral proteins of the microtubule of amyloplast. These results suggested that channels are remnants of the microtubule in the amyloplast which developed from the plastid that was located around the nucleus in endosperm cells before biosynthesis of sugar and storage in starch granules (Benmoussa et al., 2010; Fannon, Gray, Gunawan, Huber, & BeMiller, 2004).

The channels connecting the surface of the granules to the hilum likely facilitate diffusion of water and during digestion, amylases directly into the granules (Jane et al., 2003; K. Wang, Henry, & Gilbert, 2014).

Atomic force microscopy examination revealed that ungelatinised potato starch granules have fewer pores (50-300 nm) on their surface (Juszczak, Fortuna, & Krok, 2003) compared to corn granules. After incubation with amylase, few random micropores (< 1 µm) appeared on potato granules (Planchot, Colonna, & Buleon,

1997; Sujka & Jamroz, 2010) compared to corn starch granules, suggesting that amylolysis occurs slowly on potato granules due to its low porosity (Sujka & Jamroz, 2010) (Figure 2.16). This phenomenon has also been reported as surface erosion (Sujka & Jamroz, 2007).

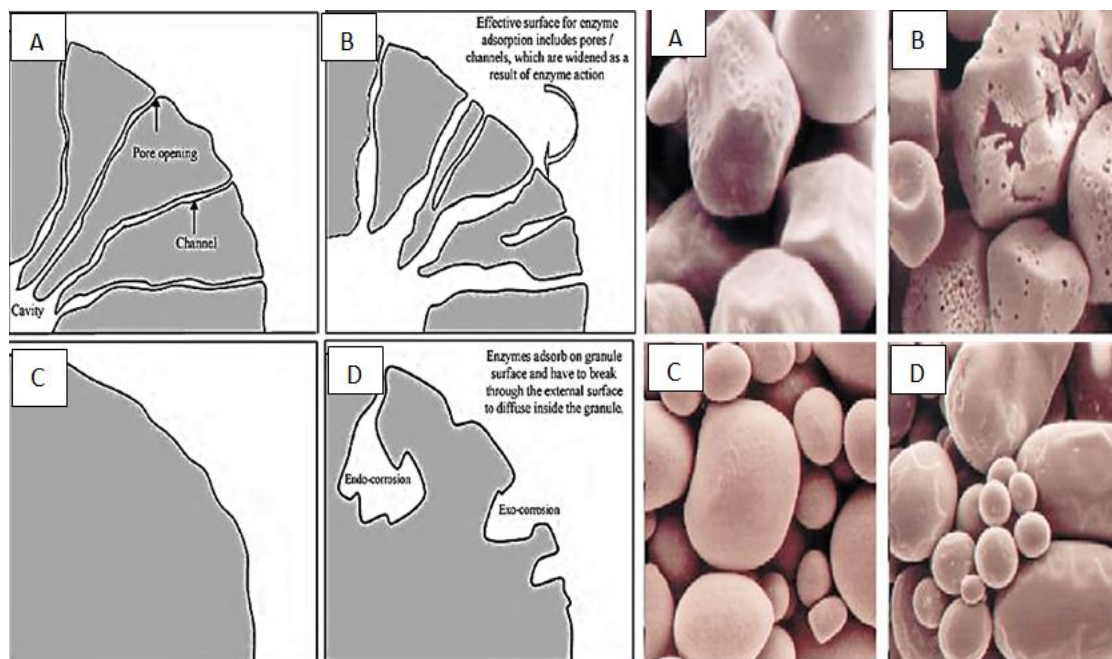


**Figure 2.16:** Diffusion of amylase and its hydrolysis patterns in raw corn and potato starches: (A) corn starch showing pores and channels; (B) corn starch hydrolysed by amylase with enlarged pores; (C) potato starch granules have fewer pores, (D) channels and cavity of potato starch by amylase. Adapted from (left: Dhital, Shrestha, & Gidley, 2010); (right: Sujka & Jamroz, 2007).

#### 2.4.2.3. Degree of gelatinisation (DG)

Not all processed starchy foods are fully gelatinised. Some starch containing foods are partially gelatinised and in this case the DG is expressed as a % of its fully gelatinised counterpart. For example, the DG of starch in muesli bars is 62% (Parada & Aguilera, 2011), cookies 4% (Lineback & Wongsrikasem, 1980) and in some extruded products 45% (Holm, Bjock, Asp, Sjoberg, & Lundquist, 1985).

Starchy foods with low DG show reduced postprandial blood glucose levels and insulin responses in human and animal studies (Ells et al., 2005; Englyst et al., 1999; Holm et al., 1988; Seal et al., 2003). Starchy foods with low DG can be prepared using low cooking temperatures (Donovan, 1979; Liu, Yu, Xie, & Chen, 2006), cooking at low water content (Gunaratne et al., 2007; Perry & Donald, 2002) or with shorter cooking times (Panlasigui et al., 1991).

Gelatinising starch suspensions at higher temperatures increases their DG and hence the rate of starch digestion. For example, the rate of digestion of waxy corn starch was doubled when gelatinised at 80°C for 5 min resulting in about 92%DG, compared to gelatinising the same starch for the same duration at 50°C (Miao, Zhang, Mu, & Jiang, 2010). The rate of amylolysis of ungelatinised (DG 0%) corn and potato starch granules was increased by 3 to 8 times when the starch was gelatinised to DG100% (G. Zhang, Ao, & Hamaker, 2006). Higher gelatinisation temperatures disrupt the molecular bonding between the pseudo-crystalline regions in starch granules (Garcia, Colonna, Bouchet, & Gallant, 1997; Shogren, 1992) increasing the bio-accessibility of amylase (Holm et al., 1988; Rendleman, 2000).

Sugars are often added in the preparation of starch based foods such as cookies, bakery goods, and confectionary. High concentrations of solutes in starch-water suspensions result in lowered DG after cooking (Gunaratne et al., 2007; Perry & Donald, 2002). For example when 6% (w/w) potato starch was gelatinised in 40% sucrose solutions the pasting volume was reduced as higher osmotic potential generated by the sugar molecules in solution inhibited swelling (Gunaratne et al.,

2007) resulting in a lowered DG (Perry & Donald, 2002). Starch granules of similar botanical source gelatinised to the same DG under similar cooking conditions had similar rates of starch digestion ( $p < 0.05$ ) (Panlasigui et al., 1991).

#### **2.4.2.4.      *Presence of insoluble and soluble dietary fibres***

Clinical studies reported that adding 20% to 25% (g/g) cellulose fibre into the diet did not significantly delay corn starch digestion but the inclusion of 1.5% (g/g) guar in bread significantly reduced the rate of wheat starch digestion (Brennan, Blake, Ellis, & Schofield, 1996; Ellis et al., 1996; Vahouny et al., 1980). The inclusion of 7.5% pea fibre and inulin plus 3% guar into pasta significantly ( $p < 0.001$ ) reduced the glucose released after 30 min (Tudorica et al., 2002) which in turn lowered the postprandial blood glucose, insulin levels (Fuentes-Zaragoza et al., 2010). Although the experimental techniques used lead to variations in amylolysis of the various starchy foods (Woolnough et al., 2008); the mechanisms associated with the addition of various dietary fibre types in delaying the rate of starch digestion are not fully understood.

The addition of guar gum at levels above about 0.5% increases the viscosity of digesta (Blackburn et al., 1984; Johnson & Gee, 1981; McRorie & McKeown, 2017; Repin, Cui, & Goff, 2016) and slows the rate of starch digestion and glucose absorption (Read & Eastwood, 1992). This has been considered to be due to increases in the unstirred water layer at the wall of the small intestine that reduces the rate of mass transfer of glucose from the digesta to the site of absorption at the gut wall (Read & Eastwood, 1992).

Studies also reported that insoluble fibres increased viscosity of digesta and could slow the rate of starch digestion (Hansen, Bach, & Eggum, 1992; Juntunen et al., 2003; Meyer et al., 2000). The mechanism by which insoluble dietary fibre increases the viscosity of digesta has been related to its WHC (Takahashi et al., 2008) and its ability to sequester the products of digestion into the voids within the fibre mass (Ou et al., 2001). Diets to which 5% (w/w) of large insoluble plant fibre particles (>500  $\mu\text{m}$ ) were added hold more free water and increased the colonic viscosity in rats compared to smaller (~300  $\mu\text{m}$ ) fibre particles (Takahashi et al., 2008). In addition, an *in-vitro* study reported that the addition of 2.0% wheat bran and 0.8% carboxymethyl cellulose into a solution containing 100 mmol/L glucose slowed the rate of apparent amylolysis of starch within the solution; this was thought to be due to the sequestration of sugar in the fibre matrix (Ou et al., 2001). However, this explanation is open to debate as glucose molecules entrapped within the fibre matrix should freely equilibrate with glucose in the free fluid within the gut (Takahashi, Karita, Ogawa, & Goto, 2005).

The measurement of amylase kinetics has shown that guar may inhibit the action of alpha-amylase through non-competitive inhibition and slow the rate of digestion. The amylase would locate but not cleave the branched glucomannan polymer structure of guar and thus be sequestered by it (Slaughter et al., 2001). This effect is eliminated when the guar is hydrolysed (Jenkins et al., 1981). A similar type of inhibition has been suggested to occur with  $\beta$ -glucan (Wood et al., 1990).



#### **2.4.2.5. Effect of shear rate**

The typical movement of digesta in the gut has been described as “*propagation in peristalsis and segmentation*” (Lentle et al., 2002), which is a slow movement. The rate of movement of digesta obtained by spatiotemporal mapping of the small intestine of the guinea pig was  $2.96 \text{ mms}^{-1}$ . Dividing the rate of propagation of digesta by the approximate radius (6.3 mm) of the small intestine; the shear rate was estimated to be  $0.47 \text{ s}^{-1}$  (Levitt, Kneip, & Levitt, 1988); similar calculations obtained a rate of  $0.58 \text{ s}^{-1}$  for *opossum* (Melville, Macagno, & Christensen, 1975),  $0.5 \text{ s}^{-1}$  for *brush-tail possum* (Lentle et al., 2002) and  $0 \text{ s}^{-1}$  at the centre to  $2 \text{ s}^{-1}$  at the wall of the small intestine for rats (Evans, Hood, Oakenfull, & Sidhu, 1992). These results suggest that the shear generated by the gut wall is generally low (Lentle et al., 2002).

Given the low shear rate and the inferred low shear stress generated in the gut, the movement digesta in the small intestine must be compensated by the elasticity of the intestinal wall and the necessarily lower viscosity of the digesta. If these conditions do not occur, the mixing of digesta in the gut would be very poor (de Loubens et al., 2013; Lentle, Stafford, et al., 2007; Shelat et al., 2015). This finding was agreed by *in-vitro* studies using dialysis tubing and rheometer where the rate of starch digestion was low at shear rate lower than  $1 \text{ s}^{-1}$  (Dhital, Bhattarai, et al., 2014, 2017; Repin et al., 2016, 2017). Therefore, when simulating *in-vitro* digestion, appropriate shear rates as found in the gut need to be considered.

## 2.5. Concluding remarks

The health benefits of dietary fibre in the human diet have been extensively studied and it is generally agreed that the addition of soluble dietary fibres elevates the viscosity of ileal digesta, while insoluble dietary fibres accelerate the rate of transit of the colonic digesta and increases stool volume while assisting with conveying toxins and other waste through the colon before they are voided in the stool. These beneficial effects have been related to level of hydration and the ability of these fibres to increase the viscosity of digesta in the gut. However the mechanisms by which water molecules are sequestered by fibre to bulk the faeces is not fully established.

Digesta is a particulate suspension that contains indigestible solid particles suspended in a continuous often Newtonian liquid phase derived from liquid components of the diet and secretions from gut cells. However, the mechanism by which fibre particles interact in the digesta and the threshold  $\phi$  at which the particles significantly interact to elevate the viscosity of digesta (Lentle & Janssen, 2010) is not fully established. Slow rates of amylolysis have been associated with high concentrations of dietary fibre in the digesta. However, the large variations in the rate of starch hydrolysis recorded by the various *in-vitro* and *in-vivo* studies discussed remain unexplained. Elucidation of this process could provide useful methods for the food processing industry to formulate foods with lowered rates of starch digestion and hence reduce glycemia and so improve health and wellbeing.

## **Chapter 3      General materials and methods**

### **3.1.            Introduction**

This chapter describes the core materials and methodologies used throughout the study into four major sections. The first section describes the selection of the commercially available food fibre and starch types used, followed by the second section describing the analytical methods used to determine chemical compositions and physical properties of selected materials. The third part covers the selection of a viscous Newtonian solution that was used to prepare a suspension of food fibres that resembled the indigestible solid particles isolated from pig digesta; also the selection of starch suspensions in which the granules had been gelatinised to different degrees by varying the cook time. All specific analysis methods are described in the appropriate chapters.

### **3.2.            Selection of materials**

The indigestible residues from food are voided in the faeces. The size, shape, chemical properties, and solubility of the particles recovered from faeces vary with diet (Lentle & Janssen, 2010). A range of insoluble fibres commonly used in the food industry were selected for their similarity to the solid particles recovered from the small intestinal and colonic digesta from pig and from human faeces.

#### **3.2.1.          *Digestive residues of pig and human***

Pig digesta was used as a model for mammalian digesta comparison as pigs have similar diets and digestive physiology to humans (Miller & Ullrey, 1987). The solid residue fractions were harvested from the small intestine and the colon of six

randomly selected pigs immediately after slaughter at an abattoir. The proximal and distal segments of the small intestine and the colon were isolated by a ligature placed medially between the pyloric valve (proximal section) and junction with the colon (distal section), digesta was collected from the proximal and distal sections into separate containers (Lentle, Hemar, Hall, & Stafford, 2005). During the preparation, the colon content of one of the pigs was lost; for this reason, the colonic contents used were collected from five pigs only (Chapter 4), whereas the intestinal contents of six pigs were represented (Chapter 5).

The physical properties of solid residues from pig digesta were compared to solid residues of a faecal sample collected from a volunteer following the diet tabulated in Table 3.1. The volunteer consumed a normal diet, with the addition of a supplement of 100 g of Kellogg's AllBran® fibre daily. Since this food product is a standard breakfast food, no ethic clearance was necessary.

**Table 3.1: Dietary records of the volunteer on three consecutive days on 100 g Kellogg's AllBran® fibre supplement.**

<b>Day</b>	<b>Breakfast</b>	<b>Lunch</b>	<b>Dinner</b>
1	40 g AllBran® 1 banana 1 cup coffee, 250 mL	30 g AllBran® 1 vegetable sandwich 250 mL orange juice	30 g AllBran® with 125 mL milk 1 apple (100g) 1 peach
2	40 g AllBran® 1 cup tea, 250 mL 1 banana	30 g AllBran® 1 cup coffee, 250 mL 100 g white rice 1 fried egg coated with chili	30 g AllBran® 1 cup coffee, 250 mL 100 g bean salad 50 g tofu, fried
3	40 g AllBran® 1 kiwi fruit 1 cup coffee, 250 mL	30 g AllBran® 100 g white rice 75 g stir fried vegetable combination with carrot, broccoli, corn, cauliflower 1 cup coffee, 250 mL	30 g AllBran® with 125 mL milk 1 apple (100g) 1 serving fried mee hoon

The nutritional values of the daily food intake for the three (3) consecutive days were calculated using NutriPRO Inc. software (Table 3.2).

**Table 3.2: Calculated nutritional values of carbohydrate, protein and fats for the daily food intake of the volunteer for three consecutive days using NutriPRO Inc. software.**

<b>Nutrients</b>	<b>DAY 1</b>	<b>DAY 2</b>	<b>DAY 3</b>	<b>Average</b>
<b>Carbohydrate (g)</b>	<b>201.62</b>	<b>151.70</b>	<b>189.05</b>	<b>180.79</b>
<i>Dietary fibre (g)</i>	<b>43.29</b>	<b>42.64</b>	<b>41.36</b>	<b>42.43</b>
- <i>Crude fibre (g)</i>	<b>3.27</b>	<b>1.45</b>	<b>1.16</b>	<b>1.96</b>
- <i>Soluble fibre (g)</i>	<b>3.83</b>	<b>3.82</b>	<b>3.23</b>	<b>3.63</b>
- <i>Insoluble fibre (g)</i>	<b>30.61</b>	<b>30.51</b>	<b>29.03</b>	<b>30.05</b>
<i>Total sugars (g)</i>	88.28	37.41	50.91	58.87
<i>Glucose (g)</i>	20.15	7.58	8.38	12.04
<i>Galactose (g)</i>	0.15	0.06	0.00	0.07
<i>Fructose (g)</i>	24.53	6.95	12.30	14.59
<i>Sucrose (g)</i>	34.43	16.35	16.83	22.54
<i>Lactose (g)</i>	6.78	0.06	6.70	4.51
<i>Maltose (g)</i>	1.75	1.77	1.66	1.73
<i>Other carbohydrate (g)</i>	22.58	22.58	22.58	22.58
<b>Protein (g)</b>	31.30	36.97	32.72	33.66
<b>Total Fat (g)</b>	13.38	31.48	17.16	20.67
<i>Saturated fat (g)</i>	3.96	4.44	2.71	3.70
<i>Polyunsaturated fat (g)</i>	4.24	11.86	8.87	8.32
<i>Monounsaturated fat (g)</i>	2.32	11.25	3.36	5.64
<i>Cholesterol (mg)</i>	20.05	210.22	6.45	78.91
<b>Total calories (kilo Joules)</b>	3786.14	3759.70	3802.25	3782.70

The calculated average daily intake of dietary fibre was 42.43 g of which about 30 g (70%) was insoluble fibre. Since most of the insoluble fibre intake was from AllBran®, the fibre particles isolated in faeces was assumed to be derived from the AllBran® consumed. Samples of pig digesta and human faeces were stored at -20°C pending further analysis. Before performing each test, the frozen samples (20 g wet weight) from each pig and from the human faeces were defrosted to room temperature. An aliquot of each sample was stirred thoroughly using a spatula to homogenise the sample before passing it through a 1 mm sieve. The resulting

samples were washed with MilliQ water three times to remove mucus and solubles and the solid residue recovered by centrifuging at 10,000 *g* for 20 min. The recovered particles were dried at 40°C (Gallenkamp, PlusII, Japan), and then ground using a mortar and pestle before storing in a sealed container pending further analysis.

### **3.2.2. Food fibres**

Four types of insoluble food fibres commonly used in the food industry and guar, a soluble food gum were chosen on the grounds that they differed in solubility and particle size distribution but fell within the range of the residual material found in the gut and recovered from pig digesta. These were: two commercially available insoluble cellulosic food fibre products derived from wheat ‘WF600’ (J. Rettenmaier & Söhne, Rosenberg, Germany) and ‘Prolux’ (Oppenheimer Pty Ltd., NSW, Australia); a finely milled food grade wood derived fibre with high lignin content (Lignocel® Type C120, J. Rettenmaier & Söhne, Rosenberg, Germany) probably derived from a species of *Pinus* (supplied by Plant and Food Research Ltd, New Zealand); and a breakfast fibre product, Kellogg’s AllBran®, derived from wheat bran containing 26.2% (dry weight basis) insoluble plant fibre (Chapter 4, Figure 4.1). AllBran® fibre consists of a high proportion of solulisable material as indicated on the nutrition information panel (Appendix 1). The soluble components may include gelatinised starch, sugars, and possibly a small amount of lipid and protein.

Guar gum is an example of soluble food grade hydrocolloid or soluble fibre containing 85% of hydratable galactomannans, the remaining 15% is mainly

moisture and a small proportion of protein, fat and mineral; no insoluble content is found in the sample as indicated in the table of nutritional data (Appendix 2) provided by Formula Foods Corporation Ltd (Christchurch, New Zealand). Guar gum is not digested in the small intestine but is a substrate for bacterial growth in the colon.

### 3.2.3. Starch

Two commercially unmodified starches commonly used by the food industry but with different processing characteristics in terms of physical, chemical, and pasting properties were used. Potato starch (WindMill, Holland) was supplied by National starch (New Zealand) and corn starch was supplied by the New Zealand Starch Company (New Zealand). The potato starch granules were between 25 and 50  $\mu\text{m}$  in their major axis and the corn starch granules between 10 and 30  $\mu\text{m}$  in diameter as determined by scanning electron microscopy (SEM) (Figure 3.1).

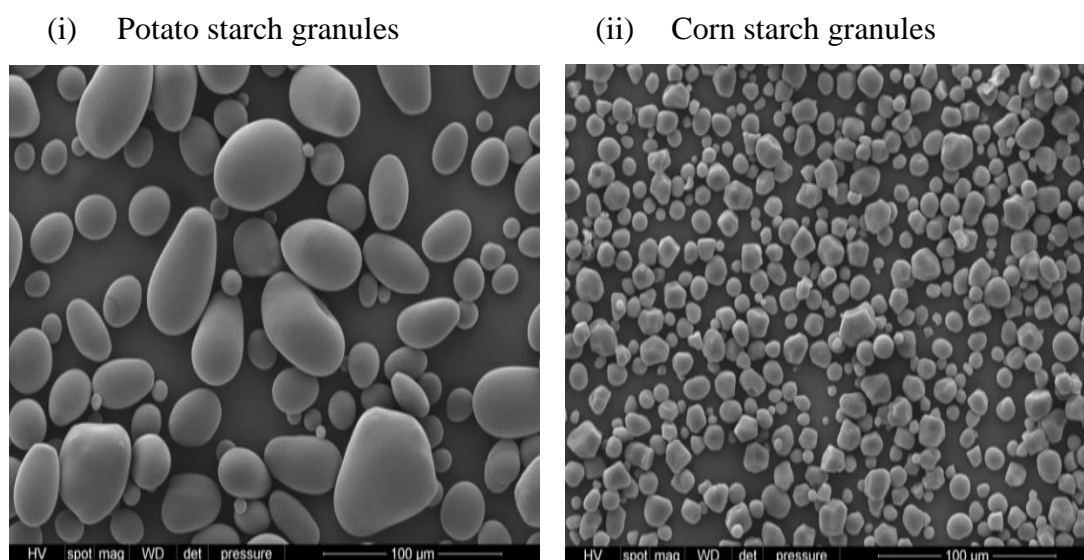


**Figure 3.1:** SEM images of the starch particles (i-ii), to the same scale.



Both contained between 20-28% of amylose and 80-75% amylopectin as indicated by the supplier, these values were similar to the published values for the proportion of amylose and amylopectin for normal potato and corn starches (Swinkels, 1985).

#### **3.2.4.            *Glass beads***

Small spherical glass beads, ~75 nm (Syntech Distributors Ltd., Auckland, New Zealand) were used as a standard material for the preparation of particulate suspensions. The reason for this was that the viscosities of suspensions of small hard regular spheres of about the same size are commonly used as model particles for work of this type (Einstein, 1906; Krieger & Dougherty, 1959; Maron & Pierce, 1956).

### **3.3.            Chemical properties of dietary fibre and starch**

#### **3.3.1.            *Proportion of cellulose, hemicellulose and lignin in food dietary fibre***

The proportion of crude insoluble fibre in the particulate materials was determined by TELARC accredited methods in the Nutrition Laboratory at Massey University (AOAC, 2005b; Robertson & van Soest, 1981). The crude fibres are composed of Acidic detergent fibre (ADF) and Neutral detergent fibre (NDF).

For the determination of NDF, each of the ‘as supplied’ food fibre samples was ground and passed through a 1 mm screen. Each of the ground samples (1 g) ( $W_1$ ) was weighed into a crucible ( $W_2$ ) and heated with acetone to solubilise fat which was then removed by filtration. The trace of acetone was removed under vacuum followed by air drying for 15 min ( $W_3$ ). The sample was then boiled in 50 mL of

neutral detergent solution containing (w/w): 3% sodium lauryl sulphate; 1.861% Na<sub>2</sub> EDTA-2H<sub>2</sub>O; 0.681% Na<sub>2</sub>B<sub>4</sub>O<sub>7</sub> · 10H<sub>2</sub>O; 0.456% Na<sub>2</sub>HPO<sub>4</sub> · 2H<sub>2</sub>O, and 1mL 2-ethoxyethanol. The pH of this solution was adjusted to between 6.95 to 7.05 using 1 M HCl or 1 M NaOH. Two mL of heat-stable α-amylase solution (20 mg/mL from *Bacillus subtilis*) was added to 50 mL of cold neutral detergent solution to hydrolyse the starch present in the fibre samples. The mixture was boiled for 30 min and then filtered through a cloth 1 h after the onset of boiling. The remaining fibre was washed three times with deionised water to remove the solubles and then with 50 mL acetone to remove water. Samples were vacuum-dried to remove acetone and then dried at 105°C for 8 h and weighed (W<sub>4</sub>). Crucibles containing fibres were ignited at 500°C furnace for 5 h to remove combustibles, cooled and reweighed (W<sub>5</sub>). The NDF reading is the sum of ADF and hemicellulose.

$$\text{NDF} = 100 \times [(W_4 - W_5) - (B_4 - B_5)] / [W_1 * W_3] \quad (\text{Equation 3.1})$$

W<sub>1</sub> = weight of ground sample

W<sub>2</sub> = weight of crucible

W<sub>3</sub> = weight of dried and cooled samples

W<sub>4</sub> = weigh of samples and crucible after treatment with solvent

W<sub>5</sub> = weigh of samples and crucible after ashing

B<sub>4</sub> = weigh of crucible after treatment with solvent

B<sub>5</sub> = weigh of crucible after ashing

ADF, which is the remaining residue of plant cell wall components, was determined gravimetrically after extraction using an acidified detergent solution that dissolved cell solubles, hemicellulose, and soluble minerals. One g of each air-dried sample (W<sub>1</sub>) was ground and passed through a 1 mm screen and weighed into a crucible

(W<sub>2</sub>). To simplify the filtration step, 1.0 g Celite was added to the crucible before the sample. The crucible was placed in the Fibertec hot extraction unit and 100 mL of cold acidic detergent solution containing (per litre) 20 g cetyltrimethylammonium bromide, 1 N sulfuric acid, octilic alcohol, and acetone was added to the crucible, with 2-4 drops n-octanol to prevent foaming and the mixture was heated to boiling point. The boiled sample was washed for three times with hot deionised water. About 30 mL of water was used and the sample was vacuum dried between washing. The crucible was placed in a cold extraction unit and filled with 25 mL acetone. The sample was filtered and this process was repeated. The remaining solvents trapped in the sample were evaporated and dried the crucible at 130°C for 2 h and cooled to room temperature in a desiccator. The cooled sample was weighed (W<sub>3</sub>). The sample was then ashed at 550°C for 2 h, transferred into 105°C oven, cooled in a desiccator, and weighed (W<sub>4</sub>). These steps were repeated with a blank crucible.

$$ADF = [(W_3 - W_2) - (B_3 - B_2)] W_1 \times 100 \quad (\text{Equation 3.2})$$

W<sub>1</sub> = weight of air dried sample

W<sub>2</sub> = weight of crucible

W<sub>3</sub> = weight of dried and cooled samples

The residue of cellulose, lignin, and heat damaged protein and a portion of cell wall protein and minerals (ash) was solubilised by 72% H<sub>2</sub>SO<sub>4</sub>, leaving the ADL (acidic detergent lignin), which was determined gravimetrically.

For ADL determination, the sample was stirred with 25 mL 72% H<sub>2</sub>SO<sub>4</sub> using a glass rod, and cooled to 15°C. After 3 h, the acid was filtered off. The sample was washed with water until acid free. The remaining solvent was evaporated and the

sample dried in the crucible at 130°C for 2 h then cooled to room temperature in a desiccator and weighed ( $W_4$ ). The sample was ashed in the crucible at 525°C for 3 h, cooled to room temperature in a desiccator and weighed ( $W_5$ ). These steps were repeated with a blank crucible.

$$ADL = [(W_4 - W_5) - (B_4 - B_5)] W_1 \times 100 \quad (\text{Equation 3.3})$$

$W_4$  = weight of samples and crucible after treatment with solvent

$W_5$  = weight of samples and crucible after ashing

### **3.3.2. Protein content**

The amount of nitrogen in the starches was analysed by the Dumas total combustion method (AOAC, 2005a) using a TruSpec CN Analyser (LECO® Corporation, St. Joseph, MI, USA). This analysis was carried out by the TELARC accredited nutrition laboratory at Massey University.

The TruSpec CN Analyser is an instrument that determines the amount of carbon and nitrogen in a range of materials, including foods, feeds, fertilisers, meats, and oilseeds. Pre-weighed samples are placed into an aluminium weighing pan and loaded into the furnace, where they are combusted rapidly at 850°C in a stream of oxygen. The products of combustion are mainly carbon dioxide, water, nitrous oxide, and nitrogen gas. The gasses then pass through a secondary furnace for further oxidation and water molecules are removed by magnesium perchlorate and sodium hydroxide. The moisture-free gas is conveyed through a heated copper catalyst using helium as a carrier gas and the nitrous oxide from the protein components is converted to nitrogen gas, and the remaining oxides and oxygen are removed. The nitrogen content of the gas stream is then determined by a thermal

conductivity detector. The crude percent protein content of each starch sample was obtained by multiplying total nitrogen content by 6.25, a conversion factor commonly used for plant proteins (AOAC, 1984).

### **3.3.3. Fat content (Soxtec™ method)**

The fat content of starch granules was estimated using a Soxtec solvent extraction method (AOAC, 1997) and was carried out by the TELARC accredited nutrition laboratory at Massey University. Two grams of the potato and corn starch samples were weighed and placed into the Soxtec filter thimbles. Round-bottom flasks (250 mL) were placed in an oven set to 125°C for 1 h to reach a constant weight. Approximately 170 mL of petroleum ether was placed into the Soxtec apparatus along with the thimbles containing the sample. The flasks were then heated and the temperature adjusted to give a distillation rate of 4 drops/second. The extraction was continued for 4 h, after which the solvent was evaporated from the sample, the remaining fat was weighed, and the proportion of fat in the starch sample calculated (Equation 3.4).

$$\% \text{Fat in starch} = [(W_2 - W_3)/W_1] * 100 \quad (\text{Equation 3.4})$$

$W_1$  = weight of empty flask (g),

$W_2$  = weight of flask and recovered fat (g),

$W_3$  = weight of starch sample prior extraction (g)

### **3.3.4. Moisture content**

Approximately 2 g of each starch sample was placed in an even thin layer on an aluminium pan. These samples were dried at 108°C in an oven overnight (Contherm Scientific, New Zealand). The dry weights were measured after cooling in a

desiccator and the moisture content (%) was calculated according to Equation 3.5 (AOAC, 1999).

$$\% \text{Moisture} = [(W_2 - W_1)/W_1] * 100 \quad (\text{Equation 3.5})$$

Where  $W_1$  = Initial weight of sample (g),

$W_2$  = Final weight of sample (g)

### **3.3.5. Water activity ( $A_w$ )**

The  $A_w$  of two grams of each of the oven dried fibre and starch samples (Section 3.3.4) was measured after cooling overnight in desiccator using a water activity meter (Dew Point AquaLab Series 4TE, Decagon Devices, USA). The  $A_w$  meter was calibrated at 25°C using the verification standards (distilled water ( $A_w=1.00$ ); 0.5 M KCl ( $A_w=0.98$ ); 6.0 M NaCl ( $A_w=0.76$ ); 8.57 M LiCl ( $A_w=0.50$ ); 13.41 M LiCl ( $A_w=0.25$ )) from Decagon (NE Hopkins Ct. Pullman, WA, USA). For each of the five water activity levels, the values were determined within the required range of 0.003 as per suggestion of the manufacturer. Samples were measured in triplicate.

### **3.4. Physical properties of fibre suspensions**

Animal digesta is considered to compose a suspension of solid particles in a Newtonian fluid (Takahashi & Sakata, 2004) with a viscosity ranging from 0.01 Pa.s to 2 Pa.s and a density close to that of water (1 g/cm<sup>3</sup>) (Abrahamsson et al., 2005; Marciani et al., 2000); whereas the density of the selected fibre particles used to prepare fibre suspensions that simulated digesta were greater than that of water and ranged between 1.400 and 1.650 g/cm<sup>3</sup>. To maintain the solid particles used in this

work in suspension during rheological measurements, a Newtonian solution of 70% fructose in water with a viscosity of 0.032 Pa.s was used as the liquid phase.

#### **3.4.1. Density of solid residues from digesta and faeces**

The volumes of the glass beads; the food fibre particles ‘as supplied’ and after “*in-vitro* digestion”; and the washed, dried and ground particles recovered from the proximal and distal parts of the small intestine were determined using a nitrogen gas pycnometer (Ultrapycnometer 1000, Quantachrome, Florida, USA). The ultrapycometer measures the volume of porous particles using Archimedes’ principle of fluid displacement and Boyle-Mariotte’s law of volume-pressure relationships (Tamari, 2004). In this case, an inert nitrogen gas rather than a liquid was used since Nitrogen gas can penetrate the finest pores of the solid particles. An ultrapycometer with 5 cm<sup>3</sup> blank vessel was calibrated using Nitrogen gas under ambient temperature and pressure with precision of 1 pascal (Pa). The volume of the blank vessel was recorded. After calibration, the pycnometer has to leave for at least 2 h to reach the equilibrium of volume between the blank vessel and the sample vessel under ambient temperature and pressure.

After equilibrium was reached, the dry particles including glass beads, plant fibres, digesta particles, and starch granules which have been kept in a desiccator overnight were placed into the sample vessel and the volume of these particles will be measured as per the instruction manual. In each case the mean volume of one gram of the test material after 5 pressure cycles was recorded. The densities of all the particle samples were determined using Equation 3.6.

$$\text{Density of solid} = (\text{weight of solid} / \text{volume of solid}) \quad (\text{Equation 3.6})$$

### **3.4.2. Density of liquid used to prepare fibre suspensions**

A liquid pycnometer is a vessel with a known volume which is used to determine the density of a given weight of liquid in. In this study, a liquid pycnometer was used to determine the density of fructose solutions.

The liquid pycnometer was first calibrated. The pre-weighed pycnometer was filled with 50 cm<sup>3</sup> MilliQ water at 37°C and reweighed. This procedure was repeated 5 times for precision. After calibration, the weight of 50 cm<sup>3</sup> at 37°C of fructose solutions ranging from 20% to 80% (w/v) with 10% intervals, and containing 0.02% (w/v) sodium azide as an antibacterial agent, were determined and the densities as a mean of 5 replicates were calculated using Equation 3.7.

$$\text{Density of liquid} = (\text{weight of liquid} / \text{volume of liquid}) \quad (\text{Equation 3.7})$$

#### **3.4.2.1. Selection of the Newtonian liquid phase**

Glass beads (density,  $\rho = 2.495 \text{ g/cm}^3$ ) are about 2.5 times the density of pure water ( $\rho = 1.000 \text{ g/cm}^3$ ). Similarly, the densities of dietary fibres ( $\rho = 1.400$  to  $1.650 \text{ g/cm}^3$ ) are greater than that of water. Therefore, Newtonian solutions of densities greater than that of water are needed to suspend glass beads and the various fibres used during viscosity measurements.

The density of a range of fructose solutions was measured using the liquid pycnometer (Sections 3.4.2.) to find a workable solution with a density as close as possible to glass beads. The apparent viscosity was also measured using a dynamic stress rheometer (model Rheometrics SR500, Rheometric Instruments, Piscataway, New Jersey, USA) equipped with cup (32 mm) and six blade vane geometry 32 mm



in length and 29.5 mm swept diameter at a range of shear rates, between  $0.1 \text{ s}^{-1}$  and  $100 \text{ s}^{-1}$  (Table 3.3).

**Table 3.3: The densities and apparent viscosities of fructose solutions at 37°C.**

Concentration of fructose solution (%)	Density of fructose solutions ( $\text{g/cm}^3$ )	Apparent viscosity of fructose solutions (Pa.s)
20	$1.089 \pm 0.001$	$0.003 \pm 0.000$
30	$1.137 \pm 0.001$	$0.004 \pm 0.000$
40	$1.193 \pm 0.001$	$0.007 \pm 0.000$
50	$1.230 \pm 0.002$	$0.010 \pm 0.000$
60	$1.273 \pm 0.001$	$0.023 \pm 0.002$
<b>70</b>	<b><math>1.350 \pm 0.007</math></b>	<b><math>0.032 \pm 0.003</math></b>
80	$1.483 \pm 0.014$	$1.900 \pm 0.020$

The viscosity of fructose solutions between 20% and 80% (w/v) showed Newtonian rheological properties (Table 3.3). Fructose solutions below 70% (w/v) show too low density to suspend glass beads during measurement and result in a rapid sedimentation. The sedimentation time ( $t$ ) was calculated from Stokes' law given by the following equation (Li et al., 2015):

$$t = \frac{18\eta h}{g(\rho_s - \rho_w)d^2} \quad (\text{Equation 3.8})$$

where,

$\eta$  = the viscosity of fructose solutions (0.032 Pa.s)

$h$  = vertical distance over which sedimentation occurs (sedimentation height, cm)

$g$  = the acceleration due to gravity ( $\text{cm}^{-2}$ )

$\rho_s$  = density of glass bead ( $2.495 \text{ g/cm}^3$ )

$\rho_w$  = density of water ( $1.000 \text{ g/cm}^3$ )

$d$  = glass bead diameter (75 nm)

The sedimentation rate in 20% (w/v) fructose solution was 10 times faster than in 70% (w/v) fructose solution. The 80% (w/v) fructose solution was too concentrated and formation of fructose crystals occurred. Therefore, 70% (w/v) fructose solution was chosen for this study.

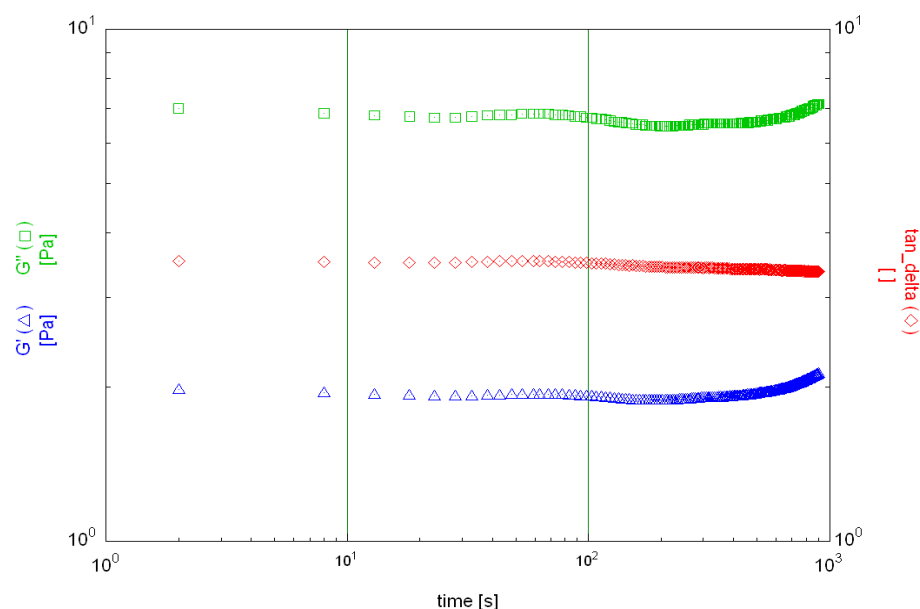


**Figure 3.2:** The small strain oscillation time sweep test on 70% (w/v) fructose in which 50% (w/v) of glass beads was suspended.

No evidence of sedimentation from the 70% (w/v) fructose/50% (w/v) glass bead suspension during small strain oscillation using 1% strain at a frequency of 1 Hz was observed (Figure 3.2). Therefore, 70% (w/v) fructose solution was selected to prepare all of the best suspensions for this work.

### 3.4.3. Microscopy

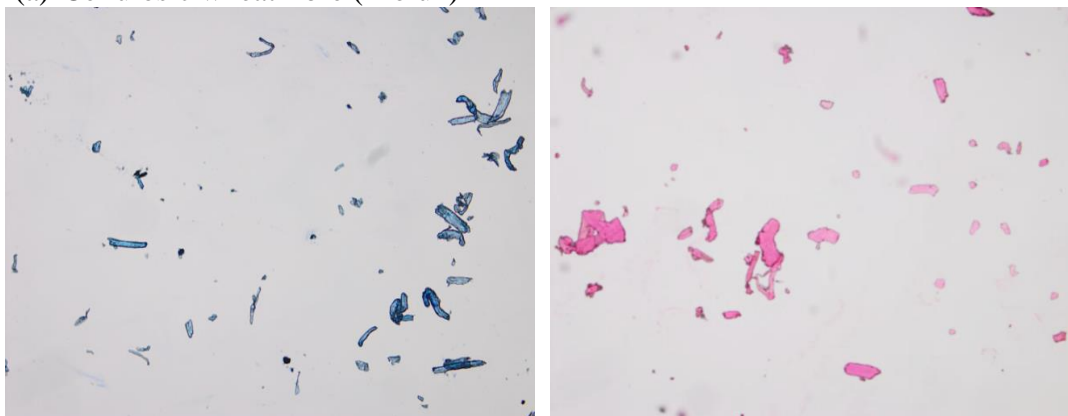
#### 3.4.3.1. Light Microscope

One mL samples of the solid residues recovered from the proximal and distal regions of the small intestine, from the colon of pig and from human faeces were washed in 0.2% sodium hypochlorite (4% (v/v), commercial Clorox bleach solution)

and incubated at room temperature for 1 h to preserve and clear the particles to assist with staining. The particles were then washed with MilliQ water twice to remove the Clorox solution and re-suspended in water.

The cellulose fibres stained using aqueous toluidine blue O which provided a better contrast for edge detection during imaging; while lignin rich fibres were stained with safranin (Figures 3.3 a, b) (Schuller & Muller, 2016; Srebotnik & Messner, 1994).

(a) Cellulosic wheat fibre (Prolux)



(b) Wood fibre (high in lignin)

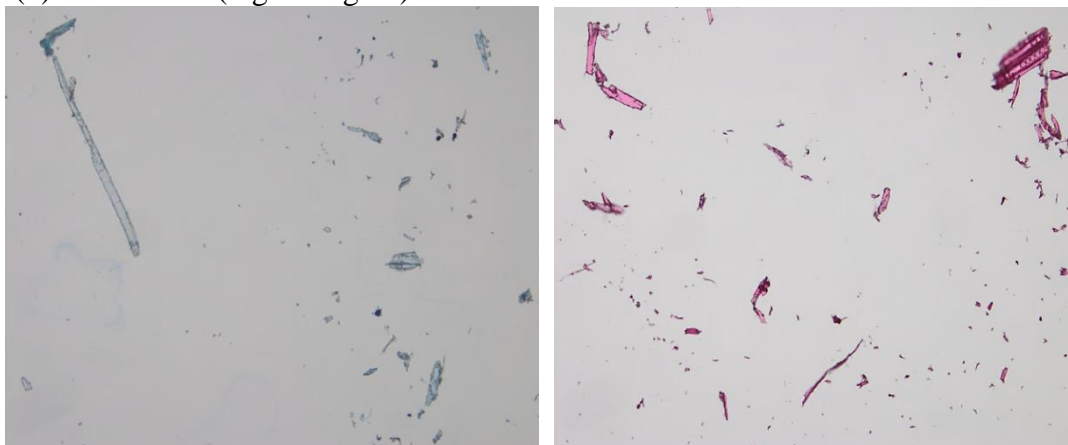


**Figure 3.3:** The light microphotography of (a) cellulosic wheat fibre (Prolux) and (b) Wood fibre stained with toluidine blue O (left) and safranin (right).

The commercially available cellulose wheat fibres (WF600 and Prolux) were therefore stained with aqueous toluidine blue O; whereas lignin enriched wood and AllBran® fibre particles; the particles recovered from human faeces and the pig colon were stained with safranin (red) overnight to facilitate edge detection during image analysing.

The stained particles were subsequently washed with MilliQ water to remove excess stain and re-suspended in water to ensure full hydration. Suspensions of each of the stained particles were photographed at a suitable magnification using an Olympus BX53 microscope (Tokyo, Japan) equipped with a digital camera and “cellSens life sciences” research imaging software (Olympus, Tokyo, Japan).

#### **3.4.3.2. Scanning electron microscope**

The morphologies of the various fibres, starch particles and glass beads were assessed by scanning electron microscopy (SEM) at the Massey University Microscopy and Imaging Centre. Each sample of the fibre particles and starch particles ‘as supplied’ and after *in-vitro* digestion, and the glass beads were attached to a mounting stub, sputter coated with gold and imaged with a FEI Quanta 200 scanning electron microscope (SEM, FEI Electron Optics, Eindhoven, The Netherlands) operated in back scattering mode at an accelerating voltage of 20.00 kV; WD (working distance) varied from 9.0 to 10.0 mm with electron detector of ETD2 (Everhart-Thornley Detector) at near vacuum ( $2.20\text{e}^{-5}$  to  $7.96\text{e}^{-5}$  Torr) using magnifications of 50x, 250x, and 1000x respectively. These parameters were adjusted until the best contrast images were obtained.

---

### 3.5. Starch digestion

#### 3.5.1. *Removal of digestible components from fibre particles*

Digestible components in the fibre particles were subjected to *in-vitro* digestion that simulated gastric and small intestinal digestion that was carried out using the method of Mishra and co-workers (Mishra, Monro, & Hedderley, 2008) with slight modifications. Fifty grams of 'as supplied' commercial fibre particles were dispersed in 250 mL of deionised water at 37°C and the pH adjusted to 2.5 ( $\pm 0.2$ ) with 1 M HCl (approximately 0.5 mL). Then 10 mL of 10% (w/v) porcine pepsin (P7000, Sigma-Aldrich, USA; activity ~250 units per mg protein) dissolved in 0.05 M HCl was added to the mixture and stirred at 130 rpm for 30 min at 37°C. The pH remained around 2.5 throughout the period of digestion. Twenty mL of a 1 M solution of NaHCO<sub>3</sub> was then added; followed by 50 mL of 0.1 M Na maleate buffer at pH 6.0 containing 0.02% (w/v) sodium azide and 1 mM CaCl<sub>2</sub>; 5mL of 2.5% porcine bile extract (B8631, Sigma-Aldrich, USA); 50 mL of 1.0% (w/v) of porcine pancreatin of 8X USP (P7545, Sigma- Aldrich, USA; the manufactures specify an activity for the preparation of 25 USP Units of amylase activity, 2.0 USP Units of lipase activity, and 25 USP Units of protease activity under standard assay condition certified by United States Pharmacopoeia, USP) dissolved in 0.1 M sodium maleate buffer at pH 6; and 1 mL of a 3260 U/mL (soluble starch) amyloglucosidase (Megazyme International, Ireland; the manufactures specify an activity for the preparation of 250 units per mg protein). The volume of digestate was subsequently made up to 550 mL with MilliQ water and the mixture stirred for 2 h at 37°C. The fibre particles were allowed to settle for 2 h and the supernatant decanted. The particles were re-suspended in MilliQ water and again decanted, this procedure

being repeated six times before the settled *in-vitro* digested fibre particles were collected and dried at 40°C for 12 h before storage for further use.

### **3.5.2. *In-vitro* digestion system - using rheometer**

A dynamic stress rheometer (model Rheometrics SR500, Rheometric Instruments, Piscataway, New Jersey, USA) equipped with cup (32 mm) and six blade vane geometry 32 mm in length and 29.5 mm swept diameter. The vane geometry (Barnes & Nguyen, 2001) provides similar shear stress and shear rate to bob geometry of similar radius and vane length (Cullen, O'Donnell, & Houska, 2002; Tabilo-Munizaga & Barbosa-Cánovas, 2005). The fidelity of the cup and vane geometry in determining viscosity was verified against that of cup and bob geometry using a Newtonian fluid (oil). Vane geometry was used to keep the starch granules and fibre particles in starch/fibre suspensions while allowing for low volume (100 µl) sub-sampling for sugar analysis at regular intervals during *in-vitro* digestion (Chapters 6 and 7).

*In-vitro* digestion was accomplished at constant temperature (37°C) and at designated shear rates; (10 s<sup>-1</sup> was used in Chapter 6; 0.1 s<sup>-1</sup>, 1 s<sup>-1</sup> and 10 s<sup>-1</sup> were used in Chapter 7). Shear was set to simulate that reported for the gastric and small intestinal conditions for animals (Mishra et al., 2008). During the course of the experiments, the humidity over the sample was maintained close to 100% to minimise evaporation from the contents of the rheometer cup.

For each of the various gelatinised starch and starch/fibre mixtures 38 g of suspension was poured into the rheometer cup and the sample equilibrated to 37°C

at the designated shear rate. The duration of digestion varied from 150 min (Chapter 6) and was reduced to 50 min (Chapter 7) as little useful data was accrued after 50 minutes.

Salivary amylase was omitted from this study may significantly reduce viscosity of the suspensions (Björck, 2006), however, the objective of this work was to compare rates of digestion of starch under controlled conditions simulating the small intestine and for this reason it was considered that a salivary phase would complicate the interpretation of the data. Variations in the rate of viscosity reduction and starch digestion resulting from the addition of dietary fibres to starch suspensions measured in this work are therefore comparable.

The *in-vitro* digestion sequence began with a gastric phase of 30 min duration. Then 3.5 mL of MilliQ water containing 250 µl of 1 M HCl, 200 µl of a solution containing 10% (w/v) of dry pepsin powder of  $\geq 250$  U/mg (P7000, Sigma-Aldrich, USA; activity ~250 units per mg protein) in 1 M HCl, and 100 µl of a 0.01% solution of lipase powder of  $\geq 20,000$  U/mg (L0382, Sigma-Aldrich, USA; activity ~20,000 units per mg protein) in MilliQ water was added to the suspension in the rheometer, lowering the pH to around 2. The subsequent small intestinal phase, which lasted for 120 min, commenced when the following reagents were added in quick succession; 500 µl of a 1 M NaHCO<sub>3</sub> solution; 1.5 mL of 1 M Na maleate buffer at pH 6 containing 0.2% (w/v) sodium azide, 1 mM CaCl<sub>2</sub>, and 0.02% bile extract (B8631, Sigma-Aldrich, USA); 100 µl of 5% pancreatin of 8 x USP (P7545, Sigma-Aldrich, USA; activity ~25 USP Units of amylase activity, 2.0 USP Units of lipase activity, and 25 USP Units of protease activity under standard assay condition

certified by United States Pharmacopoeia, USP) dissolved in 0.1 M sodium maleate buffer at pH 6; and 100  $\mu$ l of a 330 U/mL (soluble starch) solution of fungal amyloglucosidase (Novozyme, Australia) in water. An initial 250  $\mu$ l subsample of the digestate was removed immediately after the addition of the malate buffer solution (time = 0 min) and subsequent 250  $\mu$ l subsamples were taken at 1, 2, 5, 10, 15, 20, 30, 60 and 120 min following the addition of all reagents. In all cases, aliquots of each subsample were added to 850  $\mu$ l chilled absolute ethanol and mixed thoroughly to halt amylolytic digestion. These aliquots were kept at -20°C pending determination of glucose. Duplicates samples were digested.

### **3.5.3.        *Determination of total starch content***

It was assumed that the rates of appearance of glucose in the liquid phase of the digestate sampled from the rheometer were in direct proportion to the rates at which starches were digested. Prior to measuring the reducing sugar levels in the digested samples, the samples were each thawed to room temperature (20°C) and centrifuged for 10 min at 2000 g (mini spin plus centrifuge, Eppendorf, Hamburg, Germany) to remove suspended particles. The concentrations of monosaccharide reducing sugars in the supernatant were then determined using a dinitrosalicylic acid (DNS) colourimetric method appropriately modified for small samples (Mishra et al., 2008).



The amount of starch digested at each time point was calculated as follows:

$$\text{Reducing sugar} = [((\text{OD} \times k) / (W \times \text{starch})) \times 0.9] \quad (\text{Equation 3.9})$$

where;

OD = optical density at 510 nm (from spectrometer);

k = conversion factor (OD to glucose mg/mL) from the standard curve for glucose (Appendix 4);

V = total volume of sample (mL);

W = weight of starch initially present (g);

0.9 = a stoichiometric conversion constant for glucose to starch.

The weight of starch before digestion in the original suspension was determined by treating three replicates of 100 mg each of the starch/fibre suspensions (Chapter 6) or each type of starch suspension (Chapter 7) with 2.0 mL of dimethyl sulphoxide (DMSO) at 100°C for 10 min to fully dissolve them. Eight mL of sodium acetate buffer containing 100 µl of a 330 U/mL (soluble starch) of amyloglucosidase solution (Novozyme, Australia) was then added to the mixture to raise the pH to 5.2 before incubation for 30 min at 37°C. The amount of glucose produced was then quantified and starch content was calculated using Equation 3.9.

### **3.6. Data analysis**

The data from experiments reported in Chapter 4 and 5 were analysed using t-tests when two treatments were being compared. For the comparison of multiple samples within a treatment one way ANOVA and using Tukey's post hoc test to determine groups with statistically similar values was used. When there were more than two treatments and multiple samples comparisons were made using generalised linear

model (GLM) with Tukey's post hoc test to distinguish pair-wise differences. All statistical analysis was carried using the MINITAB Statistical Software suite (Version 15, USA). The distribution of the data was evaluated for normality using the Anderson-Darling normality test. Data sets that were not normality distributed were transformed using the function of "Johnson transformation" in the MINITAB software. After the statistical analysis, all data points were then re-transformed and reported as original data values. For the comparisons made in this section, P values  $< 0.05$  were considered to represent significant differences among the data. All graphs were plotted using Sigma Plot® software (Version 12.3, USA).

In Chapter 6 and 7, *in-vitro* digestion was carried out on a combination of starch and fibre suspensions among which the starch suspensions were gelatinised to different DG. The rate of starch digestion calculated over the 120 min (Chapter 6) and 20 min (Chapter 7) of *in-vitro* digestion were compared by fitting a common function to the pooled results for all treatments using CurveExpert software (Version 1.4) to determine whether all treatments showed a similar general form of digestion. The best fit describing the changes in starch concentration and viscosity with time was an exponential decay function of the form:

$$y = ae^{-(bx)} \quad (\text{Equation 3.10})$$

where

$a$  = the intercept of the y axis (starch or viscosity) at time = 0 (set to 100%);

$b$  = the coefficient of the slope (the rate of change with time);

$x$  = the elapsed time to a starch or viscosity value  $y$ .

The decline in the viscosity of the starch/fibre suspensions plateaued after about 20 min of digestion after which digestion proceeded at a much slower rate. Therefore, differences between individual treatments were plotted with transformed Ln-transformed proportional starch and viscosity values of for each treatment against time. Functions for the relative reduction in starch concentration were similarly calculated. The Ln-transformed proportional starch and viscosity values were fitted to a straight line of the form:

$$\text{Ln } y = \text{Ln } m + n \cdot \text{Ln } t \quad (\text{Equation 3.11})$$

where

$m$  is the intercept of the y axis (starch or viscosity) at time =0 (set to 100%) ;

$n$  is the coefficient of the slope (the rate of change with time);

$t$  is the elapsed time to a starch or viscosity value  $y$ .

The  $T_{1/2}$  values for starch digestion (the time taken to convert 50% of starch into sugars) and for the relative reduction in apparent viscosity (time taken to halve the apparent viscosity from the start value of 100%) were determined by substitution into Equation 3.11.

The relationship between the proportion of starch digested ( $a$ ) and the proportional viscosity ( $v$ ) was best described by the sigmoidal function that was fitted using Sigma Plot software:

$$Y = A + [(B) / (1 + \exp(-(s-C)/D))] \quad (\text{Equation 3.12})$$

where

$A$  = proportional viscosity at the minimum proportion of starch (in this case close to 0%);

$B$  = maximum proportion of starch that could be digested during the RDS phase (in this case close to 100%);

$C$  = inflection point at which the plot changes concavity (in this case near 80% starch remaining);

$D$  = slope coefficient;

$s$  = the proportion of starch at a given viscosity.

## Chapter 4 Quantification of water partitioned in undigested and digested dietary fibres

DRC 16



MASSEY UNIVERSITY  
GRADUATE RESEARCH SCHOOL

### STATEMENT OF CONTRIBUTION TO DOCTORAL THESIS CONTAINING PUBLICATIONS

(To appear at the end of each thesis chapter/section/appendix submitted as an article/paper or collected as an appendix at the end of the thesis)

We, the candidate and the candidate's Principal Supervisor, certify that all co-authors have consented to their work being included in the thesis and they have accepted the candidate's contribution as indicated below in the *Statement of Originality*.

Name of Candidate: Yap Sia Yen

Name/Title of Principal Supervisor: Prof. Roger Lentle

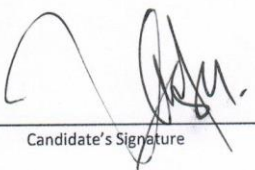
**Name of Published Research Output and full reference:**

Allan, K. Hardacre, Sia-Yen, Yap, Roger, G. Lentle, Patrick, W. M. Janssen, John, A. Monro. (2014). The partitioning of water in aggregates of undigested and digested dietary particles. *Food Chemistry*. 142: 446-454


In which Chapter is the Published Work: Chapter 4

Please indicate either:

- The percentage of the Published Work that was contributed by the candidate: 70%  
and / or
- Describe the contribution that the candidate has made to the Published Work:  
The candidate has carried out all lab work, data analysis and drafted the manuscript.

  
Candidate's Signature

4/10/16  
Date

  
Principal Supervisor's signature

4/10/16  
Date

#### **4.1. Abstract**

Two cellulose rich commercially available food fibres derived from wheat, a lignin rich wood fibre and a breakfast cereal fibre with high hemicellulose content were each hydrated before and after *in-vitro* digestion. The degree of hydration of the fibres was compared with fibre particles recovered from the colonic digesta of pigs and from human faeces. Total water and the extra- and intra-particulate water components were determined using a combination of centrifugation, drying, gas pycnometry and image analysis. The density of commercial wheat fibres before and after *in-vitro* amylolytic digestion were significantly greater ( $p > 0.05$ ) than that of 'as supplied' wood and AllBran® particles. The water of saturation ( $W_s$ ) of wood particles and AllBran®, measured after *in-vitro* digestion was up to double that of wheat fibres after *in-vitro* digestion, and increased with particle size and loss of soluble material following digestion, but was not associated with the chemical composition of the fibres. Fibre that had undergone *in-vitro* digestion, and that had been recovered from the colonic materials of pig or from human faeces, sequestered about 3% of the  $W_s$  into intra-particulate spaces, the remainder occupying extra-particulate spaces. Therefore, it is speculated that large quantities of fibre must be eaten to sequester toxins that locate into the intra-particulate space of dietary fibre.

#### **4.2. Introduction**

The human diet consists of solid and liquid materials. These materials are digested by enzymes as they traverse the gastrointestinal tract and the solubilised materials are absorbed through the gut wall. A substantial proportion of insoluble, non-nutrient solid material is voided as faeces. It is noteworthy that these insoluble particles may slow the mixing of digesta and the rate of digestion (Lentle & Janssen,

2008). However, they are believed to promote the gut health in the colon (Marlett et al., 2002). The consumption of large quantities of insoluble fibrous particles in the diet is associated with a lower incidence of colonic carcinoma (Larsson et al., 2005) and diverticulitis (Painter & Burkitt, 1971). The reduction in colonic carcinoma has been related to the ability of these particulate materials to sequester unconjugated bile acids and other potential carcinogens (Vahouny et al., 1980; Zacherl et al., 2011). The reduction in diverticulitis has been related to the ability of fibrous particles to retain water and to increase faecal bulk (Rezapour, Ali, & Stollman, 2017; William & Olmsted, 1936). Bulky but compressible colonic material facilitates peristaltic contraction and reduces intra-luminal pressure generated by the gut wall. Consequently, the movement of a plug of viscous digesta with high solid volume content in the colon may be improved by the flow of extra-particulate fluid associated with solid particulates (Lentle, Janssen, & Hume, 2009). However, if the digesta contains a high proportion of small, more or less spherical particles the flow of extra-particulate fluid may be reduced and prevent or slow flow in the digesta (Wrick et al., 1983).

Generally, there is a significant amount of vegetable matter in the remnant of solid components of digesta following enzymatic and fermentative digestion (Ehle, Robertson, & van Soest, 1982; Holloway, Tasman-Jones, & Lee, 1978). This material comprises a range of cellular residues that vary in size and shape but generally have a long axis much greater than the short. The chemical compositions of these components mainly comprised of cellulose in association with a variable amount of lignin. The ratio of cellulose to lignin depends on the type and amount of food consumed. The proportion of cellulose and lignin in cereals and vegetables

(Anderson & Bridges, 1988; Rani & Kawatra, 1994) is generally lesser than 4% on a dry weight basis (dwb), but may be up to 12% in asparagus and 25% in pears (Bunzel, Seiler, & Steinhart, 2005). More than 40% of the cellulose consumed may be fermented by colonic bacteria, but cellulose associated with lignin is less digestible (William & Olmsted, 1936).

Water held by the solid particles in digesta is located either in the extra-particulate or the intra-particular spaces (Eastwood & Morris, 1992). Extra-particulate water ( $W_E$ ) occupies the voids between the packed particles, whereas intra-particulate water ( $W_I$ ) occupies pores within the matrix of the particle and is associated with the chemical structures that form the particle surfaces. Therefore,  $W_I$  is less mobile than  $W_E$ . The reduction in the water content of digesta as it traverses the length of the colon (Lentle, Janssen, et al., 2009), is more likely the result of absorption from the  $W_E$  rather than from the intra-particulate fraction (Robertson & Eastwood, 1981b).

The relative proportions of  $W_E$  and  $W_I$  in compacted particles will vary with their permeability and the physical and chemical characteristics of the particles. The proportion of water in the particle mass varies with the size and shape distribution, and degree of compaction (Lentle & Janssen, 2008; Lentle, Janssen, et al., 2009). It is difficult to distinguish between  $W_E$  and  $W_I$ . In an intact particle, water may sequester in the lumen spaces within the cellular structures. However, when the intact walls of the particles are disrupted much of the intra-particulate fraction will be lost and the proportion of  $W_I$  will decrease (Ferguson & Harris, 1997). Conversely, water that is bonded to chemical structures on the surfaces of particles will not be freely exchangeable, and hence will be included as the intra-particulate



fraction. Grinding reduces the amount of  $W_I$  by destroying the cellular structures of the particles, but also reduces the amount of  $W_E$  as the small particles resulting from grinding occupy spaces between larger particles (Auffret et al., 1994).

Studies have suggested that bacterial toxins and deconjugated bile acids produced from digestion process may be bound to the matrices of dietary fibre by chemical or physical interactions (Florén & Nilsson, 1982; Robertson & Eastwood, 1981b) and a proportion of these substances may be sequestered into  $W_I$  (Story & Kritchevsky, 1976). Lignin-rich fibres were shown to adsorb more  $W_I$  at a given equilibrium humidity than fibres with a high cellulose content (Hill et al., 2008). Furthermore, comparisons of absorption/desorption isotherms of fibrous particles from a number of different sources (Hill et al., 2008) suggested that water binding capacity was directly related to the proportion of lignin. It is hypothesised that the crystallinity of cellulose rich particles have lower capacity for binding  $W_I$ , while lignin deposited between the cellulose microfibrils disrupted the crystalline structure of cellulose, forming micro-pores that are able to sequester about 5% it's weight of water at a relative humidity of 60% as shown in the absorption/desorption isotherms (Hill et al., 2008). Hence, the number of such pores and the characteristics of the surfaces within and between the particles are important in determining the WHC and binding of various solutes (Eastwood & Morris, 1992; Zuman, Ainso, Paden, & Pethica, 1988).

To date, there is a lack of study on quantifying the relative proportions of the  $W_E$  and  $W_I$  that associate with the finely milled particles commonly used in commercially formulated foods. Therefore, a range of fibrous particles that exhibited

differing degrees of lignification and that are of size distribution commonly found in foods were used to quantify the relative proportions of  $W_E$  and  $W_I$ . The effect of simulated gastric and small intestinal digestion of the particles on the relative proportions of these water fractions were examined and compared with those recovered from human faeces and pig digesta.

### **4.3. Materials and methods**

#### **4.3.1. *Proximate chemical compositions of fibre particulates***

The proportions of cellulose, hemicellulose and lignin in each of food fibres used were determined (Chapter 3, Section 3.3.).

#### **4.3.2. *Physical characteristics of fibre particulates***

The physical characteristics, including moisture content and water activity of all commercial fibre particles ‘as supplied’ and after *in-vitro* digestion were analysed (Chapter 3, Section 3.4.).

#### **4.3.3. *Particulates recovered from human faeces and pig digesta***

The solid particulates from human faecal and pig colon digesta samples were extracted and prepared for analysis (Chapter 3, Section 3.2.1.).

#### **4.3.4. *Selection of drying temperature for digesta particles***

The commercial fibre particles ‘as supplied’, contained low but significant amounts of moisture, typically between 6% and 8%, while fibre samples recovered from gut contents were saturated. Removal of this water by drying at 108°C caused irreversible changes in their ability to reabsorb water, which were not seen when

samples were dried at 40°C. Samples used for pycnometry measurements were therefore conducted on the undried ‘as supplied’ fibre. When drying was required, for example the samples subjected to *in-vitro* digestion and the solid particulates harvested from digesta, drying was carried out at 40°C to ensure that tightly bound water was not removed and that the rehydration properties of the fibres were retained.

Separate aliquots of all particle types were dried in a forced draft oven at 108°C to a constant weight for about 2 h to determine their ‘absolute’ moisture content (Chapter 3, Section 3.3.4). The water removed by drying at 108°C was tightly bound. When the tightly bound water was removed from the fibre particles, the volume of the fibres determined by pycnometry was reduced by 6.7%. Given the low  $A_w$  of the ‘as supplied’ fibres ( $A_w = 0.4\text{--}0.6$ ) and the high temperature required to remove this water, it is likely that the tightly bound water component in the ‘as supplied’ fibre is not available for the sequestration of gut solutes.

#### **4.3.5. *In-vitro* digestion of commercial fibre particles**

Each fibre particle sample used was subjected to *in-vitro* digestion (Chapter 3, Section 3.5.2.) for the removal of soluble fractions from food fibre, particularly sugars and starch. This step ensures that only indigestible fractions of fibre were retained for subsequent measurements.

#### **4.3.6. *SEM***

SEM micrographs of commercial fibre particles before and after *in-vitro* digestion were prepared (Chapter 3, Section 3.4.3.2.) and they were used to compare the

surface characteristics of different fibre materials and to determine surface changes resulting from *in-vitro* digestion.

#### **4.3.7.        *Light microscope***

Commercially available food fibres and solid particles recovered from human faeces and the colon digesta of pigs were prepared as described (Chapter 3, Section 3.4.3.1). All of these fibres were used in the following study (Section 4.3.8).

#### **4.3.8.        *Determination of the volume of fibre particles***

All fibre particles were initially stained with either safranin or aqueous toluidine blue O (Chapter 3, Section 3.4.3.1.) and were subsequently washed to remove excess stain after which they were subdivided into two aliquots. The first set of aliquots was dehydrated by passing through 50%, 70%, 90% and finally 98% (v/v) ethanol, the second set of aliquots was washed with water to ensure the particles were fully hydrated.

The calculated volume of water removed by drying of either the ‘as supplied’ fibres; the *in-vitro* digested fibre dried at 40°C; and the fibre recovered from the gut samples and dried at 40°C were further dried at 108°C and the dry volume of the fibres calculated from the volume of water removed (assuming the density of water is 1 g/mL).

The volumes of 1000 randomly selected images of individual particles, from each of the dehydrated and fully hydrated samples were calculated using a custom macro written for ImageJ (<http://www.rsb.info.nih.gov/ij/>) image analysis software. This

macro first skeletonised the image of each particle to derive its fundamental dimensions and subsequently calculated the volume of each particle as a series of connected cylinders, each of radius equal to the mean width of the particle and of length equal to the sum of the individual connected cylinders. All calculations assumed that the fibres were of circular section and that all of the volume of the dehydrated fibres was contributed by cell walls. The latter assumption may have led to small errors as some of the fibre particles could have contained internal voids. The particles were then assigned on the basis of their volume into one of five categories;  $0-10^4 \mu\text{m}^3$ ,  $10^4-10^5 \mu\text{m}^3$ ,  $10^5-10^6 \mu\text{m}^3$ ,  $10^6-10^7 \mu\text{m}^3$ , and  $>10^7 \mu\text{m}^3$ . The number of particles in each category was determined along with total particle volume.

#### **4.3.9. Determination of the water content of saturated particles**

##### **4.3.9.1. Water of saturation ( $W_s$ )**

Subsamples of 0.1 g of each of the four types of ‘as supplied’ and *in-vitro* digested fibre particles that were dried at 40°C were re-suspended in excess MilliQ water in 2 mL pre-weighed, capped centrifuge tubes for 24 h at 37°C to rehydrate the particles. The hydration time was chosen to mimic the estimated transit time of digesta in the human gut (Burkitt et al., 1972) and was sufficient to fully hydrate the particles (Robertson & Eastwood, 1981a). The fully hydrated particles were subsequently packed by centrifugation to form a clearly defined pellet in which it was presumed the volume of  $W_E$  was minimised. As particles from different plant sources varied in their physical and chemical properties, they required the application of differing centrifugation forces to achieve comparable packing (Cummings, Jenkins, & Wiggins, 1976; Eastwood & Mitchell, 1976). Hence the  $g$  force was progressively

increased until a clear line of separation formed between the compacted fibre pellet and the supernatant. WF600 and Prolux fibre particles required 3000 g for 20 min; wood particles and AllBran® 5000 g for 20 min and particles from pig digesta and human faeces 10,000 g for 20 min. The supernatant was subsequently decanted and the mass of the each fully hydrated pellets determined.

The water retained after centrifugation by the fully saturated particle mass in the pellet ( $W_s$ ) was calculated as the difference between the volume of the oven dried (108°C) fibres determined using gas pycnometry, and the volume of hydrated particles determined from the wet centrifuged pellets (assuming that the density of water was 1 g/mL). The  $W_s$  values for five pellets for each particle type (Waldern, 1971) were determined from which the mean and standard deviation were calculated.

#### **4.3.9.2.      *Water holding capacity (WHC)***

The WHC (Robertson & Eastwood, 1981b) of the pellets described above were determined after centrifugation at 6000 g for 15 min to remove weakly held water. Similarly, the WHC of cellulose fibres from cotton decreased as the centrifugation g force was increased to a maximum of 6500 g (Boulos et al., 2000). It was found that 6000 g was insufficient to precipitate all of the insoluble particles from suspensions of human faeces and pig digesta, hence WHC could not be determined for these materials.

### 4.3.9.3. *Intra-particulate and extra-particulate water*

The volume proportion of the fully saturated pellets occupied by  $W_E$  was calculated as the difference between  $W_S$  and the volume of the  $W_I$ . The proportion of  $W_I$  in fully hydrated particles was calculated as the difference in the volumes of fully hydrated and dehydrated particles. In each case the particle volumes of 5 replicates of 200 randomly selected hydrated and 200 randomly selected dehydrated particles were determined using image analysis.

The proportions of  $W_E$  and  $W_I$  were then calculated as a proportion of  $W_S$  using:

**Proportion of intra-particulate water =**

$$[(\text{Fully hydrated volume} - \text{dehydrated volume}) / \text{dehydrated volume} \times 100]$$

**(Equation 4.1)**

**Total intra-particulate water =**

$$\text{Weight of dry fibre used to determine } W_S \times \text{Volume \% of shrinkage}$$

**(Equation 4.2)**

$$\text{Total extra-particulate water} = W_S - \text{Total } W_I \quad \text{(Equation 4.3)}$$

### 4.3.10. *Statistical analysis*

Differences among the variables measured were compared statistically using one way ANOVA with Tukey's post-hoc comparisons between treatments calculated using the MINITAB Statistical Software suite (Chapter 3, Section 3.6). For Table 4.1, comparisons between the digestion treatments were made using the two sample t-test. Other details of data analysis were as described in Chapter 3, Section 3.6.

Graphs were plotted using Sigma Plot® software (Version 12.3, USA) or with Microsoft Excel.

#### 4.4. Results

##### 4.4.1. Chemical composition of fibre particles

The chemical composition of the “as supplied” fibre particles varied (Figure 4.1). The chemical compositions of cellulosic and wood fibres were mainly cellulose; whereas the AllBran® fibre composed of more than 70% soluble components.

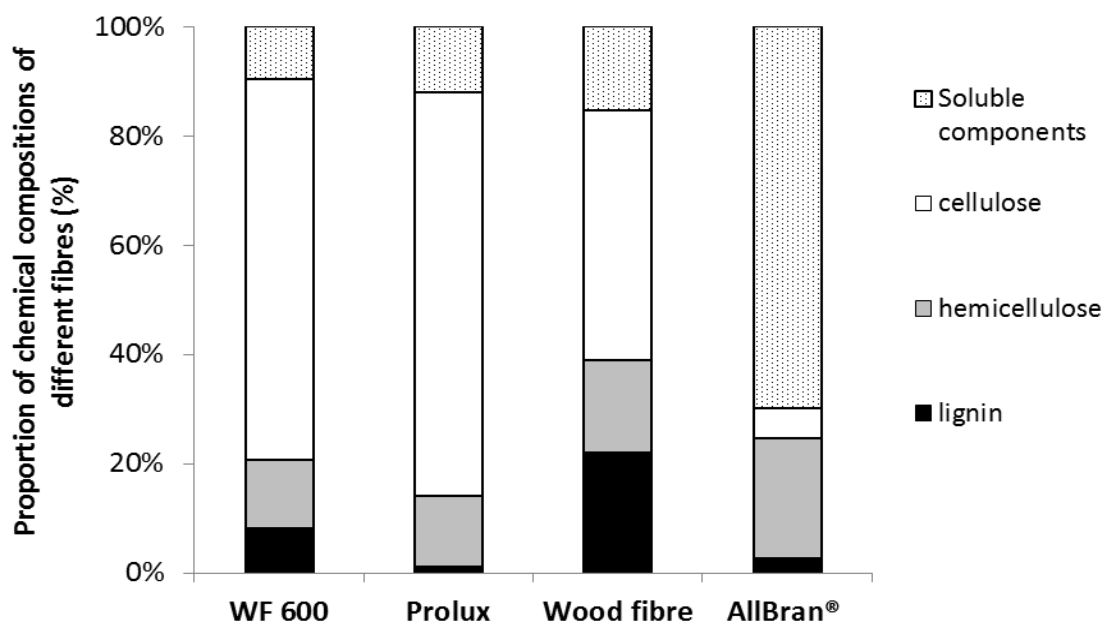


**Figure 4.1:** Chemical compositions of the “as supplied” fibre particles

Generally, the proportion of solubles was low and similar for the WF600 (~10%), Prolux (~12%) and wood particles (~15%), but the solubles (~70%) in AllBran® particles was about five to seven times greater than the particles used (Figures 4.1 and 4.2) and probably due to its formulation as a breakfast food. The soluble portion of fibres was lost during the *in-vitro* digestion process. After *in-vitro* digestion, the



chemical composition of AllBran® was different to the other fibre types with a much greater proportion of hemicellulose (Figure 4.2).

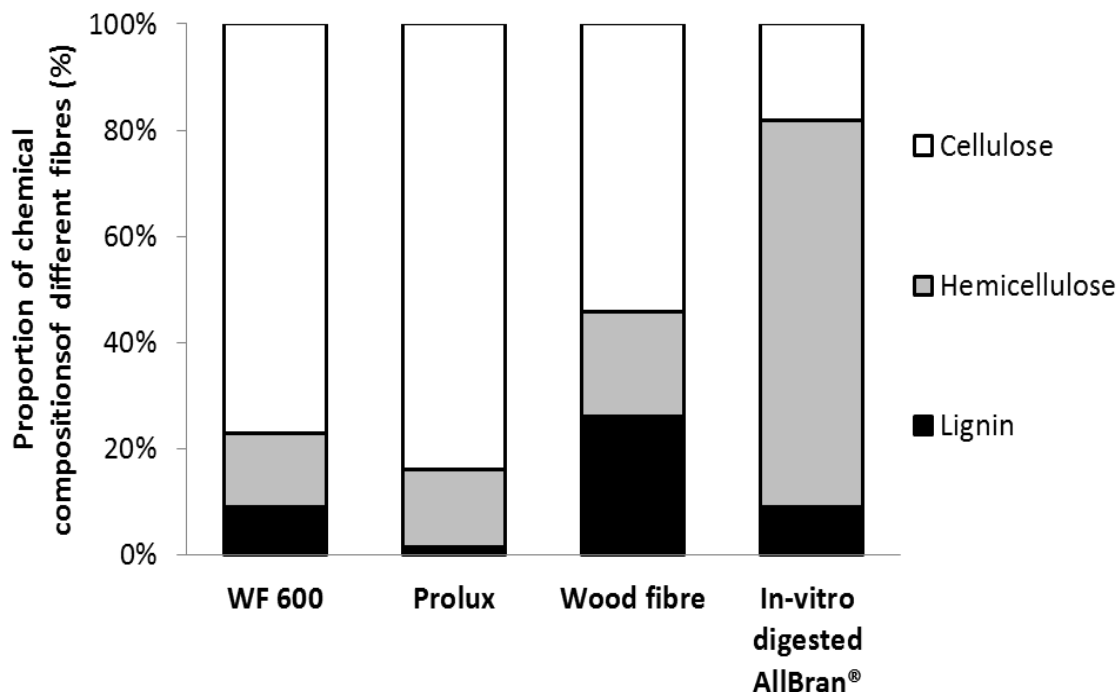


**Figure 4.2: Chemical compositions of the fibre particles after *in-vitro* digestion**

The chemical compositions of the two wheat fibres (WF600 and Prolux) were broadly similar before and after *in-vitro* digestion, although after removal of solubles by *in-vitro* digestion, more than 70% of the fibre component was cellulose and the proportion of lignin was low (Figures 4.1 and 4.2). The only exception was the ratio of lignin to cellulose for WF600 which was about seven times greater (1: 8.7) than that of the Prolux (1: 65.6) fibre. This result suggested that Prolux may have undergone chemical de-lignification during the manufacturing process, or it may have been derived from a different part of the wheat plant.

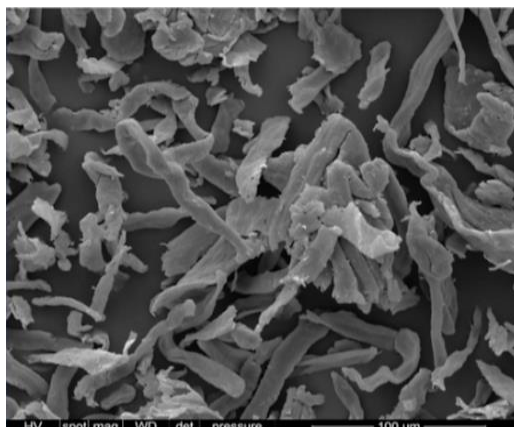
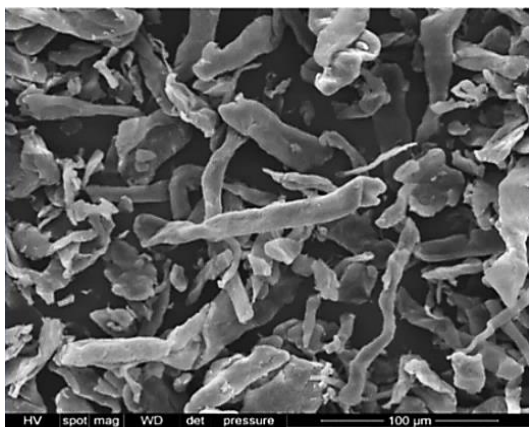
The wood particles were 26% lignin, which was the highest among the tested samples, and more than 20 times the lignin present in the Prolux particles. Since the proportions of lignin, cellulose, and hemicellulose; and the ratios of solubles to insolubles in these four fibres were different, the effects of these constituents on the fractions of  $W_E$  and  $W_I$  were measured before and after *in-vitro* digestion.

#### **4.4.2. Particle morphology**

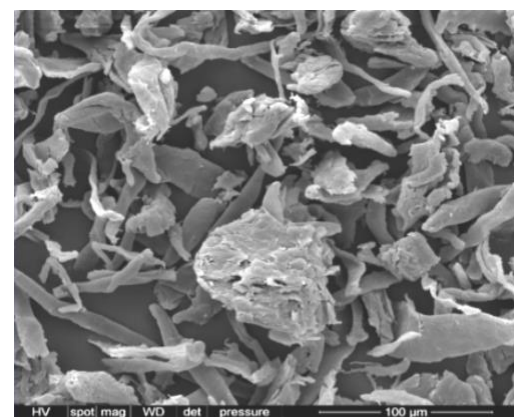
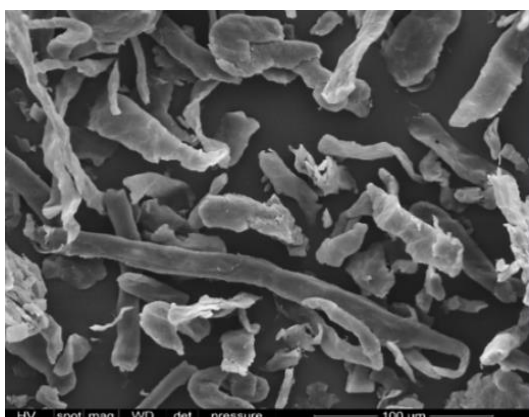
##### **4.4.2.1. Scanning electron micrographs**

WF600 and Prolux particles (Figures 4.3 a, b) had a relatively smooth surface, probably as a consequence of the process used to disaggregate the plant cells during preparation. Wood particles had a much rougher surface, presumably as a result of the mechanical grinding process used to form the particles (Figure 4.3 c). The AllBran® particles (Figure 4.3 d) were made from the tough bran layer covering the wheat grains and had a wide particle distribution size. After *in-vitro* digestion (Figure 4.3 d) which is presumed to remove all solubles and starch present, the bran particles were exposed along with internal voids of the cells comprising the bran. Conversely, *in-vitro* digestion had little effect on appearance of either the WF600 or the Prolux particles which contained relatively small proportions of soluble materials (Figures 4.1 and 4.2), although the surface texture of the wood particles appeared to be rougher following digestion.

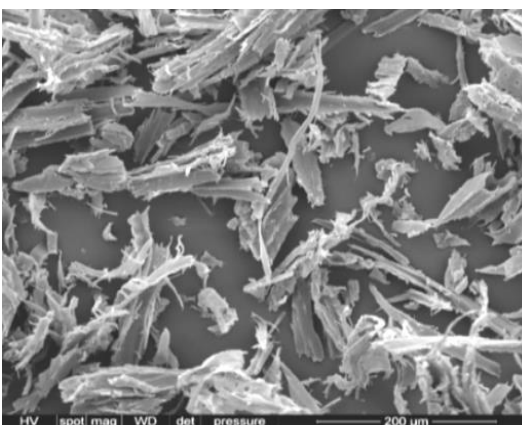
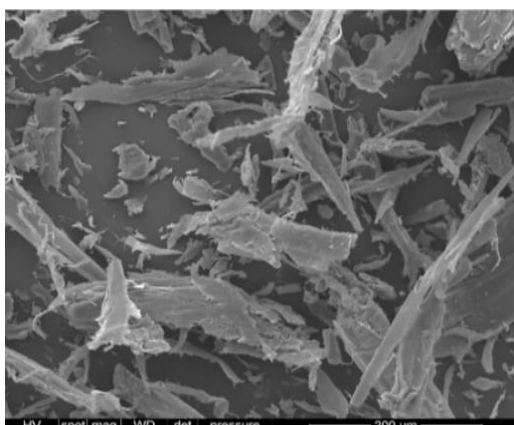
(a) WF600



(b) Prolux



(c) Wood



(d) AllBran®

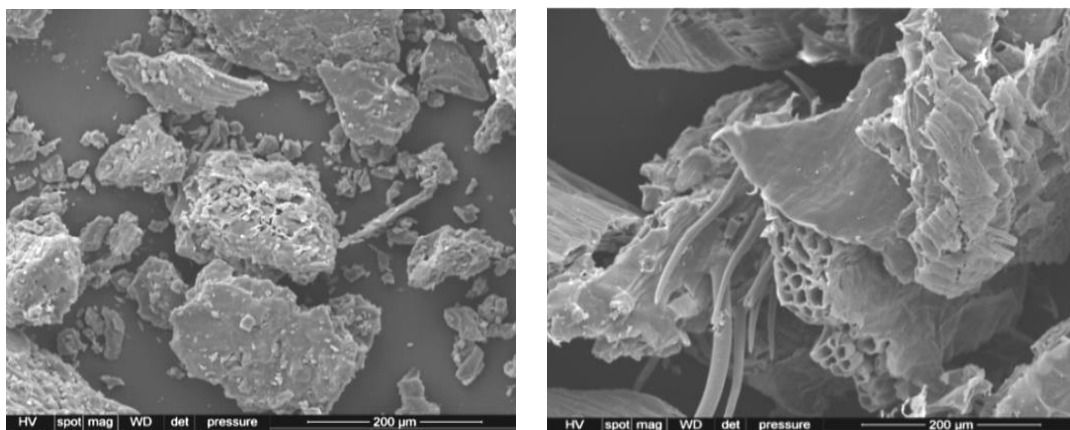
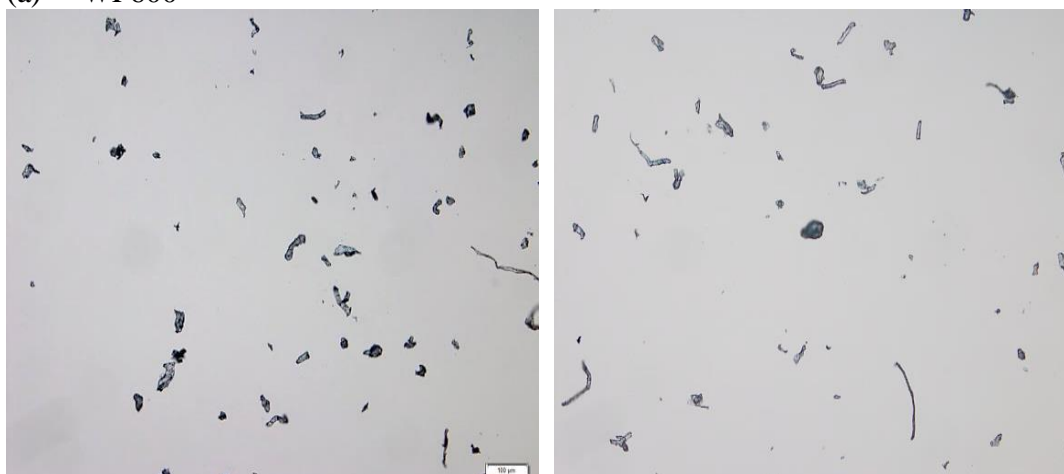


**Figure 4.3:** SEM images of the various commercial fibre particles used. Left column: commercial fibre particles ‘as supplied’; Right column: commercial fibre particles after *in-vitro* digestion.

#### 4.4.2.2. Light micrographs

The WF600 and Prolux particles were stained well with aqueous toluidine blue O to highlight the cellulose component. The particle sizes of these cellulosic fibres were smaller and more elongated in shape (Figures 4.4 a, b) than wood and AllBran® particles (Figures 4.4 c, d) and remained similar after *in-vitro* digestion (Figure 4.4).

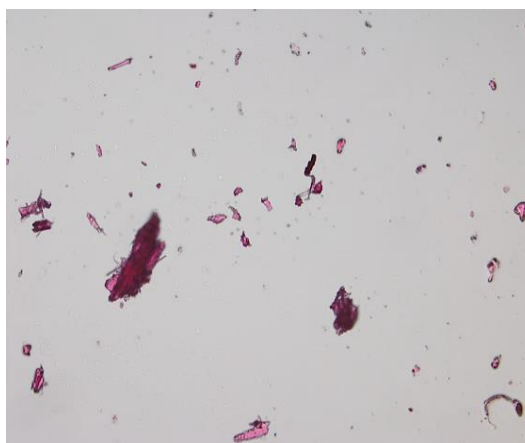
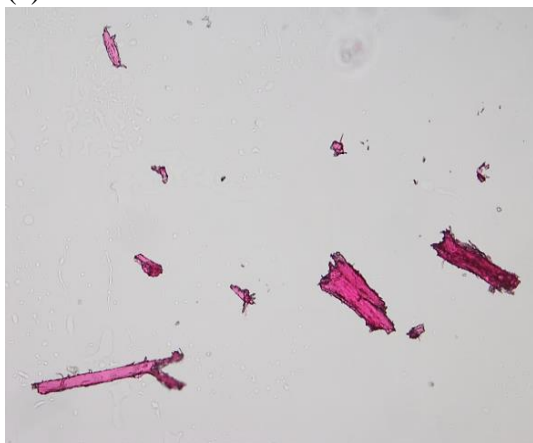
(a) WF600



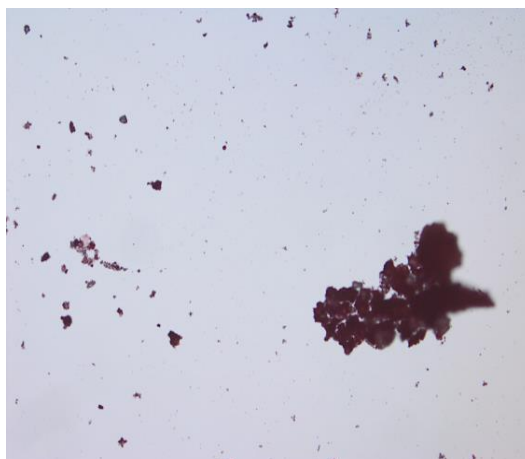
(b) Prolux



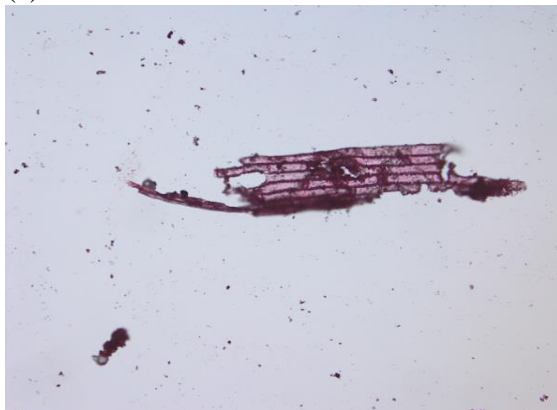
(c) Wood



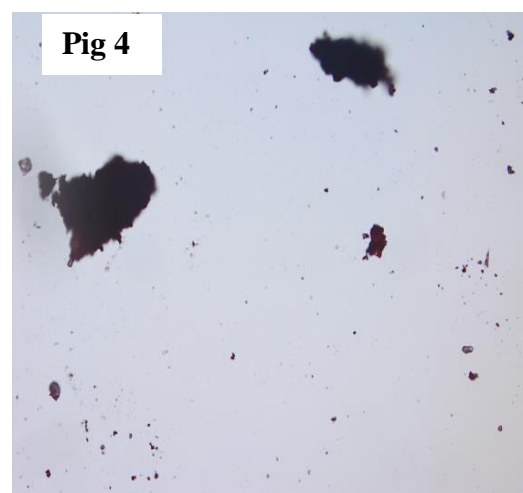
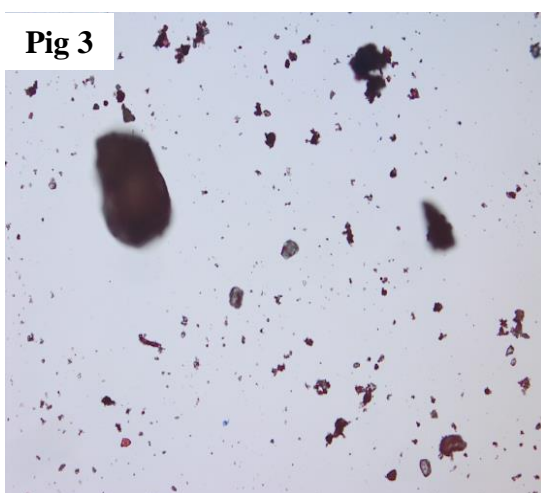
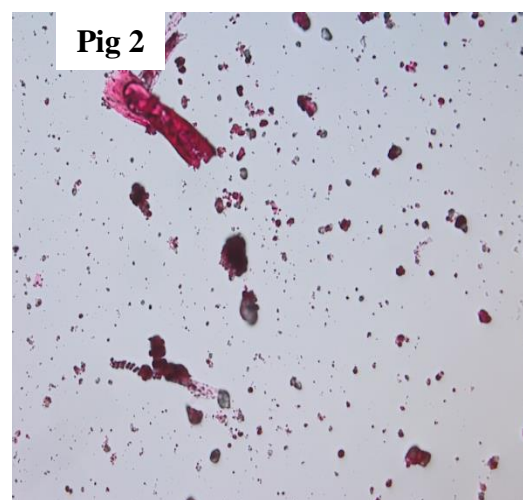
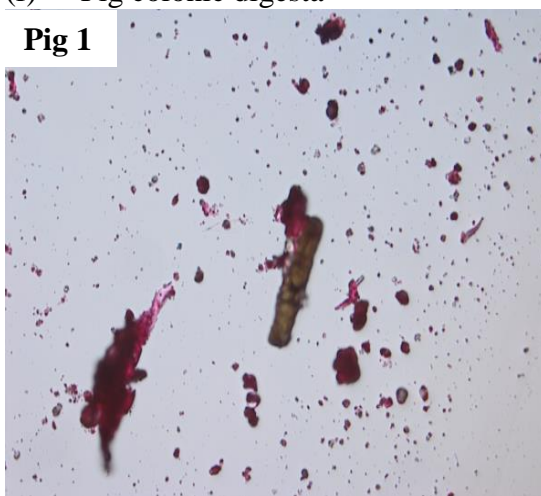
(d) AllBran®



(e) Human faecal materials recovered after high AllBran® diet



(f) Pig colonic digesta





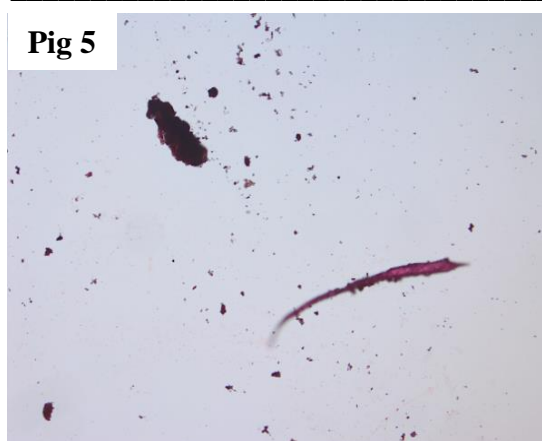
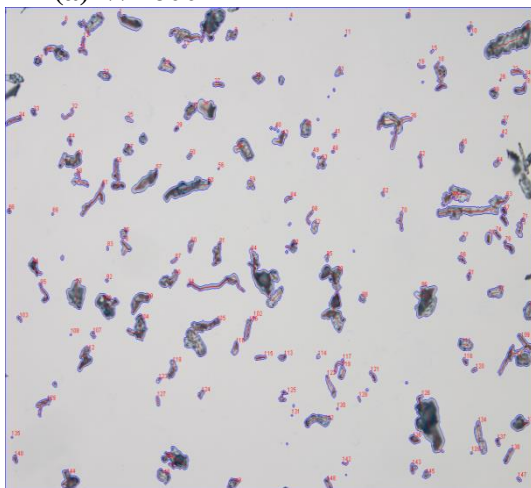


**Figure 4.4:** Light microscope images of (a) WF600 and (b) Prolux wheat fibres after staining with Toluidine blue O; particles from (c) wood, (d) AllBran®, (e) human faeces and (f) pig digesta were stained with safranin. For fibre particles from (a) to (d): (Left) commercial fibre particles ‘as supplied’; (Right) commercial fibre particles after *in-vitro* digestion. All photos were taken in the same scale as WF600.

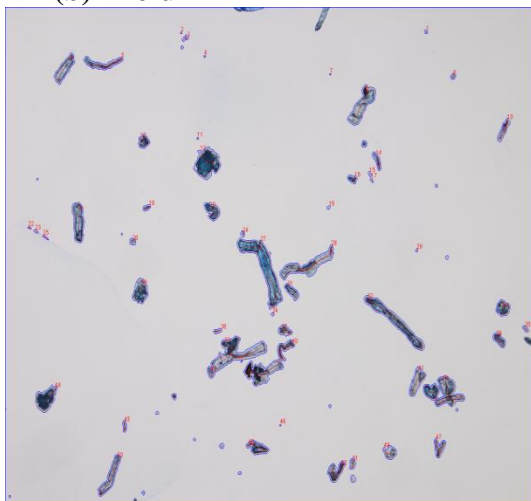
The particles of wood, AllBran®, and those recovered from the colonic materials of pig digesta and from human faeces were stained with safranin red, a lignin-specific dye, dissolved in aqueous ethanol (Figure 4.4). These results suggested that lignin content in these particles remained high even after digestion. This result is in accordance with assumption that the particles recovered from human faeces following a high AllBran® fibre diet was dominated by residues of AllBran® fibre (Chapter 3, Table 3.1). The sizes and shapes of these particles were diverse, and varied from smaller rectangular shape to the larger elongated shape (Figure 4.4).

The volumes of stained fibre particles and solid particles recovered from the pig digesta and human faeces were analysed using Image J software (Figures 4.5 a-f).

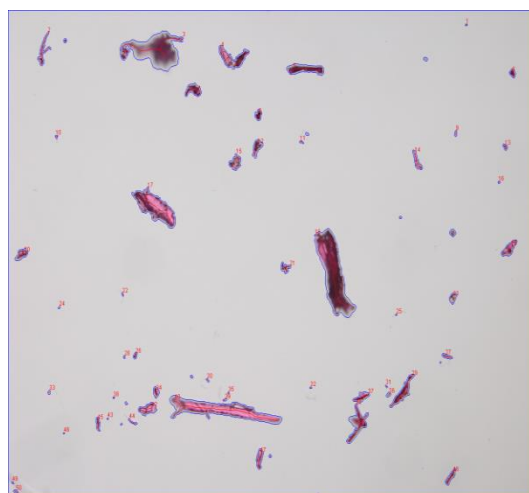
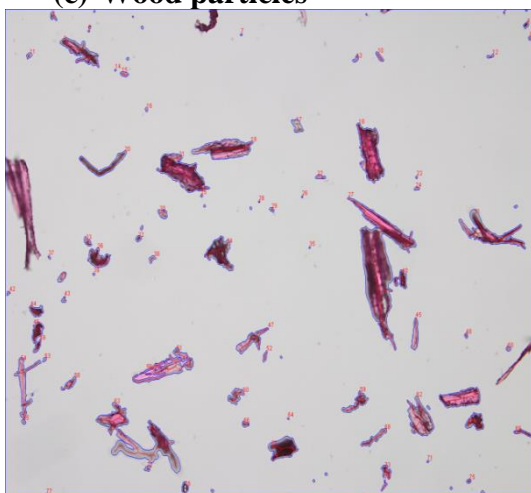
**(a) WF600**



**(b) Prolux**

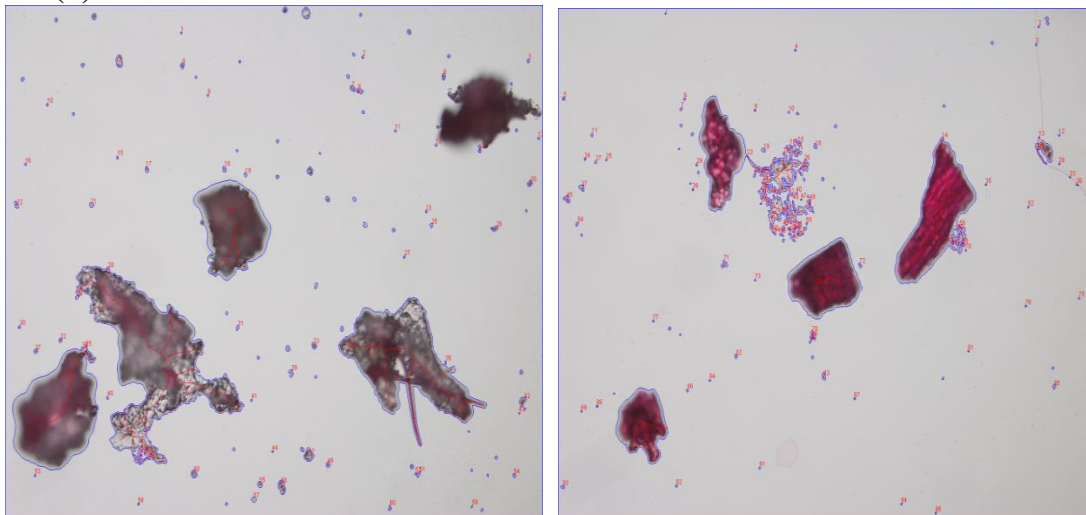


**(c) Wood particles**





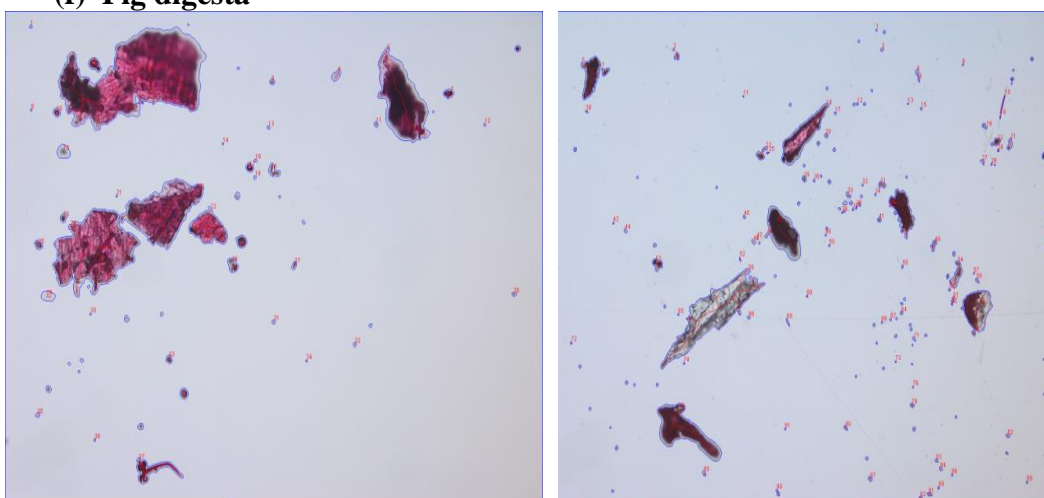
**(d) AllBran®**



**(e) Human faeces**



**(f) Pig digesta**



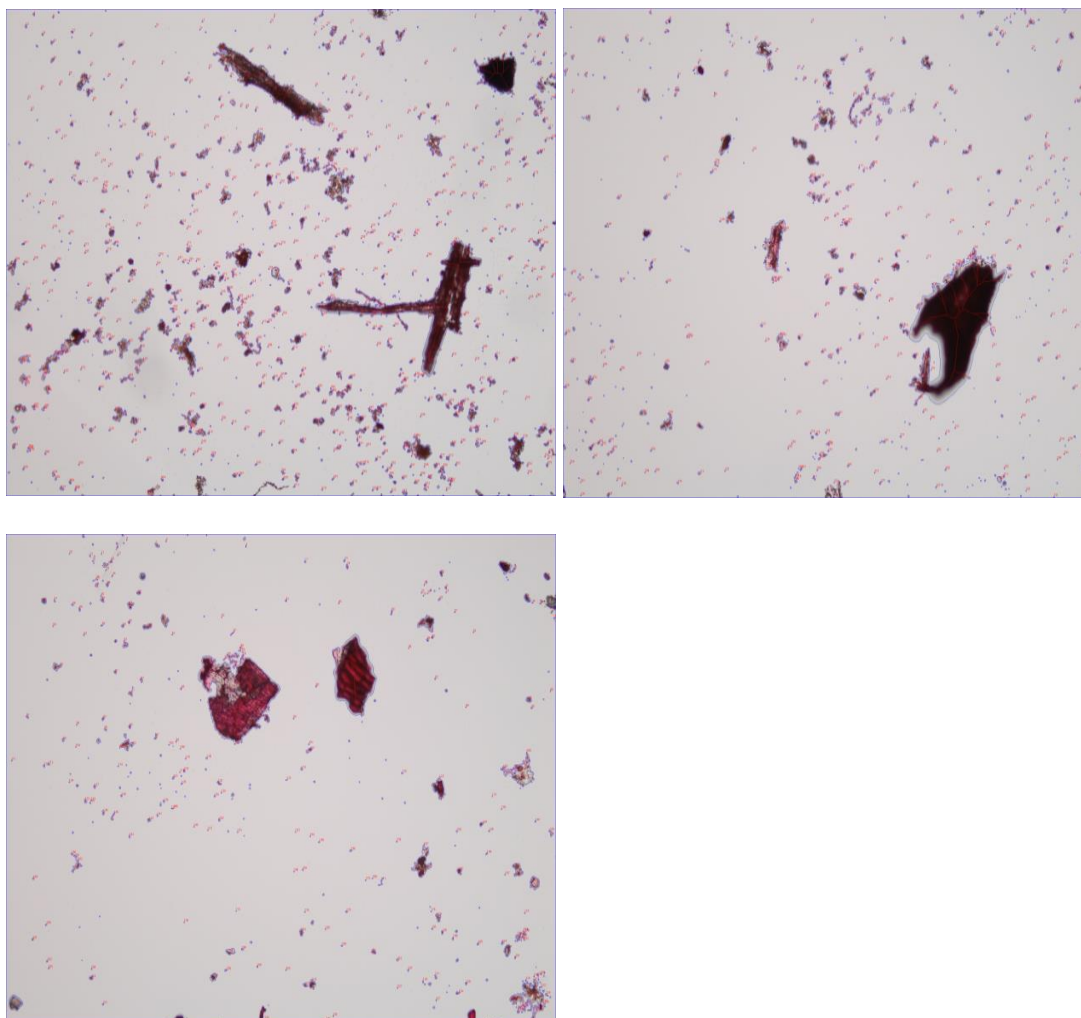


**Figure 4.5:** Light microscope images after analysis of volume using Image J software (a) WF600 and (b) Prolux wheat fibres after staining with Toluidine blue O; particles from (c) wood, (d) AllBran®, (e) human faeces and (f) pig digesta were stained with safranin. For fibre particles from (a) to (d): (Left) commercial fibre particles ‘as supplied’; (Right) commercial fibre particles after *in-vitro* digestion. All photos were taken in the same scale.

#### 4.4.3. *Distributions of particles*

##### 4.4.3.1. *Cumulative distribution of particles*

The volumes of each particle type was calculated from Image J analysis and plotted against the cumulative volume (Figures 4.6 a,b). Since the volume of cellulosic

wheat fibres (WF600 and Prolux) are way far too small to be identified on the same scale on the graph, therefore the results were replotted in Figure 4.6 b.

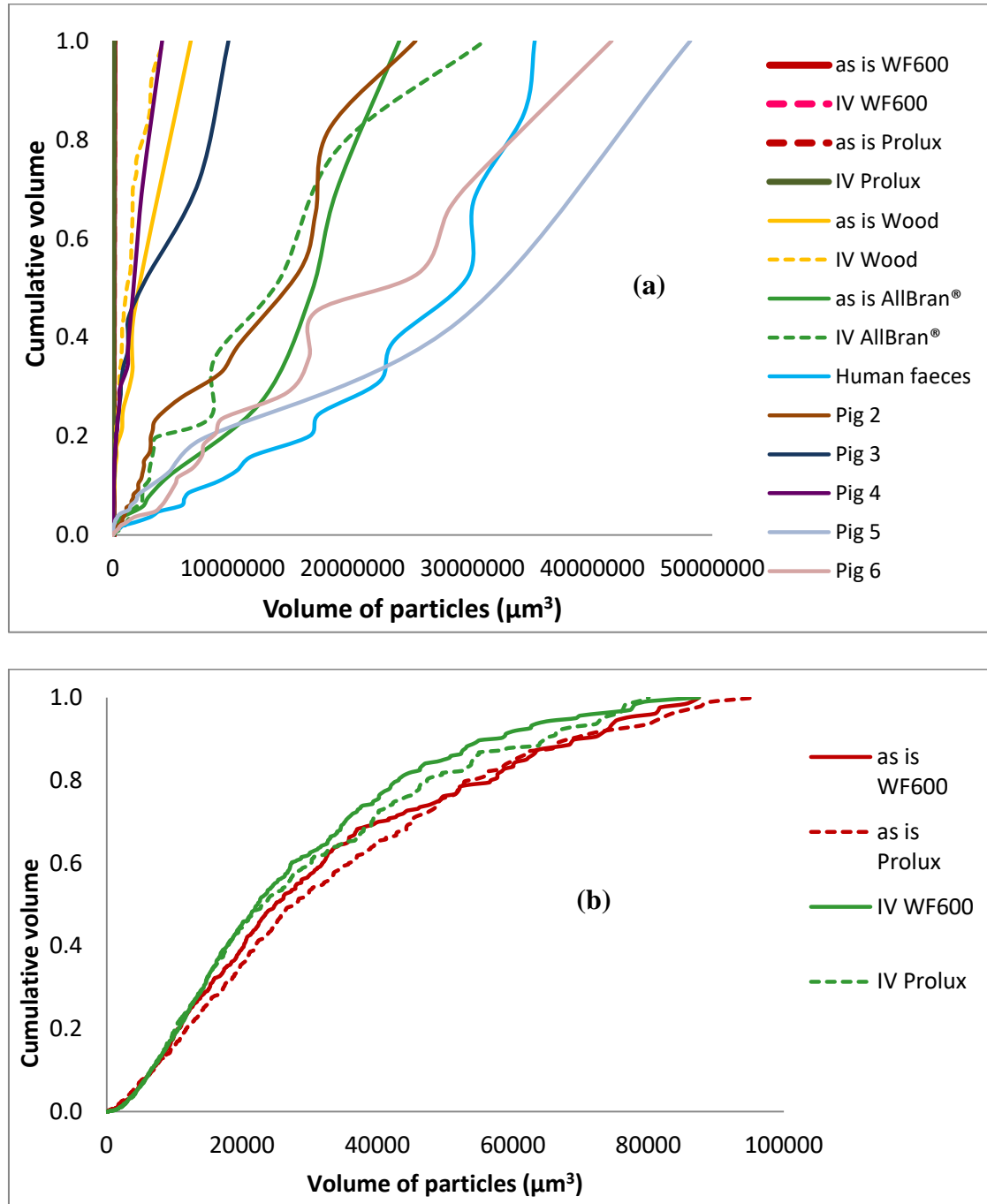


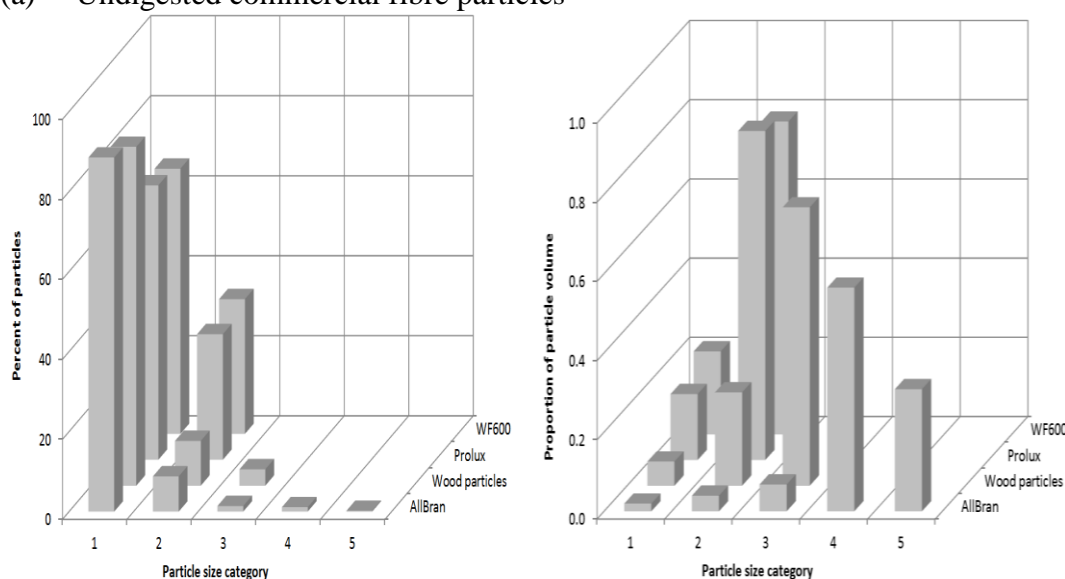
**Figure 4.6:** Volume of particles plotted against cumulative volume weighted from Image J analysis; (a) all commercial fibre types before and after *in-vitro* digestion (IV) and solid particles recovered from human faeces and pig digesta; (b) Cellulosic WF600 and Prolux wheat fibres before and after *in-vitro* digestion.

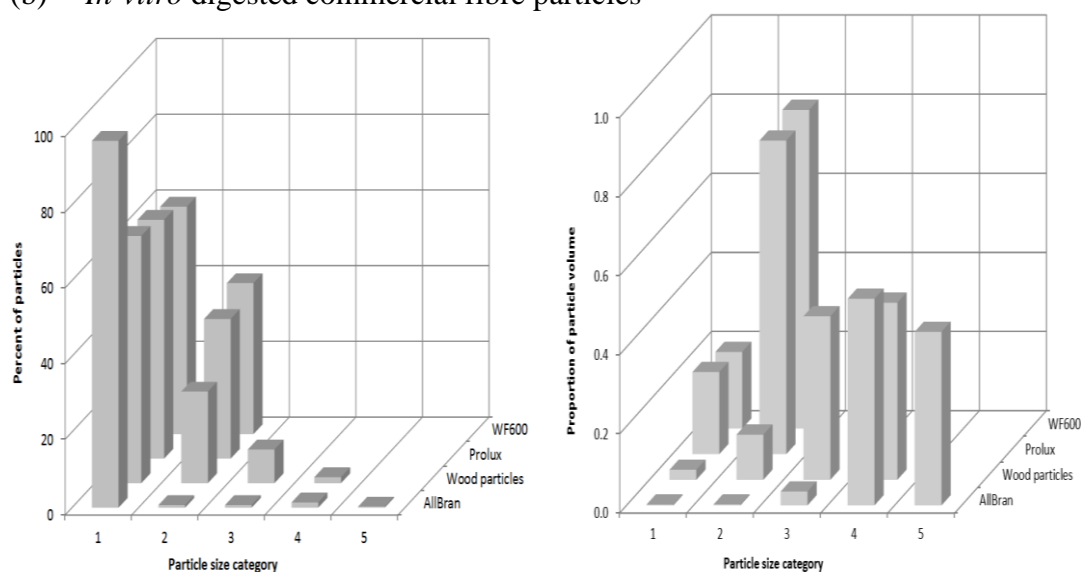
Volume of the commercial wheat fibre particles was smaller and the distribution was more uniform than the wood particles, AllBran® fibre and solids recovered from the human faeces and pig digesta (Figures 4.6 a, b). Therefore, to understand the pattern of distribution of these particles and the effect of digestion on the changes of particles volume, these particles were grouped into different categories according to their volume fractions (Section 4.4.3.2).

#### 4.4.3.2. *Distribution of particles volume*

All commercial fibre types contained more than 60% of small (category 1) particles (Figures 4.5 a–c, left), but they accounted for less than 20% of the total particle volume (Figures 4.5 a–c, right).

(a) Undigested commercial fibre particles



(b) *In-vitro* digested commercial fibre particles

## (c) Digesta fibres

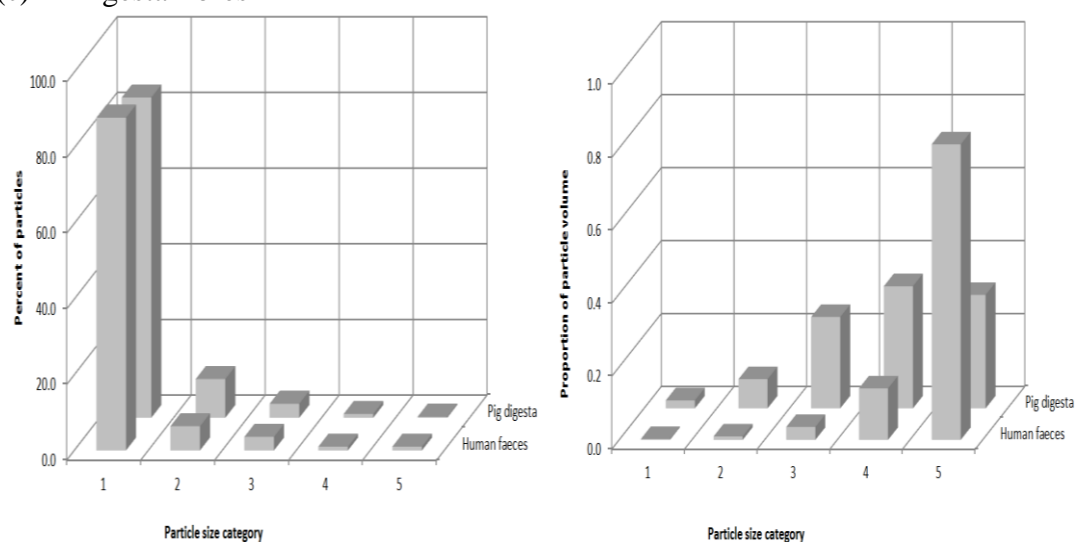


**Figure 4.7:** Percent of particles (left) and the proportion of particle volume (right) for each of the 5 size categories. (a) Commercial fibre particles before *in-vitro* digestion, (b) commercial fibre particles following *in-vitro* digestion, (c) Particles collected from colonic pig digesta and human faeces.

Generally, low numbers of large particles accounted for most of the volume of the hydrated fibre particles. For example, four particles in the largest size (category 5) of AllBran® (Figure 4.5 a, left) accounted for 30% of the volume fraction (Figures 4.5 a, right). Similarly, more than 80% of the particles isolated from pig digesta and

human faeces were of size category 1 (Figure 4.5 c), but less than 5% of the large particles in the sample accounted for 80% of the volume.

The distributions of the volume fractions of particles from digesta and faeces for all the size categories (Figure 4.5, right) were different from those of the commercially manufactured fibre particles. For the commercially sourced fibres, most of volume was represented by category 2 and 3 particles, while for particles from digesta and faeces most of the volume was represented by category 4 and 5 particles. Following *in-vitro* digestion the distributions of the size and volume fractions remained near identical except for AllBran® for which the number of particles in category 1 increased by about 8% and in category 5 the number decreased by about 20% (Figures 4.5 a and b).

#### **4.4.4. Particle density**

The density of the ‘as supplied’ WF600 particles ( $1.56 \text{ g/cm}^3$ ) determined by gas pycnometry was significantly ( $p < 0.05$ ) greater than density of the Prolux particles ( $1.53 \text{ g/cm}^3$ ). The densities of ‘as supplied’ WF600 and Prolux wheat fibre particles were lower than reported values for pure cellulose ( $\sim 1.60 \text{ g/cm}^3$ ), but greater than those reported for pure lignin (absolute density  $1.40 \text{ g/cm}^3$ ) (Walker, 2006).

The densities of the ‘as supplied’ wood particles ( $1.47 \text{ g/cm}^3$ ) and of particles from AllBran® after digestion ( $1.38 \text{ g/cm}^3$ ) were similar to those for the particles washed from human faeces (Table 4.1). The density of the solid particles isolated from the colonic digesta of pigs was 22% greater than that from human faecal material, perhaps due to the ingestion of small dense particles (possibly soil) with their diet.

The densities of all oven-dried commercial fibre particles were generally 5% to 6.5% higher than that of densities of the ‘as supplied’ particles (Table 4.1), with the exception of the *in-vitro* digested AllBran® particles where the density of the oven-dried material was 10% lower than the ‘as supplied’ counterpart. The density of particulates from human faeces and pig digesta dried at 40°C increased by 5.8% (human) and 2.8% (pig) after oven drying at 108°C.

#### **4.4.5. Hydration of particles**

The  $W_S$  values of pellets of the ‘as supplied’ WF600 and Prolux particles were similar (Table 4.1) and close to the values reported from previous studies which have been done on similar plant fibre materials (Rosell, Santos, & Collar, 2009; Sanchez-Alonso et al., 2006). The larger undigested wood and AllBran® fibre particles had  $W_S$  values 30% and 50% greater respectively than those of the wheat fibre particles. The  $W_S$  values for the WF600, Prolux and wood particles were largely unaltered following *in-vitro* digestion. However, the  $W_S$  value for larger AllBran® particles after *in-vitro* digestion was significantly greater ( $p < 0.05$ ) than all other commercial fibre particles.

The  $W_S$  values of the pellets of particles from the colonic digesta of pigs and from human faeces were greater than pellets of particles of Prolux and WF600, both before and after *in-vitro* digestion. However, these particles isolated from digesta and from human faeces had similar  $W_S$  values to those for the wood particles (Table 4.1). The  $W_S$  values are comparable to those reported for WHC (Robertson & Eastwood, 1981b). The variation in  $W_S$  values reported in this study was generally

lower than for WHC. For the reasons noted earlier, WHC could not be determined for particles from human or pig digesta.



**Table 4.1:** The hydration characteristics of centrifuged pellets of various fibres before and after *in-vitro* digestion.

Parameter	WF600		Prolux		Wood particles		AllBran®		Human faeces	Pig digesta
	'As supplied'	I-V digest	'As supplied'	I-V digest	'As supplied'	I-V digest	'As supplied'	I-V digest		
Fibre density, 'as supplied' (g/cm <sup>3</sup> )‡	1.56±0.01 <sup>a</sup> [1.53, 1.59]	1.57±0.01 <sup>a</sup> [1.55, 1.58]	1.53±0.02 <sup>b</sup> [1.50, 1.56]	1.54±0.02 <sup>b</sup> [1.52, 1.57]	1.46±0.02 <sup>c</sup> [1.43, 1.48]	1.47±0.02 <sup>c</sup> [1.46, 1.49]	1.34±0.02 <sup>d</sup> [1.31, 1.37]	1.38±0.02 <sup>d</sup> [1.36, 1.40]	1.44±0.02 <sup>^</sup> [1.42, 1.47]	1.75±0.25 <sup>^</sup> [2.01, 1.39]
Fibre density (108 °C) (g/cm <sup>3</sup> ) ‡	1.67±0.01 <sup>a</sup> [1.67, 1.68]	1.67±0.00 <sup>a</sup> [1.65, 1.69]	1.61±0.01 <sup>b</sup> [1.60, 1.62]	1.61±0.01 <sup>b</sup> [1.59, 1.62]	1.57±0.01 <sup>c</sup> [1.56, 1.59]	1.58±0.01 <sup>bc</sup> [1.57, 1.59]	1.49±0.02 <sup>e*</sup> [1.47, 1.52]	1.53±0.01 <sup>d*</sup> [1.51, 1.55]	1.53±0.02 [1.51, 1.55]	1.79±0.26 [2.07, 1.42]
W <sub>s</sub> (g water. g dry fibre <sup>-1</sup> ) †	4.93±0.09 <sup>d</sup> [3.95, 5.93]	5.08±0.07 <sup>d</sup> [4.00, 5.83]	4.89±0.01 <sup>d</sup> [3.46, 5.75]	4.73±0.10 <sup>d</sup> [3.66, 5.89]	6.60±0.07 <sup>bc</sup> [6.01, 7.68]	6.76±0.06 <sup>b</sup> [6.11, 7.50]	6.53±0.05 <sup>c*</sup> [6.04, 7.11]	10.34±0.12 <sup>a*</sup> [11.81, 8.74]	6.12±0.08 [5.27, 7.09]	5.60±0.62 [4.75, 6.35]
WHC (g water. g dry fibre <sup>-1</sup> ) †	4.75±0.33 <sup>d</sup> [4.32, 5.12]	4.96±0.31 <sup>d</sup> [4.67, 5.37]	4.23±0.29 <sup>d</sup> [3.81, 4.44]	4.41±0.43 <sup>d</sup> [4.02, 5.02]	6.43±0.35 <sup>bc</sup> [6.02, 6.83]	6.90±0.48 <sup>b</sup> [6.45, 7.57]	6.24±0.43 <sup>c*</sup> [5.69, 6.72]	8.00±0.35 <sup>a*</sup> [7.59, 8.41]	ND	ND

ND = not determined; 'As supplied' ("Undigested " particles); I-V digest (particles digested *in-vitro*)

‡ Values are means of five replicates samples dried at 108°C ± standard deviation

^ Values are means of five replicates samples dried at 40°C ± standard deviation

† Values are means of four replicates samples ± standard deviation

Numbers representing the range (±) are standard deviation from the mean value presented

<sup>a-c</sup> means in a row followed by different superscripts are significantly different (One way ANOVA and Tukey's pair wise test, p<0.05)

\* Values are significantly different (Two sample t-test, p<0.05) between the "as supplied" fibres and fibres after *in-vitro* digestion.

[LL , UL] Values are 95% confidence interval (CI) of lower limit (LL) and upper limit (UL) of samples mean value.

#### 4.4.6. Intra- and extra-particulate water

All of the particulates used in this study had a uniformly low proportion of  $W_I$  (<8%) relative to  $W_S$ , therefore more than 90% of water retained by the sample was in the  $W_E$  fraction (Table 4.2).

**Table 4.2: Relative proportions of dry matter,  $W_E$  and  $W_I$  in the water saturated centrifuged particle pellets prepared for the measurement of  $W_S$ .**

Fibre types	Relative proportions (%)		
	Dry matter	$W_I$	$W_E$
WF600	$15.51 \pm 3.21$	$4.34 \pm 0.99$	$80.15 \pm 4.20$
Digested WF600	$14.87 \pm 2.52$	$2.42 \pm 0.49$	$82.72 \pm 3.01$
Prolux	$15.92 \pm 4.09$	$4.48 \pm 0.97$	$79.61 \pm 5.04$
Digested Prolux	$16.45 \pm 3.73$	$2.72 \pm 0.65$	$80.83 \pm 4.37$
Wood particles	$11.96 \pm 0.56$	$3.33 \pm 0.22$	$84.71 \pm 0.72$
Digested wood particles	$11.53 \pm 0.44$	$2.70 \pm 0.22$	$85.77 \pm 0.58$
AllBran®	$12.73 \pm 0.47$	$7.83 \pm 0.84$	$79.44 \pm 1.06$
Digested AllBran®	$8.09 \pm 0.43$	$2.78 \pm 0.86$	$89.13 \pm 0.67$
Human faeces	$13.75 \pm 0.83$	$2.05 \pm 0.70$	$84.20 \pm 1.53$
Pig digesta	$5.19 \pm 0.70$	$2.33 \pm 0.68$	$92.49 \pm 1.30$

The proportion of  $W_I$  was lowest for the undigested wood particles (3.3%) followed by WF600 and Prolux particles (4.3% and 4.5% respectively). The ‘as supplied’ AllBran® particles had the greatest proportion of  $W_I$  (7.8%). The proportion of  $W_I$  in all particles was reduced after *in-vitro* digestion. AllBran® particles, which had the highest proportion of solubles (Figure 4.2) and the greatest proportion of large

particles (Figure 4.5), also had the greatest reduction in  $W_I$  (63%) following *in-vitro* digestion.

The reduction in  $W_I$  following *in-vitro* digestion was less for fibres that contained a lower proportion of solubles. Hence  $W_I$  for WF600 and Prolux particles was reduced by 40% and for wood particles by 19% following digestion. The proportion of  $W_I$  associated with particles isolated from digesta is uniformly low and remarkably similar to that from the fibre preparations after *in-vitro* digestion.

#### 4.5. Discussion

The true densities of the ‘as supplied’ WF600 and Prolux wheat particles determined by gas pycnometer (Figure 4.2, Table 4.1) were less than the reported density of pure cellulose ( $\sim 1.6 \text{ g/cm}^3$ ) (Walker, 2006) suggesting that the density of lignin is less than pure cellulose (Mwaikambo & Ansell, 2001). The densities of wood particles and particles of *in-vitro* digested AllBran® after drying at  $108^\circ\text{C}$  are similar to those of cellulose-based wood particles dried at  $105^\circ\text{C}$  (Stamm, 1929) and to solid particles recovered from human faeces (Table 4.1). The density of colonic solid particles of pigs was greater than reported values for pure lignin (Walker, 2006) and only a small variation in density resulted when the drying temperature was increased from  $40^\circ\text{C}$  to  $108^\circ\text{C}$ . These results suggested that solid material of high density, such as soil, may have been ingested with the food.

This study showed that the commercial fibre products used and the solid particulates from human and pig digesta can retain at least 80% of water when hydrated, even after centrifugation using sufficient  $g$  force to form a clearly defined pellet. Clearly,

the rigidity of the particles was sufficient to retain a high proportion of voids between the particles after centrifugation. Similarly,  $W_s$  was greater in particulate systems comprised of larger particles and this fits well with the hypothesis that the volume of the extra-particulate voids volume will increase when particles are larger (Auffret et al., 1994).

The centrifugation technique used to compact the particles from suspensions may not represent the compaction of particles in the digestive tract. However, this technique was valuable in determining the proportions of  $W_E$  and  $W_I$  in hydrated pellets. The proportion of water immobilised as  $W_E$  and  $W_I$  by the hydrated fibre comprising the pellet is expected to be much lower than that in the small intestine (Lentle, Stafford, et al., 2009). However, as the digest moves into the colon,  $W_E$  will be progressively reduced by the absorption of water at the gut wall (Lentle, Stafford, et al., 2009). The  $W_s$  of material recovered from the colon of pigs and from human faeces after washing and centrifugation were similar to that of centrifuged pellets of all the *in-vitro* digested fibres, except the *in-vitro* digested AllBran®. The  $W_s$  of the *in-vitro* digested AllBran® was about 70% to 85% higher than that of digesta from the colon of pigs and from human faeces (Table 4.1). Furthermore, the values for  $W_s$  obtained in this part of the study were broadly similar to the values obtained using the WHC method (Robertson & Eastwood, 1981b).

There was no relationship between either  $W_s$  or  $W_I$  and the proportion of lignin or cellulose in the particles, either before or after *in-vitro* digestion. Other work hypothesised that the hydrophobic nature of lignin (Eastwood, 1973) and the

crystalline structure of cellulose will reduce the WHC of particulate systems (Cadden, 1987; Hill et al., 2008; Stephen & Cummings, 1979).

The  $W_S$  determined using packing conditions developed in this study demonstrated that the  $W_I$  fraction was no more than 3% of  $W_S$  in pellets of any of the commercial fibre particle types examined, including particles that were recovered from digesta, and was therefore a relatively unimportant component of the water budget of the hydrated fibre. Using the centrifugation conditions optimised in this study, any significant variation in the  $W_S$  calculated for the food fibres or for undigested particles recovered from the human gut was assumed to be confined to the extra-particulate fraction. It is therefore reasonable to assume that the solid fraction of digesta can sequester no more than 3% of  $W_S$  as  $W_I$ .

If it is assumed that around 500 mL of chyme traverses the human colon in a day (Kanaghinis, Lubran, & Coghill, 1963), and this material contains between 86% and 77% moisture (Cummings & Macfarlane, 1991) it follows that 14% to 23% will be hydrated solid materials. The estimated daily loss of 3%  $W_I$  from these hydrated materials will be of the order of only 3.5 mL. In a healthy adult, 0.06 mmol/L bile acids (2-12 g/day) circulate in the body; of these, 95% reabsorb into the enterohepatic circulation and the remaining 5% (0.2-0.6 g/day) are excreted in faeces (Bajor, Gillberg, & Abrahamsson, 2010; Kullak-Ublick, Paumgartner, & Berr, 1995; Low-Beer & Pomare, 1973). Out of the maximum amount of total deconjugated bile that could be excreted in faeces (0.6 g), only 3% are able to be sequestered into  $W_I$  fraction, which is equivalent to about 0.0018 g deconjugated bile acids (Bajor et al., 2010), and this fraction is negligible. It is possible that a

proportion of deconjugated bile is held on the surfaces of lignified fibres via hydrophobic interactions (Eastwood et al., 1976; Hofmann, 1999), although *in-vivo* and *in-vitro* studies do not support this (Hillman et al., 1986; Zacherl et al., 2011).

Sequestration by binding to particles would seem to be the most important mechanism to sequester water and solubles, given the finding that the bulk of water held in association with fibre particles was extra-particulate and could move during gut activity. Such movement would allow the mass flow of nutrients including short chain fatty acids, and toxins such as deconjugated bile held in the gut contents, to interact with the intestinal mucosa. The reduction in the proportions of soluble material, the concomitant changes in the  $W_I$  and  $W_E$  fractions and the change in the various types of particles after *in-vitro* digestion, all shed some light on the mechanisms by which the particles hold water.

The decrease in  $W_I$  and large (> 60%) increase in  $W_E$  for the AllBran® particles after *in-vitro* digestion that removed the soluble component, suggests that the bulk of  $W_I$  was, for this product held in association with soluble material. The removal of this soluble material from the fibres creates voids which can then retain the  $W_E$  fraction of water associated with the AllBran®. For the other fibre products used, decrease in  $W_I$  and increases in  $W_E$  were smaller than for AllBran® as was the loss of solubles following *in-vitro* digestion. The smaller but proportionate decrease in the  $W_I$  and increase in  $W_E$  as a proportion of  $W_S$  in fibre particles with a lower proportion of solubles i.e. WF600 and Prolux following *in-vitro* digestion further supports this hypothesis.

---

#### 4.6. Conclusions

The novel combination of data from image analysis and gravimetric techniques used in this study provides new information regarding the distribution of the  $W_E$  and  $W_I$  components of  $W_S$  associated with fully hydrated insoluble fibres before and after *in-vitro* digestion. The  $W_S$  held in the centrifuged pellets of hydrated particles was greater in samples with larger mean particle size but did not vary systematically with the lignin or cellulose content. After solutes were removed by *in-vitro* digestion, the proportion of  $W_I$  was reduced to less than 3% of  $W_S$  regardless of the lignin or cellulose content. This small fraction  $W_I$  would be insufficient to dissolve, sequester, and excrete significant of dietary or biliary toxins.

The low proportion of  $W_I$  (less than 3%) means that about 97% of  $W_S$  of all of the insoluble fibre material assessed (commercial and digesta) is associated with the extra-particulate component. This result implies that most of the water present in the colon is mobile and hence available for moving solutes, such as fatty acids and non-organic ions during peristalsis, from the lumen to the gut wall for absorption. It is also likely that this water facilitates the mass flow of digesta from the small intestine to the colon. The high proportion of water trapped in extra-particulate voids between fibre particles will also aid in maintaining a high proportion of water in the stool. This  $W_E$  fraction bulks the stool, aids the movement of stool through the colon, and reduces the stool transit time. This is believed to have a protective effect against diverticulosis which is normally associated with long stool transit time and low stool volume.

Digestion of particles with high soluble contents decreased the proportion of  $W_I$  and for this reason the water fraction would be expected diminish in the distal gut. Therefore, very large amounts of coarse fibre must be consumed if significant quantities of toxins are to be sequestered in the  $W_I$ .



---

## **Chapter 5    The effect of the solid phase of digesta on the viscosity of digesta**

### **5.1.            Abstract**

The measurement of digesta viscosity is difficult due to settling and compositional changes that occur during digestion. The current work determined whether the relative viscosity ( $\eta_r$ ) of digesta could be accurately determined from DMC,  $\phi_{\max}$ , and  $\phi$  using the Maron-Pierce equation with  $\phi_{\max}$  being derived from the aspect ratios (Rs) of the particulate fraction.

The relationships between  $\eta_r$ , DMC, R,  $\phi$ , and  $\phi_{\max}$  were verified using data obtained from suspensions of plant fibres in a Newtonian liquid (70% aqueous fructose solution). The plant fibres were used after *in-vitro* digestion; in all cases the viscosity of the fibre suspension was similar to that of digesta from the small intestine of the pig.

The concentration of solids in all suspensions was expressed as DMC and  $\phi$ , which were quantified using a combination of centrifugation, washing, drying, and gas pycnometer. The Rs of spherical glass beads and the food fibres after *in-vitro* digestion varied between 1 and 6, determined using imaging analysis. Viscosity measurements were carried out in a rotation mode using cup and vane geometry at a shear rate of  $100 \text{ s}^{-1}$ . The relationship between the relative viscosity ( $\eta_r$ ), and the ratio  $\phi/\phi_{\max}$  was fitted using the Maron-Pierce equation (Equation 2.3).

Multiple stepwise regressions showed that the Maron-Pierce equation characterised the viscosity of digesta well, and strongly suggests that digesta behaves as a particulate suspension especially when  $\phi \leq 0.20$  or  $\phi/\phi_{\max} \leq 0.6$ . The predicted  $\eta_r$  and the measured  $\eta_r$  of the food fibres using Maron-Pierce equation were similar.

The  $\phi_{\max}$  was the only unknown in the Maron-Pierce equation and it is difficult to determine for a suspension with solid particles of different R. Therefore, a simpler empirical linear equation relating  $\phi_{\max}$  with R for the food fibres and glass bead suspensions was derived from Equation 2.6. It was found that  $\phi_{\max}$  could be accurately predicted from  $\phi_{\max} = 0.528 - 0.042 R$  with an  $R^2 = 0.99$ .

## 5.2. Introduction

Digesta from the small intestine comprises a suspension of macerated plant material (Lentle & Janssen, 2011) in a liquid with water like properties. The solid food residues are suspended in a continuous liquid phase containing various secretions from the gut (Lentle et al., 2008; Shelat et al., 2015). As the digesta traverses the small intestine, digestible solid food components and various liquids are reabsorbed into the blood stream, and the less digestible solids accumulate in the digesta. Therefore, the volume fraction of liquid decreases in proportion to the volume fraction of solid particles and the viscosity of the ileal digesta increases when it traverses the colon (McRorie et al., 2000).

The effect of solid particles in the solid phase on the viscosity of digesta is not well understood (Lentle et al., 2005; Takahashi et al., 2004). Solid particles in the

digesta vary in physical properties such as WHC, density, distribution of particle volume, size, and shape (Chapter 4); and chemical properties, such as content of cellulose, hemicellulose and lignin (Chapter 4). The density and chemical properties of these particles remained similar after *in-vitro* digestion, but not the particles volume distribution (Chapter 4). Viscosity of dog ileal digesta decreases from 17 Pa.s to 0.0008 Pa.s measured at  $1 \text{ s}^{-1}$ , after removal of solid particles by centrifugation at 12,000 g (Dikeman, Barry, et al., 2007); whereas the liquid phase of chicken cecal digesta was 0.0006 Pa.s (Razdan & Pettersson, 1996). These results suggested that the viscosity of a suspension which has similar solid particles to digesta is dependent on the solid volume fraction ( $\phi$ ) of particles suspended in the continuous phase (Lentle & Janssen, 2010).

Generally, the concentration of solid particles in digesta is reported as DMC (Piel et al., 2005; Takahashi et al., 2004; Takahashi & Sakata, 2004). The DMC of the intestinal contents of chickens increased by 17.5% as it traversed from the fore gut to the colon and the viscosity of digesta increased from 1.2 Pa.s to 73 Pa.s measured at a shear rate of  $1 \text{ s}^{-1}$  (Takahashi et al., 2004). Viscosity of digesta does not increase linearly with DMC, but in a power law function with DMC (Lentle, Stafford, et al., 2009). This relationship resembles that of solid particle suspensions in which the viscosity is proportional to  $\phi/\phi_{\max}$  (Chapter 2.3.2.2., Equation 2.3, the Maron-Pierce equation ( $\eta_r = (1 - \phi/\phi_{\max})^{-2}$ )). The Maron-Pierce equation was derived for solid spherical particles suspended in a Newtonian liquid (monodisperse system) and where the whole suspension is Newtonian measured over the high shear or low shear plateaus (Figure 2.11) (Krieger & Dougherty, 1959). However, solid particles

of digesta may be elastic and are not spherical and for this reason this section of the work seeks to determine if the Maron-Pierce equation can be used to model the viscosity of digesta.

Digesta contains solid particles of varying shape, in which this variation could be simplified in a single measurement known as aspect ratio (R) (Chapter 2, Section 2.3.2.3.). It is considered as a polydisperse system where the smaller particles are trapped in voids between larger particles (Lentle & Janssen, 2008, 2010; Takahashi & Sakata, 2004). Differences in R values of solid particles in a suspension may give different arrangement and packing in a polydisperse suspension and hence the  $\phi_{\max}$  of the solid particles in the suspension (Probstein, Sengun, & Tseng, 1994; Wierenge & Philipse, 1996). The relative viscosity ( $\eta_r = \eta_a/\eta_s$ , where  $\eta_a$  is apparent viscosity and  $\eta_s$  is the viscosity of the liquid phase in which the particles are suspended), of a polydisperse suspension is similar to that of a monodisperse suspension when measured in the high shear region ( $\geq 100 \text{ s}^{-1}$ ) (Probstein et al., 1994).

The R values of solid particles in digesta vary with diet (Guerin et al., 2001; Lentle & Janssen, 2010), and they range from 2 to 8 as quantified by image analysis software for animals fed with a high plant fibre diet (Jalali, Nørgaard, Weisbjerg, & Nadeau, 2012; Jalali, Nørgaard, Weisbjerg, & Nielsen, 2012; Krämer et al., 2013). The  $\phi_{\max}$  of a particulate suspension can be estimated from the average of the R values of the solid particles it contains (Pabst, Berthold, et al., 2006) by substituting these R values into the Equation 2.6 (Pabst, Berthold, et al., 2006).

The objective of this study was to determine whether the whole digesta resembles a particulate suspension and whether the relative viscosities of digesta could be accurately determined from  $\phi_{\max}$  and  $\phi$  using the Maron-Pierce equation where  $\phi_{\max}$  was derived from the aspect ratios (R) of the particulate fraction using empirical data.

### **5.3. Materials and Methods**

#### **5.3.1. Solid particles**

The sources and physical characteristics of the glass beads, and four food- and plant-derived fibres used in the test suspensions were described earlier (Chapter 3, Section 3.2), along with the procedures for recovering and describing particles from digesta (Chapter 3, Section 3.2.1.).

The suspensions of spherical rigid glass beads with a density of 2.49 g/cm<sup>3</sup> and a mean diameter of 75 nm and R close to 1. These particles, although quite unlike those of digesta and the fibres used in this work, are a commonly used reference material in work of this nature (Kitano et al., 1981; Mueller et al., 2010). Food fibres were subjected to 2 h of *in-vitro* digestion with porcine pancreatin at 37°C to remove soluble materials and starch associated with these fibres (Chapter 3, Section 3.5.1.).

#### **5.3.2. Dry matter contents (DMC)**

Frozen digesta samples collected from the proximal and distal small intestine of pigs were thawed to room temperature, sieved, and washed according to the method

described in Chapter 3, Section 3.2.1. Two grams of each of these digesta samples was dried at 40°C to a constant weight (14 to 18 days depending on the moisture content of the digesta). The dried digesta were weighed and their dried weights were recorded as DMC.

### **5.3.3. Density of solid particles from pig digesta**

Each of the true volume of the dried solid particles isolated from ileal pig digesta was measured using gas pycnometer (Chapter 3, Section 3.4.1.). The densities of these samples were then calculated (Equation 3.6).

### **5.3.4. Solid volume fraction ( $\phi$ )**

It was assumed that the continuous phase of digesta is a Newtonian fluid with a density close to that of water, in which solid particles are suspended (Chapter 3, Sections 3.4.1. and 3.4.2.). The  $\phi$  of digesta is the sum of the volumes of the solid components and it was calculated from:

$$\phi = [(m_s / d_s) / V_l] \quad (\text{Equation 5.1})$$

where

$m_s$  = mass of hydrated solids;

$d_s$  is the mean density of the solids;

$V_l$  = the volume of suspending liquid per unit volume of digesta.

### **5.3.5. Apparent viscosity of pig digesta**

The apparent viscosity of the approximate 40 mL digesta collected from the small intestine was measured in duplicate using a dynamic stress rheometer (model

Rheometrics SR500, Rheometric Instruments, Piscataway, New Jersey, USA) equipped with cup (32 mm) and six blade vane geometry 32 mm in length and 29.5 mm swept diameter. The samples were maintained at 37°C throughout each experiment and care was taken to ensure settling of the suspensions did not occur during the measurement period. Suspensions of each of the ileal digesta were pre-sheared at 0.1 s<sup>-1</sup> for 5 min (Marti et al., 2005), then the shear rate was ramped from 0 s<sup>-1</sup> to 100 s<sup>-1</sup> over 60 s, maintained at 100 s<sup>-1</sup> for 120 s, and finally returned to 0 s<sup>-1</sup> over 60 s. Each determination was repeated twice for each digesta sample used for this work.

### 5.3.6. *Fitting the Maron-Pierce equation for fibre and glass bead suspensions*

Suspensions of each of the particle types with various values of  $\phi$  were used to determine the relationship between  $\eta_r$  and  $\phi/\phi_{\max}$  and its fit to the Maron-Pierce equation ( $\eta_r = (1 - \phi/\phi_{\max})^{-2}$ ) (Equation 2.3). Food fibre samples after *in-vitro* digestion were made into aqueous 70% fructose suspensions with a viscosity of 0.032 Pa.s. The glass beads suspensions were prepared with concentration ( $\phi$ ) of 0.10, 0.20, 0.30, and 0.35, and suspensions of the various food fibres after subjected to *in-vitro* digestion with  $\phi$  of 0.01, 0.02, 0.05, 0.10, 0.15, and 0.20. Due to the differences in  $\phi_{\max}$  for the various particle types, the  $\phi$  resulted in values for  $\phi/\phi_{\max}$  between 0 and 0.73 for glass beads and 0 and 0.71 for the fibre suspensions (Figure 5.3).

Suspensions of each of the particle types with various values of  $\phi$  were pre-sheared at 0.1 s<sup>-1</sup> for 5 min (Marti et al., 2005), then the shear rate was ramped from 0 s<sup>-1</sup> to

100 s<sup>-1</sup> over 60 s, maintained at 100 s<sup>-1</sup> for 120 s, and finally returned to 0 s<sup>-1</sup> over 60 s. When viscosities were measured in the high shear rate range, the following assumptions were made (Folgar & Tucker III, 1984; Pabst, Gregorova, et al., 2006):

1. The fibre particles were sufficiently large that Brownian motion was negligible and other factors including electrostatic and van der Waals forces were also negligible.
2. The Newtonian 70% (w/v) fructose solution was sufficiently viscous to maintain the particles in suspension for the period required for the accurate determination of  $\eta_r$  at the shear rate of 100 s<sup>-1</sup>.
3. There was no wall slip effect in the rheometer.
4. The aspect ratio (R) of fibre particles can be used to predict  $\eta_r$  with appropriate constants.
5. Only whole suspensions demonstrating Newtonian properties at shear rate of 100 s<sup>-1</sup> were selected for fitting into the Equation 2.3.

The Maron-Pierce equation (Equation 2.3) was developed using the high shear rate of 100 s<sup>-1</sup>, whereas this shear rate was also used in this work to fit into the equation. Highly viscous suspensions demonstrated a more solid-like property when sheared at low shear rate, e.g. at 0.1 s<sup>-1</sup> within a short period of measuring time (Barnes, 1989). At a very low shear rate, the viscosity of a suspension is independent to shear rate (Newtonian). The constant viscosity that prevails at the low shear rates is called the zero-shear viscosity. Viscous suspensions that demonstrate yield stress are unable to be measured by a rheometer in the zero shear viscosity range. Hence,



it is unavoidable to measure the viscosities at higher shear rate to fit the results into Equation 5.2.

Although the high shear rate mixes the suspensions vigorously and will be applying enormous amount more force than the gut can apply to produce the same shear rate. Studies reported that  $\eta_r$  values derived from Maron-Pierce model using suspensions containing solid particles with Rs ranging from 1 to 5 were varied from 3% to 8% when ramp tests were performed at  $0.03 \text{ s}^{-1}$  to  $12 \text{ s}^{-1}$  (Mueller, Llewellyn, & Mader, 2011; Mueller et al., 2010) and at  $1000 \text{ s}^{-1}$  (Pabst, Gregorova, et al., 2006). In this study, the average relative errors (%) (Equation 5.2) for  $\eta_r$  fitted into Maron-Pierce equation were ranging from 3.5% to 8.4% (Table 5.2), and these values were similar to the values reported in similar studies (Mueller et al., 2011; Mueller et al., 2010; Pabst, Gregorova, et al., 2006).

**Average relative error = (A / B) x 100 (Equation 5.2)**

A = average of absolute errors,

B = average values of relative viscosities

Plots of  $\eta_r$  against  $\phi/\phi_{\max}$  for the various fibres at various values of  $\phi$  were fitted using the Maron-Pierce model. Subsequently,  $\eta_r$  and  $\eta_a$  were calculated for the values of  $\phi$  determined for porcine small intestinal digesta using the Maron-Pierce equation. The calculated values for  $\eta_r$  and  $\eta_a$  were finally compared with measured values of  $\eta_a$  for both fibre and digesta suspensions.

### 5.3.7. *Image analysis*

The preparation of solid particles recovered from the pig digesta was described in detail elsewhere (Chapter 3, Section 3.4.3.1.). The images of these particles were obtained using an Olympus BX53 microscope (Tokyo, Japan) equipped with a digital camera and “cellSens life sciences” research imaging software (Olympus, Tokyo, Japan) (Chapter 4, Section 4.3.8). Fibre volume was calculated from length and width assuming that all fibres were of uniform circular cross section. However it is impossible from the two dimensional images to tell if the ‘width’ recorded was a large or small axis and it was assumed from the large number of particles assessed (1000) for each fibre type that sufficient particles were measured to capture such variation.

Glass beads are unstainable using staining materials that were used to stain fibre particles and poor quality images were obtained from the contrast techniques of light microscopy; hence, the morphology of glass beads was assessed by scanning electron microscopy (SEM) (Chapter 3, Section 3.4.4.2.).

### 5.3.8. *Data analysis*

The various values for  $\phi_{\max}$  obtained for each of the test fibres were calculated from the raw data (Figure 5.3) using a rearrangement of the Maron-Pierce equation. Hence, using the experimentally determined values of  $\phi$  (Chapter 3, Section 3.4.1.) and values for  $\eta_r$  derived from  $\eta_r = \eta_a/\eta_s$  obtained at a shear rate of  $100 \text{ s}^{-1}$ ,  $\phi_{\max}$  is given by the reciprocal of the slope coefficient obtained from the simple linear regression of  $(1 - \sqrt{1/\eta_r})$  against  $\phi$  using SYSTAT software (Version 12, USA).

The calculated values of  $\phi_{\max}$  were then regressed against the corresponding experimentally determined values of  $R(X)$  (Figure 5.4) and the coefficients for the slope ( $m$ ) and intercept ( $c$ ) determined, hence  $\phi_{\max} = c - mX$  (Equation 2.4). These same coefficients ( $c$  and  $m$ ) were then used to predict  $\phi_{\max}$  for each of the samples of pig digesta from the mean of experimentally determined values for the  $R$  derived from image analysis.

The calculated values for  $\phi_{\max}$  (above) and the experimentally determined values for  $\phi$  based on estimations of fibre volume using image analysis were substituted into the Maron-Pierce equation (Equation 2.3) to predict the relative viscosity of pig digesta ( $\eta_r$ ). Finally, the predicted values for  $\eta_r$  were compared by simple linear regression against the experimentally determined apparent viscosities ( $\eta_a$ ) of the digesta.

Given that  $\eta_r = \eta_a / \eta_s$  where  $\eta_r$  is the relative viscosity and  $\eta_s$  is the viscosity of the liquid phase in which the particles are suspended,  $\eta_r$  can therefore be estimated from the experimentally determined values for  $\eta_a$  for the suspensions at a given shear rate by assuming values for  $\eta_s$  of 0.0007 Pa.s (water at 37°C) or up to 0.08 Pa.s for digesta at a shear rate of 100 s<sup>-1</sup>.

The relationship of DMC,  $\phi$ , and  $\phi/\phi_{\max}$  to the apparent viscosity of pig digesta was verified using multiple stepwise regressions in MINITAB (Version 17, USA) from

which the  $R^2$  and p-values were compared to determine where significant differences lay.

The differences of duplicate measurements in DMC,  $\phi$ , and  $\phi/\phi_{\max}$  of solid particles of digesta isolated from the proximal and distal regions of the small intestine of six pigs, the average R values for glass beads and for each fibre after *in-vitro* digestion and the estimated  $\phi_{\max}$  for each fibre type were statistically analysed using one way ANOVA and Tukey's post hoc test. Other details of data analysis were as described in Chapter 3, Section 3.6.

## 5.4. Results

### 5.4.1. *Validation of parameters used to characterise the viscosity of digesta*

DMC of solid particles has been related to increases in the viscosity of digesta. The viscosity increases with the  $\phi/\phi_{\max}$  of solid particles contained in the pig digesta, and was a better parameter to predict the viscosity of digesta compared to the DMC and  $\phi$  (Equation 5.3).

The DMC and  $\phi$  of the particles recovered from the solid phase of pig digesta were determined (Table 5.1). The DMC recovered from the small intestine of the six pigs varied from 10% to 26% (Table 5.1). This was similar to the DMC of 11% to 20% reported for pigs fed a range of plant fibre types (Ehle, Jeraci, Robertson, & van Soest, 1982; Mavromichalis et al., 2000; Stanogias & Pearce, 1985). The  $\phi$  of solid particles recovered from the pig digesta varied from 0.10 to 0.48 (Table 5.1).

**Table 5.1: Values for DMC,  $\phi$  and  $\phi/\phi_{\max}$  for particulates recovered from the small intestine (SI) of pigs.**

Region of SI	Viscosity ( $\eta_a$ ) at 100 s <sup>-1</sup> † (Pa.s)	$\eta_r$ (ratio) #	DMC† (g/g)	$\phi$ † (mL/mL)	$\phi_{\max}$ †† (mL/mL)	$\phi/\phi_{\max}$ †† (ratio)
<b>Proximal</b>						
1	0.022	16.92	15.50	0.22	0.36	0.61
2	0.028	21.54	13.00	0.24	0.36	0.67
3	0.019	14.62	13.00	0.22	0.37	0.59
4	NM	NM	23.00	0.31	0.41*	0.76*
5	NM	NM	26.00	0.46	0.48*	0.96*
6	0.004	3.78	15.00	0.10	0.30	0.37
<b>Average</b>			<b>17.58</b>	<b>0.26</b>	<b>0.38</b>	<b>0.66</b>
<b>Distal</b>						
1	0.010	7.69	13.00	0.14	0.33	0.42
2	0.018	13.85	12.00	0.13	0.29	0.45
3	0.016	12.31	10.50	0.16	0.33	0.49
4	0.019	14.62	11.50	0.18	0.34	0.53
5	0.007	5.38	14.00	0.14	0.33	0.42
6	0.020	15.38	14.50	0.20	0.35	0.57
<b>Average</b>			<b>12.58</b>	<b>0.15</b>	<b>0.33</b>	<b>0.48</b>

NM = not measureable by vane geometry at 100 s<sup>-1</sup>, 37°C.

SI = the small intestine;  $\eta_r$  (relative viscosity) =  $\eta_a/\eta_o$ , where  $\eta_a$  is the apparent viscosity of the suspension,  $\eta_o$  is the viscosity of the suspending liquid.  $\phi$  = measured values,

$\phi_{\max} = 0.528 - 0.042 R$ .

\* values were outliers

# values were derived from  $\eta_s$  assuming the liquid phase of digesta ( $\eta_o$ ) is equivalent to 0.0013 Pa.s (viscosity of liquid phase of pig digesta measured at 100 s<sup>-1</sup>, 37°C). (Takahashi & Sakata, 2004)

† values were from the small intestine of six pigs

†† values are derived from Equation 5.4.

The multiple stepwise regressions that models  $\eta_r$  from the DMC,  $\phi$  and  $\phi/\phi_{\max}$

(df = 3, F = 84.36, p < 0.001, R<sup>2</sup> = 0.98) was showed in Equation 5.3 :

$$\eta_r = (0.58 \pm 4.35) + (-0.70 \pm 0.22 \text{ DMC}) + (-59.19 \pm 21.39 \phi) + (53.31 \pm 4.55 \phi/\phi_{\max})$$

**(Equation 5.3)**

Equation 5.3 showed that  $\phi/\phi_{\max}$  is a more important variable in predicting the  $\eta_r$  of pig digesta (p < 0.001) than the DMC. Pig digesta can therefore be characterised as a

simple particulate suspension for which the viscosity at a given shear rate is proportional to  $\phi/\phi_{\max}$ . The validation steps are described in Sections 5.4.2. and 5.4.3.

#### 5.4.2. *Model particle system*

The spherical glass beads were larger, their surfaces smoother and their aspect ratios ( $R$ ) are close to 1 (Figure 5.1) than those of the food fibre particles ( $R > 4$ ) (Figure 5.2).

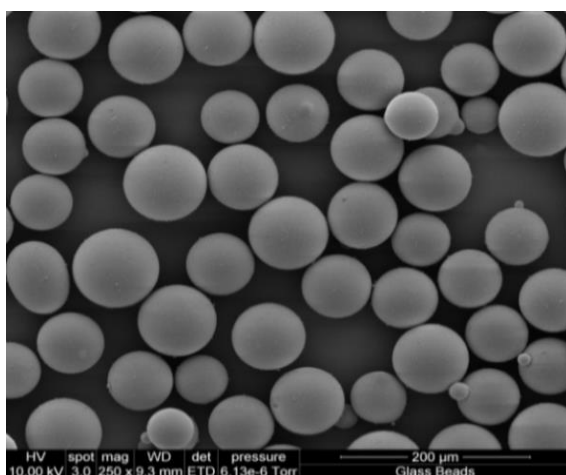


**Figure 5.1:** SEM micrograph of glass beads.

The cellulosic WF600 and Prolux wheat fibre particles were smaller in size and had smoother surfaces than those of the wood and larger AllBran® particles (Figure 5.2). Only *in-vitro* digested particles are shown as they are more comparable with solid particles recovered from pig digesta.

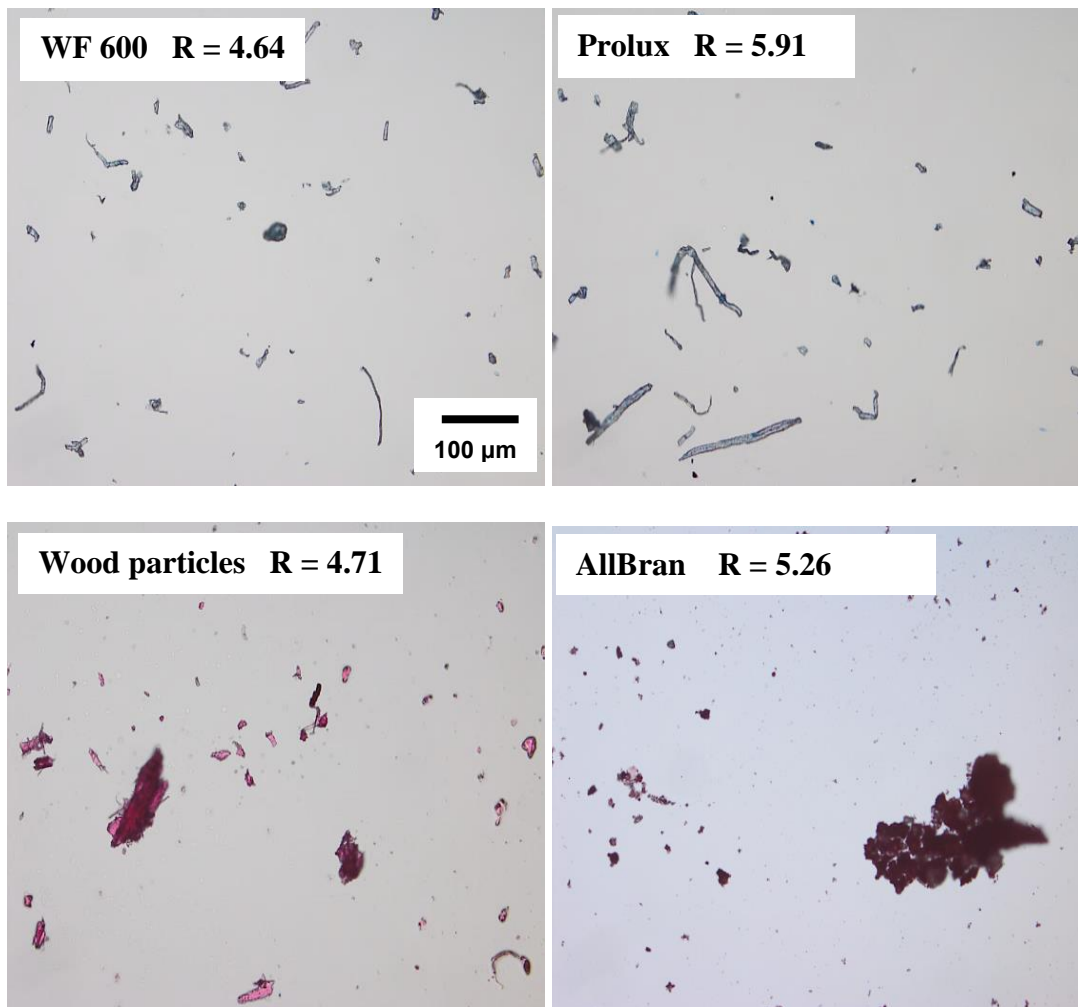


**Figure 5.2:** Light micrographs (x200) of food particles recovered from *in-vitro* digestion with various R values.

The viscosity of glass bead suspensions in 70% (w/v) fructose could be measured up to a  $\phi$  value of 0.35; whereas the viscosities for food fibre systems were only measurable up to 0.20 (Table 5.2). Beyond these limits, viscosity of the suspension was either too great to be measured by the equipment used or did not demonstrate Newtonian characteristics and therefore was not used to fit into the Equation 2.3.

**Table 5.2: The relative viscosities ( $\eta_r$ ) and, the estimated  $\phi_{\max}$  of the fibre suspensions using *in-vitro* digested particles at a range of  $\phi$ . Results relative to the viscosity of glass bead suspensions.**

	Glass beads	WF 600	Prolux	Wood particles	AllBran®
$R^\dagger$	$1.02 \pm 0.00$ c	$4.64 \pm 0.30^b$	$5.91 \pm 0.35^a$	$4.71 \pm 0.37^b$	$5.26 \pm 0.29^a$ b
$\phi_{\max}^\ddagger$	$0.55 \pm 1.00$ a	$0.33 \pm 0.01^b$	$0.28 \pm 0.01^c$	$0.33 \pm 0.01^b$	$0.29 \pm 0.01^b$ c
$(\phi)(v/v)$	Relative viscosity ( $\eta_r$ ) <sup>†</sup>				
0	$1.00 \pm 0.00$	$1.00 \pm 0.00$	$1.00 \pm 0.00$	$1.00 \pm 0.00$	$1.00 \pm 0.00$
0.01		$1.05 \pm 0.01$	$1.17 \pm 0.07$	$1.17 \pm 0.03$	$1.04 \pm 0.01$
0.02		$1.09 \pm 0.01$	$1.33 \pm 0.03$	$1.19 \pm 0.03$	$1.18 \pm 0.02$
0.05		$1.21 \pm 0.03$	$1.39 \pm 0.08$	$1.32 \pm 0.03$	$1.34 \pm 0.01$
0.10	$1.51 \pm 0.06$	$2.39 \pm 0.13$	$2.49 \pm 0.06$	$1.70 \pm 0.08$	$1.94 \pm 0.22$
0.15		$4.17 \pm 0.28$	$3.94 \pm 0.62$	$3.72 \pm 0.67$	$3.41 \pm 0.06$
0.20		$6.20 \pm 0.58$	$10.83 \pm 1.7$	$6.78 \pm 0.38$	$9.30 \pm 0.77$
			1		
0.25	$2.13 \pm 0.22$	NM	NM	NM	NM
0.30	$4.04 \pm 0.45$				
0.35	$8.13 \pm 1.33$				
0.40	NM				
$R^2$ of M-P equation	0.96	0.96	0.99	0.99	0.99
Average relative error (%)	8.40	3.69	6.85	5.10	3.54

Note: NM = not measurable; R = aspect ratio, M-P = Maron-Pierce

<sup>†</sup> Values are means of duplicate samples  $\pm$  standard deviation.

<sup>‡</sup> Values are means of six pigs  $\pm$  standard deviation.

a–c Means in a column followed by different superscripts are significantly different (One-way ANOVA and Tukey's pair wise test,  $p < 0.05$ )

The  $\phi_{\max}$  of a suspension is inversely proportional to the R values of the solid particles suspended in it (Table 5.2); but at a given  $\phi$ , the  $\eta_r$  of a suspension increases with R. For example, the  $\phi_{\max}$  for glass beads ( $R = 1$ ) was about 0.55, while the  $\phi_{\max}$  for Prolux fibre ( $R = 5.9$ ) was about 0.28 (Table 5.2).



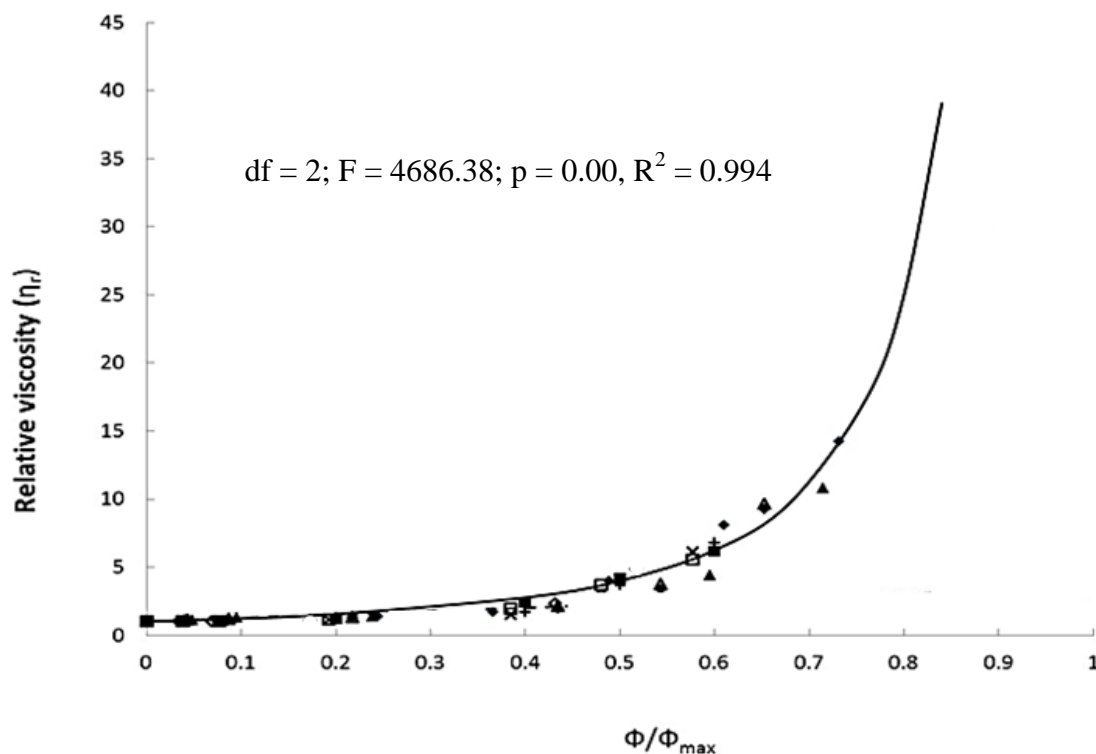


**Figure 5.3:** The relationship between  $\eta_r$  of the food fibre suspensions to  $\Phi/\Phi_{\max}$ ; ■ = WF600 after *in-vitro* digestion, ▲ = Prolux after *in-vitro* digestion; + = wood fibre after *in-vitro* digestion, ◆ = AllBran® after *in-vitro* digestion, x = glass beads, and — Maron-Pierce equation fit. Apparent viscosity of the suspending 70% fructose solution,  $\eta_s = 0.032$  Pa.s.

When viscosity approached infinity, the maximum solid volume fraction ( $\Phi_{\max}$ ) was calculated from fits of the apparent viscosity at a shear rate of  $100 \text{ s}^{-1}$  and  $\Phi$  described in the Section 5.3.6. Plotting relative viscosities against the  $\Phi/\Phi_{\max}$  show that the data for the suspensions used for this work fitted closely to the Maron-Pierce model ( $R^2 = 0.994$ ) for values of  $\Phi/\Phi_{\max} < 0.2$  (Table 5.2, Figure 5.3) and solid particles with R values between 1 and 6.

The  $\eta_r$  of suspensions with higher R values diverged slightly from the predicted values as these particles either tend to “align” at high shear rate or tend to agglomerate in solutions of greater viscosity therefore decreasing  $\eta_r$  (Pabst, Gregorova, et al., 2006).

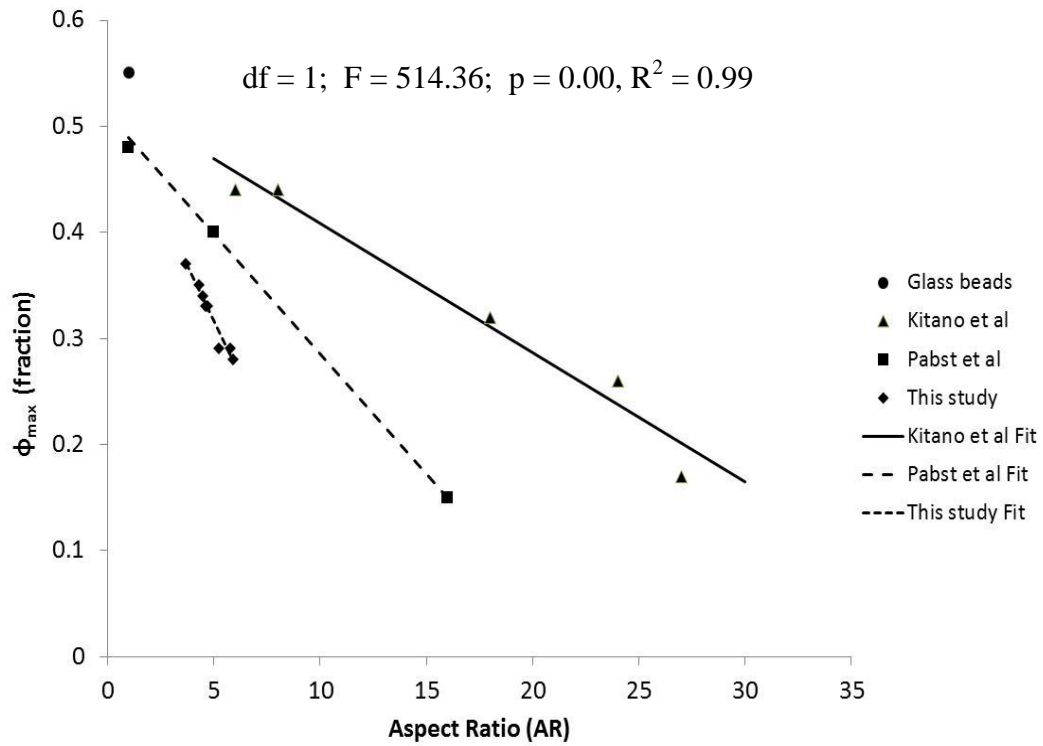


**Figure 5.4:** The relationship between  $\phi_{\max}$  and aspect ratio (R) for the glass bead and fibre suspensions from this study and for other suspensions (Kitano et al., 1981; Pabst, Gregorova, et al., 2006). Coefficients from the linear regression: This study (Equation 5.4);  $\phi_{\max} = 0.528 - 0.042 R$ , Kitano;  $\phi_{\max} = 0.54 - 0.0125 R$ , Pabst;  $\phi_{\max} = 0.51 - 0.0223 R$ .

The values of  $\phi_{\max}$  determined from the above approach were used to derive the constants  $c$  and  $m$  for the equation relationship  $\phi_{\max} = c + mR$ , where  $R$  is the aspect ratio of the fibres (Figures 5.1 and 5.2) as them used by Kitano and Pabst (Kitano et al., 1981; Pabst, Gregorova, et al., 2006).

**Table 5.3: Comparisons of constants relating  $\phi_{\max}$  with R for various studies.**

	<b>Kitano et al., 1981</b>	<b>Pabst, Gregorova, et al., 2006</b>	<b>This study</b>
Equation	(Equation 2.5) $\phi_{\max} = 0.54 - 0.0125 R$	(Equation 2.6) $\phi_{\max} = 0.51 - 0.0223 R$	(Equation 5.4) $\phi_{\max} = 0.528 - 0.042 R$
Slope coefficient “ <i>m</i> ”	-0.0125	-0.0223	-0.042
$R_{\ddagger}$ (pig digesta)	$4.17 \pm 1.21$	$4.17 \pm 1.21$	$4.17 \pm 1.21$
$\phi_{\max} \#$ (pig digesta)	$0.49 \pm 0.02$	$0.42 \pm 0.03$	$0.35 \pm 0.05$

$\ddagger$  Average R values of particles recovered from digesta collected from the small intestine of six pigs

# values estimated using the Equation 5.4.

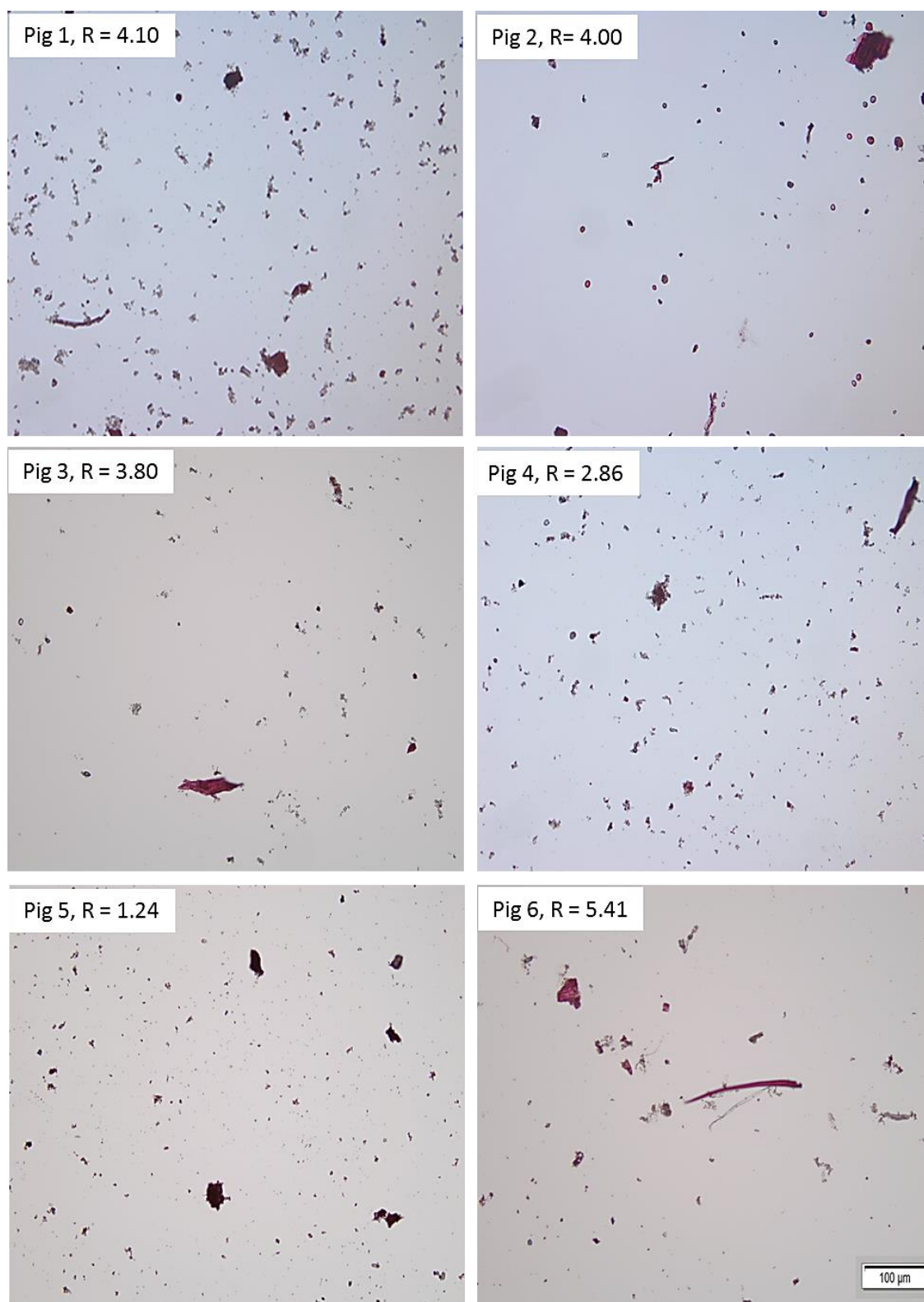
The linear fit of these data and hence the ability of R to predict  $\phi_{\max}$  was very good ( $R^2 > 0.99$ ) with all data converging near the data point for glass beads ( $\bullet$ ,  $R=1$ ). Values for the intercept were similar for this study (0.528) and those determined by Kitano and Pabst (0.54 and 0.51 respectively) (Table 5.3). Whilst the equations derived herein have similarities with those of Kitano and Pabst (Table 5.3), the value obtained for the slope (*m*) was greater than those obtained previously using different suspending liquids and fibre types.

#### **5.4.3. Properties of particles from pig digesta**

As expected, the morphology of the solid residues recovered from the small intestine (Figure 5.5) was similar to that of the solid materials recovered from the proximal colon (Chapter 4, Section 4.4.2.). Furthermore, all of these particles (Figure 5.5) appeared to have a cellular structure similar to plant materials as they all stained red with safranin indicating that they probably contained a proportion of lignin (Vazquez-Cooz & Meyer, 2002). The particulates recovered from the proximal and

distal segments of the small intestine were irregular with the length generally much greater than the diameter, and with R values varying from 1.2 to 5.6 (Figure 5.4). They were generally similar to the *in-vitro* digested food fibre fragments (Chapter 4, Section 4.4.2.) and were comparable with that of all fibre particles used ( $R > 4$ ) (Table 5.2).

**(a) Solid particles recovered from the proximal pig intestine**



(b) Solid particles recovered from the distal pig intestine

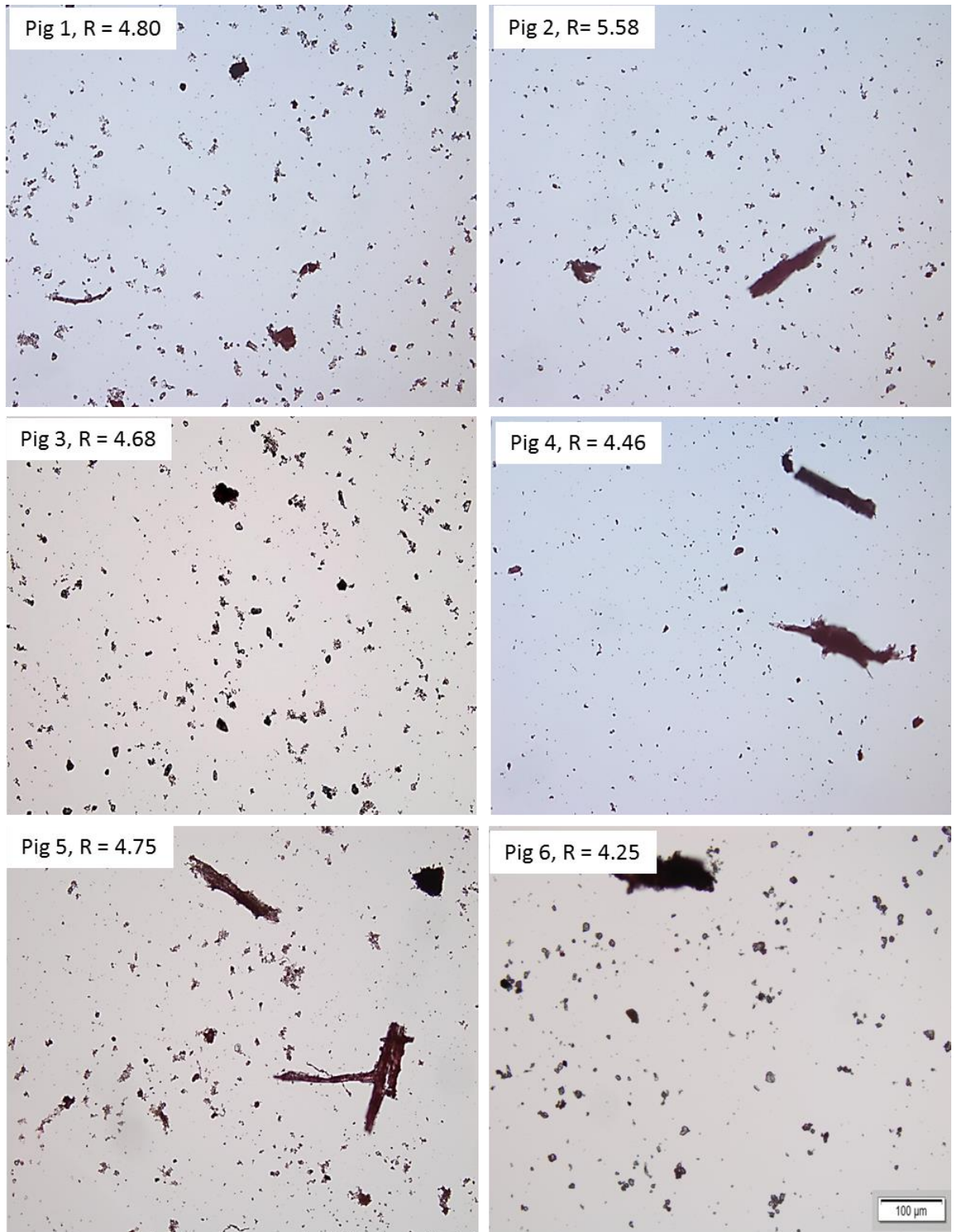


**Figure 5.5:** Optical microscopic images (x200) of digesta particles recovered from (a) the proximal; (b) the distal segments of porcine small intestine.

The larger particles recovered from pig digesta (Figure 5.5), were similar in terms of general size and shape to those of digested Allbran® (Figure 5.2; note the change in size scale of the images) and both contained similar proportions (> 85%) of very small particles that contributed to less than 20% of the total volume (Chapter 4, Section 4.4.3). In summary, the physical characteristics of the test particles used in this work varied from isometric hard smooth spheres with an  $R \sim 1$  to flexible plant derived particles that exhibited a range of surface morphologies and were of isometric shape with skewed particle number and volume distributions and had mean  $R$ s that sometimes exceeded 4.

## 5.5. Discussion

This work has shown that the maximum solid volume fraction ( $\phi_{\max}$ ) is a better predictor ( $p < 0.001$ ) of relative viscosity of suspensions containing finely divided plant fibre particles similar to those recovered from ileal pig digesta than either  $\phi$  alone or DMC (Equation 5.3). Although the apparent viscosity of digesta increases with DMC (Bartelt et al., 2002; McRorie et al., 2000) and follows a power law function (Lentle et al., 2005), the fit is often poor when the suspension contains elastic particles with different  $R$ . This is because the DMC fraction is only closely related to particle weight for a given particle density.

The  $\phi_{\max}$  of a suspension is difficult to determine. In this study, a simple accurate method of estimating it in polydisperse suspensions was used to determine  $R$  for the particles suspending in it and, once a standard curve relating viscosity to  $\phi$  is determined for a similar particle type, then the  $\phi_{\max}$  can be predicted for a range of particle types for which the  $R$  values are within the range of the standard curve

(Figure 5.4, Table 5.3). The estimated  $\phi_{\max}$  for glass bead was 0.55, and this value is close to empirical values of the published work (Farris, 1968; Pusey & Megan, 1986).

It was clear from our data and from the data published by Pabst and Kitano (Kitano et al., 1981; Pabst, Gregorova, et al., 2006) that  $\phi_{\max}$  increases as the R of the suspended particles decreases to unity (glass beads). The  $\phi_{\max}$  for the test fibre suspensions used in this work lay between 0.28 and 0.33 (Table 5.2) which was within the ranges described by these authors. However, there were considerable differences between the regression coefficients obtained for the fibre suspensions in this study and those obtained by Pabst for wollastonite fibres and starch granules in 60% saccharose, and by Kitano for various fibres in polymer melts (Kitano et al., 1981; Pabst, Gregorova, et al., 2006).

Although the variations in aspect ratio and consequently  $\phi_{\max}$  were considerably smaller than those reported in previous work (Kitano et al., 1981; Pabst, Gregorova, et al., 2006) the form of the relationship between R and  $\phi_{\max}$  was similar and  $R^2$  was high particularly when glass beads were omitted from the equation, a reasonable approach given that they are structurally very different from the fibre suspensions used in this study.

With the exception of the glass bead suspensions, the rheological behaviour of the various plant fibre and food particles used for this study were generally similar to those found in the small intestine of the pig. Although the size, shape, and surface characteristics of the particulate matter in digesta may influence the overall viscosity



(Pabst, Gregorova, et al., 2006), the fine particulate fraction present in all sampled fibres and in the gut may not contribute greatly to the rheological properties of the suspensions presumably because of their small volumetric proportion (Chapter 4) and their ability to occupy voids between the larger particles. This finding is in agreement with findings for the caecal contents of the pig where removal of the large particulate fraction significantly reduced viscosity (Takahashi & Sakata, 2002).

The  $\phi_{\max}$  (Table 5.3) could be used to postulate the  $\phi/\phi_{\max}$  of suspensions containing solid particles of similar R values. The ratio of average  $\phi/\phi_{\max}$  for pig digesta from the proximal small intestine was 0.66 and it was higher than that of from the distal small intestine (average  $\phi/\phi_{\max} = 0.57$ ) (Table 5.1). The higher ratio of  $\phi/\phi_{\max}$  in the proximal segment suggests that viscous digesta emptied from the stomach into the proximal small intestine contains a higher proportion of solid particles, but that part of these solid particles were digested, decreasing the overall volume fraction of the solid particles in the digesta as it transverses down to the distal segment.

The  $\phi_{\max}$  decreases as the R value for particles increases (Table 5.2). It is anticipated that animals will attain satiety faster when their diet contains particles with greater R values. The feed intake of ruminants fed with grass silage (R = 5.5) was 41% higher than for animals fed on grass silage for which the mean R = 7.5 (Jalali et al., 2012). Although much of the discussion to this point has revolved about relative viscosity of the suspensions, the mixing of digesta in the gut is dependent on the weak shear developed by peristalsis and the apparent viscosity of the non-Newtonian suspensions of digesta; these aspects of the work will be developed in Chapter 7.

## 5.6. Conclusions

The viscosity of the gut contents is closely related to the ratio of  $\phi/\phi_{\max}$ ; due to the density of particles viscosity is not always well predicted from DMC. The relationship between the  $R$  of the particles and  $\phi_{\max}$  previously described by Kitano et al. and by Pabst et al. (Kitano et al., 1981; Pabst, Gregorova, et al., 2006) and the relationship between maximum solid volume fraction and relative viscosity described by the Maron-Pierce model (Maron & Pierce, 1956) hold for the components of digesta. Hence it is possible to obtain reliable estimates for the relative viscosities of small samples of digesta of <1 mL that are below the volumes required for reliable rheometry by determining the mean aspect ratio and the volume fraction of the particles it contains. The relationship between  $\phi_{\max}$  and  $R$  derived using various standardised test suspensions of fibres ( $\phi_{\max} = 0.528 - 0.042 R$ ) will have general application for animal digesta when values of  $R$ s are between about 2 and 6.

Since the viscosity of the fibre suspensions made in this work resembles that of pig digesta, this work is considered to model the effect of  $\phi$  on viscosity. An extension of these effects on *in-vitro* digestion at physiological particle concentrations and shear rates (Chapter 6) will provide useful insights on the effect of  $R$ s and solid volume fraction on digestion.

## Chapter 6 The effect of fibre and gelatinised starch type on the rate of amylolysis and apparent viscosity reduction during *in-vitro* digestion at a physiological shear rate

DRC 16



MASSEY UNIVERSITY  
GRADUATE RESEARCH SCHOOL

### STATEMENT OF CONTRIBUTION TO DOCTORAL THESIS CONTAINING PUBLICATIONS

(To appear at the end of each thesis chapter/section/appendix submitted as an article/paper or collected as an appendix at the end of the thesis)

We, the candidate and the candidate's Principal Supervisor, certify that all co-authors have consented to their work being included in the thesis and they have accepted the candidate's contribution as indicated below in the *Statement of Originality*.

Name of Candidate: Yap Sia Yen

Name/Title of Principal Supervisor: Prof. Roger Lentle

#### Name of Published Research Output and full reference:

Allan, K. Hardacre, Sia-Yen, Yap, Roger, G. Lentle, John, A. Monro. (2015). The effect of fibre and gelatinised starch type on amylolysis and apparent viscosity during in-vitro digestion at a physiological shear rate. *Carbohydrate Polymers*. 123:80-88


In which Chapter is the Published Work: Chapter 6

Please indicate either:

- The percentage of the Published Work that was contributed by the candidate: 70% and / or
- Describe the contribution that the candidate has made to the Published Work:  
The candidate has carried out all laboratory work, data analysis and drafted the manuscript.

  
Candidate's signature

4/10/16  
Date

  
Principal Supervisor's signature

4/10/16  
Date

---

**6.1. Abstract**

Suspensions of pre-gelatinised starches from potato and corn were digested *in-vitro* with amylase in the presence of 0.4% (w/v) of the soluble fibre, guar or finely milled insoluble fibre derived from two commercially available wheat fibre products; a finely ground wood fibre or a coarse breakfast cereal fibre (AllBran®). The starch and solubles content of AllBran® were removed by aqueous digestion with alpha-amylase. The fibre was then washed and dried at low temperature (40°C) before use. *In-vitro* digestion was carried out at 37°C at a low, constant and physiologically relevant shear rate of 10 s<sup>-1</sup> in a rheometer fitted with cup and vane geometry. The proportion of starch digested was determined from the amount of reducing sugar released using the DNS assay described earlier. The viscosity of the suspension declined asymptotically over 120 min as the proportion of starch declined. The relationship between the proportion of viscosity remaining and the proportion of RDS with time was modelled over the first 20 min of digestion as a linear function of the Ln-transformed data. In the presence of 6.8% to 9.8% of finely milled cellulosic particles derived from wheat (WF600, Prolux), the rate of amylolysis over the first 20 min of digestion of the starches was similar to starch alone but was reduced in the presence of the wood, and AllBran® particles by about 20% and dissolved guar by up to 50%. These results suggest that in all cases the reduction in the rate of digestion was due to competitive inhibition of amylase by NSP sequences that mimic aspects of the starch polymer. The small insoluble cellulosic wheat fibre particles used in this work did not affect the rate of starch digestion in low shear systems, possibly because they contained no competing polysaccharides that reduced the rate of amylolysis. In diets, fibre added to reduce

the rate of digestion of starch must be carefully selected for its effect in reducing the rate of amylolysis.

## **6.2. Introduction**

The addition of significant quantities of soluble or insoluble dietary fibres in the human diet increases the apparent viscosity of the gut contents (Marlett et al., 2002) and reduces mixing in the gut (Blackburn & Johnson, 1981; Jenkins et al., 2004). Highly viscous digesta may hinder the penetration of enzymes into substrates (Tester & Sommerville, 2003) which in turn is likely to reduce rate of transport of liberated nutrients from the lumen of the intestine to sites of absorption at the intestinal mucosa.

Dietary fibre may reduce the overall rate of carbohydrate digestion, which in turn reduces the rate at which glucose is released and subsequently absorbed (Braaten et al., 1991; Braaten et al., 1994; Jenkins et al., 1987). For this reason, dietary fibre may be useful in lowering post-prandial blood glucose levels and may aid in the treatment of type II diabetes. However, the control of post-prandial blood glucose levels using fibre varies with the type (either soluble or insoluble), the amount of fibre consumed (Björck et al., 1994; Samra & Anderson, 2007) and the size of the particles (Granfeldt, Hagander, & Björck, 1995).

The digestibility of starch is influenced by its physical structure. Fully gelatinised starch is digested up to 8 times faster than non-gelatinised starch (Holm et al., 1988) and the digestibility of various fractions (RDS, SDS, or RS) within gelatinised starch differ significantly (Chapter 2, Section 2.4) (Butterworth et al., 2012; Englyst et al.,

1999). The fraction of gelatinised starch categorised as RDS is thought to account for the initial postprandial rise in blood glucose and insulin (Noda et al., 2008). Correspondingly, the fractions of SDS and RS starch appear to have little influence on the post-prandial levels of glucose and insulin. These components are considered to have little relevance in representing physico-chemical properties of the starch (Butterworth et al., 2012).

The rate of starch digestion varies with a number of factors; for non-gelatinised starch, the rate of digestion depends on

- the granule morphology- such as the size and shape, the surface to volume ratio, and the surface porosity (Sujka & Jamroz, 2007);
- the chemical composition, especially the ratio of amylose and amylopectin, the protein and lipid contents, and chemical components such as phosphorus (Biliaderis, 1991; Naguleswaran, Vasanthan, Hoover, & Bressler, 2014);

For starch, the rate of digestion depends on:

- The degree to which the starch is gelatinised (Holm et al., 1988; Wang & Copeland, 2013);
- The presence of other chemical components, notably the proportion of dietary fibres (Nebesny, Rosicka, & Tkaczyk, 2004; Noda et al., 2008; Snow & Odea, 1981), and the proportion of RS (Björck et al., 1987). These components could “mask” starch granules from exposure to digestive enzymes (Parada & Aguilera, 2011).

The rate of digestion of gelatinised starch can be modelled in various ways. During the early stages of digestion, regressions of Ln-transformed starch concentration with time were shown to accurately model the rate of digestion of various types of fully gelatinised starch and the raw starch to follow the first order kinetic (Chapter 2, Section 2.4) (Butterworth et al., 2012); but this model does not apply in the starch system to which fibres have been added. The rate of starch digestion has been compared using a coefficient derived from the Ln regression, but the mechanisms of amyolysis of starch is not well described (Edwards, Warren, Milligan, Butterworth, & Ellis, 2014).

While reduction in amyolysis in the presence of various fibres have been reported for the *in-vitro* digestion of starch, few of these studies have related differences in the levels of blood glucose *in-vivo* to the rate of glucose production during *in-vitro* digestion (Butterworth et al., 2012; Englyst & Hudson, 1996; Woolnough et al., 2008). One such study, showed that the rate of increase in the concentration of glucose in venous blood in the hepatic portal system of pigs fed a range of partially purified cereal starches was generally lower than that during *in-vitro* digestion but that the correlation improved when the effects of physiological processes such as gastric emptying were incorporated into the model (Björck et al., 1987; Blackburn et al., 1984; Goni et al., 1997; Holm et al., 1985; van Kempen et al., 2010; Vangsøe et al., 2016). Similarly, the adjustment of *in-vitro* data for rates of apparent glucose disposal in humans increased the accuracy of predicting the glycaemic response to human foods (Monro & Mishra, 2010). Hence it appears that digestion *in-vitro* can be used to estimate the effects of starch structure on digestive processes *in-vivo* if allowance is made for the *in-vivo* factors involved in glucose homeostasis.

In this study, an *in-vitro* system (Chapter 3, Section 3.5.2.) was used to determine the effects of the addition of soluble or insoluble fibre to suspensions containing gelatinised starch on the rate of starch digestion. The changes in the apparent viscosities and the digestion of fully gelatinised potato and corn starches alone and when mixed with either of two finely divided wheat fibre types, a finely ground wood fibre, a modified commercial high fibre breakfast cereal (AllBran®) or guar gum were measured. The four types of insoluble fibre were chosen on the grounds that they differed chemically, in solubility and in particle size distribution (Chapter 4).

### **6.3. Materials and methods**

#### **6.3.1. Fibre types**

The details on selection of fibre particles and chemical compositions are described in Chapter 3, Sections 3.2.2. and 3.3.

#### **6.3.2. Preparation of AllBran® fibre**

All fibre materials used in the study contained small amount (<10%) of solubles (Chapter 4), except the commercial AllBran® which was composed of about 70% of solubles components (Chapter 4, Figure 4.1). AllBran® was therefore subjected to *in-vitro* digestion (Section 3.5.1.) before being used in this study. After *in-vitro* digestion, the particles were re-suspended in MilliQ water, and the suspension was mixed using a stirrer at 200 rpm for 30 min and the water was decanted again. This procedure was repeated six times before the settled *in-vitro* digested fibre particles were collected and dried at 40°C for 12 h before storage for further use (Section



3.5.1.). Any loosely bound soluble compounds on the surface of AllBran® will likely have been removed after the series of washing steps.

### **6.3.3.            *The concentration of fibres used***

The objective of this work was to approximate conditions in the small intestine; the concentration of insoluble dietary fibre used was determined from the mean concentration of indigestible particulates in the digesta from the small intestine from six slaughtered pigs (Chapter 5). The mass fraction of solids isolated from the small intestine varied from 10% to 46% (Chapter 5). However, adding fibres of more than 10% mass fraction into the 10% (w/v) suspension induced very high viscosity; out of the measurable range of the rheometer. This was probably due to the high viscosity of the non-Newtonian 10% (w/v) starch suspensions used. For this reason, the solid mass fraction of fibres used in this work was set to the values closest to the mass fraction of solids isolated from the intestinal distal segment, and these ranged from 6.8%-9.8%. The viscosity of a 0.4% (w/w) guar solution was similar to that of a 6.8%-9.8%, suspension of hydrated insoluble fibre.

### **6.3.4.            *Starch***

High protein and fat contents in starch granules have been reported to delay the gelatinisation. These components of potato and corn starches were analysed (Chapter 3, Sections 3.3.2 and 3.3.3.)

### **6.3.5.            *Pasting temperature***

Suspensions of 10% (w/w) of potato and corn starches in cold water were gelatinised in an RVA (RVA-4, Newport Scientific, Warriewood, Australia) the pasting

temperature (PT), and the temperature at maximum viscosity (PV) were determined. The starch suspensions were initially stirred at 900 rpm for 60 s to suspend the starch granules; the rate was subsequently reduced to 160 rpm which was maintained throughout the remainder of the procedure. The samples were heated from 55°C to 95°C at 2°C/min, and the temperature held at 95°C for 5 min and the samples subsequently cooled over 5 min to 55°C. The experiment was also repeated with 5%, 7.5% and 15% (w/w) for each of the two types of starch used, to determine the effect of starch concentration on the PT and PV (Table 6.1). These experiments were repeated in triplicate with the potato and corn starch suspensions and the mean PV and PT for each experiment were determined.

**Table 6.1: The PT and peak hot PV for the four concentrations of the two starches.**

Starch concentration (%) (w/w)	PT (°C)‡	PV (Pa.s)‡
<b>Potato</b>		
5.0	86.0 ± 1.0 <sup>b</sup>	1.59 ± 0.01 <sup>f</sup>
7.5	69.1 ± 0.4 <sup>c</sup>	6.84 ± 0.00 <sup>d</sup>
10.0	68.0 ± 0.5 <sup>c</sup>	12.12 ± 0.01 <sup>b</sup>
15.0	63.7 ± 0.5 <sup>d</sup>	12.74 ± 0.01 <sup>a</sup>
<b>Corn</b>		
5.0	95.0 ± 0.7 <sup>a</sup>	0.09 ± 0.00 <sup>h</sup>
7.5	92.7 ± 0.4 <sup>b</sup>	1.01 ± 0.01 <sup>g</sup>
10.0	90.0 ± 0.8 <sup>b</sup>	3.48 ± 0.01 <sup>e</sup>
15.0	85.3 ± 0.5 <sup>b</sup>	8.86 ± 0.00 <sup>c</sup>

Note: PT, pasting temperature; PV, pasting viscosity.

‡ Mean values in a column with different superscripts (a-g) are significantly different (One way ANOVA and Tukey's pair wise test,  $p < 0.05$ )

Preliminary studies showed that, as the concentration of a starch suspension increased, the PV also increased but the PT decreased (Table 6.1). The PV of potato starch was significantly ( $p < 0.05$ ) higher than corn starch (Table 6.1). For example, 10% (w/w) potato starch has a peak hot PV of 12.1 Pa.s which was about 3.5 times

higher than corn starch at the same concentration. The PTs for 7.5% (potato) and 10% (w/w) (corn) starch suspensions were similar (Table 6.1), whereas the PVs for starch concentrations below 10% (w/w) were low, particularly for the corn starch suspension. Low viscosity starch suspensions cannot suspend the fibres for the duration of the rheology experiments. Therefore, a standardise concentration of starch, a 10% (w/w) starch suspension, was selected for the following experiments.

### **6.3.6. Preparation of starch/fibre suspensions**

The digestion mixtures were prepared by suspending 10% (w/w) of non-gelatinised potato or corn starch with appropriate weights of one of the four insoluble fibres (Section 6.3.3.) or 0.4% (w/w) of guar in MilliQ water. These starch/fibre suspensions were held at room temperature for 1 h to ensure that fibres were fully hydrated before the suspensions were fully gelatinised by heating for 30 min in a water bath maintained at the temperature (PT) appropriate for the degree of gelatinisation required for the starch type and concentration (Table 6.1).

During gelatinisation, the suspensions were mixed at 100 rpm for the first 10 min, to maintain the fibre particles suspended evenly in the suspensions. After 10 min, the viscosity of the suspensions increased and the stirrer speed was reduced to 50 rpm for the remaining 20 min to minimise damage to the gelatinised starch granules. The starch/fibre suspensions were then cooled to 45°C before loading into the rheometer cup for *in-vitro* digestion.

All suspensions were prepared at PTs that were pre-determined using RVA (Table 6.1); potato starch/fibre suspensions were prepared at 68°C while corn starch/fibre

suspensions at 90°C. All parameters were carefully maintained at similar levels to ensure that the changes of environmental factors on the gelatinisation were minimal. The PT was standardised for all treatments to ensure that changes in viscosity and rate of starch digestion were the effect of different fibre types. Addition of fibres might increase the PT, but less than 10% of insoluble fibres and 0.4% guar gum were added into the suspensions, which would generally have no effect on the PT on potato starch and little effect on corn starch suspensions (Ragae & Abdel-Aal, 2006).

#### **6.3.7. *In-vitro digestion using rheometer***

The details of the *in-vitro* digestion methodology used for this section were previously described (Chapter 3, Section 3.5.2). Briefly, 38 g of gelatinised starch or starch/fibre mixture was poured into the rheometer cup and the sample equilibrated to 37°C before the *in-vitro* digestion commenced. The digestate was continuously mixed at a constant shear rate of  $10\text{ s}^{-1}$  as this shear rate was able to keep the fibres suspended in the suspensions and it was close to reported physiological shear rates (Lentle et al., 2007). The *in-vitro* digestion started with a gastric phase (30 min), followed by adding an enzyme suite containing mixtures of pepsin, lipase, and acid. The subsequent small intestinal phase (120 min) was commenced after adding a mixture of  $\text{NaHCO}_3$  solution, bile extract, pancreatin, and fungal amyloglucosidase. Subsamples were taken at 1, 2, 5, 10, 15, 20, 30, 60, and 120 min following the addition of all reagents (Table 6.2).

**Table 6.2: Experimental treatments of starch/fibre suspensions used.**

Treatment	Replicates	Starch	Fibre	Treatment abbreviation		Sampling time
				Potato	Corn	
Control	2	P or C	None	P	C	10 (T0 to T120)
1,6	2	P or C	WF600	PWF600	CWF600	10 (T0 to T120)
2,7	2	P or C	Prolux	PPr	CPr	10 (T0 to T120)
3,8	2	P or C	Wood	PW	CW	10 (T0 to T120)
4,9	2	P or C	AllBran®	PAb	CAb	10 (T0 to T120)
5,10	2	P or C	Guar	PG	CG	10 (T0 to T120)

The experimental design comprised 2 starches x 5 fibres x 10 sample times x 2 replications (200 data points each for the rheological measurements and sugar analyses).

Note: P, potato (treatments 1-5); C, corn (treatments 6-10); T0, time at which the simulated small intestinal *in-vitro* digestion began; T120, time at which digestion was stopped.

### **6.3.8. Total starch and sugar determination**

The details of the total starch assay were previously described (Chapter 3, Section 3.5.3.). The amount of glucose released for each subsampled listed (Table 6.2) was calculated, and they were also generally classified into three sub-fractions: i.e. RDS, SDS, and RS. This classification is based on the extent of digestibility of starch after 20 min (RDS), 20-120 min (SDS), and more than 120 min (RS) in the *in-vitro* condition (Chapter 2, Section 2.4). This step was included to compare the effect of various dietary fibres on the arbitrary amount of glucose released in the RDS fraction. The rate amylolysis was calculated using Ln-transformed data (Section 6.3.10).

### **6.3.9. SEM of starch granules**

The details of the preparation of the starch for SEM micrographs are described earlier (Chapter 3, Section 3.4.3.).

---

**6.3.10. Data analysis**

The relative reductions in residual starch calculated over the first 120 min of *in-vitro* amylolytic digestion, were explored by fitting a common curve to the pooled results for all treatments using CurveExpert software (Version 1.4) to determine whether all treatments showed a similar general form of decline. To quantify differences between individual treatments, separate plots of Ln-converted values for each treatment against time were then fitted using a linear function (SigmaPlot® Version 12.3.3). Plots of the relative reduction in apparent viscosity were similarly developed and fitted, details were described in Chapter 3, Section 3.6., Equation 3.11. The  $T_{1/2}$  values for starch digestion (the time taken to the convert 50% of the starch into sugars) and for relative reduction in apparent viscosity (time taken to halve the apparent viscosity) were determined for each of the 10 treatments and the two controls. The magnitudes of the  $T_{1/2}$  values for relative starch content and relative change in apparent viscosity were each compared using the GLM procedure in the Minitab statistical suite (MINITAB Statistical Software Version 16, Minitab Inc, <http://www.minitab.com>) with Tukey's post-hoc test to distinguish pair-wise differences. The residuals of data from analyses were checked using the Anderson–Darling test and found to be normally distributed. The pasting temperature and pasting viscosity measured using RVA were analysed using t-tests when two treatments were being compared. p values  $\geq 0.05$  were considered to indicate significant differences.

The relationship between the proportion of starch digested and the proportional viscosity was best described graphically by fitting a common curve to the pooled data from the various treatments using SigmaPlot® Version 12.3.3. Plot for each

treatment on the relationship between the proportion of starch digested and the proportional viscosity was plotted using SigmaPlot® Version 12.3.3. This relationship was best fitted with an exponential decay function,  $y = ae^{-(bx)}$  (Equation 3.10, Chapter 3, Section 3.6).

Comparisons of slope coefficients for the Equation 3.10 were based on the distribution of student's t-test (t-value) determined from

$$t = \frac{b_1 - b_2}{SE_{b_1 - b_2}} \quad (\text{Equation 6.1})$$

where

$b_1$  = mean slope coefficient determined from the first analysis

$b_2$  = mean slope coefficient determined from the second analysis, and

$SE_{b_1 - b_2}$  = standard error of the comparison i.e.

$$SE_{b_1 - b_2} = \sqrt{SE_{b_1}^2 + SE_{b_2}^2} \quad (\text{Equation 6.2})$$

Similarly, comparisons with theoretical values were based on student's t-test (t

values) determined from 
$$t = \frac{b - b_0}{SE_b} \quad (\text{Equation 6.3})$$

where

$b$  is the mean slope coefficient determined by curve fitting,

$b_0$  is the theoretical exponent, and

$SE_b$  is the standard error of the slope.

Probabilities were determined for ( $n=2$ ) degrees of freedom, where  $n$  was the number of replicate used in each group. Other details of data analysis were as described in Chapter 3, Section 3.6.

## 6.4. Results

### 6.4.1. Fibre types

The details of chemical compositions and morphology of four of the insoluble fibre particles were previously described in Chapter 4, Section 4.4. Similar proportions of soluble or digestible components were present in the WF600 (~10%), Prolux (~12%), wood particles (~15%) and guar (~10%) fibres but the soluble or digestible components of AllBran® fibre were all removed by *in-vitro* digestion (Figure 6.1). The AllBran® particles contained a relatively high proportion of hemicelluloses with lower proportions of cellulose and lignin (Figure 6.1). Guar contained a high proportion of galactomannans and about 15% soluble components (Figure 6.1), mainly moisture and small amounts of protein, lipid and minerals (Appendix 2).

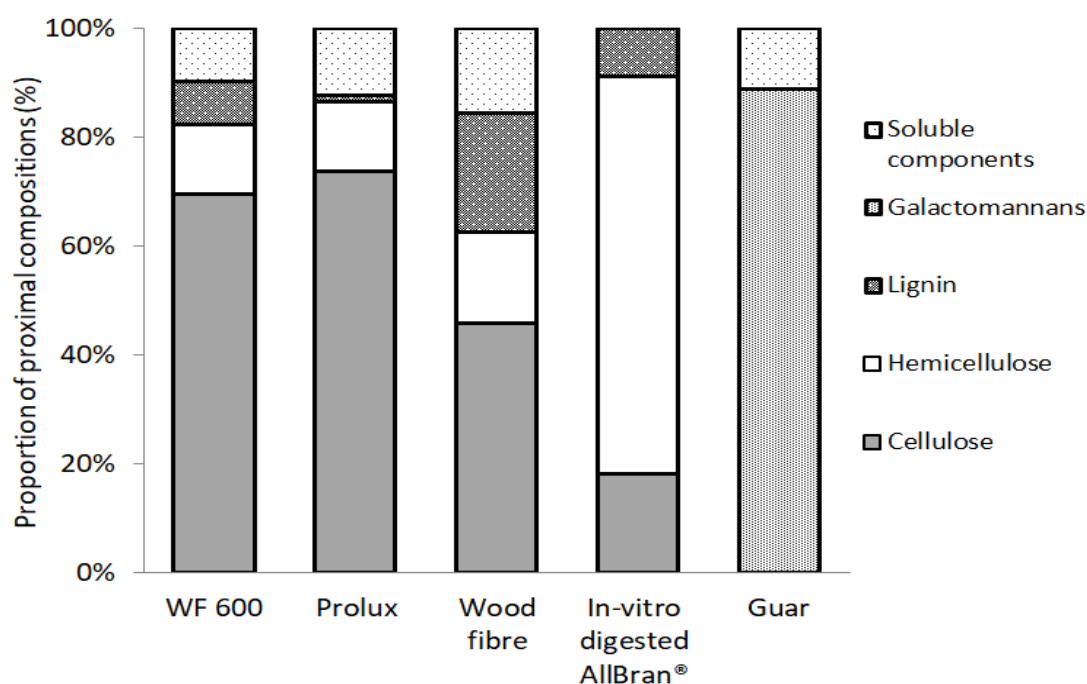


**Figure 6.1: Chemical compositions of the five fibre types.**



### 6.4.2. *Physico-chemical properties of starches*

Potato starch had a protein content (0.9%) around two thirds that of the corn starch (1.5%) and contained a negligible amount of lipid compared with corn starch (0.1%). The starch granules in potato are of greater mean diameter (10-60  $\mu\text{m}$ ) than those of corn (2-20  $\mu\text{m}$ ) and the surfaces of potato starch granules were generally smoother than those of corn in which small pores were evident (Figure 6.2 i, ii).

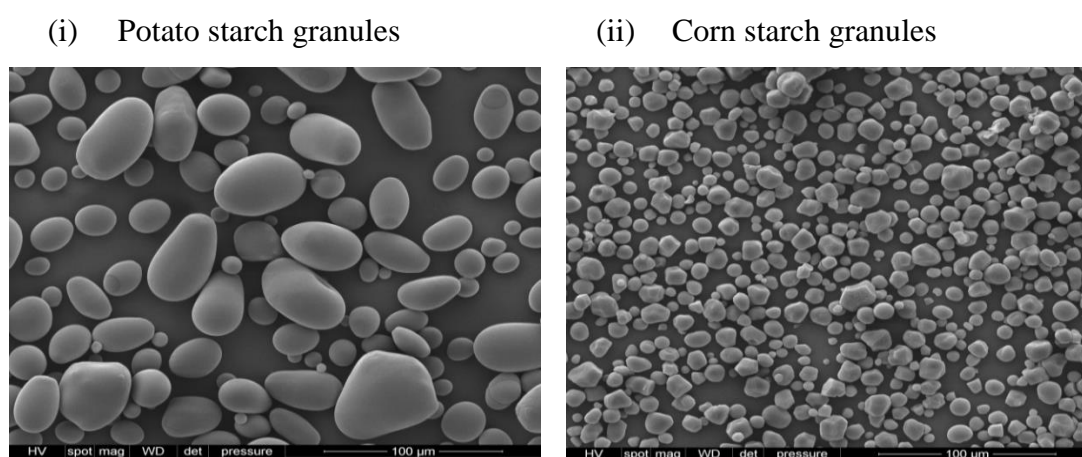


**Figure 6.2:** SEM images of the starch particles (i-ii), to the same scale.

### 6.4.3. *RDS, SDS, and RS as a proportion of total starch*

About 50% of the gelatinised P and C starch was classed as RDS and the proportions of RS were also similar for these starches (Figure 6.3). Due to the small amounts of starch present in the ‘as supplied’ fibre products, the total starch measured using this procedure was slightly greater than the 10% added to the suspensions. However, this effect was compensated for when expressed as proportion of total digested.

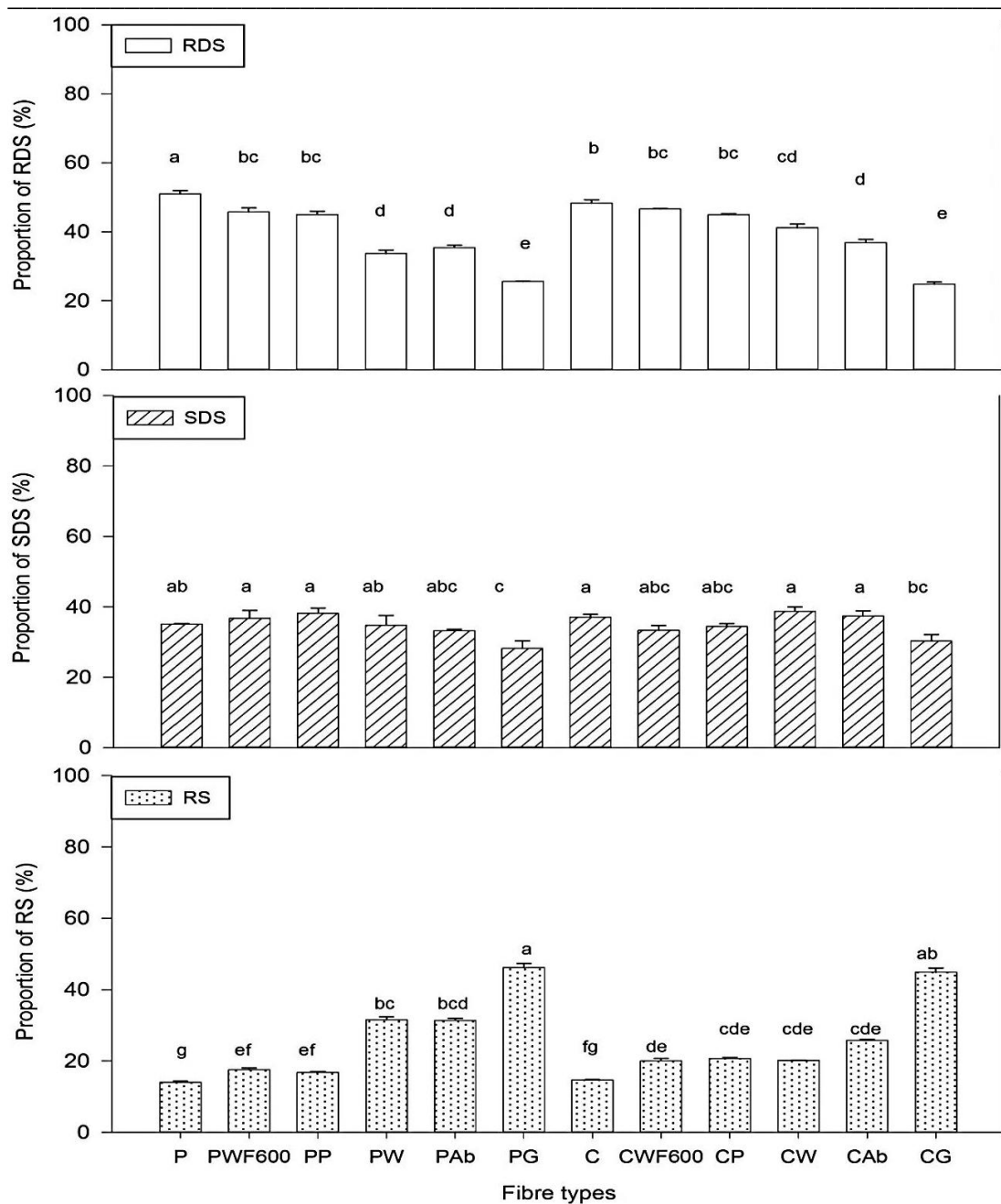


**Figure 6.3:** Proportions of RDS, SDS, and RS as a percentage of total starch, with and without the inclusion of the fibre types. P, potato starch; C, corn starch; WF600, WF600 wheat fibre; P, Prolux wheat fibre; W, wood fibre; Ab, *In-vitro* digested AllBran®; G, guar gum; RDS, rapidly digestible starch; SDS, slowly digestible starch; RS, resistant starch. Mean values labelled with different superscripts (a–e) are significantly different (GLM and Tukey's pair wise test,  $p \leq 0.05$ ).

The addition of either insoluble or soluble fibre (guar) to the gelatinised starches significantly increased ( $p < 0.05$ ) the proportion of RS. This was particularly evident for the guar/starch suspensions where the proportion of RS increased by about 30% (Figure 6.3) with concomitant decreases in RDS. The addition of wood fibre or AllBran® significantly decreased ( $p < 0.05$ ) the proportion of RDS for both potato and corn starch suspensions (Figure 6.3). Similarly, RDS decreased significantly ( $p < 0.05$ ) when wheat fibres (WF600 and Prolux) were added but only for suspensions containing potato starch but not for corn starch suspensions. These results suggest that the AllBran® fibre particles and possibly the wood particles can reduce the proportion of RDS more than the small cellulosic WF600 and Prolux particles but the larger effect occurs with the addition of guar.

#### **6.4.4. Relationship between viscosity and starch**

In the presence of gelatinised starches, the addition of fibre increased the apparent viscosity of starch suspensions, the percentage increment varying with the types of fibre and starch used at the beginning of digestion ( $T_0$ ) (Table 6.3). Thus, the viscosities of suspensions that contained potato starch at  $T=0$  min varied between 60.2 Pa.s and 80.6 Pa.s and viscosities of suspensions containing corn starch were between 8.9 Pa.s and 37.1 Pa.s, with the lower values associated with starch alone (Table 6.3). The higher viscosities in the treatment containing potato starch compared to corn starch were expected as the corn starch had a much lower PV (Table 6.1). The apparent viscosities of all suspensions rapidly decreased as starch was digested. Similar observations were reported by Repin and co-workers (Repin et al., 2016) in the study using different insoluble fibres on tapioca starch digestion and in studies using soluble fibres such as oat gum, soluble flaxseed gum, fenugreek

gum, and cereal soluble fibres on tapioca starch and corn starch digestion (Dhital et al., 2014; Repin et al., 2017).

In all treatments, the changes in the apparent viscosities were effectively completed after 20 min of digestion and the reduction of viscosities thereafter was negligible. In most cases, final viscosities were significantly lower ( $p < 0.05$ ) for suspensions containing starch only, and as expected, greater for those containing added fibre, particularly guar (Table 6.3).

**Table 6.3:** Viscosity (Pa.s) of the potato (P) and corn (C) starch suspensions with the various fibre types before intestinal digestion (0 min) and during *in-vitro* intestinal digestion at 20 and 120 min.

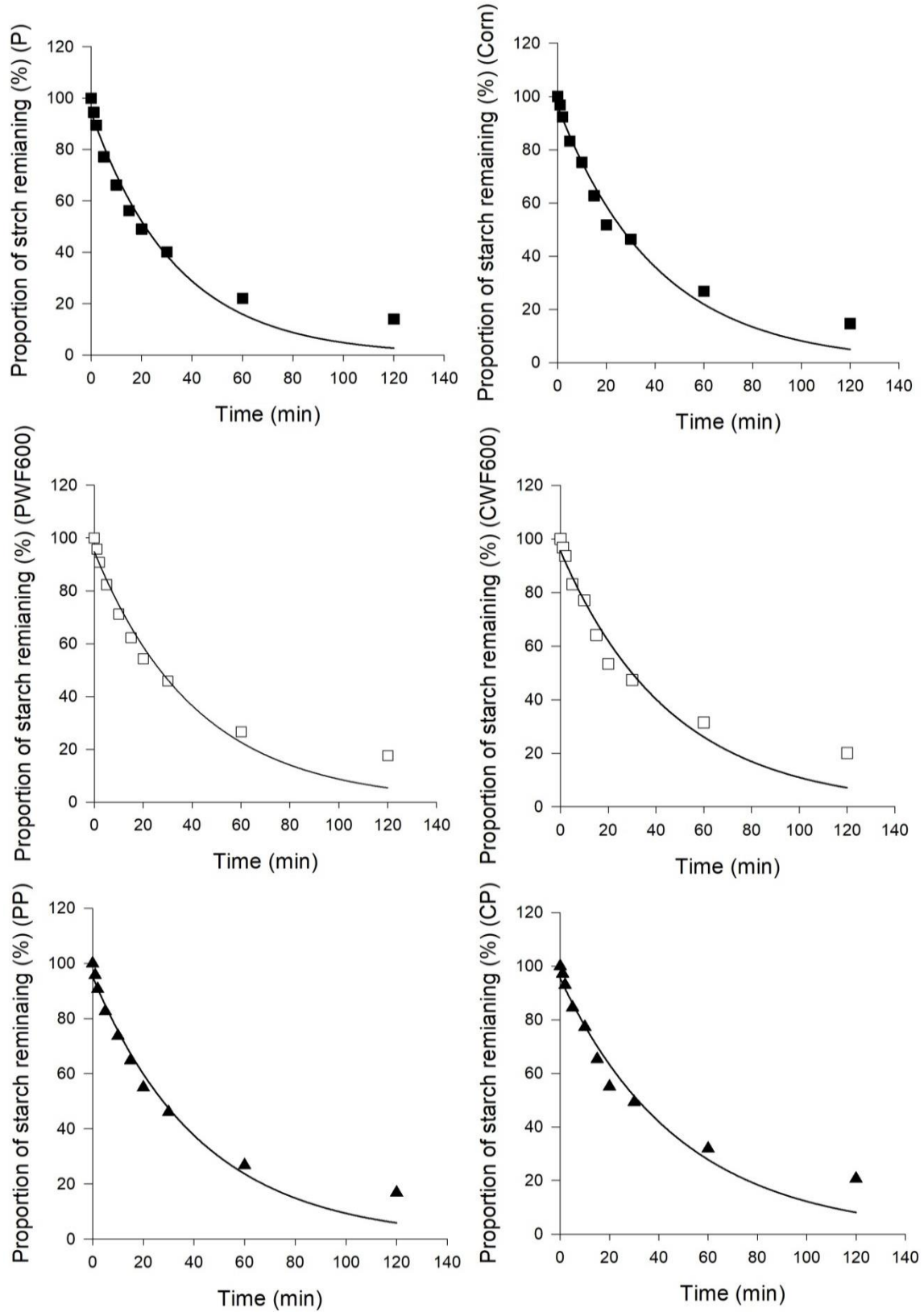
Digestion (min) ‡	P	PWF600	PP	PW	PAb	PG
Pa.s						
0	60.17 <sup>cd</sup>	65.54 <sup>bc</sup>	80.63 <sup>a</sup>	71.41 <sup>bc</sup>	63.00 <sup>cd</sup>	77.96 <sup>ab</sup>
20	0.03 <sup>g</sup>	0.05 <sup>def</sup>	0.06 <sup>ef</sup>	0.48 <sup>bc</sup>	0.15 <sup>bc</sup>	0.56 <sup>ab</sup>
120	0.01 <sup>f</sup>	0.02 <sup>e</sup>	0.03 <sup>de</sup>	0.11 <sup>bc</sup>	0.02 <sup>e</sup>	0.26 <sup>b</sup>

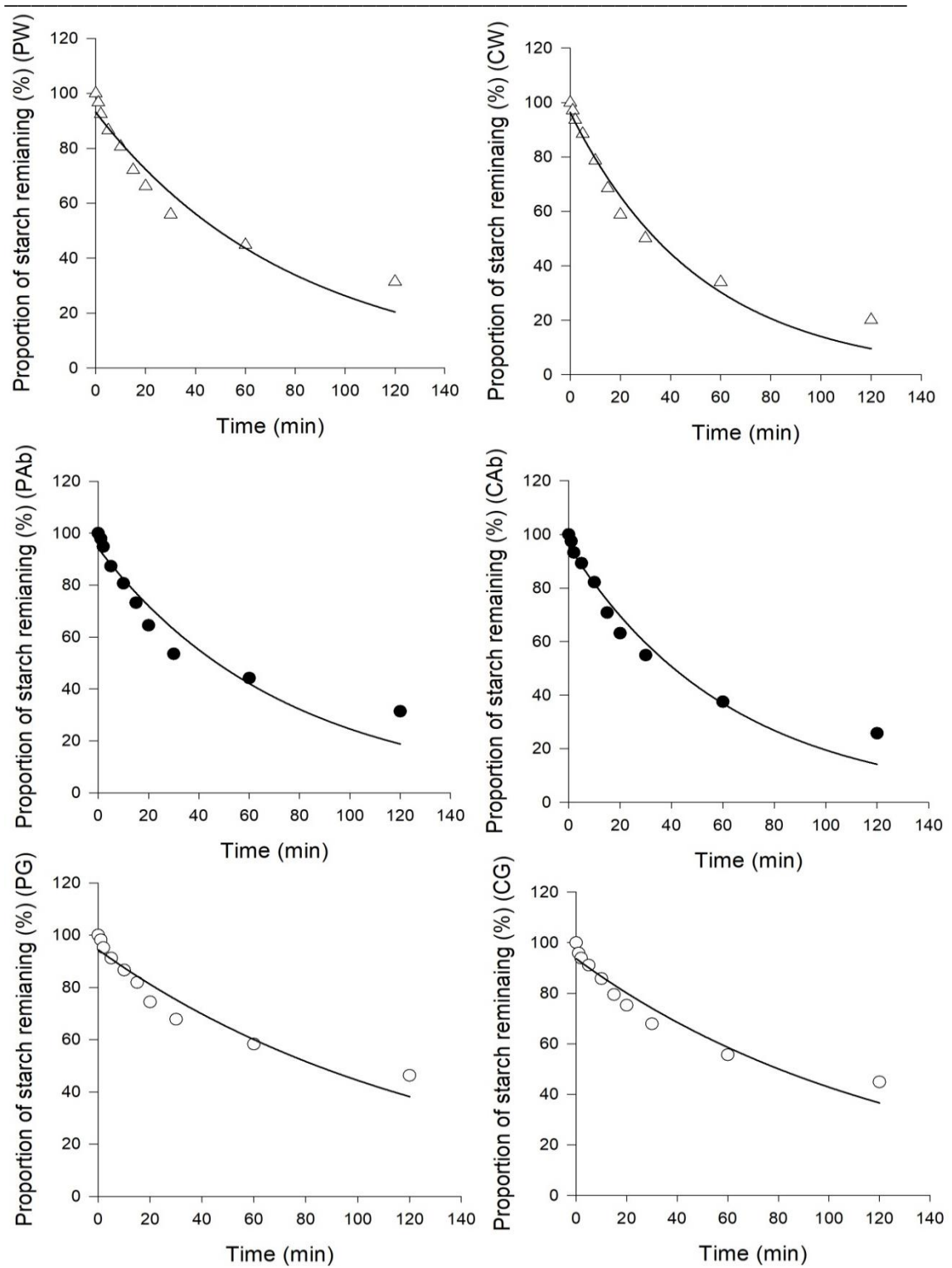
  

Digestion (min) ‡	C	CWF600	CP	CW	CAb	CG
Pa.s						
0	8.87 <sup>f</sup>	22.59 <sup>e</sup>	19.94 <sup>e</sup>	19.58 <sup>e</sup>	31.65 <sup>e</sup>	37.07 <sup>de</sup>
20	0.08 <sup>fg</sup>	0.15 <sup>cdef</sup>	0.14 <sup>cdef</sup>	0.19 <sup>cde</sup>	0.41 <sup>bcd</sup>	2.80 <sup>a</sup>
120	0.03 <sup>de</sup>	0.09 <sup>cd</sup>	0.10 <sup>bc</sup>	0.13 <sup>bc</sup>	0.19 <sup>bc</sup>	0.74 <sup>a</sup>

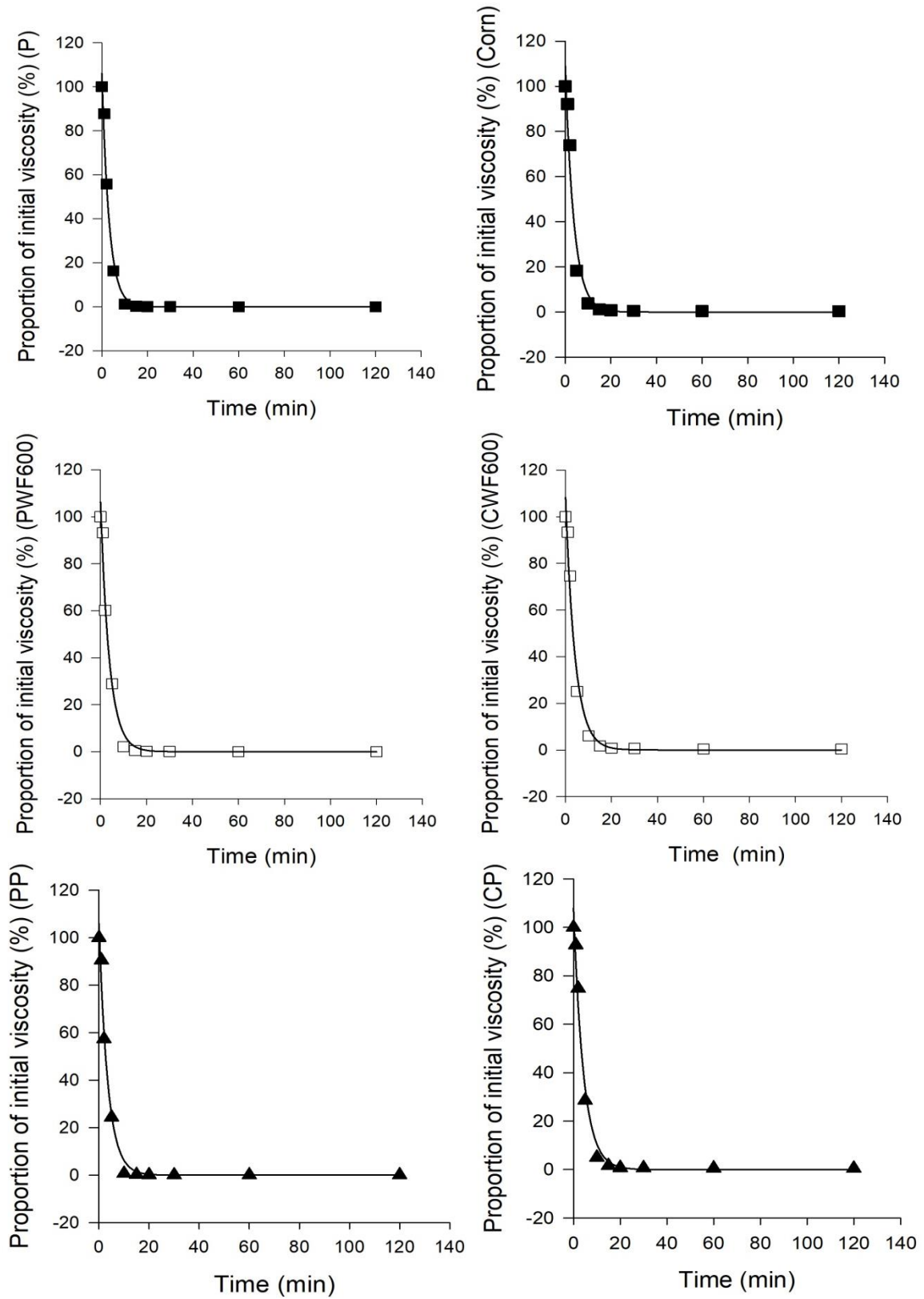
Note: ‡ Mean values in a row with different superscripts (a-g) are significantly different (GLM and Tukey's pair wise test,  $p < 0.05$ ). Other notation similar to Figure 6.3.

For each treatment, the best curve fit ( $R^2 > 0.95$ ) describing the general relationship between relative starch content and rate of digestion, and between relative viscosity and digestion time were exponential (Figures 6.4 and 6.5). Apparent viscosity declined much faster than expected from the proportion of starch remaining and had effectively reached a nadir at 20 min when less than 40% of the starch had been hydrolysed.





**Figure 6.4:** The proportion of starch remaining during *in-vitro* digestion of the ■ = Control starch (left, potato; right, corn), and various starch/fibre suspensions, □ = WF600, ▲ =Prolux fibre, △= Wood fibre, ● = AllBran® fibre, ○ = Guar. Each point is the mean of two replicates. The line is the best fit for all points using an exponential decay function (Equation 3.10).



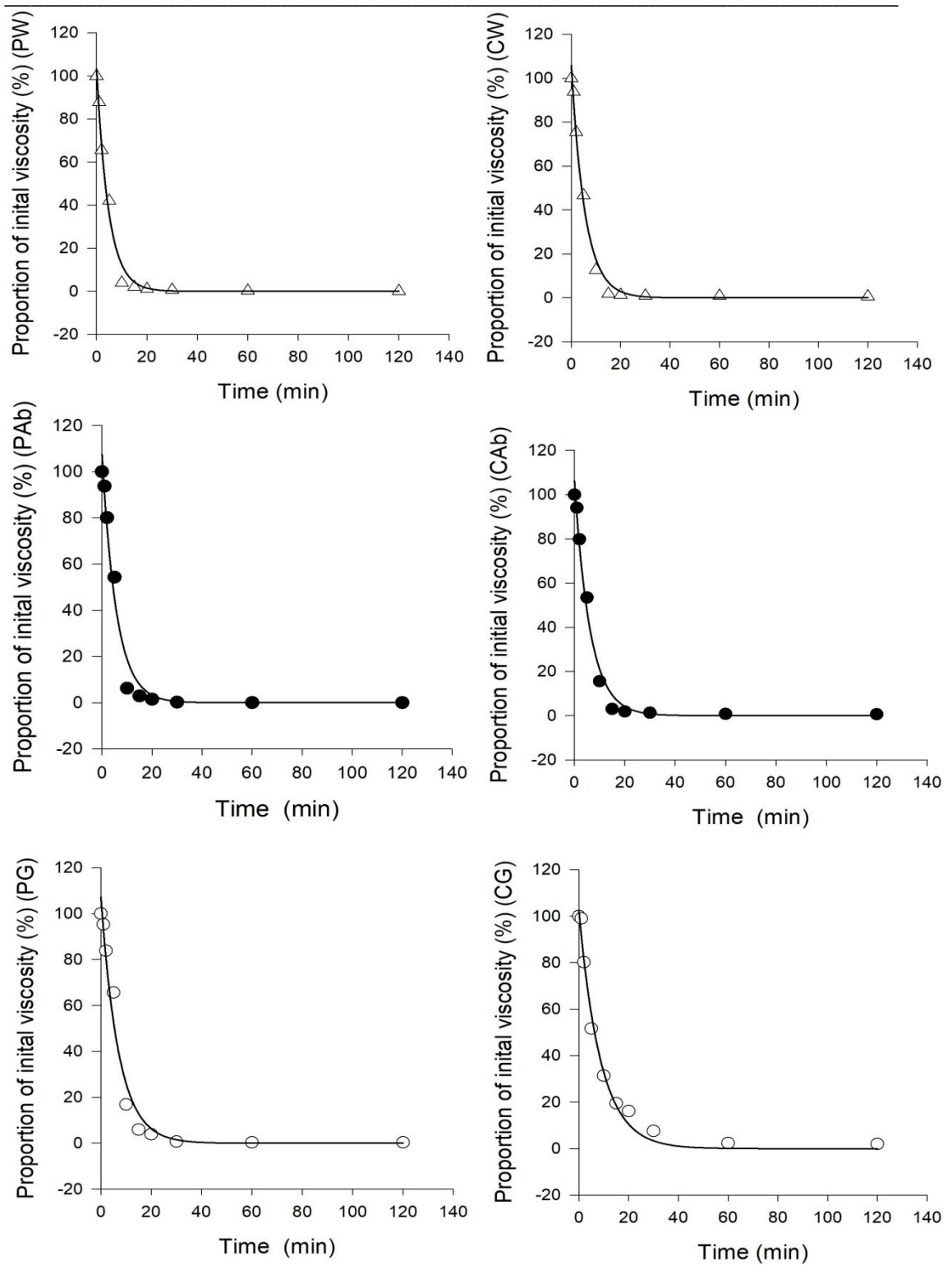


**Figure 6.5:** The proportion of apparent viscosity measured during *in-vitro* digestion of the  $\blacksquare$  = Control starch (left, potato; right, corn), and various starch/fibre suspensions,  $\square$  = WF600,  $\blacktriangle$  = Prolux fibre,  $\triangle$  = Wood fibre,  $\bullet$  = AllBran® fibre,  $\circ$  = Guar. Each point is the mean of two replicates. The line is the best fit for all points using an exponential decay function (Equation 3.10).



To further investigate the effect of addition of each fibre on the rate of digestion, the slopes (coefficient  $b$ ) derived from the exponential decay equation (Equation 3.10) for the rate of reduction in the proportion of starch and in the initial viscosity in the suspensions were compared (Tables 6.4 and 6.5).

**Table 6.4: Differences in coefficients  $a$  and  $b$  from Eq. 3.10 ( $y = ae^{-(bx)}$ ) for the relative rate of decay in the proportion of potato and corn starch for six treatments over 120 min of stimulated small intestinal digestion.**

Treatments	Coefficient $a$ , y-intercept ‡	Coefficient $b$ , slope ( $\text{min}^{-1}$ ) ‡	$R^2$
<b>P</b>	$94.33 \pm 4.17$	$0.03 \pm 0.01$	0.97
<b>PWF600</b>	$94.83 \pm 0.90$	$0.02 \pm 0.00$	0.97
<b>PP</b>	$95.21 \pm 2.85$	$0.02 \pm 0.00$	0.97
<b>PW</b>	$93.11 \pm 2.64^*$	$0.01 \pm 0.00^*$	0.93
<b>PAb</b>	$94.18 \pm 0.30^*$	$0.01 \pm 0.00^*$	0.92
<b>PG</b>	$94.37 \pm 1.37^*$	$0.01 \pm 0.00^*$	0.92
<b>C</b>	$96.32 \pm 3.28$	$0.03 \pm 0.00$	0.97
<b>CWF600</b>	$95.43 \pm 1.61$	$0.02 \pm 0.00$	0.95
<b>CP</b>	$95.43 \pm 2.03$	$0.02 \pm 0.01$	0.96
<b>CW</b>	$96.35 \pm 3.10^*$	$0.02 \pm 0.00^*$	0.97
<b>CAb</b>	$95.71 \pm 4.57^*$	$0.02 \pm 0.00^*$	0.96
<b>CG</b>	$93.65 \pm 1.09^*$	$0.01 \pm 0.00^*$	0.93

Note: ‡ mean value  $\pm$  95% confidence interval for mean within a column followed by (\*) superscript is significantly different (using t-test,  $p < 0.05$ ) compared to starch alone (P, C) treatments

**Table 6.5: Differences in coefficients  $a$  and  $b$  from Eq. 3.10 ( $y = ae^{-(bx)}$ ) for the reduction in initial viscosity of potato and corn starch for six treatments over 120 min of stimulated small intestinal digestion.**

Treatments	Coefficient $a$ , y-intercept ‡	Coefficient $b$ , slope ( $\text{min}^{-1}$ ) ‡	$R^2$
<b>P</b>	106.04 ± 10.04	0.32 ± 0.04	0.99
<b>PWF600</b>	106.32 ± 23.99	0.26 ± 0.05	0.99
<b>PP</b>	105.91 ± 15.40	0.28 ± 0.15	0.99
<b>PW</b>	103.21 ± 21.36	0.21 ± 0.02*	0.99
<b>PAb</b>	107.27 ± 22.60	0.17 ± 0.05*	0.98
<b>PG</b>	107.25 ± 19.96	0.14 ± 0.01*	0.98
<b>C</b>	108.88 ± 8.62	0.26 ± 0.06	0.98
<b>CWF600</b>	108.34 ± 2.71	0.24 ± 0.01	0.98
<b>CP</b>	107.91 ± 5.84	0.23 ± 0.03	0.99
<b>CW</b>	105.86 ± 1.34	0.18 ± 0.01*	0.99
<b>CAb</b>	106.27 ± 4.40	0.16 ± 0.01*	0.99
<b>CG</b>	102.48 ± 20.86	0.11 ± 0.04*	0.98

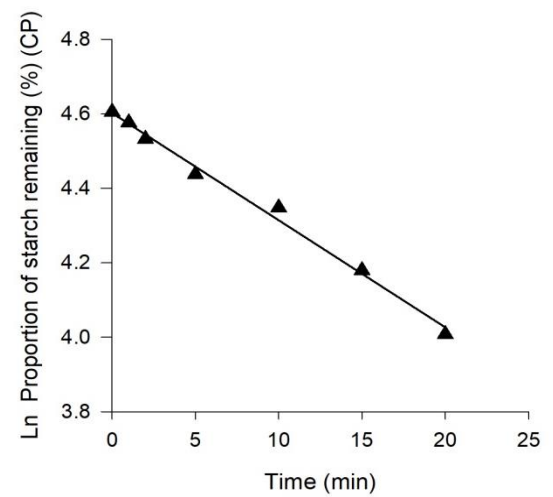
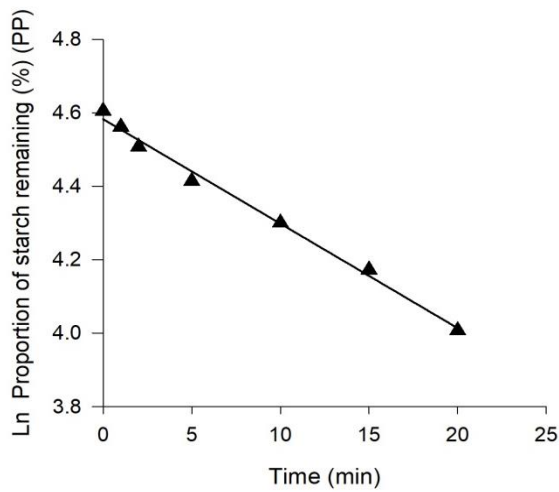
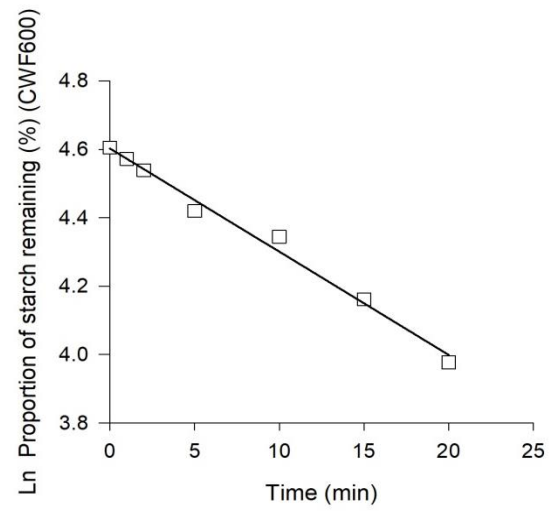
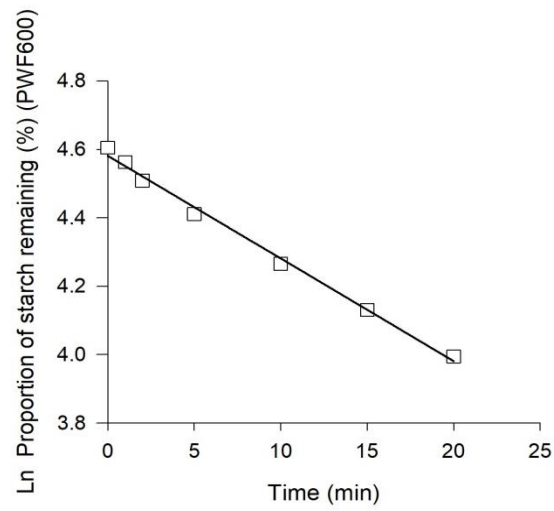
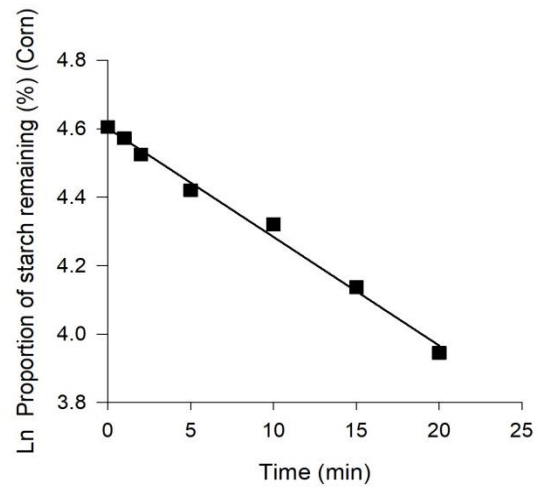
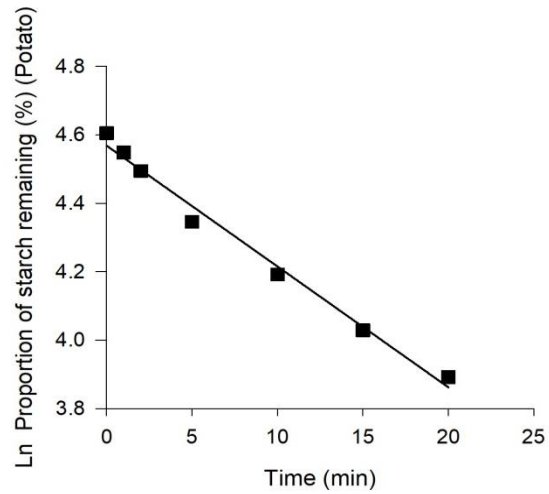
Note: ‡ mean value ± 95% confidence interval for mean within a column followed by (\*) superscript is significantly different (using t-test,  $p < 0.05$ ) compared to starch alone (P, C) treatments

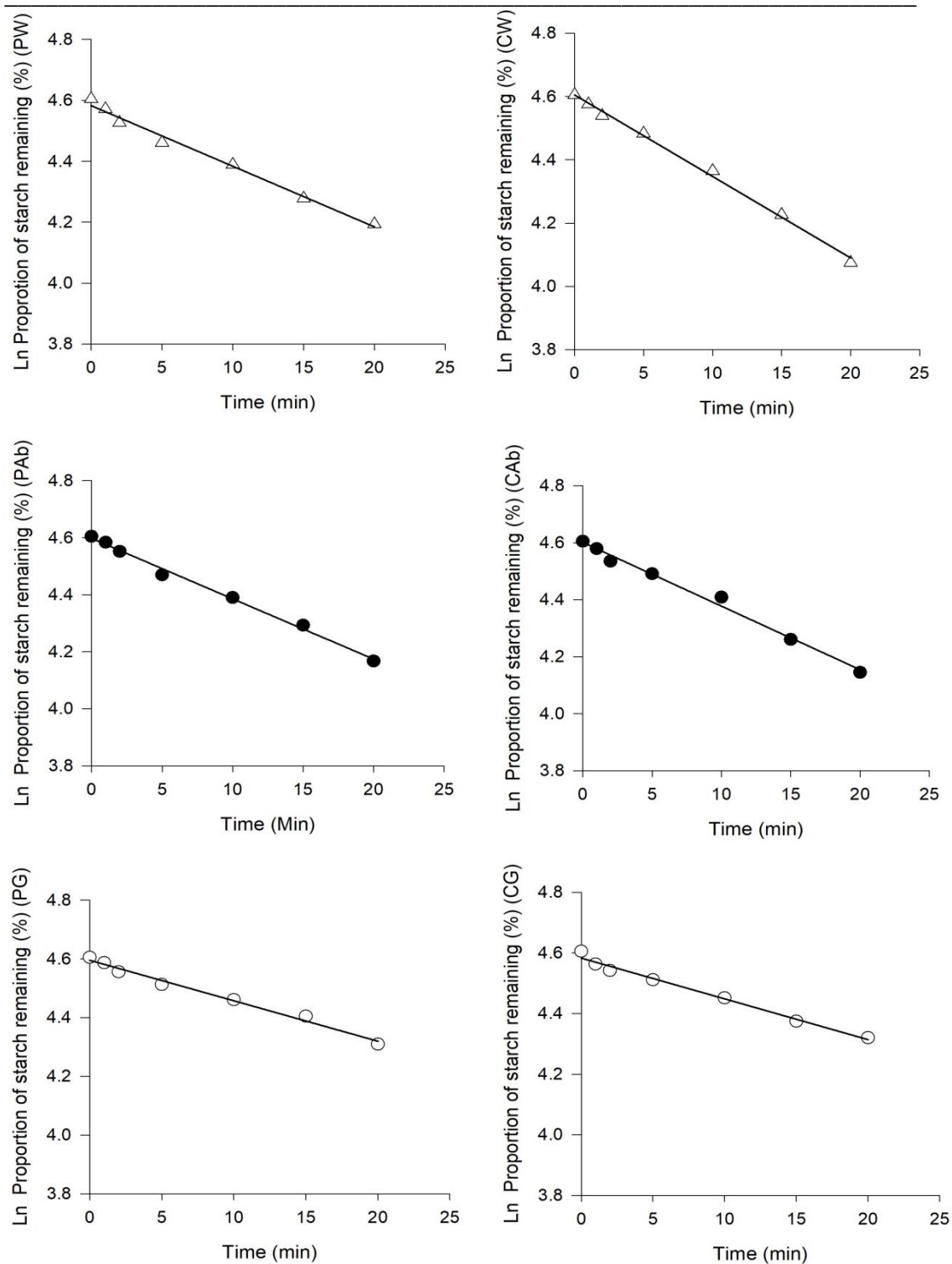
The rate of decay (slope) in the proportion of starch and in initial viscosity, both in the suspensions that contained starch alone and suspensions with added cellulosic wheat fibres, were similar, but the slope was significantly ( $p < 0.05$ ) different in suspensions with added wood fibre, AllBran®, and guar (Tables 6.4 and 6.5). Similar values of slope, ranged from 0.15 to 0.36  $\text{min}^{-1}$  were reported (Dhital et al., 2014; Repin et al., 2016, 2017) in studies using different insoluble and soluble fibres on the digestion of tapioca and maize starch.

Generally, after 20 min of digestion, the changes in the rate of amylolysis and the rate of initial viscosity reduction were negligible. Changes in the rate of viscosity reduction reached a plateau after 20 min, which might result from the limitation of the vane geometry or from hydrolysis of the gelatinised starch into smaller molecular weight products such as maltose which occupy a smaller volume fraction.

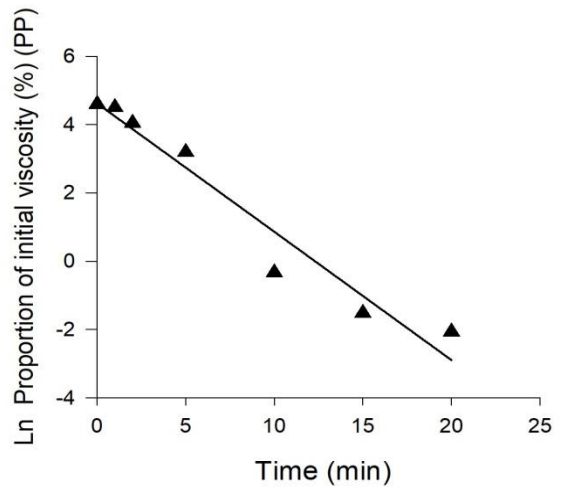
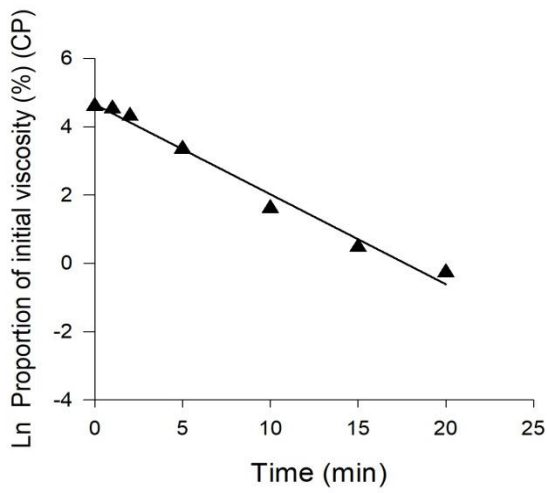
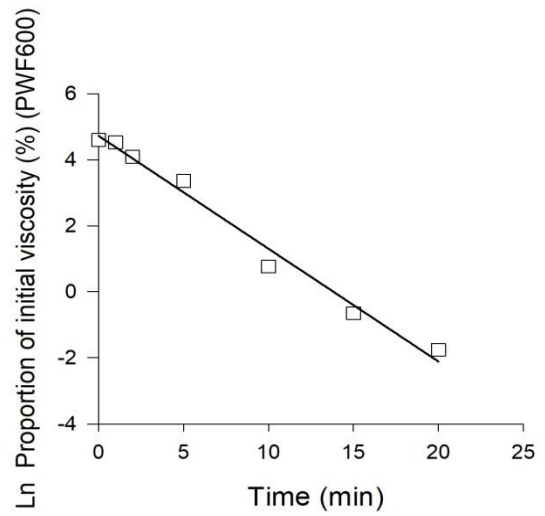
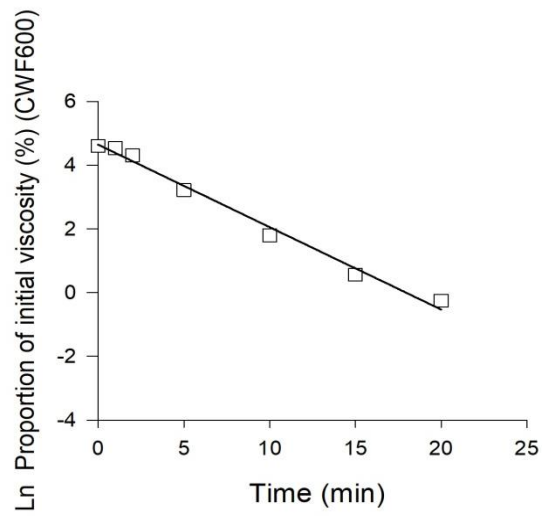
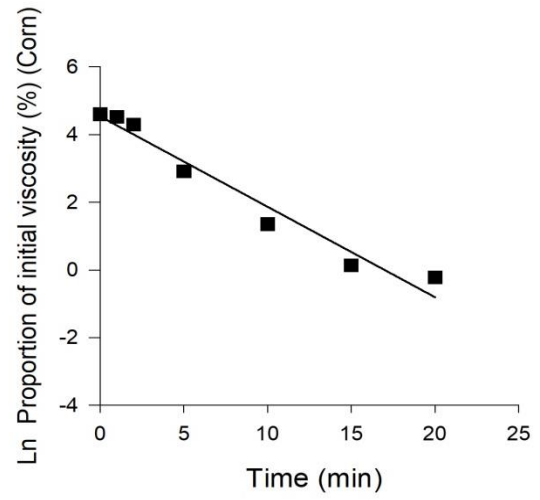
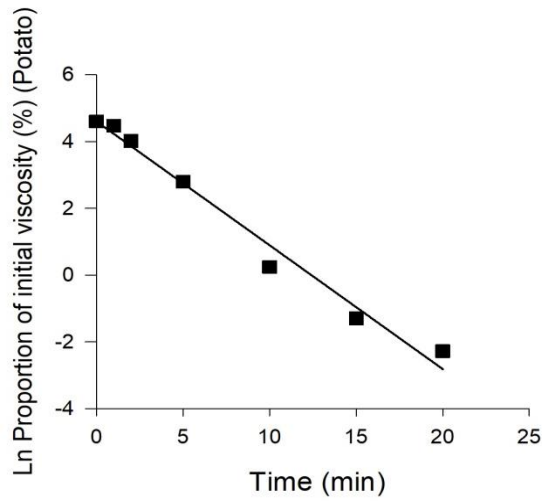
Therefore, only the major changes in the rate in both parameters within the RDS region were plotted (Figures 6.6 and 6.7) and were focused in the on following discussion.

The plots of the Ln-transformed relative proportion of starch remaining and apparent viscosity for each treatment with time of digestion were linear (Equation 3.11), and regressions determined for each fibre type had  $R^2$  values of 0.95 or better. The best curve fit to describe the relationships for the proportion of starch remaining and apparent viscosity was plotted using pooled results (Figures 6.6 and 6.7).





**Figure 6.6:** The proportion of starch remaining (Ln-transformed data) during the first 20 min (Figure 6.4) of *in-vitro* digestion of the ■ = Control starch (left, potato; right, corn), and various starch/fibre suspensions, □=WF600, ▲=Prolux fibre, △=Wood fibre, ●=AllBran® fibre, ○ = Guar. Each point is the mean of two replicates. The line is the linear regression (Equation 3.11) fitted to all points.



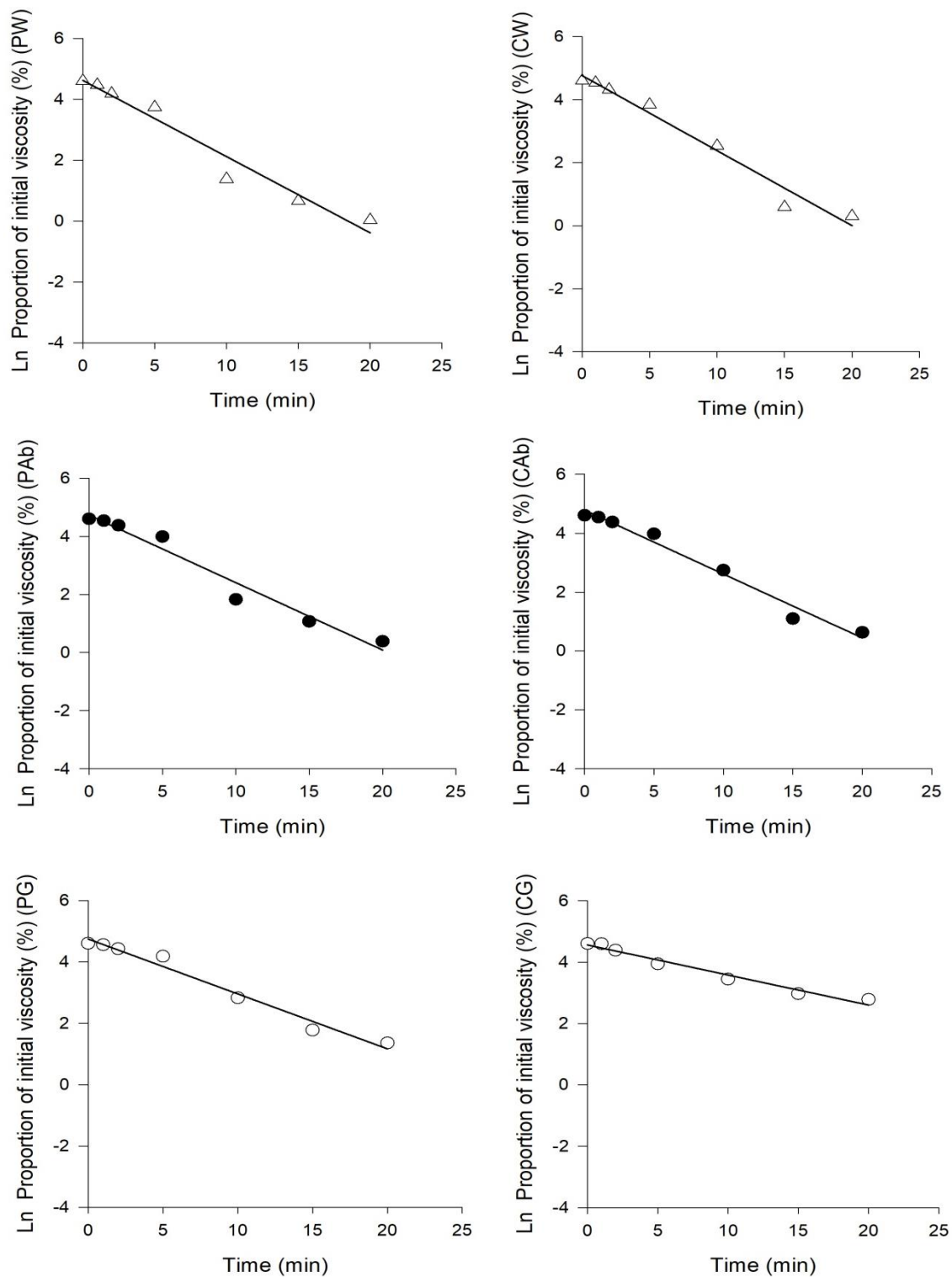


**Figure 6.7:** The proportion of initial viscosity measured (Ln-transformed data) during the first 20 min (Figure 6.5) of *in-vitro* digestion of ■ = Control starch (left, potato; right, corn), and various starch/fibre suspensions, □ = WF600, ▲ = Prolux fibre, △ = Wood fibre, ● = AllBran® fibre, ○ = Guar. Each point is the mean of two replicates. The line is the linear regression (Equation 3.11) fitted to all points.

For each of the treatments, the relationship between the rate of amylolysis and the rate of viscosity reduction in the RDS region was linear when plotted using Ln-data (Figures 6.6 and 6.7). To further investigate the effect of each fibre on the rate of starch digestion and the rate of reduction in the initial viscosity of the suspensions, the slopes (coefficient  $b$ ) derived from Equation 3.11 were compared (Tables 6.6 and 6.7).

**Table 6.6: Differences in constants  $m$  and  $n$  ( $\ln Y = \ln m + n \cdot \ln t$ ), the relative rate of decay in the proportion of potato and corn starch for six treatments over 20 min of stimulated small intestinal digestion.**

Treatments	Coefficient $m$ , y-intercept ‡	Coefficient $n$ , slope ( $\text{min}^{-1}$ ) ‡	$R^2$
<b>P</b>	$4.57 \pm 0.04^b$	$-0.035 \pm 0.01^f$	0.99
<b>PWF600</b>	$4.58 \pm 0.01^{ab}$	$-0.03 \pm 0.01^{de}$	0.99
<b>PP</b>	$4.58 \pm 0.02^{ab}$	$-0.03 \pm 0.01^{cd}$	0.99
<b>PW</b>	$4.58 \pm 0.05^{ab}$	$-0.02 \pm 0.01^b$	0.99
<b>PAb</b>	$4.60 \pm 0.01^a$	$-0.02 \pm 0.00^b$	0.99
<b>PG</b>	$4.60 \pm 0.03^{ab}$	$-0.01 \pm 0.00^a$	0.99
<b>C</b>	$4.60 \pm 0.08^a$	$-0.03 \pm 0.01^e$	0.99
<b>CWF600</b>	$4.60 \pm 0.00^a$	$-0.03 \pm 0.00^{de}$	0.99
<b>CP</b>	$4.60 \pm 0.01^a$	$-0.03 \pm 0.01^{cde}$	0.99
<b>CW</b>	$4.61 \pm 0.00^a$	$-0.03 \pm 0.00^c$	1.00
<b>CAb</b>	$4.60 \pm 0.05^a$	$-0.02 \pm 0.00^b$	0.99
<b>CG</b>	$4.58 \pm 0.01^{ab}$	$-0.01 \pm 0.00^a$	0.99

**Note:** ‡ mean value  $\pm$  95% confidence interval for mean within a column followed by (a-f) superscript is significantly different (using ANOVA,  $p < 0.05$ ) compared to starch alone (P, C) treatments



**Table 6.7: Differences in constants  $m$  and  $n$  ( $\text{Ln } Y = \text{Ln } m + n \cdot \text{Ln } t$ ), the relative rate of decay in viscosity as a proportion of initial viscosity for potato and corn starch suspensions for six treatments over 20 min of stimulated small intestinal digestion.**

Treatments	Coefficient $m$ , y-intercept $\ddagger$	Coefficient $n$ , slope ( $\text{min}^{-1}$ ) $\ddagger$	$R^2$
<b>P</b>	$4.60 \pm 0.20^{\text{de}}$	$-0.37 \pm 0.21^{\text{gh}}$	0.98
<b>PWF600</b>	$4.73 \pm 0.11^{\text{abcd}}$	$-0.34 \pm 0.04^{\text{g}}$	0.98
<b>PP</b>	$4.62 \pm 0.76^{\text{cde}}$	$-0.38 \pm 0.09^{\text{h}}$	0.95
<b>PW</b>	$4.62 \pm 0.08^{\text{cde}}$	$-0.25 \pm 0.05^{\text{def}}$	0.96
<b>PAb</b>	$4.73 \pm 0.22^{\text{abcd}}$	$-0.23 \pm 0.01^{\text{cd}}$	0.97
<b>PG</b>	$4.74 \pm 0.44^{\text{abc}}$	$-0.18 \pm 0.06^{\text{b}}$	0.97
<b>C</b>	$4.54 \pm 0.43^{\text{e}}$	$-0.27 \pm 0.04^{\text{f}}$	0.96
<b>CWF600</b>	$4.64 \pm 0.01^{\text{bcde}}$	$-0.26 \pm 0.01^{\text{def}}$	0.99
<b>CP</b>	$4.66 \pm 0.06^{\text{abcde}}$	$-0.26 \pm 0.00^{\text{ef}}$	0.98
<b>CW</b>	$4.77 \pm 0.10^{\text{ab}}$	$-0.24 \pm 0.03^{\text{cde}}$	0.97
<b>CAb</b>	$4.78 \pm 0.18^{\text{a}}$	$-0.22 \pm 0.04^{\text{c}}$	0.98
<b>CG</b>	$4.56 \pm 0.26^{\text{e}}$	$-0.10 \pm 0.02^{\text{a}}$	0.97

**Note:**  $\ddagger$  mean value  $\pm$  95% confidence interval for mean within a column followed by (a-f) superscript is significantly different (using ANOVA,  $p < 0.05$ ) compared to starch alone (P, C) treatments

The slope (coefficient of regression) was the rate of decline of remaining starch and apparent viscosity. The values for these slopes were calculated both in an exponential decay equation using proportional data (Equation 3.10), and in a linear equation using Ln data (Equation 3.11) were similar (Tables 6.4, 6.5, 6.6 and 6.7).

The amount of starch remaining after 20 min of digestion varies between 45% and 70% depending on the fibre types present. The rate of digestion and the reduction in apparent viscosity of starch alone were altered little by the addition of the smaller cellulosic wheat fibre (WF600 and Prolux) particles. However, the slopes of the linear relationship of starch remaining for potato and corn suspensions slowed significantly ( $p < 0.05$ ) when wood particles or AllBran® fibres were added, and slowed to a greater extent when guar was added (Tables 6.8). These results were greatly similar to the slopes coefficients given in Tables 6.4, 6.5, 6.6 and 6.7.

**Table 6.8: Differences in the relative rate of digestion of potato and corn starch ( $\text{min}^{-1}$ ) for six treatments over 20 min of stimulated small intestinal digestion.**

Treatments	Rate of digestion ( $\text{min}^{-1}$ ) ‡	Treatments	Rate of digestion ( $\text{min}^{-1}$ ) ‡
<b>P</b>	$14.09 \pm 0.17^a$	<b>C</b>	$13.07 \pm 0.20^a$
<b>PWF600</b>	$12.46 \pm 0.17^b$	<b>CWF600</b>	$12.62 \pm 0.03^{ab}$
<b>PP</b>	$12.43 \pm 0.14^b$	<b>CP</b>	$12.16 \pm 0.02^{ab}$
<b>PW</b>	$9.32 \pm 0.17^c$	<b>CW</b>	$11.13 \pm 0.14^{bc}$
<b>PAb</b>	$9.80 \pm 0.09^c$	<b>CAb</b>	$9.98 \pm 0.12^{bc}$
<b>PG</b>	$7.07 \pm 0.01^d$	<b>CG</b>	$6.71 \pm 0.07^c$

**Note:** ‡ mean value  $\pm$  95% confidence interval for mean within a column followed by (a-f) superscript is significantly different (using ANOVA,  $p < 0.05$ ) compared to starch alone (P, C) treatments

Calculations from the functions used to model the rate of starch hydrolysis and the reduction in viscosity during the RDS phase show that the differences in the rates have important implications for the time taken to reduce the proportion of starch remaining by 50%, expressed as the  $T_{1/2}$  value (Table 6.9).  $T_{1/2}$  values varied from 18.6 min (potato) and 21.7 min (corn) to almost 50 min for both in the presence of guar (Table 6.9). The  $T_{1/2}$  values obtained from this study are in close agreement with the values using cooked potato, wheat starch, and white bread (19.8, 17.3, and 19 min, respectively) (Butterworth et al., 2012).

**Table 6.9:**  $T_{1/2}$  values (min) for starch digestion and viscosity for the two starch controls (P, C) and 10 treatments during 120 min of *in-vitro* digestion of suspensions of various fibres with potato (left) and corn (right) starch.

Treatment	$T_{1/2}$ starch (min) <sup>‡</sup>	$T_{1/2}$ viscosity (min) <sup>‡</sup>	Treatments	$T_{1/2}$ starch (min) <sup>‡</sup>	$T_{1/2}$ viscosity (min) <sup>‡</sup>
<b>P</b>	18.60±0.71 <sup>e</sup>	1.85±0.07 <sup>f</sup>	<b>C</b>	21.70±0.42 <sup>d</sup>	2.33±0.18 <sup>e</sup>
<b>PWF600</b>	21.45±1.06 <sup>d</sup>	2.35±0.07 <sup>e</sup>	<b>CWF600</b>	22.90±0.00 <sup>cd</sup>	2.83±0.04 <sup>de</sup>
<b>PP</b>	22.40±1.27 <sup>cd</sup>	1.88±0.18 <sup>f</sup>	<b>CP</b>	23.65±0.92 <sup>cd</sup>	2.83±0.04 <sup>de</sup>
<b>PW</b>	33.65±1.06 <sup>b</sup>	2.80±0.07 <sup>de</sup>	<b>CW</b>	26.95±0.49 <sup>bc</sup>	3.60±0.14 <sup>bc</sup>
<b>PAb</b>	32.45±1.06 <sup>b</sup>	3.53±0.11 <sup>cd</sup>	<b>CAb</b>	30.85±0.21 <sup>b</sup>	4.00±0.00 <sup>bc</sup>
<b>PG</b>	49.45±0.92 <sup>a</sup>	4.65±0.07 <sup>b</sup>	<b>CG</b>	49.85±1.91 <sup>a</sup>	6.60±0.42 <sup>a</sup>

Data points are derived by solving from the linear regressions fitted to the data for each treatment in Figures 6.6 and 6.7.

Note: <sup>‡</sup> Mean values ± standard error for mean in a column with different superscripts (a-f) are significantly different (GLM and Tukey's pair wise test,  $p < 0.05$ ). Other notation similar to Figure 6.3.

The corresponding  $T_{1/2}$  values for the reduction in viscosity varied similarly between 1.8 min and 6.6 min (Table 6.9), apparent viscosity decreasing much faster than starch concentration. The  $T_{1/2}$  values for the reduction of apparent viscosity in suspensions containing two wheat fibres were similar to suspensions containing starches alone, while suspensions containing wood and AllBran® fibres increased  $T_{1/2}$  values significantly ( $p < 0.05$ ) (Table 6.9). Differences in the  $T_{1/2}$  values for viscosity between the two starches were small and less than 2 min averaged over all treatments.

The relationship between viscosity and the proportion of starch digested for the various treatments over the first 20 min of digestion fitted well as a sigmoid function ( $R^2 \geq 0.98$ ) for each starch type (Figure 6.8). The reduction of apparent viscosity for each of the treatments began when hydrolysis commenced and all reductions in

viscosity were effectively complete when about 30% of the starch was digested (Figure 6.8).

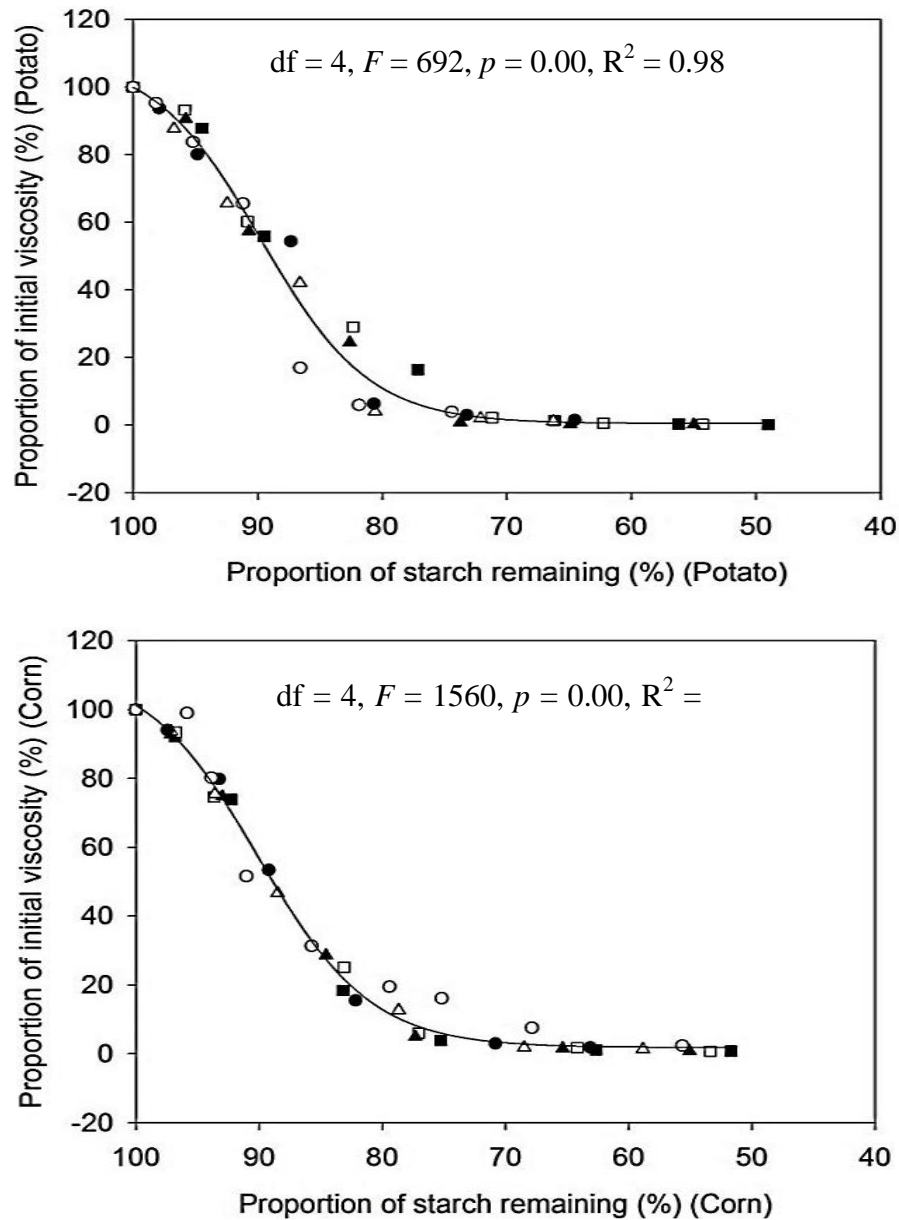


**Figure 6.8:** The relationship between the proportion of starch remaining in suspension and apparent suspension viscosity during 20 min of *in-vitro* digestion for ■ = Control starch (left, potato; right, corn), and various starch/fibre suspensions, □ = WF600, ▲ = Prolux fibre, △ = Wood fibre, ● = AllBran® fibre, ○ = Guar. Each point is the mean of two replicates.

It is noteworthy that the correlation coefficient ( $R^2$ ) for this relationship was high for both potato and corn starch, with the data points for the various fibre treatments being very close to the fitted line. Hence, when the effect of time is factored out, the relationship between the amount of starch remaining and apparent viscosity appeared to differ in three phases, a brief early phase when apparent viscosity declined relatively slowly as starch was digested, a subsequent phase when the rate of decline of starch content and relative viscosity were in proportion and a final phase when the starch content continued to decline rapidly but the reduction in viscosity was effectively complete. There was no consistent variation in the form of the relationship between starch types or fibre treatments indicating that the presence of the various fibres had no effect on the relationship between starch present and apparent viscosity.

## **6.5. Discussion**

The concentration of starch selected for this work was based on viscosity and pasting properties; the viscosity of the suspension had to be as high as possible at the beginning of digestion so that viscosity was retained in the measurable range for as long as possible during digestion. When the concentration of potato starch was 15% (w/w) (Table 6.1), the viscosity of the gelatinised paste was too great to measure properly; while at 5% (w/w) the viscosity was too low. A concentration of 10% offered the greatest workable viscosity for both potato and corn starches.

Adding guar gum and some insoluble plant fibres at concentrations and viscosities similar to those in the small intestine of pigs (Chapter 5) slowed the rate of digestion of gelatinised starch suspensions (Table 6.8). The results were broadly similar to the

reported effects with other fibre combinations (Butterworth et al., 2012; Dhital et al., 2014; Gupta & Premavalli, 2011; Repin et al., 2016; Repin et al., 2017).

In this study, the technique of *in-vitro* digestion at a constant shear rate ( $10 \text{ s}^{-1}$ ) in a rheometer fitted with cup and vane geometry allowed the rates at which starch was hydrolysed in the presence of different fibre types to be compared during the period when apparent viscosities of the suspensions were decreasing due to hydrolysis of starch. Since the viscosities of suspensions decreased rapidly within the first 10 min of digestion, and the changes of slope in the digestion curve are greatly affected by intervals of sub-sampling (Butterworth et al., 2012); therefore, digestate was sub-sampled at more frequent intervals (Figure 6.5). By increasing the sub-sampling intervals, the rate of decay in apparent viscosities and total starch content in suspensions containing different fibre types during the first 20 minutes of digestion could be accurately modelled using an exponential decay function ( $R^2 > 0.95$ ) (Figures 6.4 and 6.5) and fitted well in a linear regression when Ln-transformed data was plotted against time ( $R^2 > 0.95$ ) (Figures 6.6 and 6.7). These results suggested that to precisely model the rate of digestion, more sub-sampling intervals should be carried out at the beginning of the digestion, but not only sub-sampled at 30 min interval (Butterworth et al., 2012).

To date, most studies have reported that adding fibres to the diet decreases the rate of carbohydrate digestion in the gut (Blackburn & Johnson, 1981; Jenkins et al., 2004), presumably due to the effects of increasing viscosity, thus slowing mixing and the transfer of sugars to sites of absorption at the gut wall (Lentle & Janssen, 2008). A body of scientific evidence has shown that the addition of dietary fibre can

increase the apparent viscosity of digesta but the effects were often difficult to detect unless the concentration of fibre was high (Blackburn & Johnson, 1981; Jenkins et al., 2004; Wood et al., 1990). However, the presence of particularly high concentrations of insoluble fibres (above a volume fraction of 0.5), such as those occurring in the colon, and resulting digesta behaves as a viscoelastic solid and demonstrates a yield stress property (Lentle, Janssen, et al., 2007; Wood, 1992; Wood et al., 1990). Under these conditions, transport processes such as nutrient absorption may be limited to diffusion and will therefore be very slow and physically compromise the rate at which starch is digested. At high concentrations (1%) a range of soluble fibres were shown to reduce blood glucose levels when incorporated in a drink containing glucose. Of these fibres, guar was among the most effective in spite of its relatively low solution viscosity compared with the other fibres used (Edwards et al., 1987).

Similarly, viscous 10% starch/fibre suspensions (Table 6.3) contained a high solid volume fraction at  $T=0$ , by which the concentration of reactants (starch granules) was in excess, and rate of amylolysis is independent of reactant concentration. The rate of amylolysis is limited by the rate of enzyme diffusion; hence these suspensions followed a zero-order reaction. This is evident when the changes in the apparent viscosity of the starch/fibres suspensions (reactants) were minimal in the first 5 minutes of amylolysis (Figures 6.4, 6.5 and 6.8). This effect became apparent only when digestate was sub-sampled at more frequent intervals in the RDS phase.

In this study, the solid volume fraction of fibres added into the suspensions was close to levels normally encountered in the small intestine (Chapter 5). Regardless of

the types of fibre added into the starch suspension, the relationship between percentage changes in apparent viscosity and percentage of starch digested was constant (Tables 6.4, 6.5, 6.6 and 6.7). This result suggests that when time is factored out, changes in suspension viscosity during digestion are only dependent on the loss of starch (solid) particles as they are hydrolysed to sugars.

The addition of various fibres to gelatinised starch did increase the apparent viscosities of all suspensions to differing extents (Table 6.3). There was no clear relationship between initial viscosity of the various mixtures and the  $T_{1/2}$  values for starch digestion. For example, the initial viscosities of suspensions with potato starch were three to four times greater than treatments using corn starch, yet the  $T_{1/2}$  values for starch digestion were similar overall and for each treatment (Table 6.9). The higher gelatinisation temperatures (PT) and lower PV (Table 6.1) for the fully gelatinised corn starch have been reported previously and are attributed to the presence of lipids that complex with the starch and to differences in the molecular organisation of the granules (Karlalas, Tester, & Morrison, 1992). The presence of fibres, namely, wood, AllBran®, and particularly guar, significantly increased both the  $T_{1/2}$  values for starch digested and the  $T_{1/2}$  values for apparent viscosities compared with those for potato and corn starches alone (Table 6.9). These high  $T_{1/2}$  values suggested that wood fibre, AllBran®, and particularly guar suppressed the hydrolytic activity of amylase; reduced the rate of starch digestion, and consequently reduced the rate of reduction in apparent viscosity.

The overall sigmoid relationship between the rate of change in apparent viscosity and the rate of change in starch content (Figure 6.8) provides some insight into the



process of digestion of starch granules. The relative initial apparent viscosity of these suspensions plateaued off (Table 6.3, Figure 6.5) and concomitantly reduced the relative amount of starch (reactant) (Figure 6.4) in the *in-vitro* system could be explained by shifting of rate of reaction from zero order to first order, and the rate of digestion is following the rate of first order kinetics after 20 min of digestion. The plateaued off of rate of amylolysis in the latter part of the digestion (after 20 min) could be due to the substrate depletion in the *in-vitro* system. However, this explanation does not consider the chemical structure of starch granules *per se*. At a closer look on the results, starch granules are not only the concentration of substrate changes with time, but also the susceptibility of starch chemical structure to the enzyme changes with time, where the digestibility of starch granules gradually moved from highly digestible starch to resistant starch. Hereby, the sigmoidal curve could be further elaborated amylolysis process.

In the beginning of the sigmoidal curve, the relative viscosity decreased at a slower rate (Figure 6.8). The delays were presumably due to the remaining ordered granule structures resisting initial digestion and thereby preserving the granule integrity from amylolysis (Planchot et al., 1995). In the second phase of digestion, as indicated by the subsequent rapid linear decline in viscosity (Figure 6.8), suggests that the gelatinised granules progressively lose size and volume in the suspension and these starch fragments become less important in determining the viscosity of the suspension (Dhital et al., 2017). Hence, when 30% of the starch has been hydrolysed, the remaining starch granule fragments are no longer contributing significantly to the solid volume fraction of the suspension, although the digestion of

the remaining starch continues. In the latter part of the graph (Figure 6.8), the curve plateaued off slowly (after 20 min digestion commenced).

As noted above, reductions in the rate of starch digestion and in the rate of decline in viscosity were greatest when wood, AllBran® fibre, and particularly guar were added to the suspensions but least when the cellulosic fibres were added. Given that these differences in digestion rate could not be directly attributed to differences in the initial viscosity conferred by the fibre type, it therefore seems that the differences may be due to other effects. In the suspensions,  $\alpha$ -amylase continuously hydrolysed starch polymers, especially amylopectin, into different lower molecular weight compounds such as maltoses, maltotrioses, and  $\alpha$ -limit dextrins. These smaller molecule fractions contain branch points resistant to  $\alpha$ -amylase (Dhital et al., 2017). As amylase is an endo-acting enzyme, it could effectively half the molecular weight of starch polymers in a single reaction and lead to the reduction of solid volume fraction of starch polymers in the *in-vitro* system. This also suggests that if a larger molecular amylopectin were hydrolysed into smaller molecular weights dextrins, it would reduce the viscosity of the whole suspension (Dhital et al., 2017). This suggestion is supported by the low rate of amylolysis (Table 6.8) and the high proportion of SDS and RS remaining in the starch/fibre suspensions with added wood, AllBran® fibres, and guar (Figure 6.3).

The slowed rate of amylolysis in the suspensions with fibres added could also be due to the non-competitive inhibition of amylase. Studies on starch digestion using amylase also reported that the active site of pancreatic amylase, which must locate on a sequence of five  $\alpha$ -(1-4) linked glucose residues within the starch polymer in

order to cleave them between sites 3 and 4 (Warren, Butterworth, & Ellis, 2012), may be non-competitively inhibited by guar. The amylase may locate on but not cleave the branched glucomannan polymer structure of guar. The active site of amylase is thus inhibited, reducing amylolytic activity (Slaughter et al., 2001). This effect is eliminated when the guar is hydrolysed (Jenkins et al., 1987). A similar type of amylase inhibition has been suggested to occur with  $\beta$ -glucans (Dhital et al., 2017; Wood et al., 1990). Hence the reductions in the rate of starch digestion in the presence of wood and AllBran® fibre and the variable effects of other soluble and insoluble fibres (Nunes & Malmlof, 1992; Vachon, Jones, Wood, & Savoie, 1988) may similarly result from amylase inhibition.

## 6.6. Conclusions

The current *in-vitro* work has provided data that may explain reductions in the rate of starch digestion when the concentrations of various dietary fibres present in digesta are close to physiological levels. The rate of amylolysis during *in-vitro* digestion of gelatinised potato and corn starch was significantly lower ( $p < 0.05$ ) in the presence of wood fibre, digested AllBran® particles, and particularly guar gum. The effects of various fibres in reducing  $T_{1/2}$  values for starch digestion and suspension viscosities was unrelated to viscosity at the physiologically relevant concentrations used in this work. Rather, the slower amylolysis rate in suspension with wood fibre, digested AllBran® particles, and particularly guar gum added may be due to non-competitive inhibition of amylase by the indigestible starch polymers such as  $\alpha$ -limit dextrans or these fibres which could block the active site of amylase. These results may assist with selecting fibre products such as guar gum, food analogues that contains similar structures to  $\alpha$ -limit dextrans, wood fibre, and

digested AllBran® particles for incorporating into diets to reduce post-postprandial glycemia and hence manage or reduce the incidence of diabetes.

## Chapter 7 The effects of degree of gelatinisation and process conditions on the digestibility of starch suspensions during *in-vitro* digestion at physiological shear rates

DRC 16



MASSEY UNIVERSITY  
GRADUATE RESEARCH SCHOOL

### STATEMENT OF CONTRIBUTION TO DOCTORAL THESIS CONTAINING PUBLICATIONS

(To appear at the end of each thesis chapter/section/appendix submitted as an article/paper or collected as an appendix at the end of the thesis)

We, the candidate and the candidate's Principal Supervisor, certify that all co-authors have consented to their work being included in the thesis and they have accepted the candidate's contribution as indicated below in the *Statement of Originality*.

Name of Candidate: Yap Sia Yen

Name/Title of Principal Supervisor: Prof Roger Lentle

#### Name of Published Research Output and full reference:

Allan, K. Hardacre, Roger, G. Lentle, Sia-Yen, Yap, John, A. Monro. (2016). Does viscosity or structure govern the rate at which starch granules are digested? Carbohydrate Polymers. 136: 667-675.

In which Chapter is the Published Work: Chapter 7

Please indicate either:

- The percentage of the Published Work that was contributed by the candidate: 70% and / or
- Describe the contribution that the candidate has made to the Published Work:  
The candidate has carried all lab work, data analysis and drafted the manuscript

  
Candidate's Signature

4/10/16  
Date

  
Principal Supervisor's signature

4/10/16  
Date

GRS Version 3- 16 September 2011

## 7.1. Abstract

The rate of digestion for native potato and corn starches was quantified before and after pre-gelatinisation to nominal DGs of 50% and 100% as determined from the peak viscosities and temperatures at which they were attained during pasting of the starches in an RVA. The starch suspensions of DG100% were further varied by holding at the PT for either 10 or 30 min. The prepared starches were characterised by  $Q$  (swelling capacity),  $S$  (water solubility index) and  $\phi_w$  (volume fraction of gelatinised starch). Ungelatinised starches were suspended in 70% (w/v) fructose solution to reduce the rate of settling for viscosity measurement while preventing gelatinisation. *In-vitro* digestion was carried out at 37°C and at a constant physiological shear rate in the range 0.1 to 10 s<sup>-1</sup> in a rheometer fitted with cup and vane. The proportion of starch digested was determined from the amount of reducing sugar released using the DNS assay. The rate of amylolysis and the viscosity of the suspension declined asymptotically over 20 min as the proportion of starch declined. The relationship between the proportion of viscosity remaining and the proportion of RDS with time was modelled as a linear function of the Ln-transformed data. Viscosity and starch concentration can be modelled with a sigmoidial function. The rate of amylolysis was increased by 25% to 40% more than in ungelatinised starch suspensions when starch samples were gelatinised to nominal DGs of 50% and 100%. In the lower shear (0.1 s<sup>-1</sup>) system, the rate of amylolysis for the starches of DG100% and cooked for 30 min was significantly higher than starch samples that were gelatinised to DG50% with 10 min cooking duration. However, the rate of amylolysis for all starch samples that were agitated at higher shear rates (1.0 s<sup>-1</sup> and 10 s<sup>-1</sup>) was similar. These results suggest that the mobility of amylase was limited at lower shear rates, therefore the digestion of starch

polymers may be localised, while high shear promoted mixing between amylase and starch polymers and accelerated the digestion process. Shear rates generated by segmentation and peristalsis ( $> 0.1 \text{ s}^{-1}$ ) is a significant factor in providing a proper mixing that aids digestion in the gut.

## 7.2. Introduction

The rapid digestion of starch can lead to the sustained elevation of postprandial blood sugar levels. Continuous elevation of blood sugar levels has been associated with the development of illnesses such as diabetes (Riccardi & Rivellese, 2000). Not all fibre types can slow the rate of starch digestion (Chapter 6), others factors such as processing methods, cooking duration (Snow & Odea, 1981) and the rate of starch shear in the physiological conditions of the gut (Lentle et al., 2002) are among important factors which affect the rate of starch digestion.

A number of *in-vivo* and *in-vitro* studies have demonstrated that different starchy foods are digested at different rates (Björck et al., 1987; Fujiwara, Hall, & Jenkins, 2017; Goni et al., 1997; Holm et al., 1988; van Kempen et al., 2010; Vangsøe et al., 2016) depending on the extent to which the starch granules are gelatinised (Englyst et al., 1992). For instance, the rate of gelatinised starch digestion by amylase is 3-10 times greater than that of the ungelatinised starch (Holm et al., 1988; Noda et al., 2008; Snow & Odea, 1981). This result faster rate of amylolysis of gelatinised starch compared to ungelatinised starch is presumably due to the effect of disruption of the physical structures of amylose and amylopectin within the starch granules when they are hydrated during gelatinisation (Gallant, Bouchet, & Baldwin, 1997) improving the accessibility of digestive enzymes to the starch molecules. The

temperature at which starch granules are cooked (Holm et al., 1988), their water content (Gunaratne et al., 2007) and the duration of cooking (Li & Yeh, 2001) can also affect the extent of gelatinisation and hence the digestibility. Thus, postprandial blood glucose levels do not always consistently rise in proportion to the quantity of starch that is consumed (Ells et al., 2005; Parada & Aguilera, 2009; Seal et al., 2003).

It is known that agents that increase the viscosity of digesta, such as inert particles, guar or beta-glucan also reduce the rate of starch hydrolysis, possibly by delaying the mixing of enzyme with substrate or by directly interfering with enzyme activity (Chapter 6). Shear stress developed by the gut has rarely been estimated but values up to 1.2 Pa have been reported (Jeffrey et al., 2003). The apparent viscosity of digesta measured at physiological shear rates of between  $0.1 \text{ s}^{-1}$  and  $10 \text{ s}^{-1}$  has been reported to range between that of water ( $\sim 0.0008 \text{ Pa.s}$ ) to  $0.1 \text{ Pa.s}$  in the small intestine (de Loubens et al., 2013), almost  $10 \text{ Pa.s}$  in the small intestine of pigs (Takahashi & Sakata, 2004) and  $73 \text{ Pa.s}$  in the caecum of chickens (Takahashi et al., 2004). High digesta viscosity would probably hinder the mixing of food with digestive enzymes (Svihus, Uhlen, & Harstad, 2005) as well as delay the rates of digestion and subsequent absorption of digestive products. Therefore, any *in-vitro* method that is used to gain insight into the dynamics of the digestion of particular substrates must replicate the viscosity and shear rate that occur in the gut, as well as the shear stress conditions that occur in the gut (Lee, Bailey, & Cartwright, 2003; Shelat et al., 2015).



The objective of the work described here was to determine relationships between the rates of enzymatic digestion of aqueous suspensions of potato and corn starch granules that have undergone various degrees of gelatinisation, and the viscosity of the suspension at shear rates within the physiological range ( $0.1\text{ s}^{-1}$ ,  $1\text{ s}^{-1}$  and  $10\text{ s}^{-1}$ ) at  $37^{\circ}\text{C}$  using an *in-vitro* system that replicated the gastric and intestinal phases of digestion (Chapter 3, Section 3.5.2). Changes in the physical states of the starch granules during digestion were inferred from the relationship between the proportion of undigested starch and viscosity. The rates at which the starches were digested were determined indirectly from the rates at which glucose was liberated during amylolysis, while the rates at which the physical state of the starch changed during digestion were determined indirectly from the rate of reduction in apparent viscosity of the digestate.

### **7.3. Materials and methods**

#### **7.3.1. Starch**

The physical and chemical properties of potato and corn starches were as previously described (Chapter 3, Sections 3.3. and 3.4.).

#### **7.3.2. Determination of %DG**

The details of selection of starch concentration and starch pasting temperature were described elsewhere (Chapter 6, Section 6.3.5.).

The %DG of starch was determined by tracking changes in viscosity of a starch suspension as it is heated to around  $95^{\circ}\text{C}$  (Gunaratne et al., 2007; Kaur, Singh, McCarthy, & Singh, 2007). The temperature at which viscosity of starch suspension

was developed to nominal of 50% and 100% of potato and corn starch suspensions, were defined as DG50% or DG100% (Figure 7.1). The DG was determined indirectly from the changes in apparent viscosity of aqueous suspensions incorporating 10% (w/w) of potato or corn starches in Milli Q water during heating between 50°C and 95°C using a RVA (Chapter 6, Section 6.3.5.).

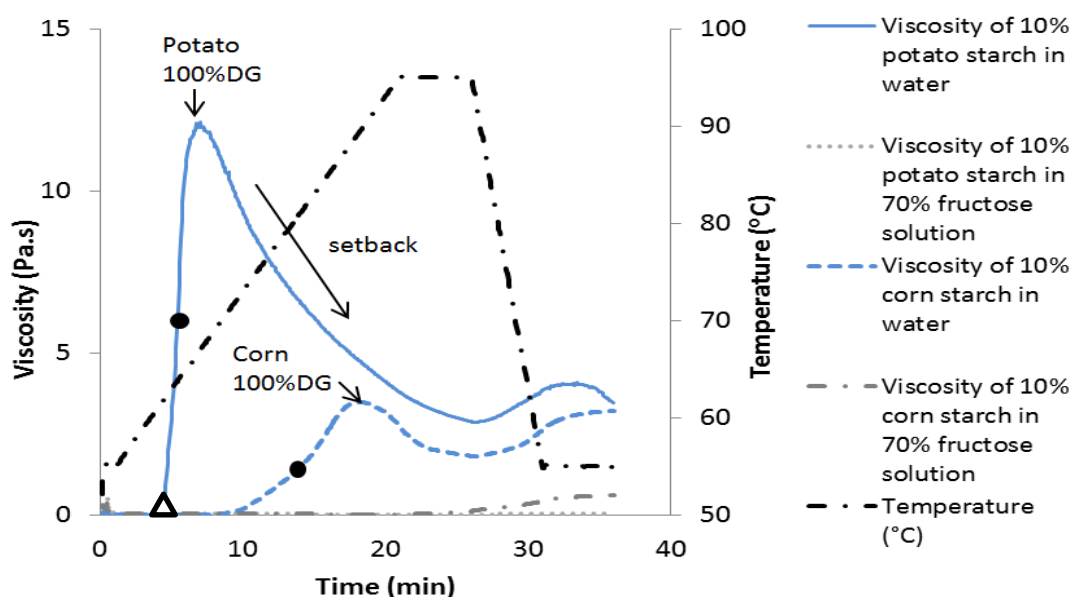


**Figure 7.1:** Rheology of starches during gelatinisation: RVA pasting profile for aqueous suspensions of 10% (w/w) potato (P) and corn (C) starch,  $\Delta$  = DG0%,  $\bullet$  = DG50%, DG100% marked on graph.

**Table 7.1:** Pasting properties of 10% (w/w) potato and corn starch suspensions determined by the RVA.

Types of starch	Percentage of DG (%)	PT (°C) <sup>‡</sup>	PV (Pa.s) <sup>‡</sup>
<b>Potato</b>	DG50% <sup>‡</sup>	63.9 ± 0.4 <sup>c</sup>	6.06 ± 0.00 <sup>b</sup>
	DG100% <sup>‡</sup>	68.0 ± 0.5 <sup>*bc</sup>	12.12 ± 0.01 <sup>*a</sup>
<b>Corn</b>	DG50% <sup>‡</sup>	82.2 ± 0.7 <sup>b</sup>	1.74 ± 0.00 <sup>c</sup>
	DG100% <sup>‡</sup>	90.0 ± 0.8 <sup>*a</sup>	3.48 ± 0.01 <sup>*b</sup>

Note : DG, degree of gelatinisation, PT, Pasting temperature; PV, Peak viscosity  
<sup>\*</sup> Means in a column followed by different superscripts are significantly different (2 samples t-test,  $p < 0.05$ )  
<sup>‡</sup> Mean values in a column with different superscripts (a-c) are significantly different (One way ANOVA and Tukey's pair-wise test,  $p < 0.05$ )

The %DG was selected from the PV values of the pasting curve (Table 7.1, Figure 7.1). The PV for potato starch gelatinised to 100%DG in water was significantly higher ( $p < 0.05$ ) than that of 50%DG (Table 7.1), although the PT for the potato suspension at DG100% was similar to that of 50%DG. Similarly, the PV for 100%DG corn starch suspension was significantly higher than that of the 50%DG (Table 7.1). Changes in the PV of potato starch happened within a narrow temperature range (Table 7.1, Figure 7.1) and the PV when the DG of corn starch was less than 50% was below the sensitivity of the rheometer. For this reason, only DG's of nominally 50% and 100% were selected to track changes in viscosity during *in-vitro* digestion.

Suspensions of gelatinised starch are stable and do not settle. However, the density of non-gelatinised granules is higher than water, thus they must be suspended in a viscous medium to reduce their rate of settling. For this reason, a 70% fructose (w/v) solution with a Newtonian viscosity of 0.032 Pa.s was used to suspend the starch granules. This was useful in determining the rheological behaviour of suspensions of starch granules but the high concentration of fructose reduced  $A_w$  ( $A_w = 0.74$ ) and gelatinisation was largely inhibited (Figure 7.1). Exploitation of the high viscosity of gelatinised starch suspensions without added fructose and the very slow rate of settling of the non-gelatinised granules in the fructose solution allowed the continuous determination of changes in viscosity during digestion within the cup and vane geometry of a rheometer.

Due to the limitation of the stress-controlled rheometer used in this study couldn't perform the temperature sweep test; starch and starch/fibre suspensions were

gelatinised at a PT defined by the %DG determined from the RVA viscogram using temperature controlled water bath. The temperature was carefully controlled throughout the gelatinisation process. The starch types, %DG, and cooking duration of the starch suspensions prepared allowed a wide range of starch effects to be explored.

### **7.3.3. Hydration properties**

The hydration properties of starch suspensions (Q), and the relative mass of the soluble solids (S), were investigated. The Q for each of the starch granule types was determined as the ratio of their wet weight, after gelatinising in an aqueous suspension, to their dry weight (Bagley & Christianson, 1982). The dry weight of the starch added (5 g) was calculated using the previously determined moisture content of the ‘as supplied’ starch. Hence Q was calculated as

$$Q \text{ (g/g)} = (\text{weight of gelatinised granules} / \text{dry weight of starch}) \quad (\text{Equation 7.1})$$

The value Q was determined by the centrifugation method using a 10% (w/v) suspension of starch granules in water, rather than 1% as previously described (Leach et al., 1959). Starches were hydrated by suspending 5 g of either P or C starch ‘as supplied’ in 45 mL of 70% (w/v) fructose solution or MilliQ water in 100 mL pre-weighed centrifuge tubes. The tubes were placed in a temperature controlled water bath at either 64°C (DG50% for potato) or 68°C (DG100% for potato) and 82°C (DG50% for corn) 90°C (DG100% for corn), as pre-determined from Section 7.3.2. Each starch suspension was constantly stirred at 150 rpm for 5 min using a magnetic stirrer bar. After 5 min, the stirring rate was decreased to 50 rpm and suspensions were incubated for a further 10 min or 30 min to achieve the

required DG. The Q and S values for potato and corn starch suspensions gelatinised for 10 or 30 min in 70% (w/v) fructose solution were generally very low and similar, therefore only the 30 min treatment was used (Appendix 3).

The Q and S values for the two starch types gelatinised for 10 or 30 min to 50% DG in water were also similar (Appendix 3). However, prolonging the cooking duration from 10 min to 30 min significantly ( $p < 0.05$ ) increased Q and S for DG100% starch suspensions. Therefore the starch suspensions used for this study were gelatinised with stirring for 10 min or 30 min at temperatures appropriate for DG100% (Appendix 3). The tubes containing the samples were then removed from the water bath and cooled in an ice bath for 5 min. Sufficient MilliQ water was then added to reach a total weight of 60 g. The tubes were then sealed and mixed gently by inverting them ten times before centrifuging for 20 min at 2200 g (Heraeus Multifuge IS-R centrifuge, Thermo Fisher Scientific, Germany). The supernatants were carefully transferred into pre-weighed aluminium containers using a pipette and dried at 108°C to reach a constant weight. The relative mass of the soluble solid (S) (Holm et al., 1985) could then be calculated:

$$S (\%) = [(Ss / st) \times 100] \quad \text{(Equation 7.2)}$$

Ss = weight of solubles in the supernatant after drying at 108°C (g);

st = dry weight of starch prior to gelatinisation (g)

The tubes with hydrated gel pellets were then reweighed. The weight of the gel pellet was determined by subtraction and substituted into Equation 7.1 to determine Q. The volume fraction of water in the hydrated granules ( $\phi_w$ ) was then calculated using the following equation (Doublier et al., 1987).

---


$$\phi_w = [(1 - (S/100)) * cQ] \quad \text{(Equation 2.8, Chapter 2)}$$

Where Q and S are derived from Equations 7.1 and 7.2 above and c is the concentration of starch (in this case 10%). Mean values for Q, S and  $\phi_w$  were determined from four replicates of each starch and gelatinisation treatments.

#### **7.3.4. Preparation of starch samples for digestion**

Gelatinised starch suspensions of 50 mL each for the digestion experiments were prepared from 10% (w/w) suspensions of potato and corn starches in MilliQ water in 150 mL beakers (Chapter 7, Sections 7.3.2 and 7.3.3.). Each starch suspension was first stirred at 150 rpm for 5 min using a magnetic stir-bar to thoroughly disperse the component granules, the stirring speed was then reduced to 50 rpm to minimise damage to the granules as they were gelatinised. Gelatinisation was carried out in a water bath for either 10 min or 30 min at the temperature previously determined Section 7.3.2 to achieve the desired %DG. A control treatment for the P and C starches alone was suspended in 70% (w/v) fructose solution at temperatures appropriate for DG100% for 30 min.

#### **7.3.5. Light microscope**

The starch granules that were gelatinised at 70% fructose solution, 30 min (FrucCk30); in water at DG100% for 10 min (DG100%Ck10), and 30 min (DG100%Ck30) were photographed at a suitable magnification using an Olympus BX53 microscope (Tokyo, Japan) equipped with a digital camera and “cellSens life sciences” research imaging software (Olympus, Tokyo, Japan). The changes in the size of starch granules for different experimental treatments were recorded (Figure 7.3).

### 7.3.6. Experiment designs for in-vitro digestion

The experimental design was a full factorial design comprising two types of starch (potato and corn) x three shear rates that covered the physiological range ( $0.1 \text{ s}^{-1}$ ,  $1 \text{ s}^{-1}$  and  $10 \text{ s}^{-1}$ ) x 4 cooking conditions (Fruc 30min, DG50% 30min, DG100% 10min and DG100% 30min) (Table 7.2).

**Table 7.2: Experimental treatments: P, Potato; C, Corn; Fruc, starch suspension cooked in 70% (w/v) fructose solution; DG50% or DG100%, 50% or 100% gelatinisation temperature treatments; Ck10 or Ck30, cooked for 10 min or 30 min.**

Treatment (3 replicates)	Shear rates ( $\text{s}^{-1}$ )	DG (%)	Duration (min)	Treatments abbreviation		Sampling points
				Potato	Corn	
1,13,25	0.1	Fruc	30	PFrucCk30	CFrucCK30	7, T0-T20
2,14,26		DG50%	30	PDG50%Ck30	C50%30min	7, T0-T20
3,15,27		DG100%	10	PDG100%Ck10	C100%10min	7, T0-T20
4,16,28		DG100%	30	PDG100%Ck30	C100%30min	7, T0-T20
5,17,29	1	Fruc	30	PFrucCk30	CFrucCK30	7, T0-T20
6,18,30		DG50%	30	PDG50%Ck30	C50%30min	7, T0-T20
7,19,31		DG100%	10	PDG100%Ck10	C100%10min	7, T0-T20
8,20,32		DG100%	30	PDG100%Ck30	C100%30min	7, T0-T20
9,21,33	10	Fruc	30	PFrucCk30	CFrucCK30	7, T0-T20
10,22,34		DG50%	30	PDG50%Ck30	C50%30min	7, T0-T20
11,23,35		DG100%	10	PDG100%Ck10	C100%10min	7, T0-T20
12,24,36		DG100%	30	PDG100%Ck30	C100%30min	7, T0-T20

### 7.3.7. In-vitro digestion

Digestion of the samples at defined shear rates was carried out in the cup of a stress-controlled rheometer equipped with propriety cup and vane geometry and operated at  $37^{\circ}\text{C}$ . The details on the procedures for *in-vitro* digestion were as described in Chapter 3, Section 3.5.2.

### 7.3.8. Rheology

The digestate was mixed at constant near physiological shear rates to keep the granules in suspension. Shear was maintained throughout the experimental period by the vane geometry rotating at the speed required to generate the requisite shear rate.

**Table 7.3:** Calculated shear stress required (*Italics*) to generate the shear rates for materials of the apparent viscosities listed. The value for shear stress = 1 (*italics, bold*) is close to the maximum reported for the small intestine and shear stress values to the right of this in each row represent suspensions with viscosities that are **unlikely to be mixed effectively in the small intestine**.

Shear rate ( $\text{s}^{-1}$ )	Apparent viscosity (Pa.s)				
	0.01	0.1	1	10	100
0.1	0.001	0.01	0.1	<b><i>1</i></b>	10
1	0.01	0.1	<b><i>1</i></b>	10	100
10	0.1	<b><i>1</i></b>	10	100	1000

The range of shear rates used ( $0.1 \text{ s}^{-1}$ ,  $1 \text{ s}^{-1}$  and  $10 \text{ s}^{-1}$ ) was based on reported values for shear rates generated by intestinal contraction (de Loubens et al., 2013). The maximum shear stress generated by the small intestine has been reported to be about 1.2 Pa (Jeffrey et al., 2003). By using the formula “shear stress = apparent viscosity x shear rate”, the sufficiency of the reported stress (Jeffrey et al., 2003) to induce the mixing of digesta at viscosities ranging between 0.01 and 100 Pa.s was judged. Hence, a maximum shear stress of 1.2 Pa would generate shear rates of about  $10 \text{ s}^{-1}$  at an apparent viscosity of 0.1 Pa.s and reduced shear rates of about  $0.1 \text{ s}^{-1}$  if the viscosity were greater at 10 Pa.s (Table 7.3). The calculations show that the shear stress required to generate shear rates in excess of  $1 \text{ s}^{-1}$  would rise rapidly and well above physiological levels once the apparent viscosity exceeded 1 Pa.s.



### **7.3.9. Total starch and sugar determination**

The total starch and the sugar that released during *in-vitro* digestion were quantified as monosaccharides (sugars) using the DNS colourimetric method (Chapter 3, Section 3.5.3). The rates of starch digestion in the RDS phase were determined (Chapter 6).

### **7.3.10. Data analysis**

The details of the data analysis were previously described (Chapter 3, Section 3.6.). The slopes of  $T_{1/2}$  (coefficient) were statistically compared using the GLM procedure in the MINITAB statistical suite (Chapter 3, Section 3.6). The relationship between the proportion of starch added to the suspension digested and the proportion of the original viscosity remaining was best described graphically for the entire dataset by fitting a common curve to the pooled data from the various treatments using SigmaPlot® Version 12.3.3. From this deviations to individual treatments could be compared.

## **7.4. Results**

### **7.4.1. Pasting properties of starches**

The increase in apparent viscosity of the aqueous suspensions of potato starch started at 58°C and continued to a peak at 68°C. The apparent viscosity at this peak was 12 Pa.s which was designated as DG100% or peak hot paste viscosity, PV (Figure 7.1). Accordingly, fifty percent gelatinisation (DG50%) was the point when the RVA viscosity was half of 12 Pa.s, i.e. 6 Pa.s, and occurred at 64°C (Table 7.1). Increases in the apparent viscosities of the aqueous suspensions of corn starch began

at 70°C and peaked at a lower viscosity of ~3.5 Pa.s at 90°C so that the DG50% point occurred when the apparent viscosity was 1.75 Pa.s at 82°C (Table 7.1).

The apparent viscosity of the potato starch suspension was consistently higher than that of the corn starch suspension for a given concentration of starch (Figure 7.1). Similarly, viscosities at the end of the gastric digestion phase and before amylolysis of the potato starch suspensions were between 2 and 8 times greater than those for corn starch suspensions at comparable shear rates (Table 7.1). Neither potato nor corn starch gelatinised when cooking was carried out in 70% (w/v) fructose solution ( $A_w = 0.74$ ), although the corn starch-in-fructose suspension exhibited a minimal increase in viscosity (0.2 Pa.s) at temperatures greater than 90°C (Figure 7.1).

#### **7.4.2. RDS as a proportion of total starch**

The proportion of RDS in corn and potato starch was similar for all corresponding treatments of the two starch types (Figure 7.2). Less than 10% of potato and corn starch that gelatinised in 70% (w/v) fructose solution was hydrolysed in the RDS phase at all shear rates applied (Figure 7.2). Both potato and corn starches, regardless their %DG and cooking duration, were hydrolysed by a similar proportion during the RDS phase of digestion when mixed at the higher shear rates used ( $1 \text{ s}^{-1}$  and  $10 \text{ s}^{-1}$ ). The proportion of both starches digested over the first 20 minutes was significantly reduced at the lower shear rate ( $0.1 \text{ s}^{-1}$ ) (Figure 7.2).

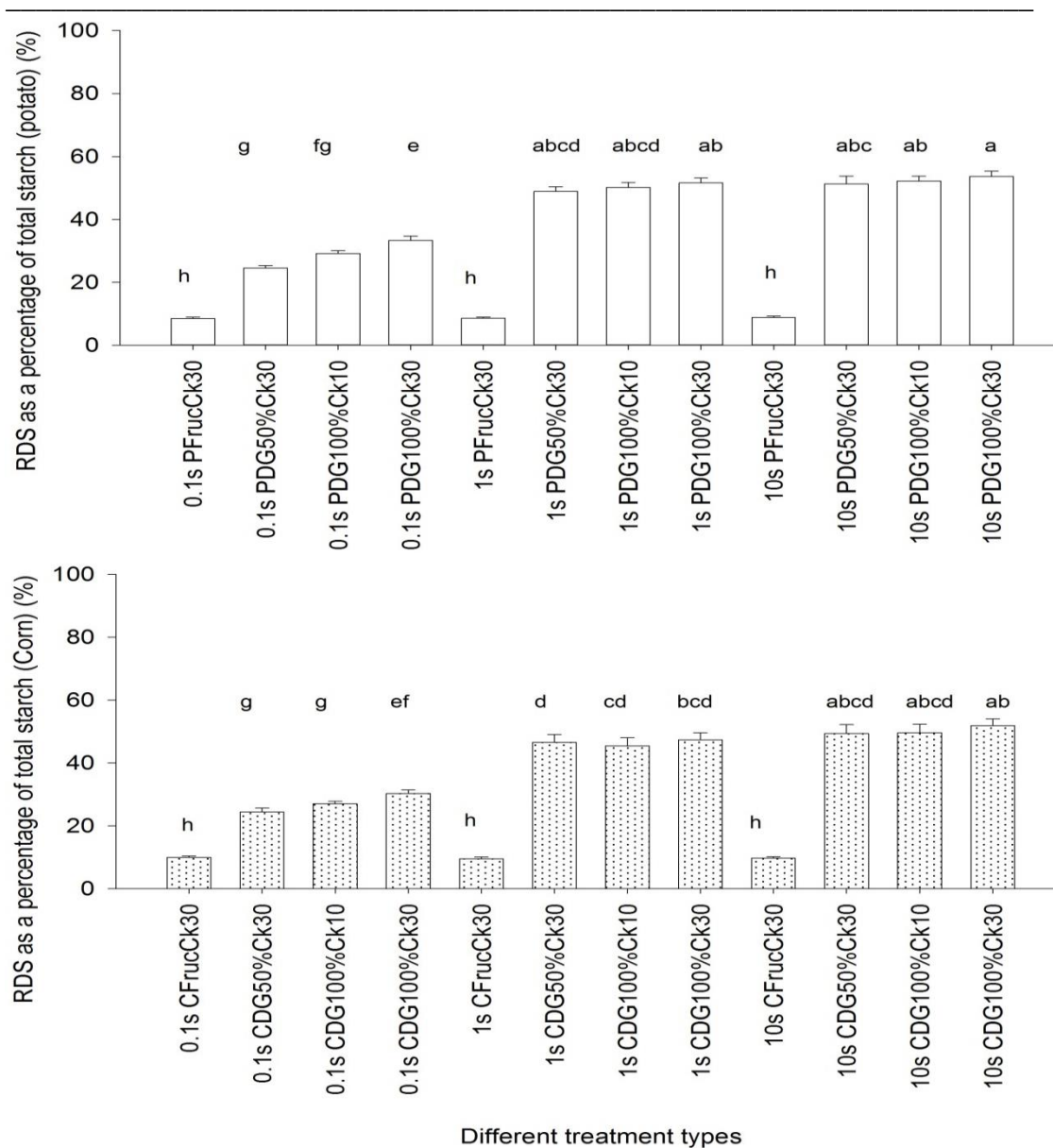


**Figure 7.2:** Differences in RDS as a percentage of total starch, with %DG and cooking duration at different shear rates (10s, shear rate at  $10 \text{ s}^{-1}$ ; 1s, shear rate at  $1 \text{ s}^{-1}$ ; 0.1s, shear rate at  $0.1 \text{ s}^{-1}$ ). Proportion of RDS was plotted as means; values with superscripts (a-h) are significantly different (Two way ANOVA and Tukey's pair-wise test,  $p < 0.05$ ). Other notation similar to Table 7.2.

### 7.4.3. Water absorption, solubility and apparent viscosity

The values for  $Q$ ,  $\phi_w$ , and  $S$  obtained for 10% (w/w) suspensions of potato and corn starch in MilliQ water increased with temperature and with duration of cooking (Table 7.4). Moreover, the increase in  $Q$ ,  $\phi_w$ , and  $S$  were accompanied by increases in the apparent viscosities of the suspensions.

**Table 7.4:** Effect of cooking duration (Ck10 min or Ck30 min) and %DG on  $Q$  (swelling factor),  $\phi_w$  (volume proportion of water in the granules), and  $S$  (weight proportion of granule solubles) and the apparent viscosity at the three (3) shear rates for all treatments at the end of the gastric digestion phase. Other notation similar to Table 7.2.

Treatments	$Q$ (g/g) ‡	$\phi_w$ ‡	$S$ (%) ‡	Apparent viscosity (Pa.s)		
				Shear rate (s <sup>-1</sup> )		
				0.1	1	10
	g/g	v/v	%			
PFrucCk30	1.27±0.12 <sup>e</sup>	0.13±0.01 <sup>d</sup>	0.93±0.17 <sup>f</sup>	0.04±0.0 <sup>h</sup>	0.04±0.0 <sup>h</sup>	0.04±0.0 <sup>h</sup>
PDG50%Ck30	7.40±0.34 <sup>d</sup>	0.69±0.03 <sup>c</sup>	6.24±0.41 <sup>e</sup>	1322.6±70.4 <sup>c</sup>	250.9±4.6 <sup>f</sup>	54.6±3.5 <sup>gh</sup>
PDG100%Ck10	8.78±0.21 <sup>c</sup>	0.79±0.02 <sup>b</sup>	9.49±0.25 <sup>d</sup>	2191.8±24.8 <sup>a</sup>	320.7±5.5 <sup>f</sup>	84.6±5.3 <sup>g</sup>
PDG100%Ck30	10.94±0.32 <sup>a</sup>	0.96±0.03 <sup>a</sup>	12.27±0.21 <sup>b</sup>	1755.1±84.7 <sup>b</sup>	309.5±5.1 <sup>f</sup>	60.2±2.9 <sup>gh</sup>
CFrucCk30	1.12±0.13 <sup>e</sup>	0.12±0.02 <sup>d</sup>	0.94±0.22 <sup>f</sup>	0.04±0.0 <sup>h</sup>	0.04±0.0 <sup>h</sup>	0.04±0.0 <sup>h</sup>
CDG50%Ck30	7.64±0.36 <sup>d</sup>	0.71±0.04 <sup>c</sup>	7.04±0.47 <sup>e</sup>	452.0±37.1 <sup>e</sup>	41.7±4.2 <sup>gh</sup>	7.6±0.5 <sup>gh</sup>
CDG100%Ck10	8.80±0.13 <sup>c</sup>	0.78±0.01 <sup>b</sup>	10.83±0.49 <sup>c</sup>	594.1±20.8 <sup>d</sup>	64.8±2.5 <sup>gh</sup>	8.4±0.1 <sup>gh</sup>
CDG100%Ck30	9.90±0.45 <sup>b</sup>	0.86±0.04 <sup>a</sup>	13.28±0.23 <sup>a</sup>	542.3±9.5 <sup>d</sup>	54.7±2.2 <sup>gh</sup>	8.9±0.2 <sup>gh</sup>

‡ values for mean and standard error within a column followed by different superscripts (a-f) are significantly different (one way ANOVA) using Tukey's post hoc pair-wise test, ( $p < 0.05$ ).

All starch granule suspensions contained close to 10% dry matter but the volume fraction of water in the granules ( $\phi_w$ ) increased with gelatinisation from 12% to 13% (fructose suspensions) to around 90% or more for the most highly gelatinised suspensions (PDG100%Ck30 and CDG100%Ck30 treatments). Hence the most highly gelatinised granules swelled to between nine and ten times their original

volume by absorbing almost all of the available water from the suspensions (Figure 7.3).

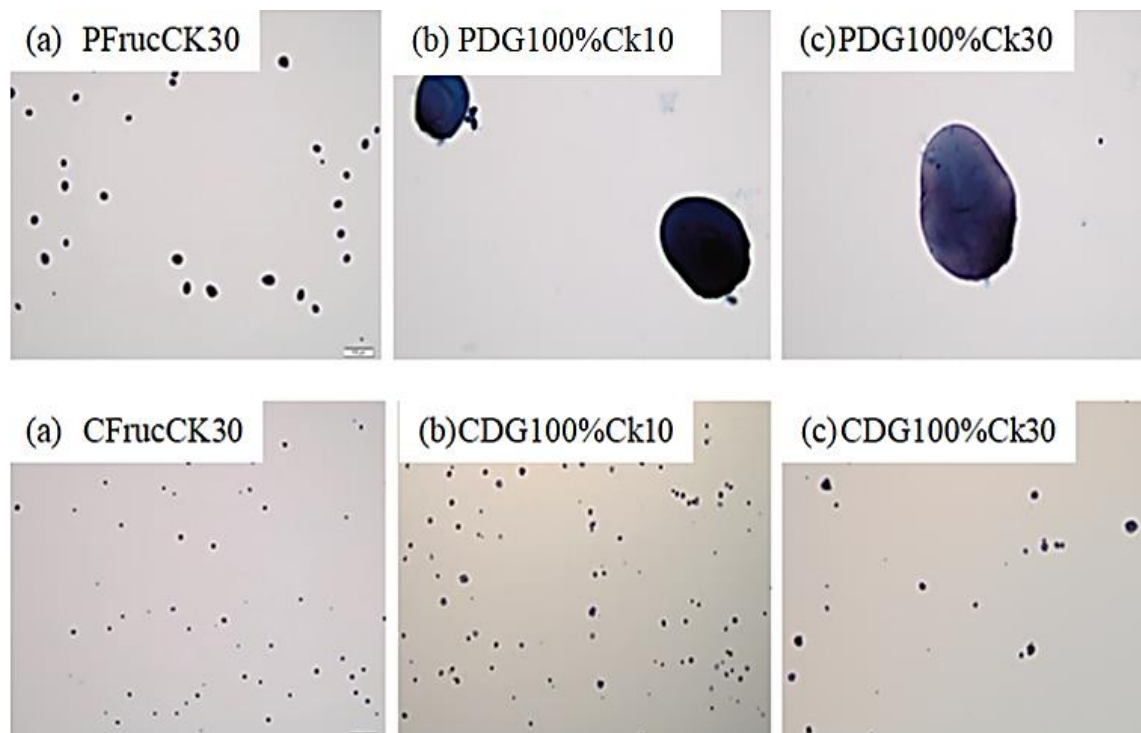


**Figure 7.3:** Light micrographs (x40) of starch granules gelatinised at different DG and cooking duration. Upper row: Potato starch, lower row: corn starch. The  $A_w$  for all starch/water suspension was 0.99 and  $A_w$  for all starch/70% fructose suspensions was 0.74.

The high  $Q$  value (10.94) for the fully gelatinised potato starch which is above the theoretical maximum of 10, may have been due to the absorption of additional water during the latter stages of the procedure for determining  $Q$  and  $S$  (Section 7.3.3.). The quantities of solubles leached from the granules into the aqueous phase ( $S$ ) were similar for potato and corn (corn  $\sim 1\%$  > potato) and increased significantly (>50 %) with %DG and to a lesser extent with duration of cooking (Table 7.4).

The values obtained for  $Q$ ,  $\phi_w$ , and  $S$  for ungelatinised 10% (w/w) potato and corn starch suspensions in MilliQ water were markedly lower than when they were suspended in the 70% (w/v) fructose solution; correspondingly, the apparent viscosities of these suspensions were negligible at all shear rates (Table 7.4).

Viscosity of potato starch suspensions was slightly lower when cooked for the longer time (30 min) compared to lesser cooking duration (10 min), although the effect is not significant in corn starch (Table 7.4). These results suggest that reducing the contact time between granules and water molecules could result in less destruction of the ordered structure of granules (Bagley & Christianson, 1982; Okechukwu & Rao, 1995) that maintains the integrity of the granule during gelatinisation (Kearsley & Sicard, 1989). This has also been reported by (Eliasson, 1986), who gelatinised potato and corn starch at 95°C for two different cooking durations, i.e. 5 min and 10 min. As shown in Figure 7.3, there is no evidence that starch ghost granule damage due to shear during the cooking process.

#### **7.4.4. Digestion of starch**

The declines in the relative starch content and relative viscosity of the suspensions with time were Ln linear in relationship over the 20 min of digestion for all treatments (Figure 7.4) with  $R^2$  higher than 0.95 for the Ln linear relationship for all treatments.

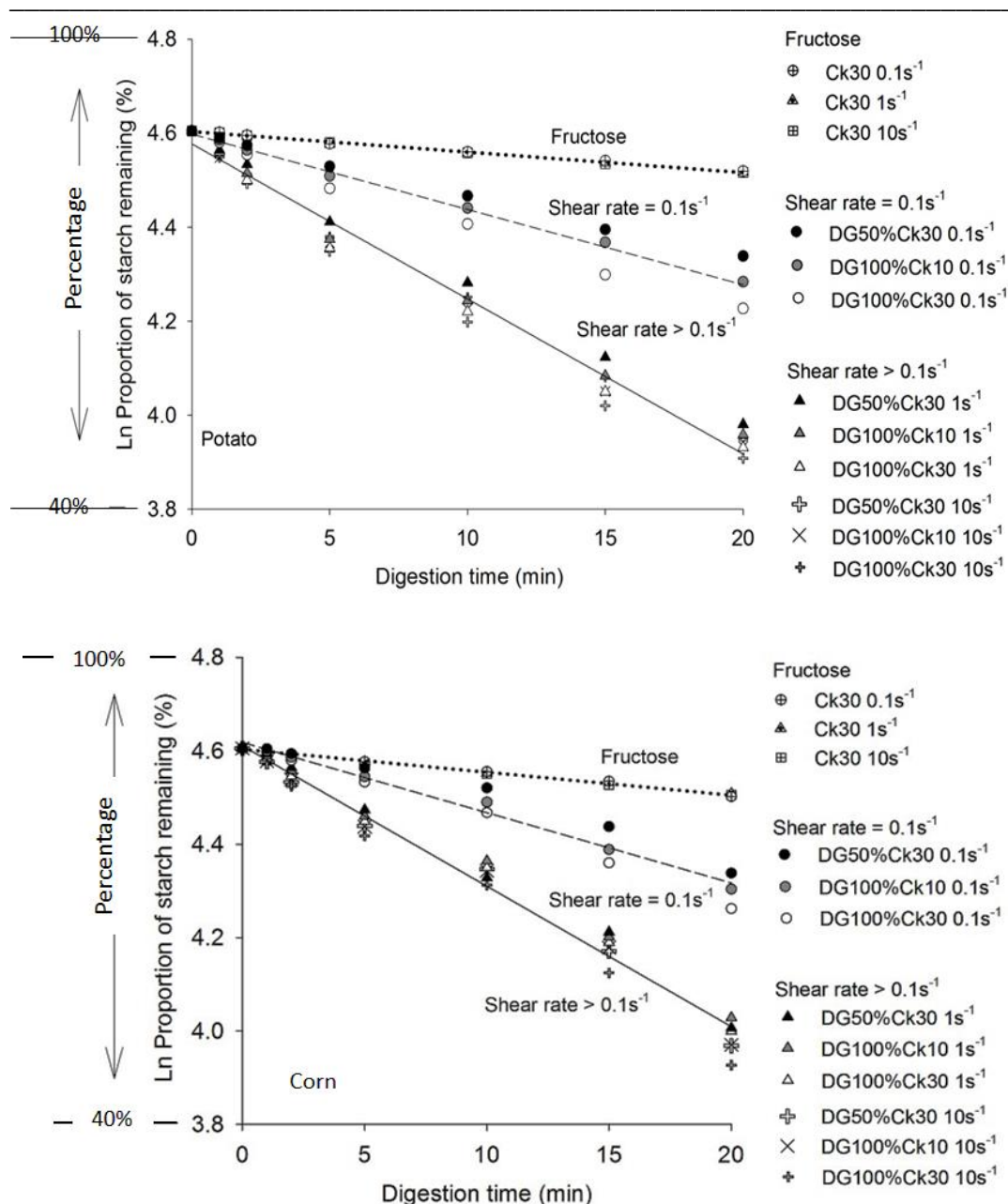


**Figure 7.4:** Ln proportion of starch remaining during the first 20 min of simulated small intestinal digestion (Start value = 100%). DG, degree of gelatinisation; Ck, cook time (min); Starch cooked in fructose and measured at shear rates of  $0.1 \text{ s}^{-1}$ ,  $1 \text{ s}^{-1}$  and  $10 \text{ s}^{-1}$  (open symbols as per legend); starch cooked in water and measured at a shear rate of  $0.1 \text{ s}^{-1}$  (filled symbols as per legend); starch cooked in water measured at a shear rate of  $1 \text{ s}^{-1}$  and  $10 \text{ s}^{-1}$  (Shear rate  $> 0.1 \text{ s}^{-1}$ ) is the remaining data. Linear regressions of the Ln-transformed data plotted against time are fitted to all data within each of the 3 data sets and are the annotated lines on the graphs.

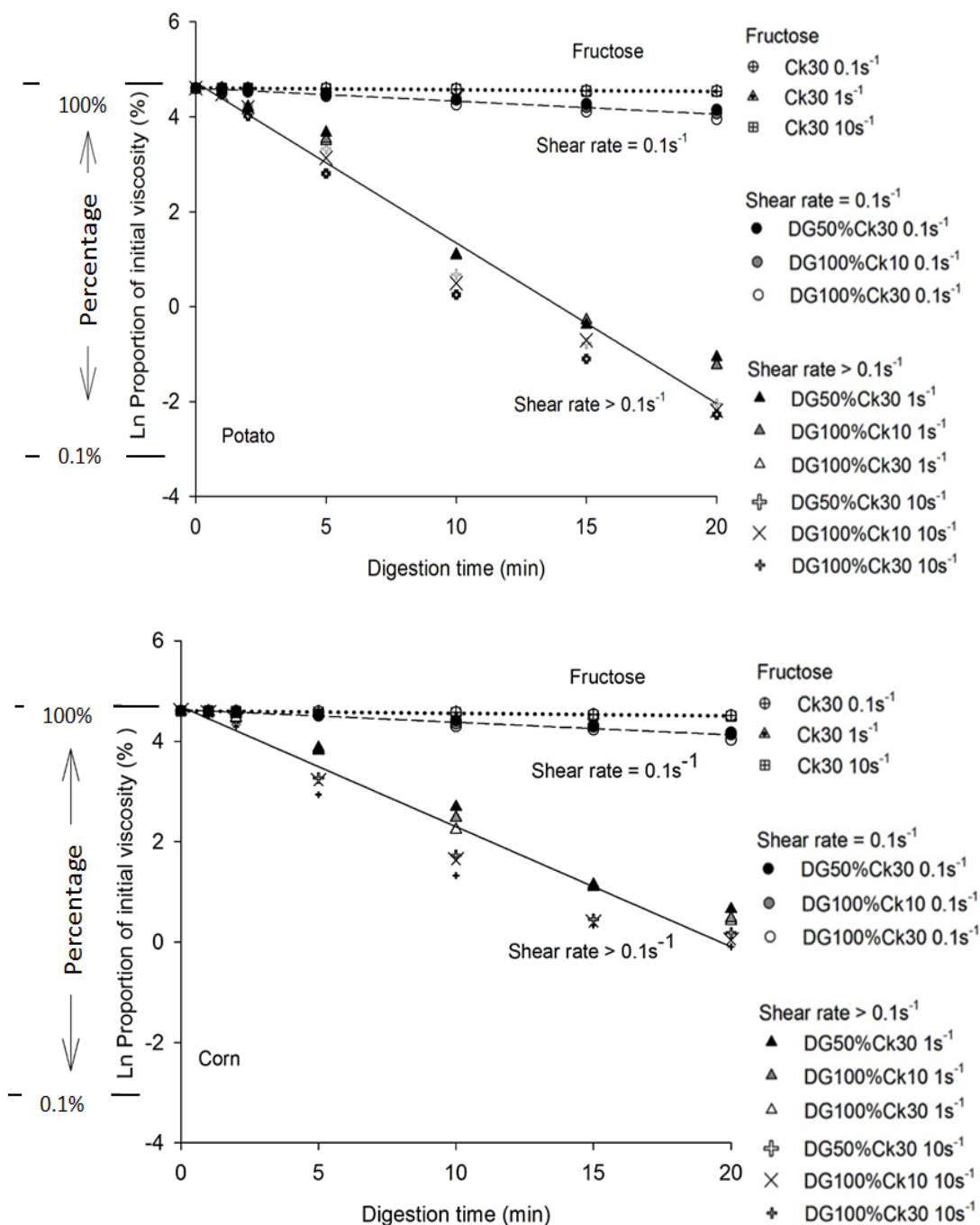


**Figure 7.5:** Ln proportion of apparent viscosity remaining during the first 20 min of simulated small intestinal digestion (Start value = 100%). Notations were similar to those in Figure 7.4.

The Ln linear relationships were categorised into three groups according to the relative rates of decline of starch content and relative rates of decline of viscosity with time (slopes) (Figures 7.4 and 7.5). The magnitude of these slopes was



influenced by the shear rate applied to the digestate and %DG of the starch granules in the digestate (Figures 7.4 and 7.5). Therefore, starches cooked in 70% (w/v) fructose solution demonstrated the lowest rates of digestion, varying between 2.3 and 2.5 min<sup>-1</sup> (Table 7.5).

**Table 7.5: Variation in the relative rate of digestion of potato (P) and corn (C) starch (min<sup>-1</sup>) for the four gelatinisation treatments and three shear rates over 20 min of simulated small intestinal digestion. Other notation similar to Table 7.2.**

Treatments	Shear rate (s <sup>-1</sup> )		
	0.1	1	10
	Rate of digestion (min <sup>-1</sup> )*		
PFrucCk30	2.33±0.09 [2.24, 2.43]	2.34±0.08 [2.26, 2.42]	2.39±0.16 [2.24, 2.43]
PDG50%Ck30	6.57±0.06 [6.52, 6.63]	13.03±0.22 [12.79, 13.21]	13.51±0.39 [2.24, 2.43]
PDG100%Ck10	7.71±0.13 [7.57, 7.81]	13.36±0.81 [13.30, 13.45]	13.72±0.26 [2.24, 2.43]
PDG100%Ck30	8.83±0.24 [8.62, 9.09]	13.76±0.10 [13.67, 13.87]	14.08±0.08 [2.24, 2.43]
CFrucCk30	2.44±0.14 [2.37, 2.54]	2.44±0.09 [2.34, 2.51]	2.50±0.03 [2.46, 2.51]
CDG50%Ck30	6.20±0.16 [6.02, 6.33]	11.91±0.17 [11.74, 12.07]	12.45±0.18 [12.27, 12.63]
CDG100%Ck10	6.88±0.15 [6.71, 7.02]	11.59±0.22 [11.38, 11.82]	12.42±0.13 [12.32, 12.57]
CDG100%Ck30	7.68±0.10 [7.60, 7.78]	12.01±0.14 [11.88, 12.16]	13.02±0.26 [12.83, 13.31]

\*[LL , UL] Values are 95% confidence interval (CI) of lower limit (LL) and upper limit (UL) of samples mean value.

Mean total starch present at the start of digestion (mg/g solids in suspension, dwb) ± standard deviation; P, 561.1 ± 15.4; C, 528.7 ± 21.8

Starches gelatinised in MilliQ water and maintained at a shear rate of  $1 \text{ s}^{-1}$  or  $10 \text{ s}^{-1}$  showed the greatest rate of digestion, ranging between  $11.9$  and  $14.3 \text{ min}^{-1}$  (Table 7.5). Rates of digestion for starches gelatinised in MilliQ water and maintained at a shear rate of  $0.1 \text{ s}^{-1}$  lay between these two extremes and ranged from  $6.2$  to  $8.8 \text{ min}^{-1}$  (Table 7.5).

Less than 10% of available starch was hydrolysed during the first 20 min of digestion when starch granules were suspended in 70% (w/v) fructose solution, regardless of the shear rate applied. However, when starch granules suspended in MilliQ water were gelatinised at shear rates of  $1 \text{ s}^{-1}$  or greater, around 50% was hydrolysed during the same period (Figure 7.4). Decreasing the shear rate from  $10 \text{ s}^{-1}$  to  $1 \text{ s}^{-1}$  had little effect on the rate of starch digestion; however a further decrease to  $0.1 \text{ s}^{-1}$  approximately halved the rate of starch digestion (Table 7.5). In treatments where gelatinisation was nearly complete, i.e. where  $\phi_w > 0.68$ , there were some slight, though non-significant, differences between the rates of digestion of corn and potato starch (Table 7.5). Hence when digesta was maintained at shear rates of  $> 1 \text{ s}^{-1}$ , potato starch was digested 8% to 14% more rapidly than corn starch and the corresponding values of  $T_{1/2}$  were about 20 min for potato and 24 min for corn starch (Table 7.6).

#### **7.4.5. Effect of %DG**

The gelatinisation and swelling of the starch granules barely occurred in 70% (w/v) fructose solution and rates of *in-vitro* digestion were correspondingly very slow (Tables 7.4 and 7.5). The viscosities of suspensions of the gelatinised starch granules were much higher (Table 7.4) and the rates of digestion were also higher

(Table 7.5). Increasing %DG from 50% to 100%, or the cooking time from 10 min to 30 min tended to increase the rates of digestion at all applied shear rates with both starches (Figure 7.4, Table 7.5) but the differences were small and generally not significant.

#### **7.4.6.        *Effects on starch viscosity***

At the beginning of the phase simulating digestion in the small intestine, the apparent viscosities of suspensions of potato starch were 3 to 10 times greater than the suspensions containing corn starch, depending on shear rate. The viscosities of all starch suspensions increased with %DG and with cooking time (Table 7.4).

Increasing the %DG from 50% to 100% after cooking for 30 min increased the apparent viscosity by around 10% of the initial value. However, for all suspensions of starch with DG100% maintained at a shear rate of  $10 \text{ s}^{-1}$ , increasing the cooking time from 10 min to 30 min reduced the apparent viscosity, although this reduction was only significant for potato starch (Table 7.4). These reductions in viscosity occurred in spite of the values for  $Q$ ,  $\phi_w$ , and  $S$  having a tendency to increase (Table 7.4). The high initial viscosity of the potato compared with corn starch had no significant effect on the rate of starch digestion at any shear rate (Table 7.5).

**Table 7.6: Variation in  $T_{1/2}$  values with starch digestion and apparent viscosity for all treatments over 20 minutes. Data points are derived by solving from the linear regression fitted to the data in Figures 7.3 and 7.4.**

Treatments	$T_{1/2}$ starch (min) ‡			$T_{1/2}$ Viscosity (min) ‡		
	Shear rate ( $s^{-1}$ )			Shear rate ( $s^{-1}$ )		
	0.1	1	10	0.1	1	10
PFrucCk30	148.6±9.6 <sup>a</sup> [138.3, 157.2]	147.9±5.0 <sup>a</sup> [142.2, 153.6]	146.8±3.3 <sup>a</sup> [143.3, 149.8]	151.2±1.6 <sup>a</sup> [150.0, 153.0]	148.±2.9 <sup>a</sup> [145.5, 151.2]	146.4±3.7 <sup>ab</sup> [143.9, 150.5]
PDG50% Ck30	52.4±1.2 <sup>bc</sup> [51.6, 53.8]	21.9±0.8 <sup>f</sup> [21.1, 22.8]	20.3±1.0 <sup>f</sup> [19.4, 21.3]	35.6±1.3 <sup>c</sup> [34.5, 37.1]	2.7±0.1 <sup>e</sup> [2.6, 2.8]	2.4±0.2 <sup>e</sup> [2.3, 2.6]
PDG100% Ck10	44.8±0.6 <sup>cd</sup> [44.2, 45.2]	20.4±0.4 <sup>f</sup> [20.1, 20.9]	19.5±0.4 <sup>f</sup> [19.0, 19.8]	35.1±0.9 <sup>c</sup> [34.6, 36.1]	2.6±0.1 <sup>e</sup> [2.5, 2.7]	2.2±0.1 <sup>e</sup> [2.1, 2.3]
PDG100% Ck30	35.8±1.3 <sup>e</sup> [34.3, 36.7]	19.3±0.6 <sup>f</sup> [18.9, 20.0]	18.5±0.4 <sup>f</sup> [18.2, 18.9]	19.9±0.3 <sup>d</sup> [19.6, 20.1]	2.5±0.1 <sup>e</sup> [2.4, 2.6]	1.9±0.1 <sup>e</sup> [1.7, 1.9]
CFrucCk30	146.0±3.1 <sup>a</sup> [144.2, 149.6]	144.2±2.8 <sup>a</sup> [141.6, 147.2]	142.7±1.7 <sup>a</sup> [140.9, 143.7]	147.2±5.8 <sup>ab</sup> [140.5, 150.6]	146.6±3.1 <sup>ab</sup> [143.3, 149.5]	140.2±7.2 <sup>b</sup> [132.0, 145.3]
CDG50%Ck3 0	55.8±0.4 <sup>b</sup> [55.4, 56.1]	25.5±0.5 <sup>f</sup> [24.9, 25.8]	23.5±0.6 <sup>f</sup> [22.9, 24.1]	44.1±0.4 <sup>c</sup> [43.8, 44.5]	4.0±0.2 <sup>e</sup> [3.8, 4.2]	2.8±0.1 <sup>e</sup> [2.7, 2.9]
CDG100%Ck 10	50.3±0.4 <sup>bc</sup> [50.2, 50.5]	25.5±0.7 <sup>f</sup> [24.7, 25.9]	23.5±0.5 <sup>f</sup> [23.0, 23.9]	38.6±0.8 <sup>c</sup> [37.9, 39.4]	4.0±0.2 <sup>e</sup> [3.8, 4.1]	2.8±0.2 <sup>e</sup> [2.6, 2.9]
CDG100%Ck 30	41.7±0.6 <sup>de</sup> [41.3, 42.4]	24.4±0.6 <sup>f</sup> [23.8, 24.8]	21.6±0.3 <sup>f</sup> [21.4, 21.9]	24.3±0.4 <sup>d</sup> [23.8, 24.6]	3.7±0.2 <sup>e</sup> [3.5, 3.8]	2.3±0.1 <sup>e</sup> [2.2, 2.4]

‡ Mean values in a column with different superscripts (a-f) are significantly different on one way ANOVA of all rows in a column using Tukey's pair-wise test,  $p < 0.05$ .

[LL , UL] Values are 95% confidence interval (CI) of lower limit (LL) and upper limit (UL) of samples mean value.

Mean total starch present at the start of digestion (mg/g solids in suspension, dwb) ± standard deviation; P, 561.1 ± 15.4; C, 528.7 ± 21.8

The amount of starch present and apparent viscosities of all suspensions of starch granules in MilliQ water decreased rapidly as starch was hydrolysed during the simulated small intestinal digestion. About 50% of the starch was digested within 25 minutes or less ( $T_{1/2} = 25$  min) at shear rates of  $10 s^{-1}$  and  $1 s^{-1}$  (Table 7.6). However, when the shear rate was lower than  $1 s^{-1}$ , it took around twice as long ( $T_{1/2} = 41$ -56 min) to digest half the starch present. The  $T_{1/2}$  for viscosities of suspensions

during digestion declined in a similar trend, where the  $T_{1/2}$  for the initial viscosity to decrease 50% was about doubled when shear rate was lower than  $1 \text{ s}^{-1}$  (Table 7.6)

#### **7.4.7. Relationship between digestion starch and % viscosity**

The relationship between the proportions of starch remaining and decreases in apparent viscosity of all suspensions gelatinised in MilliQ water and digested at higher shear rates of  $1 \text{ s}^{-1}$  or  $10 \text{ s}^{-1}$  was best fitted (degree of freedom = 7,  $F = 986$ ,  $p < 0.05$ ,  $R^2 > 0.97$ ) with a sigmoid function (Chapter 3, Equation 3.12) (Figure 7.6).

For digestates maintained at the higher shear rates ( $1 \text{ s}^{-1}$  and  $10 \text{ s}^{-1}$ ), in which the apparent viscosities were relatively low at the beginning of the digestion ( $< 320 \text{ Pa.s}$ ), there was a brief initial phase, in which viscosity declined relatively slowly as starch was digested. This was followed by a phase in which the relationship between the decline in relative viscosity as the starch was digested was linear with a slope coefficient of around  $-4\%$  viscosity per % of starch digested. This was followed by a final phase during which the starch content continued to decline but with little further reduction in viscosity (Figure 7.6).

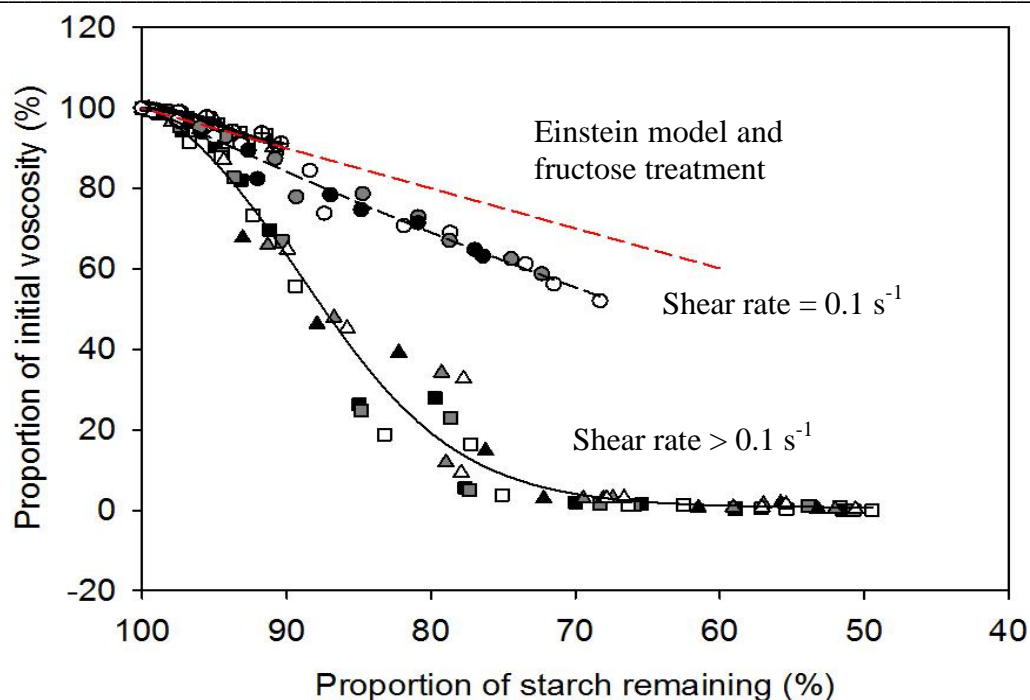


**Figure 7.6:** The relationship between the proportion of undigested starch and the proportion of apparent viscosity remaining for all treatments during the 20 min of digestion;  $\boxplus = 10 \text{ s}^{-1}$  FrucCk30,  $\blacksquare = 10 \text{ s}^{-1}$  DG50%Ck30,  $\blacksquare = 10 \text{ s}^{-1}$  DG100%Ck10,  $\square = 10 \text{ s}^{-1}$  DG100%Ck30,  $\triangle = 1 \text{ s}^{-1}$  FrucCk30,  $\blacktriangle = 1 \text{ s}^{-1}$  DG50%Ck30,  $\triangle = 1 \text{ s}^{-1}$  DG100%Ck10,  $\triangle = 1 \text{ s}^{-1}$  DG100%Ck30,  $\oplus = 0.1 \text{ s}^{-1}$  FrucCk30,  $\bullet = 0.1 \text{ s}^{-1}$  DG50%Ck30,  $\bullet = 0.1 \text{ s}^{-1}$  DG100%Ck10,  $\circ = 0.1 \text{ s}^{-1}$  DG100%Ck30,  $---$  Shear rate at  $0.1 \text{ s}^{-1}$ ,  $---$  Shear rate at 10 and  $1 \text{ s}^{-1}$  ( $R^2 = 0.97$ ),  $---$  Predicted from the Einstein model and Fructose treatment data. All treatments set to 100% starch and viscosity at the start of digestion. Digestion proceeds from left to right.

In treatments where the digestate was maintained at the lowest shear rate ( $0.1 \text{ s}^{-1}$ ) and in treatments where starch granules were suspended in 70% (w/v) fructose (circles, Figure 7.6), the relationships were linear with slope coefficients of less than  $-2\%$  viscosity per % of starch digested, the rate of decline for the fructose treatment being less than that for the low shear treatment (Figure 7.6). For both potato and corn starch samples digested at shear rates of  $> 0.1 \text{ s}^{-1}$ , the relative viscosity was low and constant after about 30% of the starch was digested (Figure 7.6). However, at the lower shear rate of  $0.1 \text{ s}^{-1}$ , the relative viscosity was higher, at around 60% of the

initial value when 30% of the starch had been digested (Figure 7.6) and the relative viscosity continued to decrease linearly as starch was digested.

## 7.5. Discussion

When the digestates were mixed at shear rates within the physiological range ( $1 \text{ s}^{-1}$  or  $10 \text{ s}^{-1}$ ), the relative rates of digestion for suspensions of potato and corn starch granules with comparable %DG were similar, in spite of large differences in their apparent viscosities (Figures 7.4 and 7.5, Table 7.5). These results indicate that the higher viscosities did not limit enzyme access to starch granules, provided that shear rates were sufficient to mix and to disperse the amylolytic enzymes throughout the digesta (Dhital, Bhattarai, et al., 2014). Dhital and co-workers found that when shear high than  $1 \text{ s}^{-1}$  was used, the rate of starch digestion was doubled (Dhital, Bhattarai, et al., 2014). However, when shear rates were reduced below those commonly encountered in the digestive tract i.e. to  $0.1 \text{ s}^{-1}$ , the rate at which starch was digested was markedly reduced (Table 7.5) suggesting that there is a threshold for shear rate that must be met or exceeded to disperse enzyme secretions in a viscous substrate (Dhital et al., 2017).

The relative apparent viscosities of all starch granule suspensions decreased exponentially over time during digestion as the Ln-transformed data showed a linear relationship (Figure 7.4). This interdependence probably reflects the relationship between the solid volume fraction and the apparent viscosity described for weakly interacting rigid particles (Krieger & Dougherty, 1959). Hence, as digestion proceeded, the solid volume fraction of the starch granules decreased with concomitant reductions in viscosity. However this model does not account for

particles softened by gelatinisation and digestion and this case will be discussed later in this section.

The  $Q$  and  $\phi_w$  obtained for suspensions of starch in fructose were low. This indicated that the granules were not, or only weakly, hydrated, hence little gelatinisation of the starch had occurred. This is in accord with work showing that pasting temperatures are increased when the aqueous phase of starch suspensions contains 40% (w/v) sucrose (Gunaratne et al., 2007) and up to 50% (w/v) sucrose (Spies & Hosene, 1982). Low levels of enzyme activity and digestion of the granules is also expected when sugar concentrations are high and  $A_w$  is correspondingly low (Drapron, 1985; Monsan & Combes, 1984; Roder et al., 2009). The low  $\phi_w$  resulted in low apparent viscosities of suspensions of potato and corn starch in 70% (w/v) fructose (Table 7.4). The values for apparent viscosities of these suspensions were close to the calculated values when  $\phi_w = 0.10$  was substituted into Einstein's empirical equation predicting viscosity from  $\phi_w$ , where  $(\eta) = \eta_s (1 + 2.5 \phi_w)$ ; in this case, a 10% (v/v) suspension of rigid spherical particles in a Newtonian liquid (70% (w/v) fructose) for which  $\eta_s = 0.032$  Pa.s.

The sigmoid relationship between the rate of change in apparent viscosity and the rate of change in starch content during digestion of gelatinised starches at shear rates between  $1 \text{ s}^{-1}$  and  $10 \text{ s}^{-1}$  where apparent viscosity is less than 321 Pa.s (Table 7.4, Figure 7.5), has not been described previously. Some clues to the cause of this sigmoidal relationship are given by the linear relationship and slower rates of decline in viscosity that occur when the starch is largely ungelatinised or when a very low shear rate ( $0.1 \text{ s}^{-1}$ ) was applied. The ungelatinised starch granules can be



considered as hard spheres and when they are in an aqueous suspension (in 70% (w/v) fructose solution), they would be expected to contribute to viscosity according to the Einstein model (Mendoza & Santamaria-Holek, 2009). Using the data for  $\phi_w$ , the solid volume fraction of the hydrated granules was determined by substituting the  $\phi_w$  value into Einstein's empirical equation,  $(\eta) = \eta_s (1 + 2.5 \phi_w)$  to calculate suspension viscosity ( $\eta$ ) from the viscosity of the suspending liquid ( $\eta_s$ ). This predicts that about 80% of the initial viscosity would remain when 30% of the starch was digested (dashed red line Figure 7.6). The relationship between apparent viscosity and the proportion of starch remaining for the poorly hydrated starch of the fructose treatments (Figure 7.6) is very close to that predicted from the Einstein model and the granules appeared to behave as hard spheres of decreasing volume throughout digestion. For all gelatinised starch treatments at the low shear rate ( $0.1 \text{ s}^{-1}$ ), the relationship between viscosity and starch concentration also declines linearly but only about 60% of the original viscosity remains when 30% of the starch is digested. Probably the imposed weak shear causes elastic distortion to the granules, resulting in apparent viscosities of the starch granules less than predicted for hard spheres.

Increasing shear from  $0.1 \text{ s}^{-1}$  to  $1 \text{ s}^{-1}$  or  $10 \text{ s}^{-1}$  reduces the viscosity predicted from the starch concentration further and results in the characteristic sigmoid curve for fully gelatinised starch at higher shear rates ( $1 \text{ s}^{-1}$  and  $10 \text{ s}^{-1}$ ) as described in Chapter 6. Presumably, the lag phase at the beginning of the sigmoid curve obtained at the higher shear rates reflects the predicted (Einstein) relationship between the solid volume fraction and viscosity. However, as the highly gelatinised and hydrated granules are rapidly degraded during digestion, elastic distortion of granules and

granule fragments generated by the imposed shear results in the rapid linear reduction in viscosity as the starch content falls (Figure 7.6). In the final phase of digestion, only softened dispersed fragments of granules remain in the aqueous phase and these fragments do not interact sufficiently to contribute significantly to viscosity. Furthermore, it is also likely that the mixing of digestates at the higher shear rates facilitated the movement of enzyme into the gelatinised granules from the digestates (Dhital, Bhattarai, et al., 2014; Dhital, Dolan, Stokes, & Gidley, 2014). At the low shear rate, mixing may be reduced the rate of digestion of the granules. The hypothesised structural changes in the starch granules during digestion are supported by TEM and SEM studies (Planchot et al., 1995). These results suggest that in continuously shaken systems, considerable internal digestion of the granules happens, weakening the granule even when the granule surface remains reasonably intact.

It is important to note that the phenomena reported occurred in suspensions of starch granules that had been continuously stirred during cooling, after cooking, and throughout *in-vitro* digestion. This, coupled with the decreased concentration of the starch as digestion proceeded and the rapid loss of starch during digestion, ensured that the gelatinised suspensions remained fully dispersed during rheological measurements. It is also noteworthy that the digestion mixture during the acid phase contained no pancreatic enzymes nor did the mixture in the alkaline phase of digestion contain the entire suite of pancreatic or brush border enzymes. This situation could have affected the rate at which starch was digested either directly or indirectly. However, given that gelatinised starches were digested rapidly, it is

presumed that the inclusion of the full suite of enzymes would not alter gross dynamics.

This study confirms that the properties and composition of potato and corn starch granules differ (Chapter 6). During gelatinisation, the extent of water absorbed and swelling of potato starch granules ( $Q$  and  $\phi_w$ ) and the consequent increase in apparent viscosity are much greater than in corn starch granules. These differences may reflect differences in fat and protein content (Chapter 6). The higher pasting temperature of corn compared to potato starch is well known (Moore, Tuschhoff, Hastings, & Schanefelt, 1984) and is thought to be related either to differences in the physical organisation of the starch within the granules (Mishra & Rai, 2006) or to the presence of hydrophobic lipid-protein complexes in the corn that resist hydration (Karlalas et al., 1992).

The increase in viscosity as  $Q$  and  $\phi_w$  increase was expected and is the basis of predicting the rheology of suspensions; however the decrease in viscosity that occurred when cooking time was increased from 10 to 30 min needs explanation. This phenomenon is a component of the well-known ‘set-back’ phase that occurs when starches are heated above the temperature at which peak hot paste viscosity occurs (Figure 7.1). The loss in viscosity probably represents a softening of starch granules as they continue to swell and absorb water following gelatinisation.

## **7.6. Conclusion**

The rates of *in-vitro* digestion of potato and corn starch granules in suspensions with apparent viscosity close to that of small intestinal digesta were not influenced by the

shear rates used provided these shear rates were close to the physiological range. Low rates of digestion occurred when shear rates used were below this range ( $0.1 \text{ s}^{-1}$ ). Conversely, small increases in the solids content of digesta will result in large increases in apparent viscosity. In systems such as the gut where shear stress is limited; mixing of the digesta will be compromised along with rates of digestion and the transport of soluble material to sites of absorption at the gut wall.

The relative reduction in apparent viscosity of the granule suspensions and the reduction in starch content during *in-vitro* digestion at physiological shear rates follow a sigmoidal relationship. This suggests that the rate of digestion in the initial phase was slow and granule integrity was more or less preserved, this stage was followed by a more rapid decline in apparent viscosity as granule integrity was lost, finishing in a phase where the still digesting starch granule remnants no longer contributed to viscosity. Conversely, when shear rates were maintained below physiological levels or when starch granules were inadequately gelatinised, the rate of starch digestion was reduced and the granule structure persisted therefore hindering the decline in apparent viscosity.

When the cooking duration of starch was increased from 10 to 30 minutes, the rate of digestion increased although the change was small. This suggests that gelatinisation in the presence of excess water is a time dependent process that may continue long after the peak hot paste viscosity is reached.

---

## **Chapter 8      General discussion and conclusions**

### **8.1.              Introduction**

The aim of this study was to investigate the effects of physico-chemical properties of different fibre types and their effect on the rate of starch digestion using an *in-vitro* digestion system that mimics to a reasonable degree the physiological conditions of small intestinal digestion. In this chapter the major questions addressed in this thesis are summarised along with the discoveries that resulted from them.

### **8.2.              Outcomes from the study**

The insoluble fibre fraction was thought to sequester toxins into intra- and extra-particulate voids, although, as shown early in this work the volume of water that can be sequestered of intra-particulate void is very small (~3%) and probably insignificant in removal of toxins from the gut. The association of high intake of insoluble fibre with reduction of in the incidence of diverticulosis and colon cancer may be due to the high proportion of water held in the mass of insoluble fibre as it transverses the colon and maintains the digesta in a soft well lubricated mass and hence ensures easy elimination of the stool (Cadden, 1987; Eastwood et al., 1983), and improves the ability of the mass of materials in the colon to sequester soluble toxins such as deconjugated biles.

In the small intestine, both soluble and insoluble fibres increase the viscosity of digesta and at sufficiently high concentrations reduce mixing of digesta, thus hindering the mass transfer of solutes during digestion (Morgan, Tredger, Wright, & Marks, 1990), hence reducing the rate of absorption of nutrients including glucose.

However, the fibre concentrations that may affect the rate of glucose absorption were unknown. To ensure the efficient operation of the gut, it would be expected that the viscosity of the contents of the small intestine would be sufficiently diluted by gastric and pancreatic secretions to a viscosity where mixing is ensured by the relatively weak musculature of the small intestine. Clearly, in terms of gut efficiency it is an advantage to be able to process the greatest amount of food in the smallest possible investment in digestive organs. The trade-off is therefore the maximum volume fraction of solids that result in the maximum viscosity that the gut can efficiently mix and ensure near complete digestion and absorption in the small intestine.

The rate of starch digestion has been reported to be reduced by high levels of soluble fibre (Fuentes-Zaragoza, et al., 2010; Tudorica et al., 2002). However, at values of  $\phi$  commonly found in the small intestine, the shear stress developed in the gut is sufficient to maintain shear rates above about  $0.1 \text{ s}^{-1}$ , a limit often reported for the small intestine and hence maintain efficient mixing and absorption (Chapter 7). However it was evident that when guar was added to the diet the rate of digestion was reduced due to inhibition of amylase activity (Slaughter et al., 2001; Warren et al., 2012), and not by restricting mixing due to increases in viscosity.

The solid volume fraction and hence viscosity of the contents of the gut are continually changing due to gut secretions, absorption of liquids and solutes and the digestion of solids, there is a need for method to estimate the viscosity of digesta based on small samples of digesta, preferentially without sacrificing the animal. This work has shown that it is possible to estimate the viscosity of the gut contents

by estimating  $\phi$  using image analysis and measuring the aspect ratio of the fibres to obtain  $\phi_{\max}$  from which the relative viscosity can be estimated by substitution into the Maron-Pierce equation ( $\eta_r = (1 - \phi/\phi_{\max})^{-2}$ ).

The composition of the simulated small intestinal digesta was prepared by mimicking digestive conditions specific to the human digestive tract with the absence of salivary amylase. These included all digestive enzymes, bile extract, ionic strength, presence of divalent cations, and pH while temperature and shear rate were controlled by carrying out the digestions in a rheometer fitted with cup and vane geometry, this also ensured that the digestion mixtures were maintained in suspension during the experiments.

The volume fraction of suspended particles used in this work and found in the pig digesta examined were all well below concentrations that could increase the viscosity of digesta to the point where the shear rate that the gut reportedly generates could not effectively mix its contents.

### **8.3. Applications**

The main objective of this study is to determine factors that lower the rate of amylolysis in the gut which in turn could help manage the incidence of Type II diabetes, diverticular disease and colonic carcinoma. This study shows the likely concentration determined as solid volume fraction of dietary fibre that will result in viscosities of digesta that reduce rates of digestion of starchy foods at the shear stress and therefore shear rates possible in the gut.

#### **8.4. Limitations**

It would have been useful to extend this study to more combinations of starch and perhaps other soluble fibres. However, due to the time and financial constraints, only a limited number of combinations were possible.

#### **8.5. Recommended future research**

- The *in-vitro* digestion system using rheometer can serve as a simple system that approximates conditions in the gut. This set-up can perform fast screening of combinations of various starches and food fibers in simulated digesta and may be used to develop food products with low glycemic impact.
- The *in-vitro* system could also be adopted to investigate the more complex food combinations including proteins, carbohydrates and fats that mimic typical food combinations.



---

## Bibliography

- Abrahamsson, B., Pal, A., Sjoberg, M., Carlsson, M., Laurell, E., & Brasseur, J. G. (2005). A novel *in-vitro* and numerical analysis of shear-induced drug release from extended-release tablets in the fed stomach. *Pharmaceutical Research*, 22, 1215-1226.
- American Dietetic Association. (2008). Position of the American dietetic association: Health implications of dietary fiber. *Journal of the American Dietetic Association*, 108, 1716-1731.
- Anderson, J. W., & Bridges, S. R. (1988). Dietary fiber content of selected foods. *The American Journal of Clinical Nutrition*, 47, 440-447.
- Anderson, J. W., Smith, B. M., & Gustafson, N. J. (1994). Health benefits and practical aspects of high-fiber diets. *The American Journal of Clinical Nutrition*, 59, 1242S-1247S.
- Annisson, G., & Topping, D. L. (1994). Nutritional role of resistant starch: Chemical structure vs physiological function. *Annual Review of Nutrition*, 14, 297-320.
- AOAC. (1984). Official Methods of Analysis of the Association of Official Analytical Chemists *Association of Official Analytical Chemists*: (14th ed.). Arlington, Virginia, USA.: AOAC International.
- AOAC. (1995). Official Method 985.29 - Total Dietary in Foods-Enzymatic-Gravimetric Method *Official Methods of Analysis* (Vol. 16<sup>th</sup> edition). Gaithersburg, M. D., USA: AOAC International.
- AOAC. (1997). AOAC 991.36 Fat (Crude) in Meat and Meat Products *AOAC Official Methods of Analysis*. Gaithersburg, M. D., USA: AOAC International.
- AOAC. (1999). A moisture by oven drying method *Official methods of analysis* (13<sup>th</sup> Edition ed.). Washington, D. C., USA: AOAC International.
- AOAC. (2005a). 968.06. Animal feed; Determination of nitrogen content by combustion using Dumas method and calculate protein (crude) content *AOAC Official Methods of Analysis* (Vol. 1, pp. 25-26). Gaithersburg, M. D., USA.: AOAC International.
- AOAC. (2005b). AOAC Official Method 2002.04 - Amylase-treated Neutral Detergent Fibre in feeds using refluxing in beakers or crucibles first action 2002 *AOAC Official Methods of Analysis* (Vol. 1). Arlington, V. A., USA: AOAC International.
- Asp, N. G., Johansson, C. G., Hallmer, H., & Siljestrom, M. (1983). Rapid enzymatic assay of insoluble, soluble dietary fibre. *Journal of Agriculture and Food Chemistry*, 31, 476-482.
- Auffret, A., Ralet, M. C., Guillon, F., Barry, J. L., & Thibault, J. F. (1994). Effect of grinding and experimental conditions on the measurements of hydration properties on dietary fibres. *Lebensm.-Wiss. u.-Technol.*, 27, 166-172.
- Aune, D., Chan, D. S. M., Lau, R., Vieira, R., Greenwood, D. C., Kampman, E., & Norat, T. (2011). Dietary fibre, whole grains, and risk of colorectal cancer: systematic review and dose-response meta-analysis of prospective studies. *British Medical Journal*, 343, 1-20.
- Bagley, E. B., & Christianson, D. D. (1982). Swelling capacity of starch and its relationship to suspension viscosity- effect of cooking time, temperature and concentration. *Journal of Texture Studies*, 13, 115-126.

- Bajor, A., Gillberg, P., & Abrahamsson, H. (2010). Bile acids : short and long term effects in the intestine *Scandinavian Journal of Gastroenterology*, 45, 645-664.
- Baker, A. A., Miles, M. J., & Helbert, W. (2001). Internal structure of the starch granule revealed by AFM. *Carbohydrate Research*, 300, 249–256.
- Baks, T., Bruins, M. E., Master, A. M., Janssen, A. E. M., & Boom, R. M. (2008). Effect of gelatinization and hydrolysis conditions on the selectivity of starch hydrolysis with  $\alpha$ -amylase from *Bacillus licheniformis*. *Journal of Agricultural and Food Chemistry*, 56, 488-495.
- Barnes, H. A. (1989). Shear-thickening ("dilatancy") in suspensions of nonaggregating solid particles dispersed in Newtonian liquids. *Journal of Rheology*, 33, 329-366.
- Bartelt, J., Jadamus, A., Wiese, F., Swiech, E., Buraczewska, L., & Simon, O. (2002). Apparent precaecal digestibility of nutrients and level of endogenous nitrogen in digesta of the small intestine of growing pigs as affected by various digesta viscosities. *Archives of Animal Nutrition*, 56, 93-107.
- Bauer, B. A., & Knorr, D. (2005). The impact of pressure, temperature and treatment time on starches: pressure-induced starch gelatinisation as pressure time temperature indicator for high hydrostatic pressure processing. *Journal of Food Engineering*, 68, 329–334.
- Becker, A., Hill, S. E., & Mitchell, J. R. (2001). Milling- A further parameter affecting the rapid visco analyser (RVA) profile. *Cereal Chemistry*, 78, 166-172.
- Bedford, M. R., & Classen, H. L. (1992). Reduction of intestinal viscosity through manipulation of dietary rye and pentosanase concentration is effected through changes in the carbohydrate composition of the intestinal aqueous phase and results in improved growth rate and food conversion efficiency of broiler chicks. *Journal of Nutrition*, 122, 560-569.
- Benmoussa, M., Hamaker, B. R., Huang, C.-P., Sherman, D. M., Weil, C. F., & BeMiller, J. N. (2010). Elucidation of maize endosperm starch granule channel proteins and evidence for plastoskeletal structures in maize endosperm amyloplasts. *Journal of Cereal Science*, 52, 22-29.
- Bertoft, E. (2007). Composition of building blocks in clusters from potato amylopectin. *Carbohydrate Polymers*, 70, 123-136.
- Bertoft, E. (2013). On the building block and backbone concepts of amylopectin structure. *Cereal Chemistry*, 90, 294-311.
- Bertoft, E., Koch, K., & Aman, P. (2012). Structure of building blocks in amylopectins. *Carbohydrate Research*, 361, 105-113.
- Biliaderis, C. G. (1991). The structure and interactions of starch with food constituents. *Canadian Journal of Physiology and Pharmacology*, 69, 60-78.
- Bingham, S. A., Day, N. E., Luben, R., Ferrari, P., Slimani, N., Norat, T., Clavel-Chapelon, F., Kesse, E., Nieters, A., Boeing, H., Tjønneland, A., Overvad, K., Martinez, C., Dorronsoro, M., Gonzalez, C. A., Key, T. J., Trichopoulou, A., Naska, A., Vineis, P., Tumino, R., Krogh, V., Bueno-de-Mesquita, H. B., Peeters, P. H. M., Berglund, G., Hallmans, G., Lund, E., Skeie, G., Kaaks, R., & Riboli, E. (2003). Dietary fibre in food and protection against colorectal cancer in the European Prospective Investigation into Cancer and Nutrition (EPIC): an observational study. *The Lancet*, 361, 1496-1501.

- Björck, I., Granfeldt, Y., Liljeberg, H., Tovar, J., & Asp, N. G. (1994). Food properties affecting the digestion and absorption of carbohydrates. *The American Journal of Clinical Nutrition*, 59, 699S-705S.
- Björck, I. (2006). Starch : Nutritional aspects. In A.-C. Eliasson (Ed.), *Carbohydrates in Food* (Second edition ed., pp. 471-522). Boca Raton: CRC Press.
- Björck, I., Nyman, M., Pedersen, B., Siljestrom, M., Asp, N. G., & Eggum, B. O. (1987). Formation of enzyme resistant starch during autoclaving of wheat starch: studies *in vitro* and *in-vivo*. *Journal of Cereal Science*, 6, 159-172.
- Blackburn, N. A., & Johnson, I. T. (1981). The effect of guar gum on the viscosity of the gastrointestinal contents and on glucose uptake from the perfused jejunum in the rat. *British Journal of Nutrition*, 46, 239-246.
- Blackburn, N. A., Redfern, J. S., Jarjis, H., Holgate, A. M., Hanning, I., Scarpello, J. H., Johnson, I. T., & Read, N. W. (1984). The mechanism of action of guar gum in improving glucose tolerance in man. *Clinical Science*, 66, 329-336.
- Blazek, J., & Copeland, L. (2008). Pasting and swelling properties of wheat flour and starch in relation to amylose content. *Carbohydrate Polymers*, 71, 380–387.
- Boek, E. S., Coveney, P. V., Lekkerkerker, H. N. W., & van der Schoot, P. (1997). Simulating the rheology of dense colloidal suspensions using dissipative particle dynamics. *Physical Review E*, 55, 3124-3133.
- Boerjan, W., Ralph, J., & Baucher, M. (2003). Lignin biosynthesis. *Annual Review of Plant Biology*, 54, 519-546.
- Boulos, N. N., Greenfield, H., & Wills, R. B. H. (2000). Water holding capacity of selected soluble and insoluble dietary fibre. *International Journal of Food Properties*, 3, 217-231.
- Braaten, J. T., Wood, P. J., Scott, F. W., Riedel, K. D., Poste, L. M., & Collins, M. W. (1991). Oat gum lowers glucose and insulin after an oral glucose load. *The American Journal of Clinical Nutrition*, 53, 1425-1430.
- Braaten, J. T., Wood, P. J., Scott, F. W., Wolynetz, M. S., Lowe, M. K., Bradley-White, P., & Collins, M. W. (1994). Oat beta-glucan reduces blood cholesterol concentration in hypercholesterolemic subjects. *European Journal of Clinical Nutrition*, 48, 465-474.
- Brand-Miller, J., Hayne, S., Perocz, P., & Colagiuri, S. (2003). Low-glycemic index diets in the management of diabetes: A meta-analysis of randomized controlled trials. *Diabetes Care*, 26, 2261-2267.
- Brennan, C. S., Blake, D. E., Ellis, P. R., & Schofield, J. D. (1996). Effects of guar galactomannan on wheat bread microstructure and on the *in vitro* and *in-vivo* digestibility of starch in bread. *Journal of Cereal Science*, 24, 151-160.
- Brenner, H. (1974). Rheology of a dilute suspension of axisymmetric Brownian particles *International Journal of Multiphase Flow*, 1, 195-341.
- Brodribb, A. J. M., & Groves, C. (1978). Effect of bran particle size on stool weight. *Gut*, 19, 60-63.
- Brown, E., & Jaeger, H. M. (2009). Dynamic jamming point for shear thickening suspensions. *Physical Review Letter*, 103, 086001-086004.
- Bul  on, A., Colonna, P., Planchot, V., & Ball, S. (1998). Starch granules: structure and biosynthesis. *International Journal of Biological Macromolecules*, 23, 85–112.

- Bunzel, M., Seiler, A., & Steinhart, H. (2005). Characterization of dietary fiber lignins from fruits and vegetables using the DFRC method. *Journal of Agriculture and Food Chemistry*, 53, 9553-9559.
- Burkitt, D. P., Walker, A. R. P., & Painter, N. S. (1972). Effect of dietary fibre on stools and transit times and its role in the causation of disease. *The Lancet*, 30, 1408-1411.
- Butterworth, P. J., Warren, F. J., Grassby, T., Patel, H., & Ellis, P. R. (2012). Analysis of starch amylolysis using plots for first-order kinetics. *Carbohydrate Polymers*, 87, 2189-2197.
- Cadden, A. M. (1987). Comparative effects of particle size reduction on physical structure and water binding properties of several plant fibers. *Journal of Food Science*, 52, 1595-1599.
- Capuano, E. (2016). The behaviour of dietary fibre in the gastrointestinal tract determines its physiological effect. *Critical Reviews in Food Science and Nutrition*, 57, 3543-3564.
- Carpita, N. C., & Gibeaut, D. M. (1993). Structural models of primary cell walls in flowering plants: consistency of molecular structure with the physical properties of the walls during growth. *The Plant Journal*, 3, 1-30.
- Champ, M., Langkilde, A. M., Brouns, F., Kettlitz, B., & Collet, Y. L. B. (2003). Advances in dietary fibre characterisation. 1. Definition of dietary fibre, physiological relevance, health benefits and analytical aspects. *Nutrition Research Reviews*, 16, 71-82.
- Chawla, R., & Patil, G. R. (2010). Soluble dietary fiber. *Comprehensive Reviews in Food Science and Food Safety*, 9, 178-196.
- Chen, J. Y., Piva, M., & Labuza, T. P. (1984). Evaluation of water binding capacity (WBC) of food fiber sources. *Journal of Food Science*, 49, 59-63.
- Chen, P., Wang, K., Kuang, Q., Zhou, S., Wang, D., & Liu, X. (2016). Understanding how the aggregation structure of starch affects its gastrointestinal digestion rate and extent. *International Journal of Biological Macromolecules*, 87, 28-33.
- Chrastil, J. (1987). Improved colorimetric determination of amylose in starches or flours *Carbohydrate Research*, 159, 154-158.
- Chudzikowski, R. J. (1971). Guar gum and its applications. *Journal of the Society of Cosmetic Chemists*, 22, 43-60.
- Codex, Commission Alimentarius. (2009). Report of the 30<sup>th</sup> session of the Codex Committee on Nutrition and Foods for Special Dietary Uses., from <http://www.codexalimentarius.org/meetings-reports/en/?sortingDate=012009>
- Cornish-Bowden, A. (2014). Effects of pH and temperature on enzymes. In A. Cornish-Bowden (Ed.), *Principles of enzyme kinetics* (pp. 101-114). London: Butterworth & Co. Ltd.
- Cosgrove, D. J. (2005). Growth of the plant cell wall. *Nature Reviews - Molecular Cell Biology*, 6, 850-861.
- Craig, S. A. S., Maningat, C. C., Seib, P. A., & Hoseney, R. C. (1989). Starch paste clarity. *Cereal Chemistry*, 66, 173-182.
- Crowe, F. L., Appleby, P. N., Allen, N. E., & Key, T. J. (2011). Diet and risk of diverticular disease in Oxford cohort of European Prospective Investigation into Cancer and Nutrition (EPIC): prospective study of British vegetarians and non-vegetarians. *British Medical Journal*, 343, 1-15.
- Cullen, P. J., O'Donnell, C. P., & Houska, M. (2002). Rotational rheometry using complex geometries - A review. *Journal of Texture Studies*, 34, 1-20.

- Cummings, J. H. (1984). Constipation, dietary fibre and the control of large bowel function. *Postgraduate Medical Journal*, 60, 811-819.
- Cummings, J. H. (2001). The effect of dietary fiber on fecal weight and composition. In G. A. Spiller (Ed.), *CRC Handbook of dietary fiber in human nutrition, Third edition* (Third edition ed., pp. 183-252). Boca Raton: CRC Press.
- Cummings, J. H., Branch, W., Jenkins, D. J. A., Southgate, D. A. T., Houston, H., & James, W. P. T. (1978). Colonic response to dietary fibre from carrot, cabbage, apple bran and guar gum. *The Lancet*, 1, 5-9.
- Cummings, J. H., Jenkins, D. J. A., & Wiggins, H. S. (1976). Measurement of the mean transit time of dietary residue through the human gut. *Gut*, 17, 210-218.
- Cummings, J. H., & Macfarlane, G. T. (1991). The control and consequences of bacterial fermentation in the human colon. *Journal of Applied Bacteriology*, 70, 443-459.
- Cummings, J. H., Pomare, E. W., Branch, H. W. J., Naylor, C. P. E., & Macfarlane, G. T. (1987). Short chain fatty acids in human large intestine, portal, hepatic and venous blood. *Gut*, 28, 1221-1227.
- Cummings, J. H., Roberfroid, M. B., Andersson, H., Barth, C., Ferro-Luzzi, A., Ghos, Y., Gibney, M., Hermansen, K., James, W. P. T., Korver, O., Lairon, D., Pascal, G., & Voragen, A. G. S. (1997). Review : A new look at dietary carbohydrate: chemistry, physiology and health. *European Journal of Clinical Nutrition*, 51, 417-423.
- Cummings, J. H., & Stephen, A. M. (2007). Review : Carbohydrate terminology and classification. *European Journal of Clinical Nutrition*, 61, S5-S18.
- Dahm, C. C., Keogh, R. H., Spencer, E. A., Greenwood, D. C., Key, T. J., Fentiman, I. S., Shipley, M. J., Brunner, E. J., Cade, J. E., Burley, V. J., Mishra, G., Stephen, A. M., Kuh, D., White, I. R., Luben, R., Lentjes, M. A. H., Khaw, K. T., & Rodwell, S. A. (2010). Dietary fiber and colorectal cancer risk: A nested case-control study using food diaries *Journal of the National Cancer Institute*, 102, 614-626.
- Davidson, M. H., & McDonald, A. (1998). Fibres: Forms and functions. *Nutrition Research*, 18, 617-624.
- de Loubens, C., Lentle, R. G., Love, R. J., Hulls, C., & Janssen, P. W. M. (2013). Fluid mechanical consequences of pendular activity, segmentation and pyloric outflow in the proximal duodenum of the rat and the guinea pig. *Journal of the Royal Society Interface*, 10, 1-12.
- de Sales, P. M., de Souza, P. M., Simeoni, L. A., Magalhaes, P. O., & Silveira, D. (2012).  $\alpha$ -amylase inhibitors: A review of raw material and isolated compounds from plant source. *Journal of Pharmacy and Pharmaceutical Sciences* 15, 141-183.
- Deffenbaugh, L. B., & Walker, C. E. (1989). Use of the Rapid-Visco-Analyzer to measure starch pasting properties. Part I: effect of sugars. . *Starch*, 41, 461-467.
- Delcour, J. A., Bruneel, C., Derde, L. J., Gomand, S. V., Pareyt, B., Putseys, J. A., Wilderjans, E., & Lamberts, L. (2010). Fate of starch in food processing: From raw materials to final food products. 1, 87-111.
- Dhingra, D., Michael, M., Rajput, H., & Patil, R. T. (2012). Dietary fibre in foods: a review. *Journal of Food Science Technology*, 49, 255-266.

- Dhital, S., Bhattarai, R. R., Gorham, J., & Gidley, M. J. (2014). Intactness of cell wall structure controls the *in-vitro* digestion of starch in legumes. *Food and Function*, 7, 1367-1379.
- Dhital, S., Dolan, G., Stokes, J. R., & Gidley, M. J. (2014). Enzymatic hydrolysis of starch in the presence of cereal soluble fibre polysaccharides. *Food and Function*, 5, 579-586.
- Dhital, S., Gidley, M. J., & Warren, F. J. (2015). Inhibition of  $\alpha$ -amylase activity by cellulose: Kinetic analysis and nutritional implications. *Carbohydrate Polymers*, 123, 305-312.
- Dhital, S., Shrestha, A. K., & Gidley, M. J. (2010). Relationship between granule size and *in vitro* digestibility of maize and potato starches. *Carbohydrate Polymers*, 82, 480-488.
- Dhital, S., Warren, F. J., Butterworth, P. J., Ellis, P. R., & Gidley, M. J. (2017). Mechanisms of starch digestion by  $\alpha$ -amylase—Structural basis for kinetic properties. *Critical Reviews in Food Science and Nutrition*, 57, 875-892.
- Dikeman, C. L., Barry, K. A., Murphy, M. R., & Fahey, G. C. J. (2007). Diet and measurement techniques affect small intestinal digesta viscosity among dogs. *Nutrition Research*, 27, 56-65.
- Dikeman, C. L., & Fahey, G. C. J. (2006). Viscosity as related to dietary fiber: A review. *Critical Reviews in Food Science and Nutrition*, 46, 649-663.
- Dikeman, C. L., Murphy, M. R., & Fahey, G. C. (2007). Diet type affects viscosity of ileal digesta of dogs and simulated gastric and small intestinal digesta. *Journal of Animal Physiology and Animal Nutrition*, 91, 139-147.
- Dona, A. C., Pages, G., Gilbert, R. G., & Kuchel, P. W. (2010). Review - Digestion of starch: *In-vivo* and *in-vitro* kinetic models used to characterise oligosaccharide or glucose release. *Carbohydrate Polymers*, 80, 599-617.
- Donovan, J. W. (1979). Phase transitions of the starch-water system. *Biopolymers*, 18, 263-275.
- Doublier, J. L. (1987). A rheological comparison of wheat, maize, paba bean and smooth pea starches. *Journal of Cereal Science*, 5, 247-262.
- Doublier, J. L., Llamas, G., & Le Meur, M. (1987). A rheological investigation of cereal starch pastes and gels. Effect of pasting procedures. *Carbohydrate Polymers*, 7, 251-275.
- Drapron, R. (1985). Enzyme activity as a function of water activity. In D. Simatos & J. L. Multon (Eds.), *Properties of water in foods* (pp. 171-190). Netherlands: Springer.
- Dreher, M. (1999). Food sources and uses of dietary fiber. In S. S. Cho, L. Prosky & M. Dreher (Eds.), *Complex carbohydrate in foods* (pp. 327-371). New York: Marcel Dekker, Inc.
- Dreher, M., Dreher, C. J., Berry, J. W., & Fleming, S. E. (1984). Starch digestibility of foods : A nutritional perspective. *CRC Critical Reviews in Food Science and Nutrition*, 20, 47-71.
- Eastwood, M. A. (1973). Vegetable fibre: its physical properties. *Proceedings of the Nutrition Society*, 32, 137-143.
- Eastwood, M. A., Anderson, R., Mitchell, W. D., Robertson, J., & Pocock, S. (1976). A method to measure the adsorption of bile salts to vegetable fiber of differing water holding capacity. *The Journal of Nutrition*, 106, 1429-1432.
- Eastwood, M. A., & Kay, R. M. (1979). An hypothesis for the action of dietary fiber along the gastrointestinal tract. *The American Journal of Clinical Nutrition*, 32, 364-367.

## Bibliography

- Eastwood, M. A., & Mitchell, W. D. (1976). Physical properties of fibre: A biological evaluation. In G. A. Spiller & R. J. Amen (Eds.), *Fibre in human nutrition* (pp. 109-129). New York: Plenum Press.
- Eastwood, M. A., & Morris, E. R. (1992). Physical properties of dietary fiber that influence physiological function: a model for polymers along the gastrointestinal tract. *The American Journal of Clinical Nutrition*, 55, 436-442.
- Eastwood, M. A., Robertson, J. A., Brydon, W. G., & MacDonald, D. (1983). Measurement of water holding properties of fibre and their faecal bulking ability in man. *British Journal of Nutrition*, 50, 539-547.
- Edwards, C. A., Blackburn, N. A., Craigen, L., Davison, P., Tomlin, J., Sugden, K., Johnson, I. T., & Read, N. W. (1987). Viscosity of food gums determined in vitro related to their hypoglycemic actions. *The American Journal of Clinical Nutrition*, 46, 72-77.
- Edwards, C. H., Warren, F. J., Milligan, P. J., Butterworth, P. J., & Ellis, P. R. (2014). A novel method for classifying starch digestion by modelling the amylolysis of plant foods using first-order enzyme kinetic principles. *Food & Function*, 5, 2751-2758.
- Ehle, F. R., Jeraci, J. L., Robertson, J. B., & van Soest, P. J. (1982). The influence of dietary fiber on digestibility, rate of passage and gastrointestinal fermentation in pigs. *Journal of Animal Science*, 55, 1071-1081.
- Ehle, F. R., Robertson, J. B., & van Soest, P. J. (1982). Influence of dietary fibers on fermentation in the human large intestine. *The Journal of Nutrition*, 112, 158-166.
- Einstein, A. (1906). A new determination of molecular dimensions. *Annalen der Physik*, 19, 289-306.
- Eliasson, A. C. (1986). Viscoelastic behaviour during the gelatinisation of starch. I. Comparison of wheat, maize, potato and waxy barley starches. *Journal of Texture Studies*, 17, 253-265.
- Eliasson, A. C., & Gudmundsson, M. (1996). Starch: Physicochemical and functional aspects. In A. C. Eliasson (Ed.), *Carbohydrates in Food* (pp. 431-504). United State of America: Marcel Dekker.
- Elleuch, M., Bedigian, D., Roiseux, O., Besbes, S., Blecker, C., & Attia, H. (2011). Dietary fibre and fibre-rich by-products of food processing: Characterisation, technological functionality and commercial applications: A review. *Food Chemistry*, 124, 411-421.
- Ellis, P. R., Rayment, P., & Wang, Q. (1996). A physico-chemical perspective of plant polysaccharides in relation to glucose absorption, insulin secretion and the entero-insular axis. *Proceedings of the Nutrition Society*, 55, 881-898.
- Ells, L. J., Seal, C. J., Kettlitz, B., Bal, W., & Mathers, J. C. (2005). Postprandial glycaemic, lipaemic and haemostatic responses to ingestion of rapidly and slowly digested starches in healthy young women. *British Journal of Nutrition*, 94, 948-955.
- Englyst, H. N. (1989). Classification and measurement of plant polysaccharides. *Animal Feed Science and Technology*, 23, 27-42.
- Englyst, H. N., & Hudson, G. J. (1996). The classification and measurement of dietary carbohydrates. *Food Chemistry*, 57, 15-21.
- Englyst, H. N., Kingman, S. M., & Cummings, J. H. (1992). Classification and measurement of nutritionally important starch fractions. *European Journal of Clinical Nutrition*, 46, S33-S50.

- Englyst, H. N., Kingman, S. M., Hudson, G. J., & Cummings, J. H. (1996). Measurement of resistant starch *in vitro* and *in vivo*. *British Journal of Nutrition*, 75, 749-755.
- Englyst, K. N., Englyst, H. N., Hudson, G. J., Cole, T. J., & Cummings, J. H. (1999). Rapidly available glucose in foods : an *in vitro* measurement that reflects the glycemic response. *The American Journal of Clinical Nutrition*, 69, 448-454.
- Evans, A. L., Hood, R. L., Oakenfull, D. G., & Sidhu, G. S. (1992). Relationship between structure and function of dietary fibre: a comparative study of the effects of three galactomannans on cholesterol metabolism in the rat. *British Journal of Nutrition*, 68, 217-229.
- Evans, I. D., & Lips, A. (1992). Viscoelasticity of gelatinised starch dispersions. *Journal of Texture Studies*, 23, 69-86.
- Fannon, J. E., Gray, J. A., Gunawan, N., Huber, K. C., & BeMiller, J. N. (2004). Heterogeneity of starch granules and the effect of granule channelization on starch modification. *Cellulose*, 11, 247-254.
- Farris, R. J. (1968). Prediction of the viscosity of multimodal suspensions from unimodal viscosity data. *Transactions of the Society of Rheology*, 12, 281-301.
- Femenia, A., Selvendran, R. R., Ring, S. G., & Robertson, J. A. (1999). Effects of heat treatment and dehydration on properties of cauliflower fiber. *Journal of Agricultural and Food Chemistry*, 47, 728-732.
- Ferguson, L. R., & Harris, P. J. (1997). Particle size of wheat bran in relation to colonic function in rats. *Lebensm.-Wiss. u.-Technol.*, 30, 735-742.
- Fermin, D., & Riley, J. (2010). Charge in colloidal systems. In T. Cosgrove (Ed.), *Colloid science: principles, methods and applications* (pp. 23-42). Chichester: John Wiley & Sons Ltd.
- Finley, J. W., Soto-Vaca, A., Heimbach, J., Rao, T. P., Juneja, L. R., Slavin, J., & Fahey, G. C. (2013). Safety assessment and caloric value of partially hydrolyzed guar gum. *Journal of Agriculture and Food Chemistry*, 61, 1756-1771.
- Fischer, P., Pollard, M., Erni, P., Marti, I., & Padar, S. (2009). Rheological approaches to food systems. *Complex and biofluids*, 10, 740-750.
- Florén, C. H., & Nilsson, A. (1982). Binding of bile salts to fibre-enriched wheat bran. *Human Nutrition Clinical Nutrition*, 36, 381-390.
- Folgar, F., & Tucker III, C. L. (1984). Orientation behavior of fibers in concentrated suspensions. *Journal of Reinforced Plastics and Composites*, 3, 98-119.
- Foschia, M., Peressini, D., Sensidoni, A., & Brennan, C. S. (2013). Review: The effects of dietary fibre addition on the quality of common cereal products. *Journal of Cereal Science*, 58, 216-227.
- Fredriksson, H., Silverio, J., Andersson, R., Eliasson, A. C., & Aman, P. (1998). The influence of amylose and amylopectin characteristics on gelatinization and retrogradation properties of different starches. *Carbohydrate Polymers*, 35, 119-134.
- Fredstrom, S. B., Lampe, J. W., Jung, H-J. G., & Slavin, J. L. (1994). Apparent fiber digestibility and fecal short-chain fatty acid concentrations with ingestion of two types of dietary fiber. *Journal of Parenteral and Enteral Nutrition*, 18, 14-19.
- Freudenheim, J. L., Graham, S., Horvath, P. J., Marshall, J. R., Haughey, B. P., & Wilkinson, G. (1990). Risks associated with source of fiber and fiber



- components in cancer of the colon and rectum. *Cancer Research*, 50, 3295-3300.
- Fuentes-Zaragoza, E., Riquelme-Navarrete, M. J., Sánchez-Zapata, E., & Pérez-Álvarez, J. A. (2010). Resistant starch as functional ingredient: A review. *Food Research International*, 43, 931-942.
- Fujiwara, N., Hall, C., & Jenkins, A. L. (2017). Development of low glycemic index (GI) foods by incorporating pulse ingredients into cereal-based products: use of *in-vitro* screening and *in-vivo* methodologies. *Cereal Chemistry*, 94, 110-116.
- Funami, T., Kataoka, Y., Omoto, T., Goto, Y., Asai, I., & Nishinari, K. (2005). Food hydrocolloids control the gelatinization and retrogradation behavior of starch. 2a. Functions of guar gums with different molecular weights on the gelatinization behavior of corn starch. *Food Hydrocolloids*, 19, 15-24.
- Furda, I. (1977). Fractionation and examination of biopolymers from dietary fiber. *Cereal Foods World*, 22, 252-254.
- Gallant, D. J., Bouchet, B., & Baldwin, P. M. (1997). Microscopy of starch: evidence of a new level of granule organization. *Carbohydrate Polymers*, 32, 177-191.
- Gallant, D. J., Bouchet, B., Buléon, A., & Pérez, S. (1992). Physical characteristics of starch granules and susceptibility to enzymatic degradation. *European Journal of Clinical Nutrition*, 46, S3-S16.
- Garcia, V., Colonna, P., Bouchet, B., & Gallant, D. J. (1997). Structural changes of cassava starch granules after heating at intermediate water contents. *Starch*, 49, 171-179.
- Genovese, D. B., Lozano, J. E., & Rao, M. A. (2007). The rheology of colloidal and noncolloidal food dispersions. *Journal of Food Science*, 72, R11-R20.
- Gérard, C., Planchot, V., Colonna, P., & Bertoft, E. (2000). Relationship between branching density and crystalline structure of A- and B-type maize mutant starches. *Carbohydrate Research*, 326, 130-144.
- Germaine, K. A., Samman, I., Fryirs, C. G., Griffiths, P. J., Johnson, S. K., & Quail, K. J. (2008). Comparison of *in-vitro* starch digestibility methods for predicting the glycaemic index of grain foods *Journal of the Science of Food and Agriculture*, 88, 652-658.
- Giacco, R., Parillo, M., Rivelles, A. A., Lasorella, G., Giacco, A., D'episcopo, L., & Riccardi, G. (2000). Long-term dietary treatment with increased amounts of fiber-rich low-glycemic index natural foods improves blood glucose control and reduces the number of hypoglycemic events in Type 1 diabetic patients. *Diabetes Care*, 23, 1461-1466.
- Goni, I., Garcia-Alonso, A., & Saura-Calixto, F. (1997). A starch hydrolysis procedure to estimate glycemic index. *Nutrition Research*, 17, 427-437.
- Gonzalez, C. A., Riboli, E., & (EPIC), and other members of European Prospective Investigation into Cancer and Nutrition. (2010). Diet and cancer prevention: Contributions from the European Prospective Investigation into Cancer and Nutrition (EPIC) study. *European Journal of Cancer*, 46, 2555-2562.
- Granfeldt, Y., Hagander, B., & Björck, I. (1995). Metabolic responses to starch in oat and wheat products. On the importance of food structure, incomplete gelatinization or presence of viscous dietary fibre. *European Journal of Clinical Nutrition*, 49, 189-199.
- Gray, G. M. (1992). Starch digestion and absorption in nonruminants. *The Journal of Nutrition*, 122, 172-177.

- Grundy, M. M.-L., Edwards, C. H., Mackie, A. R., Gidley, M. J., Butterworth, P. J., & Ellis, P. R. (2016). Re-evaluation of the mechanisms of dietary fibre and implications for macronutrient bioaccessibility, digestion and postprandial metabolism. *British Journal of Nutrition*, 116, 816-833.
- Guillon, F., & Champ, M. (2000). Structural and physical properties of dietary fibres, and consequences of processing on human physiology. *Food Research International*, 33, 233-245.
- Gujral, H. S., Haros, M., & Rosell, C. M. (2004). Improving the texture and delaying staling in rice flour chapati with hydrocolloids and  $\alpha$ -amylase. *Journal of Food Engineering*, 65, 89-94.
- Gunaratne, A., Ranaweera, S., & Corke, H. (2007). Thermal, pasting, and gelling properties of wheat and potato starches in the presence of sucrose, glucose, glycerol, and hydroxypropyl  $\beta$ -cyclodextrin. *Carbohydrate Polymers*, 70, 112-122.
- Gupta, P., & Premavalli, K. S. (2011). *In-vitro* studies on functional properties of selected natural dietary fibres. *International Journal of Food Properties*, 14, 397-410.
- Hanashiro, I., Abe, J. I., & Hizukuri, S. (1996). A periodic distribution of chain length of amylopectin as revealed by high performance anion-exchange chromatography *Carbohydrate Research*, 283, 151-159.
- Hansen, I., Bach, K. E. K., & Eggum, B. O. (1992). Gastrointestinal implications in the rat of wheat bran, oat bran and pea fibre. *British Journal of Nutrition*, 68, 451-462.
- Harris, P. J., & Ferguson, L. R. (1993). Dietary fibre: its composition and role in protection against colorectal cancer. *Mutation Research*, 290, 97-110.
- Hasinoff, B. B., Dreher, R., & Davey, J. P. (1987). The association reaction of yeast alcohol dehydrogenase with coenzyme is partly diffusion-controlled in solvents of increased viscosity. *Biochimica et Biophysica Acta*, 911, 53-58.
- Hasjim, J., Lavau, G. C., Gidley, M. J., & Gilbert, R. G. (2010). *In-vivo* and *in-vitro* starch digestion: Are current *in-vitro* techniques adequate? *Biomacromolecules*, 11, 3600-3608.
- Heaton, K. W., Marcus, S. N., Emmett, P. M., & Bolton, C. H. (1988). Particle size of wheat, maize and oat test meals: effects on plasma glucose and insulin responses and on the rate of starch digestion *in vitro*. *The American Journal of Clinical Nutrition*, 47, 675-682.
- Heller, S. N., Hackler, L. R., Rivers, J. M., van Soest, P. J., Roe, D. A., Lewis, B. A., & Robertson, J. (1980). Dietary fiber: the effect of particle size of wheat bran on colonic function in young adult men. *The American Journal of Clinical Nutrition*, 33, 1734-1744.
- Hellman, N. N., & Melvin, E. H. (1950). Surface area of starch and its role in water sorption. *Journal of the American Chemical Society*, 72, 5186-5188.
- Higley, J. S., Love, S. L., Price, W. J., Nelson, J. E., & Huber, K. C. (2003). The rapid visco analyzer (RVA) as a tool for differentiating potato cultivars on the basis of flour pasting properties. *American Journal of Potato Research*, 80, 195-206.
- Hill, C. A. S., Norton, A., & Newman, G. (2008). The water vapour sorption behavior of natural fibers. *Journal of Applied Polymer Science*, 112, 1524-1537.

## Bibliography

- Hillman, L., Peters, S., Fisher, A. C., & Pomare, E. W. (1986). Effects of the fibre components pectin, cellulose, and lignin on bile salt metabolism and biliary lipid composition in man. *Gut*, 27, 29-36.
- Hillman, L., Peters, S., Fisher, A., & Pomare, E. W. (1983). Differing effects of pectin, cellulose and lignin on stool pH, transit time and weight. *British Journal of Nutrition*, 50, 189-195.
- Hizukuri, S. (1986). Polymodal distribution of the chain lengths of amylopectin and its significance. *Carbohydrate Research*, 147, 342-347.
- Hofmann, A. F. (1999). The continuing importance of bile acids in liver and intestinal disease. *Archives international Medical*, 159, 2647-2658.
- Hollmann, J., Themeier, H., Neese, U., & Lindhauer, M. G. (2013). Dietary fibre fractions in cereal foods measured by anew integrated AOAC method. *Food Chemistry*, 140, 586-589.
- Holloway, W. D., & Greig, R. I. (1984). Water holding capacity of hemicelluloses from fruits, vegetables and wheat bran. *Journal of Food Science*, 49, 1632-1633.
- Holloway, W. D., Tasman-Jones, C., & Lee, S. P. (1978). Digestion of certain fractions of dietary fiber in humans. *The American Journal of Clinical Nutrition*, 31, 927-930.
- Holm, J., Bjock, I., Asp, N. G., Sjoberg, L. B., & Lundquist, I. (1985). Starch availability *in vitro* and *in vivo* after flaking, steam-cooking and popping of wheat. *Journal of Cereal Science*, 3, 193-206.
- Holm, J., Lundquist, I., Bjorck, I., Eliasson, A. C., & Asp, N. G. (1988). Degree of starch gelatinization, digestion rate of starch *in vitro*, and metabolic response in rats. *The American Journal of Clinical Nutrition*, 47, 1010-1016.
- Hoover, R. (2001). Composition, molecular structure, and physicochemical properties of tuber and root starches: a review. *Carbohydrate Polymers*, 45, 253-267.
- Howling, D. (1980). The influence of the structure of starch on its rheological properties. *Food Chemistry*, 6, 51-61.
- Hur, S. J., Lim, B. O., Decker, E. A., & McClements, D. J. (2011). *In-vitro* human digestion models for food applications. *Food Chemistry*, 125, 1-12.
- Imberty, A., Buléon, A., Tran, V., & Pérez, S. (1991). Recent advances in knowledge of starch structure. *Starch*, 43, 375-384.
- Jacobs, H., & Delcour, J. A. (1998). Hydrothermal Modifications of Granular Starch, with Retention of the Granular Structure: A Review. *Journal of Agricultural and Food Chemistry* 46, 2895-2905.
- Jacobs, L. R. , & Lupton, J. R. (1986). Relationship between colonic luminal pH cell proliferation, and colon carcinogenesis in 1,2-dimethylhydrazine treated rats fed high fiber diets. *Cancer Research*, 46, 1726-1734.
- Jacobson, M. R., Obanni, M., & BeMiller, J. N. (1997). Retrogradation of starches from different botanical sources. *Cereal Chemistry*, 74, 511-518.
- Jalali, A. R., Nørgaard, P., Weisbjerg, M. R., & Nadeau, E. (2012). Effect of stage of maturity of grass at harvest on intake, chewing activity and distribution of particle size in faeces from pregnant ewes. *Animal*, 6, 1774-1783.
- Jane, J. (2006). Current understanding on starch granule structures. *Journal of Applied Glycoscience*, 53, 205-213.
- Jane, J., Ao, Z., Duvick, S. A., Wiklund, M., Yoo, S. H., Wong, K. S., & Gardner, C. (2003). Structures of amylopectin and starch granules: How are they synthesized? *Journal of Applied Glycoscience*, 50, 167-172.

- Jeffrey, B., Udaykumar, H. S., & Schulze, K. S. (2003). Flow fields generated by peristaltic reflex in isolated guinea pig ileum: impact of contraction depth and shoulders. *American Journal of Physiology - Gastrointestinal and Liver Physiology*, 285, G907–G918.
- Jeffrey, D. J., & Acrivos, A. (1976). The rheological properties of suspensions of rigid particles. *AIChE Journal*, 22, 417-432.
- Jenkins, D. J. A., Leeds, A. R., Gassull, M. A., Cochet, B., & Alberti, K. G. M. M. (1977). Decrease in postprandial insulin and glucose concentrations by guar and pectin. *Annals of Internal Medicine*, 86, 20-23.
- Jenkins, D. J. A., Marchie, A., Augustin, L. S. A., Ros, E., & Kendall, C. W. C. (2004). Viscous dietary fibre and metabolic effects. *Clinical Nutrition Supplements*, 1, 39-49.
- Jenkins, D. J. A., Thorne, M. J., Wolever, T. M. S., Jenkins, A. L., Rao, A. V., & Thompson, L. U. (1987). The effect of starch-protein interaction in wheat on the glycemic response and rate of *in vitro* digestion. *The American Journal of Clinical Nutrition*, 45, 946-951.
- Jenkins, D. J. A., Wolever, T. M. S., Taylor, R. H., Barker, H., Fielden, H., Baldwin, J. M., Bowling, A. C., Newman, H. C., Jenkins, A. L., & Goff, D. V. (1981). Glycemic index of foods: a physiological basis for carbohydrate exchange. *The American Journal of Clinical Nutrition*, 34, 362-366.
- Johansen, H. N., & Knudsen, K. E. B. (1994). Effects of wheat-flour and oat mill fractions on jejunal flow, starch degradation and absorption of glucose over an isolated loop of jejunum in pigs. *British Journal of Nutrition*, 72, 299-313.
- Johnson, I. T., & Gee, J. M. (1981). Effect of gel-forming gums on the intestinal unstirred layer and sugar transport *in-vitro*. *Gut*, 22, 398-403.
- Juhász, R., & Salgó, A. (2008). Pasting behavior of amylose, amylopectin and their mixtures as determined by RVA curves and first derivatives. *Starch*, 60, 70-78.
- Juntunen, K. S., Laaksonen, D. E., Autio, K., Niskanen, L. K., Holst, J. J., Savolainen, K. E., Liukkonen, K. H., Poutanen, K. S., & Mykkanen, H. M. (2003). Structural differences between rye and wheat breads but not total fiber content may explain the lower postprandial insulin response to rye bread. *The American Journal of Clinical Nutrition*, 78, 957-964.
- Juszczak, L., Fortuna, T., & Krok, F. (2003). Non-contact Atomic Force Microscopy of starch granules surface. Part I. Potato and tapioca starches. *Starch*, 55, 1-7.
- Kanaghinis, T., Lubran, M., & Coghill, N. F. (1963). The composition of ileostomy fluid. *Gut*, 4, 322-338.
- Karlalas, J., Tester, R. F., & Morrison, W. R. (1992). Properties fo damaged starch granules. I. Comparison of a micromethod for the enzymic determination of damaged starch with the standard AACC and Farrand methods. *Journal of Cereal Science*, 16, 237-251.
- Karlsson, M. E., & Eliasson, A. C. (2003). Gelatinization and retrogradation of potato (*Solanum tuberosum*) starch in situ as assessed by differential scanning calorimetry (DSC). *Lebensmittel - Wissenschaft und Technologie : Food Science and Technology*, 36, 735-741.
- Kaur, L., Singh, J., McCarthy, O. W., & Singh, H. (2007). Physico-chemical, rheological and structural properties of fractionated potato starches. *Journal of Food Engineering*, 82, 383–394.
- Kelsay, J. L., Goering, H. K., Behall, K. M., & Elizabeth, S. (1981). Effect of fiber from fruits and vegetables on metabolic responses of human subjects: fiber

- intakes, fecal excretions, and apparent digestibilities. *The American Journal of Clinical Nutrition*, 34, 1849-1852.
- Kendall, C. W. C., Esfahani, A., & Jenkins, D. J. A. (2010). The link between dietary fibre and human health. *Food Hydrocolloids*, 24, 42-48.
- Khan, K., Jovanovski, E., Ho, H. V. T., Marques, A. C. R., Zurbau, A., Mejia, S. B., Sievenpiper, J. L., & Vuksan, V. (2017). The effect of viscous soluble fiber on blood pressure: A systematic review and meta-analysis of randomized controlled trials. *Nutrition, Metabolism and Cardiovascular Diseases*, *In press, accepted manuscript*. doi: 10.1016/j.numecd.2017.09.007
- Kim, H. S., & Huber, K. C. (2010). Physicochemical properties and amylopectin fine structures of A- and B-type granules of waxy and normal soft wheat starch. *Journal of Cereal Science*, 51, 256-264.
- Kitano, T., Kataoka, T., & Shirota, T. (1981). An empirical equation of the relative viscosity of polymer melts filled with various inorganic fillers. *Rheology Acta*, 20, 207-209.
- Klucinec, J. D., & Thompson, D. B. (2002). Amylopectin nature and amylose-to-amylopectin ratio as influences on the behavior of gels of dispersed starch. *Cereal Chemistry*, 79, 24-35.
- Knudsen, K. E. B. (2001). The nutritional significance of "dietary fibre" analysis. *Animal Feed Science and Technology*, 90, 3-20.
- Knutson, C. A., & Grove, M. J. (1994). Rapid method for estimation of amylose in maize starches. *Cereal Chemistry*, 71, 469-471.
- Koh, A., Vadder, F. D., Kovatcheva-Datchary, P., & Bäckhed, F. (2016). From dietary fiber to host physiology : Short-chain fatty acids as key bacterial metabolites. *Cell*, 165, 1332-1345.
- Kong, B. W., Kim, J. I., Kim, M. J., & Kim, J. C. (2003). Porcine pancreatic  $\alpha$ -amylase hydrolysis of native starch granules as a function of granule surface area. *Biotechnology Progress*, 19, 1162-1166.
- Konstantinov, S. R. (2017). Diet, microbiome, and colorectal cancer. *Best Practice & Research Clinical Gastroenterology*, *In Press*, 1-7.
- Krämer, M., Nørgaard, P., Lund, P., & Weisbjerg, M. R. (2013). Particle size alterations of feedstuffs during *in-situ* neutral detergent fiber incubation. *Journal of Dairy Science*, 96, 4601-4614.
- Krieger, I. M., & Dougherty, T. J. (1959). A mechanism for non-Newtonian flow in suspensions of rigid spheres. *Transactions of the Society of Rheology* 3, 137-152.
- Kullak-Ublick, G. A., Paumgartner, G., & Berr, F. (1995). Long term effects of cholecystectomy on bile acid metabolism. *Hepatology*, 21, 41-45.
- Larsson, S. C., Giovannucci, E., Bergkvist, L., & Wolk, A. (2005). Whole grain consumption and risk of colorectal cancer: a population-based cohort of 60 000 women. *British Journal of Cancer*, 92, 1803-1807.
- Leach, H. W., McCowen, L. D., & Schoch, T. J. (1959). Structure of the starch granule I. Swelling and solubility patterns of various starches. *Cereal Chemistry*, 36, 534-544.
- Lee, J. T., Bailey, C. A., & Cartwright, A. L. (2003). Guar meal germ and hull fractions differently affect growth performance and intestinal viscosity of broiler chickens. *Poultry Science*, 82, 1589-1595.
- Lentle, R. G., Hemar, Y., Hall, C. E., & Stafford, K. J. (2005). Periodic fluid extrusion and models of digesta mixing in the intestine of a herbivore, the

- common brushtail possum (*Trichosurus vulpecula*). *Journal of Comparative Physiology B*, 175, 337-347.
- Lentle, R. G., & Janssen, P. W. M. (2008). Physical characteristics of digesta and their influence on flow and mixing in the mammalian intestine: a review. *Journal of Comparative Physiology B*, 178, 673-690.
- Lentle, R. G., & Janssen, P. W. M. (2010). Manipulating digestion with foods designed to change the physical characteristics of digesta. *Critical Reviews in Food Science and Nutrition*, 50, 130-145.
- Lentle, R. G., & Janssen, P. W. M. (2011). Part 1 The digestion of particle suspensions. In R. G. Lentle & P. W. M. Janssen (Eds.), *The physical processes of digestion* (pp. 9-10). New York: Springer.
- Lentle, R. G., Janssen, P. W. M., Asvarujanon, P., Chambers, P., Stafford, K. J., & Hemar, Y. (2007). High definition mapping of circular and longitudinal motility in the terminal ileum of the brushtail possum *Trichosurus vulpecula* with watery and viscous perfusates. *Journal of Comparative Physiology B*, 177, 543-556.
- Lentle, R. G., Janssen, P. W. M., Asvarujanon, P., Chambers, P., Stafford, K. J., & Hemar, Y. (2008). High-definition spatiotemporal mapping of contractile activity in the isolated proximal colon of the rabbit. *Journal of Comparative Physiology B*, 178, 257-268.
- Lentle, R. G., Janssen, P. W. M., & Hume, I. D. (2009). The roles of filtration and expression in the processing of digesta with high solid phase content. *Comparative Biochemistry and Physiology, Part A*, 154, 1-9.
- Lentle, R. G., Stafford, K. J., Bekkour, K., Aserevujanon, P., Sylvester, S., & Hemar, Y. (2009). Changes in the viscoelastic behaviour of the rumenal digesta mat of sheep fed on pasture or chaffed lucerne hay. *Journal of Animal Physiology and Animal Nutrition*, 94, 495-504.
- Lentle, R. G., Stafford, K. J., Hemar, Y., Aseruvujanon, P., Mellor, D. J., & Moughan, P. J. (2007). Changes in the physical properties of stomach digesta during fasting in tammar wallabies (*Macropus eugenii eugenii*). *Australian Journal of Zoology*, 55, 383-389.
- Lentle, R. G., Stafford, K. J., Kennedy, M. S., & Haslett, S. J. (2002). Rheological properties of digesta suggest little radial or axial mixing in the forestomach of the Tammar (*Macropus eugenii*) and the Parma (*Macropus parma*) Wallaby. *Physiological and Biochemical Zoology*, 75, 572-582.
- Levitt, M. D., Kneip, J. M., & Levitt, D. G. (1988). Use of laminar flow and unstirred layer models to predict intestinal absorption in the rat. *The Journal of Clinical Investigation*, 81, 1365-1369.
- Li, B. W., Andrews, K. W., & Pehrsson, P. R. (2002). Individual sugars, soluble, and insoluble dietary fiber contents of 70 high consumption foods. *Journal of Food Composition and Analysis*, 15, 715-723.
- Li, C., Mense, A. L., Brewer, L. R., Lau, C., & Shi, Y-C. (2017). *In-vitro* bile acid binding capacity of wheat bran with different particle sizes. *Cereal Chemistry*, 94, 654-658.
- Li, C., & Uppal, M. (2010). Canadian Diabetes Association National Nutrition Committee clinical update on dietary fibre in diabetes: food sources to physiological effects. *Canadian Journal of Diabetes*, 34, 355-361.
- Li, J. Y., & Yeh, A. I. (2001). Relationships between thermal, rheological characteristics and swelling power for various starches. *Journal of Food Engineering*, 50, 141-148.

- Li, M., Witt, T., Xie, F., Warren, F. J., Halley, P. J., & Gilbert, R. G. (2015). Biodegradation of starch films : The roles of molecular and crystalline structure. *Carbohydrate Polymers*, 122, 115-122.
- Lille, M., Nurmela, A., Nordlund, E., Metsä-Kortelainen, S., & Sozer, N. (2017). Applicability of protein and fiber-rich food materials in extrusion-based 3D printing. *Journal of Food Engineering, In Press*, 1-8.
- Limpisut, P., & Jindal, V. K. (2002). Comparison of rice flour pasting properties using brabender viscoamylograph and rapid visco analyser for evaluating cooked rice texture. *Starch*, 54, 350–357.
- Lindeboom, N., Chang, P. R., & Tylera, R. T. (2004). Analytical, biochemical and physicochemical aspects of starch granule size, with emphasis on small granule starches: a review. *Starch*, 56, 89-99.
- Lineback, D. R., & Wongsrikasem, E. (1980). Gelatinisation of starch in baked products. *Journal of Food Science* 45, 71-74.
- Liu, H., Yu, L., Xie, F., & Chen, L. (2006). Gelatinization of cornstarch with different amylose/amylopectin content. *Carbohydrate Polymers*, 65, 357-363.
- Liu, J. M., & Zhao, S. L. (1990). Scanning electron microscope study on gelatinisation of starch granules in excess water. *Starch*, 42, 96-98.
- Liu, Y., & Sopade, P. A. (2011). Modelling starch digestion in sweetpotato with biphasic digestograms. *Journal of Food Engineering*, 104, 307-315.
- López, E. C., Rolee, A., & Meste, M. L. (2004). Study of starch granules swelling by the blue dextran method and by microscopy. *Starch*, 56, 576-581.
- Lovegrove, J. A., Commane, D. M., Jackson, K. G., Karani, V., Kennedy, O. B., Kuhnle, G. G., Spencer, J. P. E., Wagstaff, C., & Yaqoob, P. (2015). The Hugh Sinclair Unit of Human Nutrition – 20 years of research 1995-2015. *Nutrition Bulletin*, 40, 303-314.
- Low-Beer, T. S., & Pomare, E. W. (1973). Regulation of bile salt pool size in man. *British Medical Journal*, 2, 338-340.
- Luallen, T. E. (1985). Starch as functional ingredient. *Food Technology*, 39, 59-63.
- Lund, D., & Lorenz, K. J. (1984). Influence of time, temperature, moisture, ingredients, and processing conditions on starch gelatinization. *Critical Reviews in Food Science and Nutrition*, 20, 249-273.
- Lunn, J., & Buttriss, J. L. (2007). Carbohydrates and dietary fibre. *British Nutrition Foundation Nutrition Bulletin*, 32, 21–64.
- Lupton, J. R., & Ferrell, R. G. (1986). Using density rather than mass to express the concentration of gastrointestinal tract constituents. *The Journal of Nutrition*, 116, 164-168.
- Maki, K. C., Beiseigel, J. M., Jonnalagadda, S. S., Gugger, C. K., Reeves, M. S., Farmer, M. V., Kaden, V. N., & Rains, T. M. (2010). Whole-grain ready-to-eat oat cereal, as part of a dietary program for weight loss, reduces low-density lipoprotein cholesterol in adults with overweight and obesity more than a dietary program including low-fiber control foods. *Journal of the American Dietetic Association* 110, 205-214.
- Marchand, L. L., Hankin, J. H., Wilkens, L. R., Kolonel, L. N., Englyst, H. N., & Lyu, L. (1997). Dietary fiber and colorectal cancer risk. *Epidemiology*, 8, 658-665.
- Marciani, L., Gowland, P. A., Spiller, R. C., Manoj, P., Moore, R. J., Young, P., Al-Sahab, S., Bush, D., Wright, J., & Fillery-Travis, A. J. (2000). Gastric

- response to increased meal viscosity assessed by echo-planar magnetic resonance imaging in humans. *The Journal of Nutrition*, 130, 122-127.
- Marlett, J. A., McBurney, M. I., & Slavin, J. L. (2002). Position of the American Dietetic Association: Health implications of dietary fibre. *Journal of the American Dietetic Association*, 102, 993-1000.
- Maron, S. H., & Pierce, P. E. (1956). Application of ree-eyring generalized flow theory to suspensions of spherical particles. *Journal of Colloid Science*, 11, 80-95.
- Marti, I., Hofler, O., Fischer, P., & Windhab, E. J. (2005). Rheology of concentrated suspensions containing mixtures of spheres and fibres. *Rheology Acta*, 44, 502-512.
- Mavromichalis, I., Hancock, J. D., Senne, B. W., Gugle, T. L., Kennedy, G. A., Hines, R. H., & Wyatt, C. L. (2000). Enzyme supplementation and particle size of wheat in diets for nursery and finishing pigs. *Journal of Animal Science*, 78, 3086-3095.
- McCleary, B. V., Clark, A. H., Dea, I. C. N., & Rees, D. A. (1985). The fine structure of carbo and guar galactomannans. *Carbohydrate Research*, 139, 237-260.
- McCormick, K. M., Panozzo, J. F., & Hong, S. H. (1991). A swelling power test for selecting potential noodle quality wheats. *Australian Journal of Agricultural Research* 42, 317-323.
- McDonald, D. E., Pethick, D. W., Mullan, B. P., & Hampson, D. J. (2001). Increasing viscosity of the intestinal contents alters small intestinal structure and intestinal growth, and stimulates proliferation of enterotoxigenic *Escherichia coli* in newly-weaned pigs. *British Journal of Nutrition*, 86, 487-498.
- McRorie, J., Brown, S., Cooper, R., Givaruangsawat, S., Scruggs, D., & Boring, G. (2000). Effects of dietary fibre and olestra on regional apparent viscosity and water content of digesta residue in porcine large intestine. *Alimentary and Pharmacology Therapeutic*, 14, 471-477.
- McRorie, J. W., & McKeown, N. M. (2017). Understanding the physics of functional fibers in the gastrointestinal tract: An evidence-based approach to resolving enduring misconceptions about insoluble and soluble fiber. *Journal of the Academy of Nutrition and Dietetics*, 117, 251-264.
- Melville, J., Macagno, E., & Christensen, J. (1975). Longitudinal contractions in the duodenum: their fluid-mechanical function. *American Journal of Physiology*, 228, 1887-1892.
- Mendoza, C. I., & Santamaria-Holek, I. (2009). The rheology of hard sphere suspensions at arbitrary volume fractions: An improved differential viscosity model. *The Journal of Chemical Physics*, 130, 044904-044901 - 044904-044907.
- Menkovska, M., Levkov, V., Damjanovski, D., Gjorgovska, N., Knezevic, D., Nikolova, N., & Andreevska, D. (2017). Content of TDF, SDF and IDF in cereals grown by organic and conventional farming – a short report. *Polish Journal of Food and Nutrition Sciences*, 67, 241-244.
- Meyer, K. A., Kushi, L. H., Jacobs, J. D. R., Slavin, J., Sellers, T. A., & Folsom, A. R. (2000). Carbohydrates, dietary fiber, and incident type 2 diabetes in older women. *The American Journal of Clinical Nutrition*, 71, 921-930.



- Miao, M., Zhang, T., Mu, W., & Jiang, B. (2010). Effect of controlled gelatinization in excess water on digestibility of waxy maize starch. *Food Chemistry*, 119, 41-48.
- Mikkonen, K. S., Rita, H., Helen, H., Talja, R. A., Hyvonen, L., & Tenkanen, M. (2007). Effect of polysaccharide structure on mechanical and thermal properties of galactomannan-based films. *Biomacromolecules*, 8, 3198-3205.
- Miller, E. R., & Ullrey, D. E. (1987). The pig as a model for human nutrition. *Annual Review of Nutrition*, 7, 361-382.
- Mishra, S., Monro, J., & Hedderley, D. (2008). Effect of processing on slowly digestible starch and resistant starch in potato. *Starch*, 60, 500-507.
- Mishra, S., & Rai, T. (2006). Morphology and functional properties of corn, potato and tapioca starches. *Food Hydrocolloids*, 20, 557-566.
- Mongeau, R., & Brassard, R. (1982). Determination of neutral detergent fiber in breakfast cereals: pentose, hemicellulose, cellulose and lignin content. *Journal of Food Science*, 47, 550-555.
- Monro, J. A., & Mishra, S. (2010). Database values for food-based dietary control of glycaemia. *Journal of Food Composition and Analysis*, 23, 406-410.
- Monsan, P., & Combes, D. (1984). Effect of water activity on enzyme action and stability. *Annals of the New York Academy of Sciences*, 434, 48-60.
- Monteiro, C. A., Levy, R. B., Claro, R. M., de Castro, I. R. R., & Cannon, G. (2010). Increasing consumption of ultra-processed foods and likely impact on human health: evidence from Brazil. *Public Health Nutrition*, 14, 5-13.
- Moore, C. O., Tuschhoff, J. V., Hastings, C. W., & Schanefelt, R. V. (1984). Applications of starches in foods In R. L. Whistler, J. N. BeMiller & E. F. Paschall (Eds.), *Starch chemistry and technology* (2nd Ed. ed.). Orlando, FL: Academic Press.
- Morgan, L. M., Tredger, J. A., Wright, J., & Marks, V. (1990). The effect of soluble- and insoluble-fibre supplementation on post-prandial glucose tolerance, insulin and gastric inhibitory polypeptide secretion in healthy subjects. *British Journal of Nutrition*, 64, 103-110.
- Morrison, W. R. (1988). Lipids in cereal starches: A review. *Journal of Cereal Science*, 8, 1-15.
- Morrison, W. R., Tester, R. F., Snape, C. W., Law, R., & Gidley, M. J. (1993). Swelling and gelatinisation of cereal starches. IV. Effects of lipid complexed amylose and free amylose in waxy and normal barley starches. *Cereal Chemistry*, 70, 385-391.
- Mueller, S., Llewellyn, E. W., & Mader, H. M. (2011). The effect of particle shape on suspension viscosity and implications for magmatic flows. *Geophysical Research Letters*, 38, 1-5.
- Mueller, S., Llewellyn, E. W., & Mader, H. M. . (2010). The rheology of suspensions of solid particles. *Proceedings of the Royal Society A*, 466, 1201-1228.
- Murphy, N., Norat, T., Ferrari, P., Jenab, M., Bueno-de-Mesquita, B., Skeie, G., Dahm, C. C., Overvad, K., Olsen, A., Tjønneland, A., Clavel-Chapelon, F., Boutron-Ruault, M. C., Racine, A., Kaaks, R., Teucher, B., Boeing, H., Bergmann, M. M., Trichopoulou, A., Trichopoulos, D., Lagiou, P., Palli, D., Pala, V., Panico, S., Tumino, R., Vineis, P., Siersema, P., van Duijnhoven, F., Peeters, P. H., Hjartaker, A., Engeset, D., González, C. A., Sánchez, M. J., Dorronsoro, M., Navarro, C., Ardanaz, E., Quirós, J. R., Sonestedt, E., Ericson, U., Nilsson, L., Palmqvist, R., Khaw, K. T., Wareham, N., Key, T. J., Crowe, F.L., Fedirko, V., Wark, P. A., Chuang,

- S. C., & Riboli, E. (2012). Dietary Fibre Intake and Risks of Cancers of the Colon and Rectum in the European Prospective Investigation into Cancer and Nutrition (EPIC). *Plos One*, 7, 1-10.
- Mwaikambo, L. Y., & Ansell, M. P. (2001). The determination of porosity and cellulose content of plant fibers by density methods. *Journal of Materials Science Letters*, 20, 2095-2096.
- Naguleswaran, S., Vasanthan, T., Hoover, R., & Bressler, D. (2014). Amylolysis of amylopectin and amylose isolated from wheat, triticale, corn and barley starches. *Food Hydrocolloids*, 35, 686-693.
- Nebesny, E., Rosicka, J., & Tkaczyk, M. (2004). Influence of conditions of maize starch enzymatic hydrolysis on physicochemical properties of glucose syrups. *Starch*, 56, 132-137.
- Noda, T., Takigawa, S., Matsuura-Endo, C., Suzuki, T., Hashimoto, N., Kottearachchi, N. S., Yamauchi, H., & Zaidul, I. S. M. (2008). Factors affecting the digestibility of raw and gelatinized potato starches. *Food Chemistry*, 110, 465-470.
- Nunes, C. S., & Malmlof, K. (1992). Effect of guar gum and cellulose on glucose absorption, hormonal release and hepatic metabolism in the pig. *British Journal of Nutrition*, 68, 693-700.
- Nyman, M., Asp, N-G., Cummings, J., & Wiggins, H. (1986). Fermentation of dietary fibre in the intestinal tract: comparison between man and rat *British Journal of Nutrition*, 55, 487-496.
- Nyman, M., & Asp, N. G. (1982). Fermentation of dietary fibre components in the rat intestinal tract. *British Journal of Nutrition*, 47, 357-366.
- Oechslin, R., Lutz, M. V., & Amado, R. (2003). Pectin substances isolated from apple cellulosic residue: structural characterisation of a new type of rhamnogalacturonan I. *Carbohydrate Polymers*, 51, 301-310.
- Okechukwu, P. E., & Rao, M. A. (1995). Influence of granule size on viscosity of corn starch suspension. *Journal of Texture Studies*, 26, 501-516.
- Ortega-Ojeda, F. E., Larsson, H., & Eliasson, A-C. (2004). Gel formation in mixtures of high amylopectin potato starch and potato starch. *Carbohydrate Polymers*, 56, 505-514.
- Ou, S., Kwok, K. C., Li, Y., & Fu, L. (2001). *In-vitro* study of possible role of dietary fiber in lowering postprandial serum glucose. *Journal of Agriculture and Food Chemistry*, 49, 1026-1029.
- Pabst, W., Berthold, C., & Gregorov, E. (2006). Size and shape characterization of polydisperse short-fiber systems. *Journal of the European Ceramic Society*, 26, 1121-1130.
- Pabst, W., Gregorova, V., & Berthold, C. (2006). Particle shape and suspension rheology of short-fiber systems. *Journal of the European Ceramic Society*, 26, 149-160.
- Painter, N. S., & Burkitt, D. P. (1971). Diverticular disease of the colon: A deficiency disease of Western civilization. *British Medical Journal*, 2, 450-454.
- Pan, D. D., & Jane, J. (2000). Internal structure of normal maize starch granules revealed by chemical surface gelatinization. *Biomacromolecules*, 1, 126-132.
- Panlasigui, L. N., Thompson, L. U., Juliano, B. O., Perez, C. M., Yiu, S. H., & Greenberg, G. R. (1991). Rice varieties with similar amylose content differ in starch digestibility and glycemic response in humans. *The American Journal of Clinical Nutrition*, 54, 871-877.

- Papathanasopoulos, A., & Camilleri, M. (2010). Dietary fiber supplements: Effects in obesity and metabolic syndrome and relationship to gastrointestinal functions. *Gastroenterology*, 138, 65–72.
- Parada, J., & Aguilera, J. M. (2009). *In-vitro* digestibility and glycemic response of potato starch is related to granule size and degree of gelatinization. *Journal of Food Science*, 74, E34-E37.
- Parada, J., & Aguilera, J. M. (2011). Review: Starch matrices and the glycemic response. *Food Science and Technology International*, 17, 187-204.
- Park, H., Xu, S., & Seetharaman, K. (2011). A novel *in-situ* atomic force microscopy imaging technique to probe surface morphological features of starch granules. *Carbohydrate Research*, 346, 847-853.
- Parker, P., & Ring, S. G. (2001). Aspects of the physical chemistry of starch. *Journal of Cereal Science*, 34, 1-17.
- Parrott, M. E., & Thrall, B. E. (1978). Functional properties of various fibers: physical properties. *Journal of Food Science*, 43, 759-766.
- Patel, H., Day, R., Butterworth, P. J., & Ellis, P. R. (2014). A mechanistic approach to studies of the possible digestion of retrograded starch by  $\alpha$ -amylase revealed using a log of slope (LOS) plot. *Carbohydrate Polymers*, 113, 182-188.
- Pérez, S., & Bertoft, E. (2010). The molecular structure of starch components and their contribution to the architecture of starch granules : A comprehensive review. *Starch*, 62, 389-420.
- Peroni, F. H. G., Rocha, T. S., & Franco, C. M. L. (2006). Some structural and physicochemical characteristics of tuber and root starches. *Food Science and Technology International*, 12, 505-513.
- Perry, P. A., & Donald, A. M. (2002). The effect of sugars on the gelatinisation of starch. *Carbohydrate Polymers*, 49, 155-165.
- Petford, N. (2009). Which effective viscosity? *Mineralogical Magazine*, 73, 167-191.
- Philips, G. O. (2013). Dietary fibre : A chemical category or a health ingredient? *Bioactive Carbohydrates and Dietary Fibre 1*, 3-9.
- Piel, C., Montagne, L., Seve, B., & Lalles, J. P. (2005). Increasing digesta viscosity using carboxymethylcellulose in weaned piglets stimulates ileal goblet cell numbers and maturation. *The Journal of Nutrition*, 135, 86-91.
- Planchot, V., Colonna, P., & Buleon, A. (1997). Enzymatic hydrolysis of  $\alpha$ -glucan crystallites. *Carbohydrate Research*, 298, 319-326.
- Planchot, V., Colonna, P., Gallant, D. J., & Bouchet, B. (1995). Extensive degradation of native starch granules by  $\alpha$ -amylase from *aspergillus fumigatus*. *Journal of Cereal Science*, 21, 163-171.
- Popov, D., Buléon, A., Burghammer, M., Chanzy, H., Montesanti, N., Putaux, J. L., Potocki-Véronèse, G., & Riek, C. (2009). Crystal structure of  $\alpha$ -amylase: a revisit from synchrotron microdiffraction analysis of single crystals. *Macromolecules*, 42, 1167-1174.
- Pouteau, C., Dole, P., Cathala, B., Averous, L., & Boquillon, N. (2003). Antioxidant properties of lignin in polypropylene. *Polymer Degradation and Stability*, 81, 9-18.
- Probstein, R. F., Sengun, M. Z., & Tseng, T-C. (1994). Bimodal model of concentrated suspension viscosity for distributed particle sizes. *Journal of Rheology*, 38, 811-829.

- Pusey, P. N., & Megan, V. W. (1986). Phase behaviour of concentrated suspensions of nearly hard colloidal spheres. *Nature*, 320, 340-342.
- Ragaei, S., & Abdel-Aal, E. S-M. (2006). Pasting properties of starch and protein in selected cereals and quality of their food products. *Food Chemistry*, 95, 9-18.
- Raghavendra, S. N., Rastogi, N. K., Raghavarao, K. S. M. S., & Tharanathan, R. N. (2004). Dietary fiber from coconut residue: effects of different treatments and particle size on the hydration properties. *European Food Research Technology*, 218, 563-567.
- Rani, B., & Kawatra, A. (1994). Fibre constituents of some foods. *Plant Foods for Human Nutrition*, 45, 343-347.
- Ratnayake, W. S., & Jackson, D. S. (2007). A new insight into the gelatinization process of native starches. *Carbohydrate Polymers*, 67, 511-529.
- Rayment, P., Ross-Murphy, S. B., & Ellis, P. R. (1995). Rheological properties of guar galactomannan and rice starch mixtures. I. Steady shear measurements. *Carbohydrate Polymers*, 28, 121-130.
- Rayment, P., Ross-Murphy, S. B., & Ellis, P. R. (1998). Rheological properties of guar galactomannan and rice starch mixtures. II. Creep measurements. *Carbohydrate Polymers*, 35, 55-63.
- Razdan, A., & Pettersson, D. (1996). Hypolipidaemic, gastrointestinal and related responses of broiler chickens to chitosans of different viscosity. *British Journal of Nutrition*, 76, 387-397.
- Read, N. W., & Eastwood, M. A. (1992). Gastro-intestinal physiology and function. In T. F. Schweizer & C. A. Edwards (Eds.), *Dietary fibre- A component of food* (pp. 103-115). London: Springer-Verlag.
- Regand, A., Chowdhury, Z., Tosh, S. M., Wolever, T. M. S., & Wood, P. (2011). The molecular weight, solubility and viscosity of oat beta-glucan affect human glycemic response by modifying starch digestibility. *Food Chemistry*, 129, 297-304.
- Renard, C. M. G. C., Crepeau, M. J., & Thibault, J. F. (1994). Influence of ionic strength, pH and dielectric constant on hydration properties of native and modified fibres from sugar-beet and wheat bran. *Industrial Crops and Products*, 3, 75-84.
- Rendleman, J. A. (2000). Hydrolytic action of  $\alpha$ -amylase on high-amylose starch of low molecular mass. *Biotechnology and Applied Biochemistry*, 31, 171-178.
- Repin, N., Cui, S. W., & Goff, H. D. (2016). Impact of dietary fibre on *in-vitro* digestibility of modified tapioca starch: viscosity effect. *Bioactive Carbohydrates and Dietary Fibre*, In Press.
- Repin, N., Kay, B. A., Cui, S. W., Wright, A. J., Duncan, A. M., & Goff, H. D. (2017). Investigation of mechanisms involved in postprandial glycemia and insulinemia attenuation with dietary fibre consumption. *Food Function*, 8, 2142-2154.
- Rezapour, M., Ali, S., & Stollman, N. (2017). Diverticular disease: An update on pathogenesis and management. *Gut and Liver*, 11, 1-8.
- Riccardi, G., & Rivellese, A. A. (2000). Dietary treatment of the metabolic syndrome - the optimal diet. *British Journal of Nutrition*, 83, S143-S148.
- Ríos-Covián, D., Ruas-Madiedo, P., Margolles, A., Gueimonde, M., de los Reyes-Gavilán, C. G., & Salazar, N. (2016). Intestinal short chain fatty acids and their link with diet and human health. *Frontiers in Microbiology*, 7, 185.
- Robertson, J., de Monredon, F. D., Dysseler, P., Guillon, F., Amado, R., & Thibault, J. F. (2000). Hydration properties of dietary fibre and resistant

- starch: a European collaborative study. *Lebensm.-Wiss. u.-Technology*, 33, 72-79.
- Robertson, J., & Eastwood, M. A. (1981a). An investigation of the experimental conditions which could affect water-holding capacity of dietary fibre. *Journal of the Science of Food and Agriculture*, 32, 819-825.
- Robertson, J., & Eastwood, M. A. (1981b). An examination of factors which may affect the water holding capacity of dietary fibre. *British Journal of Nutrition*, 45, 83-88.
- Robertson, J., & Eastwood, M. A. (1981c). A method to measure the water-holding properties of dietary fibre using suction pressure. *British Journal of Nutrition*, 46, 247-255.
- Robertson, J., & van Soest, P. J. (1981). The detergent system of analysis. In W. P. T. James & O. Theander (Eds.), *The analysis of dietary fibre in food* (pp. 123-158). New York and Basel: Marcel Dekker.
- Robin, J. P., Mercier, C., Charbonnière, R., & Guilbot, A. (1974). Lintnerized starches: Gel filtration and enzymatic studies of insoluble residues from prolonged acid treatment of potato starch. *Starch*, 51, 389-406.
- Robinson, G., Ross-Murphy, S. B., & Morris, E. R. (1982). Viscosity-molecular weight relationships, intrinsic chain flexibility, and dynamic solution properties of guar galactomannan. *Carbohydrate Research*, 107, 17-32.
- Roder, N., Gerard, C., Verel, A., Bogracheva, T. Y., Hedley, C. L., Ellis, P. R., & Butterworth, P. J. (2009). Factors affecting the action of  $\alpha$ -amylase on wheat starch: Effects of water availability. An enzymic and structural study. *Food Chemistry*, 113, 471-478.
- Rosell, C. M., Santos, E., & Collar, C. (2009). Physico-chemical properties of commercial fibres from different sources: A comparative approach. *Food Research International*, 42, 176-184.
- Sacilik, K., Ozturk, R., & Keskin, R. (2003). Some physical properties of hemp seed. *Biosystems Engineering*, 86, 191-198.
- Saha, B. C. (2003). Hemicellulose bioconversion. *Journal of Industrial Microbiology and Biotechnology*, 30, 279-291.
- Samra, R. A., & Anderson, G. H. (2007). Insoluble cereal fiber reduces appetite and short-term food intake and glycemic response to food consumed 75 min later by healthy men. *The American Journal of Clinical Nutrition*, 86, 972-979.
- Sanchez-Alonso, I., Haji-Maleki, R., & Borderias, A. J. (2006). Effect of wheat fibre in frozen stored fish muscular gels. *European Food Research Technology*, 223, 571-576.
- Sangnark, A., & Noomhorm, A. (2004). Chemical, physical and baking properties of dietary fiber prepared from rice straw. *Food Research International*, 37, 66–74.
- Schirmer, M., Höchstötter, A., Jekle, M., Arendt, E., & Becker, T. (2013). Physicochemical and morphological characterization of different starches with variable amylose/amylopectin ratio. *Food Hydrocolloids*, 32, 52-63.
- Schuller, A., & Muller, J. L. (2016). Histological methods to detect the clubroot pathogen *Plasmodiophora brassicae* during its complex life cycle. *Plant Pathology*, 1-15. doi: 10.1111/ppa.12520
- Schulze, M. B., Schulz, M., Heidemann, C., Schienkiewitz, A., Hoffmann, K., & Boeing, H. (2007). Fiber and magnesium intake and incidence of type 2 diabetes : A prospective study and meta-analysis. *Archive of Internal Medicine*, 167, 956-965.

- Seal, C. J., Daly, M. E., Thomas, L. C., Bal, W., Birkett, A. M., Jeffcoat, R., & Mathers, J. C. (2003). Postprandial carbohydrate metabolism in healthy subjects and those with type 2 diabetes fed starches with slow and rapid hydrolysis rates determined *in-vitro*. *British Journal of Nutrition*, 90, 853–864.
- Selvendran, R. R. (1984). The plant cell wall as a source of dietary fibre : chemistry and structure. *The American Journal of Clinical Nutrition*, 39, 320-337.
- Shelat, K. J., Nicholson, T., Flanagan, B. M., Zhang, D., Williams, B. A., & Gidley, M. J. (2015). Rheology and microstructure characterisation of small intestinal digesta from pigs fed a red meat-containing Western-style diet. *Food Hydrocolloids*, 44, 300-308.
- Shogren, R. L. (1992). Effect of moisture content on the melting and subsequent physical aging of corn starch. *Carbohydrate Polymers*, 19, 83-90.
- Skrabanja, V., Elmståhl, H. G. M. L., Kreft, I., & Björck, I. (2001). Nutritional properties of starch in buckwheat products: studies *in-vitro* and *in-vivo*. *Journal of Agricultural and Food Chemistry*, 49, 490-496.
- Slaughter, S. L., Ellis, P. R., & Butterworth, P. J. (2001). An investigation of the action of porcine pancreatic  $\alpha$ -amylase on native and gelatinised starches. *Biochimica et Biophysica Acta*, 1525, 29-36.
- Slavin, J. L., Brauer, P. M., & Marlett, J. A. (1981). Neutral detergent fiber, hemicellulose and cellulose digestibility in human subjects. *The American Journal of Clinical Nutrition*, 111, 287-297.
- Snow, P., & Odea, K. (1981). Factors affecting the rate of hydrolysis of starch in food. *The American Journal of Clinical Nutrition* 34, 2721-2727.
- Southgate, D. A. T. (1969). Determination of carbohydrates in foods I. - Available carbohydrate. *Journal of Science and Food Agriculture*, 20, 326-330.
- Southgate, D. A. T. (1976). The analysis of dietary fibre. In G. A. Spiller & R. J. Amen (Eds.), *Fiber in human nutrition* (pp. 73-107). New York Plenum Press.
- Southgate, D. A. T., Bailey, B., Collinson, E., & Walker, A. F. (1976). A guide to calculating intakes of dietary fibre. *Journal of Human Nutrition*, 30, 303-313.
- Spies, R. D., & Hosney, R. C. (1982). Effect of sugars on starch gelatinisation. *Cereal Chemistry* 59, 128-131.
- Srebotnik, E., & Messner, K. (1994). A simple method that uses differential staining and light microscopy to assess the selectivity of wood delignification by white rot fungi. *Applied and Environmental Microbiology*, 60, 1383-1386.
- Srichuwong, S., Sunarti, T. C., Mishima, T., Isono, N., & Hisamatsu, M. (2005). Starches from different botanical sources II: Contribution of starch structure to swelling and pasting properties. *Carbohydrate Polymers*, 62, 25-34.
- Stamm, A. J. (1929). Density of wood substance, adsorption by wood and permeability of wood. *Journal of Physical Chemistry*, 33, 398-414.
- Stanogias, G., & Pearce, G. R. (1985). The digestion of fibre by pigs. *British Journal of Nutrition*, 53, 513-530.
- Steeneken, P. A. M. . (1989). Rheological properties of aqueous suspensions of swollen starch granules. *Carbohydrate Polymers*, 11, 23-42.
- Stephen, A. M., Champ, M. M. J., Cloran, S. J., Fleith, M., van Lieshout, L., Mejbörn, H., & Burley, V. J. (2017). Dietary fibre in Europe: current state of knowledge on definitions, sources, recommendations, intakes and

- relationships to health. *Nutrition Research Reviews*, 1-42. doi: 10.1017/S095442241700004X
- Stephen, A. M., & Cummings, J. H. (1979). Water-holding by dietary fibre in vitro and its relationship to faecal output in man. *Gut*, 20, 722-729.
- Stickel, J. J., & Powell, R. L. (2005). Fluid mechanics and rheology of dense suspensions *Annual Review of Fluid Mechanics*, 37, 129-149.
- Story, J. A., & Kritchevsky, D. (1976). Comparison of the binding of various bile acids and bile salts *in vitro* by several types of fiber. *The Journal of Nutrition*, 106, 1292-1294.
- Sturtzel, S., & Elmadfa, I. (2008). Intervention with dietary fiber to treat constipation and reduce laxative use in residents of nursing homes. *Annals of Nutrition and Metabolism*, 52, 54-56.
- Sujka, M., & Jamroz, J. (2007). Starch granule porosity and its changes by means of amylolysis. *International Agrophysics*, 21, 107-113.
- Sujka, M., & Jamroz, J. (2010). Characteristics of pores in native and hydrolyzed starch granules. *Starch*, 62, 229-235.
- Svihus, B., Uhlen, A. K., & Harstad, O. M. (2005). Effect of starch granule structure, associated components and processing on nutritive value of cereal starch: A review. *Animal Feed Science and Technology*, 122, 303-320.
- Swinkels, J. J. M. (1985). Composition and properties of commercial native starches. *Starch*, 37, 1-5.
- Tabilo-Munizaga, G., & Barbosa-Cánovas, G. V. (2005). Rheology for the food industry. *Journal of Food Engineering*, 67, 147-156.
- Taiz, L., & Zeiger, E. (2002). Cell walls: Structure, biogenesis, and expansion. In T. Lazar (Ed.), *Plant Physiology* (pp. 313-338). Sunderland: Sinauer Associates.
- Takahashi, T. (2010). Cellulose. In S. S. Cho & P. Samuel (Eds.), *Fibre ingredients, food applications and health benefits* (pp. 263-282). Boca Raton: CRC Press.
- Takahashi, T., Furuichi, Y., Mizuno, T., Kato, M., Tabara, A., Kawada, Y., Hirano, Y., Kubo, K. Y., Onozuka, M., & Kurita, O. (2008). Water-holding capacity of insoluble fibre decreases free water and elevates digesta viscosity in the rat. *Journal of the Science of Food and Agriculture*, 89, 245-250.
- Takahashi, T., Goto, M., & Sakata, T. (2004). Viscoelastic properties of the small intestinal and caecal contents of the chicken. *British Journal of Nutrition*, 91, 867-872.
- Takahashi, T., Karita, S., Ogawa, N., & Goto, M. (2005). Crystalline cellulose reduces plasma glucose concentrations and stimulates water absorption by increasing the digesta viscosity in rats. *The Journal of Nutrition*, 135, 2405-2410.
- Takahashi, T., & Sakata, T. (2002). Large particles increase viscosity and yield stress of pig cecal contents without changing basic viscoelastic properties. *The Journal of Nutrition*, 132, 1026-1030.
- Takahashi, T., & Sakata, T. (2004). Viscous properties of pig cecal contents and the contribution of solid particles to viscosity. *Nutrition*, 20, 377-382.
- Takano, A., Kamiya, T., Tomozawa, H., Ueno, S., Tsubata, M., Ikeguchi, M., Takagaki, K., Okushima, A., Miyata, Y., Tamaru, S., Tanaka, S., & Takahashi, T. (2013). Insoluble fiber in young barley leaf suppresses the increment of postprandial blood glucose level by increasing the digesta viscosity. *Evidence-Based Complementary and Alternative Medicine*, 2013, 1-10.

- Tamari, S. (2004). Optimum design of the constant-volume gas pycnometer for determining the volume of solid particles. *Measurement Science and Technology* 15, 549-558.
- Taylor, R. (1990). Management of constipation-High fibre diets work. *British Medical Journal*, 300, 1063-1064.
- Tester, R. F. (1997). Properties of damaged starch granules: composition and swelling properties of maize, rice, pea and potato starch fractions in water at various temperatures. *Food Hydrocolloids*, 11, 293-301.
- Tester, R. F., Karkalas, J., & Qi, X. (2004). Review : Starch-composition, fine structure and architecture. *Journal of Cereal Science*, 39, 151-165.
- Tester, R. F., & Morrison, W. R. (1990). Swelling and gelatinization of cereal starches. I. Effects of amylopectin, amylose, and lipids. *Cereal Chemistry*, 67, 551-557.
- Tester, R. F., & Sommerville, M. D. (2003). The effect of non-starch polysaccharides on the extent of gelatinisation, swelling and  $\alpha$ -amylase hydrolysis of maize and wheat starches. *Food Hydrocolloids*, 17, 41-54.
- Tester, R. F., & Sommerville, M. D. (2000). Swelling and enzymatic hydrolysis of starch in low water systems. *Journal of Cereal Science*, 33, 193-203.
- Thakur, B. R., Singh, R. K., Handa, A. K., & Rao, M. A. (1997). Chemistry and uses of pectin - A review. *Critical Reviews in Food Science and Nutrition*, 31, 47-73.
- Theander, O., Westerlund, E., Aman, P., & Graham, H. (1989). Plant cell walls and monogastric diets. *Animal Feed Science and Technology*, 23, 205-225.
- Tobaruela, E. C., de O. Santos, A., de Almeida-Muradian, L. B., Araujo, E. S., Lajolo, F. M., & Menezes, E. W. (2018). Application of dietary fiber method AOAC 2011.25 in fruit and comparison with AOAC 991.43 method. *Food Chemistry*, 238, 87-93.
- Topping, D. L., & Clifton, P. M. (2001). Short-chain fatty acids and human colonic function: Roles of resistant starch and nonstarch polysaccharides. *Physiological Reviews*, 81, 1031-1064.
- Trowell, H. (1978). The development of the concept of dietary fiber in human nutrition. *The American Journal of Clinical Nutrition*, 31, S3-S11.
- Trowell, H., Southgate, D. A., Wolever, T. M., Leeds, A. R., Gassull, M. A., & Jenkins, D. J. (1976). Letter : Dietary fibre redefined. *The Lancet*, 307, 967.
- Tudorica, C. M., Kuri, V., & Brennan, C. S. (2002). Nutritional and physicochemical characteristics of dietary fiber enriched pasta. *Journal of Agricultural and Food Chemistry*, 50, 347-356.
- Vachon, C., Jones, J. D., Wood, P. J., & Savoie, L. (1988). Concentration effect of soluble dietary fibers on postprandial glucose and insulin in the rat. *Canadian Journal of Physiology and Pharmacology*, 66, 801-806.
- Vahouny, G. V., Tombes, R., Cassidy, M. M., Kritchevsky, D., & Gallo, L. L. (1980). Dietary fibers: V. Binding of bile salts, phospholipids and cholesterol from mixed micelles by bile acid sequestrants and dietary fibers. *Lipids*, 15, 1012-1018.
- Vamadevan, V., & Bertoft, E. (2015). Review : Structure-function relationships of starch components. *Starch*, 67, 55-68.
- van der Maarel, M. J. E. C., van der Veen, B., Uitdehaag, J. C. M., Leemhuis, H., & Dijkhuizen, L. (2002). Properties and applications of starch-converting enzymes of the  $\alpha$ -amylase family. *Journal of Biotechnology*, 94, 137-155.



- Van Der Werff, J. C., De Kruif, C. G., & Hoff, V. (1989). Hard-sphere colloidal dispersions : The scaling of rheological properties with particle size, volume fraction, and shear rate. *Journal of Rheology*, 33, 421-454.
- van Kempen, T. A. T. G., Regmi, P. R., Matte, J. J., & Zijlstra, R. T. (2010). *In-vitro* starch digestion kinetics, corrected for estimated gastric emptying, predict portal glucose appearance in pigs. *The Journal of Nutrition*, 140, 1227–1233.
- Vangsøe, C. T., Ingerslev, A. K., Theil, P. K., Hedemann, M. S., Lærke, H. N., & Knudsen, K. E. B. (2016). *In-vitro* starch digestion kinetics of diets varying in resistant starch and arabinoxylan compared with in vivo portal appearance of glucose in pigs. *Food Research International*, 88, 199-206.
- Vanholme, R., Demedts, B., Morreel, K., Ralph, J., & Boerjan, W. (2010). Lignin biosynthesis and structure. *Plant Physiology*, 153, 895-905.
- Vazquez-Cooz, I., & Meyer, R. W. (2002). A differential staining method to identify lignified and unlignified tissues. *Biotechnic & Histochemistry*, 77, 277-282.
- Veendam, J. J. M. S. (1985). Composition and properties of commercial native starches. *Starch*, 1, 1-5.
- Waigh, T. A., Gidley, M. J., Komanshek, B. U., & Donald, A. M. (2000). The phase transformations in starch during gelatinisation: a liquid crystalline approach. *Carbohydrate Research*, 328, 165-176.
- Waldern, D. E. (1971). A rapid micro-digestion procedure for neutral and acid detergent fibre *Canadian Journal of Animal Science*, 51, 67-69.
- Walker, J. (2006). Water in wood. In J. Walker (Ed.), *Primary wood processing: Principles and practice* (2 ed., pp. 69-91). Netherlands: Springer.
- Wang, K., Henry, R. J., & Gilbert, R. G. (2014). Causal relations among starch biosynthesis, structure, and properties. *Springer Science Review*, 2, 15-33.
- Wang, L., & Seib, P. A. (1996). Australian salt-noodle flours and their starches compared to US wheat flours and their starches. *Cereal Chemistry*, 73, 167-175.
- Wang, Q., & Ellis, P. R. (2014). Oat  $\beta$ -glucan: physico-chemical characteristics in relation to its blood-glucose and cholesterol-lowering properties. *British Journal of Nutrition*, 112, S4-S13.
- Wang, S., & Copeland, L. (2013). Molecular disassembly of starch granules during gelatinization and its effect on starch digestibility: a review. *Food & Function*, 4, 1564-1580.
- Warren, F. J., Butterworth, P. J., & Ellis, P. R. (2012). Studies of the effect of maltose on the direct binding of porcine pancreatic  $\alpha$ -amylase to maize starch. *Carbohydrate Research*, 358, 67-71.
- Warren, F. J., Zhang, B., Waltzer, G., Gidley, M. J., & Dhital, S. (2015). The interplay of  $\alpha$ -amylase and amyloglucosidase activities on the digestion of starch in *in-vitro* enzymic systems. *Carbohydrate Polymers*, 117, 192-200.
- Weickert, M. O., & Pfeiffer, A. F. H. (2008). Metabolic effects of dietary fiber consumption and prevention of diabetes. *The Journal of Nutrition*, 138, 439-442.
- Weill, C., Burch, R., & Van Dyk, J. (1954). An  $\alpha$ -amyloglucosidase that produces  $\beta$ -glucose. *Cereal Chemistry*, 31, 150-158.
- Wierenge, A. M., & Philipse, A. P. (1996). Low-shear viscosities of dilute dispersions of colloidal rodlike silica particles in cyclohexane. *Journal of Colloid and Interface Science*, 180, 360-370.

- William, R. D., & Olmsted, W. H. (1936). The effect of cellulose, hemicellulose and lignin on the weight of the stool: a contribution to the study of laxation in man. *The Journal of Nutrition*, 11, 433-449.
- Williams, B. A., Grant, L. J., Gidley, M. J., & Mikkelsen, D. (2017). Gut fermentation of dietary fibres: Physico-chemistry of plant cell walls and implications for health. *International Journal of Molecular Sciences*, 18, 1-25.
- Wood, P. J. (1992). Aspects of the chemistry and nutritional effects of non starch polysaccharides of cereals. In Alexander R. J. & H. F. Zobel (Eds.), *Developments in Carbohydrate Chemistry* (pp. 293-314). St Paul: American Association Cereal Chemists Inc.
- Wood, P. J., Braaten, J. T., Scott, F. W., Riedel, D., & Poste, L. M. (1990). Comparisons of viscous properties of oat and guar gum and the effects of these and oat bran on glycemic index. *Journal of Agriculture and Food Chemistry*, 38, 753-757.
- Woolnough, J. W., Monro, J. A., Brennan, C. S., & Bird, A. R. (2008). Simulating human carbohydrate digestion *in-vitro* : a review of methods and the need for standardisation. *International Journal of Food Science and Technology*, 43, 2245-2256.
- Wrick, K. L., Robertson, J. B., van Soest, P. J., Lewis, B. A., Rivers, J. M., Roe, D. A., & Kackler, L. R. (1983). The influence of dietary fibre source on human intestinal transit and stool output. *The Journal of Nutrition*, 113, 1464-1479.
- Yangilar, F. (2013). The application of dietary fibre in food industry: structural features, effects on health and definition, obtaining and analysis of dietary fibre: A review. *Journal of Food and Nutrition Research*, 1, 13-23.
- Zacherl, C., Eisner, P., & Engel, K. H. (2011). *In-vitro* model to correlate viscosity and bile acid-binding capacity of digested water-soluble and insoluble dietary fibres. *Food Chemistry*, 126, 423-428.
- Zaidul, I. S. M., Nik Norulaini, N. A., Mohd. Omar, A. K., Yamauchi, H., & Noda, T. (2007). RVA analysis of mixtures of wheat flour and potato, sweet potato, yam, and cassava starches. *Carbohydrate Polymers*, 69, 784-791.
- Zhang, B., Dhital, S., & Gidley, M. J. (2013). Synergistic and antagonistic effects of  $\alpha$ -amylase and amyloglucosidase on starch digestion. *Biomacromolecules*, 14, 1945-1954.
- Zhang, G., Ao, Z., & Hamaker, B. R. (2006). Slow digestion property of native cereal starches. *Biomacromolecules*, 7, 3252-3258.
- Zhao, G., Zhang, R., Dong, L., Huang, F., Tang, X., Wei, Z., & Zhang, M. (2018). Particle size of insoluble dietary fiber from rice bran affects its phenolic profile, bioaccessibility and functional properties. *LWT - Food Science and Technology* 87, 450-456.
- Zielinski, G., DeVries, J. W., Craig, S. A. S., & Bridges, S. R. (2013). Dietary fibre methods in Codex Alimentarius : Current status and ongoing discussions. *Cereal Food World*, 58, 148-152.
- Zuman, P., Ainso, S., Paden, C., & Pethica, B. A. (1988). Sorptions on lignin, wood and celluloses. I. bile salts. *Colloids and Surfaces*, 33, 121-132.

## Appendix 1

### Appendix 1: Nutrition information panel for as is Kellogg's AllBran®

Kellogg's® All-Bran® Original		
<b>Nutrition Facts</b>		
Serving Size $\frac{1}{2}$ cup (31g)		
Amount Per Serving	Cereal	with $\frac{1}{2}$ cup skim milk
<b>Calories</b>	80	120
Calories from Fat	10	10
% Daily Value**		
<b>Total Fat</b> 1g*	<b>2%</b>	<b>2%</b>
Saturated Fat 0g	<b>0%</b>	<b>0%</b>
Trans Fat 0g		
Polyunsaturated Fat 0.5g		
Monounsaturated Fat 0g		
<b>Cholesterol</b> 0mg	<b>0%</b>	<b>0%</b>
<b>Sodium</b> 80mg	<b>3%</b>	<b>6%</b>
<b>Potassium</b> 350mg	<b>10%</b>	<b>16%</b>
<b>Total Carbohydrate</b> 23g	<b>8%</b>	<b>10%</b>
Dietary Fiber 10g	<b>40%</b>	<b>40%</b>
Sugars 6g		
<b>Protein</b> 4g	<b>4%</b>	<b>12%</b>
<b>Vitamin A</b>	<b>10%</b>	<b>15%</b>
<b>Vitamin C</b>	<b>10%</b>	<b>10%</b>
<b>Calcium</b>	<b>10%</b>	<b>25%</b>
<b>Iron</b>	<b>25%</b>	<b>25%</b>
<b>Vitamin D</b>	<b>10%</b>	<b>25%</b>
<b>Thiamin</b>	<b>25%</b>	<b>30%</b>
<b>Riboflavin</b>	<b>25%</b>	<b>35%</b>
<b>Niacin</b>	<b>25%</b>	<b>25%</b>
<b>Vitamin B<sub>6</sub></b>	<b>100%</b>	<b>100%</b>
<b>Folic Acid</b>	<b>100%</b>	<b>100%</b>
<b>Vitamin B<sub>12</sub></b>	<b>100%</b>	<b>110%</b>
<b>Phosphorus</b>	<b>35%</b>	<b>45%</b>
<b>Magnesium</b>	<b>25%</b>	<b>30%</b>
<b>Zinc</b>	<b>10%</b>	<b>15%</b>
<b>Copper</b>	<b>10%</b>	<b>10%</b>
* Amount in cereal. A serving of cereal plus skim milk provides 1g total fat, 0mg cholesterol, 130mg sodium, 540mg potassium, 29g total carbohydrates (12g sugars) and 8g protein.		
** Percent Daily Values are based on a 2,000 calorie diet. Your daily values may be higher or lower depending on your calorie needs:		
	Calories	2,000 2,500
Total Fat	Less than	65g 80g
Sat. Fat	Less than	20g 25g
Cholesterol	Less than	300mg 300mg
Sodium	Less than	2,400mg 2,400mg
Potassium		3,500mg 3,500mg
Total Carbohydrate		300g 375g
Dietary Fiber		25g 30g
Protein		50g 65g

**Ingredients:** Wheat bran, sugar, malt flavor, contains 2% or less of salt.

**Vitamins and Minerals:** Calcium carbonate, vitamin C (sodium ascorbate and ascorbic acid), reduced iron, niacinamide, vitamin B<sub>6</sub> (pyridoxine hydrochloride), vitamin B<sub>2</sub> (riboflavin), folic acid, vitamin B<sub>1</sub> (thiamin hydrochloride), vitamin A palmitate, vitamin B<sub>12</sub>, vitamin D.

**CONTAINS WHEAT INGREDIENTS.**

## Appendix 2

### Appendix 2: Nutrition information for as supplied guar gum given by the food company

**Texture Innovation Center**  
 10552 Philadelphia Road | White Marsh, MD 21162 USA  
 (800) 899-3953 | (410) 273-7300 | (410) 335-4935 Fax

**Operations**  
 4609 Richlynn Drive | Belcamp, MD 21017 USA  
 (800) 221-3953 | (410) 273-7300 | (410) 273-0289 Fax  
 ticgums.com



**TIC GUMS**  
 We're your Gum Guru

#### TIC Pretested® Gum Guar 8/22

#### PRODUCT DATA

TIC Pretested® Gum Guar 8/22 is a high viscosity, fine mesh guar gum. Used for where rapid hydration required. Gum Guar 8/22 is used in instant soup mixes, instant gravies and also in liquid sauces and baked goods, where either viscosity or water control is required. Typical usage level varies from 0.1% to 0.5%. Gum Guar 8/22 is stable over a wide pH range, but in liquid products should not be used when the pH is below 4.0. Hydrates in cold water, but actually performs better when heated and cooled.

Typical Usage Level	0.1% to 1%
Solubility	Cold Water Soluble
Suggested Uses	Instant Beverages, Instant Soup Mixes, Instant Cocoa, Sauces, Marinades, Gravies, Bakery Mixes, Suspension, Thickener
Label Declaration	Guar Gum
Country of Origin	Made in USA from imported guar splits
CFR #	21 CFR 184.1339
CAS #	9000-30-0
EU #	413
HS Tariff #	1302.32
Minimum Qty	
Standard Packing	50# Bags, 2,000# per pallet
Lead Time	10 business days
Storage & Handling	Each container is identified with the product name and lot number. Store in cool dry place for maximum shelf life.

Kosher	Y	(Y/N)
Kosher for Passover	N	(Y/N)
Halal	Y	(Y/N)
Allergen	N	(Y/N)

All Natural Y\* (Y/N)

Shelf-Life 2 years

**TIC Gums Natural Definition Disclaimer:** When deciding which of its product offerings to classify as "natural" or "all natural," TIC Gums applies the following internal definition to either term interchangeably: "A finished product derived from naturally occurring raw materials that were processed without modifying the native chemical structure of any of the materials." Our processes may involve more than minimal processing of the raw materials to maximize functionality with processing aids that may be synthetic or that may be derived from ingredients developed through the use of recombinant DNA technology. TIC Gums will consider an ingredient "natural" or "all natural" when there has been no modification to its native chemical structure. TIC Gums makes no representations regarding the consistency of its definition of "natural" or "all natural" with any legal or regulatory lexicon, or dictionary. TIC Gums makes no representations in particular as to whether this definition is superior to or in conformance with definitions of "natural" or "all natural" promulgated by the USDA, Health Canada, or the FDA. Each customer must make its own decision regarding what definition of "natural" or "all natural" the customer will utilize in describing its own products. As part of its decision-making process, each customer should obtain independent regulatory and legal advice regarding the definition of "natural" or "all natural" most appropriate for that customer. Each customer is solely responsible for determining the nature and content of any claims that may or should appear on its own products. Each customer is also solely responsible for compliance with all pertinent legal requirements worldwide.

#### NUTRITIONAL INFORMATION

Calories (Total)	363 Kcal	Sodium	33 mg	Insoluble Dietary Fiber	0.0 g
%Calories from Fat	2.00 %	Potassium	249 mg	Simple Carbohydrates	0 g
Calories from Fat	9.00 Kcal	Calcium	51 mg	Complex Carbohydrates	0 g
Total Fat	1.00 g	Total Carbohydrates	85.00 g	Protein	4 g
Trans Fat	0.00 g	Soluble Dietary Fiber	85 g	Vitamins, Other Minerals	*ND
Cholesterol	0 mg				

(per 100 grams). This data is from analysis and calculation and should be considered "typical" and not a specification. Data is reported on an "as is" basis. Total fat and protein values are rounded to the nearest whole number.

\* Calculated based on typical assay of component(s)

\* N.D.: Not determined

\*\*Total Calories are calculated in compliance with FDA Regulations requiring the inclusion of 4 Kcal/g for all soluble dietary fiber. However dietary fiber by definition consists of plant material that is resistant to hydrolysis by endogenous enzymes of the mammalian digestive tract. TIC GUMS has participated in discussions with the FDA as part of the Calorie Control Council to amend the FDA regulations to 2Kcal/g.

If all nutritional information is listed as "0" then these findings have yet to be evaluated.

#### SPECIFICATIONS

Bacteriological	Minimum	Maximum
Aerobic Plate Count (AOAC 988.18, 2.5g)	0	2500 cfu
Combined Yeast and Mold (BAM)	0	200 /g
E. coli (AOAC 989.11, 2.5g)	Negative /g	-
S. aureus (BAM)	Negative /10g	-
Salmonella - 25g (AOAC 999.09)	Negative /25g	-
Total Coliforms (AOAC 989.11)	0	33 /g
Mesh	Minimum	Maximum
US#100 Mesh On	0	5 %
US#200 Mesh Through	85	100 %
Physical and Chemical	Minimum	Maximum
Flavor (Typical)	Typical	-
Moisture (Infrared)	0	15 %
Odor (Typical)	Typical	-
pH (viscosity solution)	5.4	7 pH
Powder Color (Visual)	Creamy White	-
Texture (Qualitative)	Free Flowing Powder	-
Viscosity (1.0% RV@20rpm, 25C)	4000	6000 cps

The information provided is based upon tests and observations made under laboratory conditions and is believed to be accurate. Test results may, however, vary depending upon testing conditions. In furnishing samples and product data and specifications, TIC Gums, Inc. makes no Warranty, either express or implied, including any warranty of merchantability or fitness for a particular purpose. It is expressly understood and agreed that it is the buyer's responsibility to determine suitability of the product for a particular purpose, product or process. To obtain a description of our testing methodologies, please contact TIC Gums, Inc. at (800) 899-3953 or (410) 273-7300.

This product, or ingredients used to make this product, have been demonstrated to conform with current Food Chemical Codex requirements

Version: 20131213.0010

GUAR 8/22

### Appendix 3

**Appendix 3: Effect of cooking duration and %DG on Q and S in potato and corn starches gelatinised in water and were compared with starches gelatinised in 70% (w/v) fructose solution**

Starch	Treatment	Cooking duration (min)	Q (g/g) ‡	S (g/g) ‡
Potato	70% (DG0%)	10	1.11±0.09 <sup>c</sup>	0.84±0.19 <sup>d</sup>
		30	1.27±0.12 <sup>c</sup>	0.93±0.17 <sup>d</sup>
	DG50%	10	6.01±0.22 <sup>b</sup>	5.90±0.66 <sup>c</sup>
		30	7.40±0.34 <sup>b</sup>	6.24±0.41 <sup>c</sup>
	DG100%	10	8.78±0.21 <sup>b</sup>	9.49±0.25 <sup>bc</sup>
		30	10.94±0.32 <sup>a</sup>	12.27±0.21 <sup>ab</sup>
Corn	70% (DG0%)	10	1.08±0.05 <sup>c</sup>	0.80±0.18 <sup>d</sup>
		30	1.12±0.13 <sup>c</sup>	0.94±0.22 <sup>d</sup>
	DG50%	10	6.86±0.69 <sup>b</sup>	6.33±0.42 <sup>c</sup>
		30	7.64±0.36 <sup>b</sup>	7.04±0.47 <sup>bc</sup>
	DG100%	10	8.80±0.13 <sup>b</sup>	10.83±0.49 <sup>bc</sup>
		30	9.90±0.45 <sup>ab</sup>	13.28±0.23 <sup>a</sup>

‡ mean values in a row followed by different superscripts (a-d) are significantly different (Two way ANOVA and Tukey's pair wise test, p<0.05)

## Appendix 4

**Appendix 4:** Standard curve of glucose curve for DNS assay

